UNIVERSIDAD AUTÓNOMA DE MADRID

Departamento de Bioquímica

NANOMEDICINA APLICADA AL TRATAMIENTO DE LA OTOTOXICIDAD PROVOCADA POR CISPLATINO Y DESCRIPCIÓN DE NUEVAS DIANAS TERAPÉUTICAS

Sergio Martin Saldaña

Madrid, 2016

Departamento de Bioquímica

Facultad de Medicina

UNIVERSIDAD AUTÓNOMA DE MADRID

NANOMEDICINA APLICADA AL TRATAMIENTO DE LA OTOTOXICIDAD PROVOCADA POR CISPLATINO Y DESCRIPCIÓN DE NUEVAS DIANAS TERAPÉUTICAS

SERGIO MARTIN SALDAÑA

Licenciado en Biología

DIRECTORES:

Julio San Román del Barrio

Rafael Ramírez Camacho

HOSPITAL UNIVERSITARIO PUERTA DE HIERRO

Grupo de Investigaciones Otológicas

INSTITUTO DE CIENCIA Y TECNOLOGÍA DE POLÍMEROS (ICTP-CSIC)

Departamento de Nanomateriales Poliméricos y Biomateriales

D. JULIO SAN ROMÁN DEL BARRIO, PROFESOR DE INVESTIGACIÓN DEL CONSEJO SUPERIOR DE INVESTIGACIONES CIENTÍFICAS Y **D. RAFAEL RAMÍREZ CAMACHO**, PROFESOR TITULAR DEL DEPARTAMENTO DE CIRUGÍA DE LA FACULTAD DE MEDICINA DE LA UNIVERSIDAD AUTÓNOMA DE MADRID Y JEFE DE SERVICIO DE OTORRINOLARINGOLOGÍA DEL HOSPITAL UNIVERSITARIO PUERTA DE HIERRO DE MADRID,

CERTIFICAN como Directores de la Tesis Doctoral titulada **"NANOMEDICINA APLICADA AL TRATAMIENTO DE LA OTOTOXICIDAD PROVOCADA POR CISPLATINO Y DESCRIPCIÓN DE NUEVAS DIANAS TERAPÉUTICAS."** presentada por **SERGIO MARTIN SALDAÑA**, que la misma ha sido realizada bajo su dirección en los laboratorios del Departamento de Nanomateriales Poliméricos y Biomateriales del Insti6tuto de Ciencia y Tecnología de Polímeros (CSIC) y del Grupo de Investigaciones Otológicas del Instituto de Investigación Puerta de Hierro-Majadahonda.

Revisado el trabajo, consideramos éste como satisfactorio y autorizamos su presentación y defensa para optar al grado de Doctor en Bioquímica, Biología Molecular, Biomedicina y Biotecnología (Biociencias Moleculares). Y para que quede constancia de ello, firmamos el presente documento.

Los Directores de la Tesis.

Fdo.: Julio San Román del Barrio Fdo.: Rafael Ramírez Camacho

A mis padres

Agradecimientos

Tras estos cuatro años de trabajo para la realización de la presente tesis, hay mucha gente a la que agradecer su ayuda, apoyo y motivación, sin la que no habría sido posible llegar a este punto.

En primer lugar, quiero agradecer a mis directores, Julio y Rafa, por darme la oportunidad de realizar este trabajo, por brindarme un proyecto con tantísimo potencial y sobre todo por cada palabra de apoyo y ánimo que he recibido por su parte desde el primer día que pisé el laboratorio.

A Almudena, de manera muy especial, quien ha sido un apoyo constante en estos años, y me ha enseñado a tener pasión por el complejo mundo de la cóclea.

Debo agradecer al grupo del Dr. Ricardo Sanz, del Hospital de Getafe, toda la ayuda que me brindaron al principio de la tesis, abriéndome las puertas de su laboratorio y ayudándome con todas las dudas que pudieron surgirme, que fueron muchas. Especialmente a Carolina y Mario, que me sufrieron los primeros 8 meses de tesis, y fueron parte fundamental en que aprendiera a manejarme con los animales.

A la gente del animalario del hospital, con quien he compartido tantas horas y me han ayudado tanto en estos cuatro años. A Lola y Aitor, por estar siempre dispuestos a echarme una mano en el quirófano, y a Martin, por toda la ayuda prestada en el animalario.

Al grupo de Biomateriales. A Blanca, por tener siempre una palabra positiva y de ánimo para todo el mundo. A Mar, por ayudarme a dar mis primeros pasos en células, y a Rosana por estar siempre dispuesta a ayudarme cuando no me daban las horas para poder con todos los ensayos. A Luis Rodríguez, por los consejos al inicio de mi "estancia" en el grupo. A Luisgar, por sus cambios repentinos de música a traición cuando uno está tan tranquilo en el laboratorio. A Luis Rojo, por enseñarme que hay que ir a muerte a por todo y que se puede ser CIENTÍFICO y no morir en el intento. A todos los estudiantes que han pasado por el grupo en este tiempo, por todos los momentos, risas y broncas, por mi parte, que hemos compartido (a Martina, Enrica, Humberto, Edu, Daniel, Angela, Maria, Eva, Luis, Raquel, Soraya, Pilar…).

A Curra, mi directora en las trincheras. Sin ti ésta tesis no hubiera sido posible. Sin toda tu ayuda, exigencia y apoyo de manera directa durante estos cuatro años, esta tesis no sería ni un cuarto de lo que hoy es, y yo no sería ni la décima parte de lo que soy ahora como proyecto de científico.

En éstos cuatro años he tenido la suerte de cruzarme con gente que ha pasado de ser compañera a ser amiga. A los chicos de Neonatología, Laura, Carlos y María, por los cafelitos de las 11, las charlas sobre futbol y el apoyo que habéis sido para mí desde el principio en el hospital. A Paco, por sus chistacos, por todas las conversaciones, científicas y no, que hemos compartido en éste tiempo. A Elma, por enseñarme a hablar mejor y bajar mi ratio palabrota/palabra, y tener siempre una sonrisa para todo el mundo. A Raquel, sin ti mi tesis directamente no existiría, por estar siempre dispuesta a ayudar incluso si tenias que estirar el día a 48 horas, y por todo el tiempo que hemos compartido al final de tu tesis. A Álvaro. A ti no te digo nada, no te vayas a poner romanticón; sencillamente gracias por estar siempre ahí incondicionalmente.

A mis amigos del máster de ciencias forenses. A Mery, Juanma, Belén, Paula, Nieves, Ali y Patri, porque sois lo mejor que me llevé de aquel máster.

A mis amigos de siempre, por aguantar mis chapas científicas todos estos años simulando interés. Hubo veces que hasta me lo creí. A Fer, Edu, Ales, Dani, Paco, Frank, Rute, Crivins, Luis, Ger, Jorge y Juan; vosotros lleváis algunos años más aguantándome y aún seguís ahí apoyando. Porque más que amigos, sois familia.

A mi familia. A mis abuelos, los que están y los que se fueron, por enseñarme a vivir y dar mis primeros pasos. A mis hermanos, Edu y Rebe, y, sobre todo, a mis padres. A ti, Papá, por auto convencerte de que soy el mejor científico del mundo, y a ti, Mamá, por escuchar mis chapas sobre nanomedicina, a pesar de que te sonaran a esperanto. A los dos, gracias por todo, por criarme, por acompañarme en la vida y apoyarme siempre. Ésta tesis es vuestra.

Por último, te lo agradezco a ti, mi *Maga* particular. Por aparecer de pronto para no irte nunca. Porque siempre vivamos nuestro capítulo 7.

A todos, INFINITAS GRACIAS.

RESUMEN

El cisplatino es un agente citostático utilizado en el tratamiento de gran variedad de tumores sólidos. Sin embargo, su potencial como antitumoral debido a su alta citotoxicidad hace que tenga serios efectos adversos, incluida la ototoxicidad. El tratamiento de la pérdida de audición derivada de la administración de cisplatino, irreversible cuando se emplean dosis elevadas del fármaco, sigue representando un gran desafío.

En la presente tesis se desarrollaron y testaron *in vitro* e *in vivo*, un total de 26 sistemas de nanopartículas poliméricas con el objetivo de paliar el efecto ototóxico derivado del tratamiento con cisplatino. Los sistemas nanoparticulados están basados en copolímeros anfifílicos derivados de la vitamina E o el α-TOS, y en ellos se vectorizaron tres moléculas con potencial otoprotector, siendo estas: 6α-metilprednisolona, dexametasona y α-TOS. Así mismo, se desarrollaron y testaron sistemas basados en una mezcla de los copolímeros anteriormente mencionados, y otros basados en un derivado metacrílico del ibuprofeno, con el fin de conseguir sistemas sensibles a pH con capacidad de liberar su carga en entornos inflamatorios, con ligera acidosis. Los prometedores resultados obtenidos a lo largo de ésta tesis doctoral tanto *in vitro* como *in vivo* (en modelo animal murino), con varias de la múltiples formulaciones testadas, apoyan el potencial clínico de las nanopartículas poliméricas para mejorar los tratamientos otoprotectores frente al cisplatino.

De igual manera, el estudio de receptores sobre expresados en el oído interno tras el tratamiento con cisplatino, que puedan servir como dianas terapéuticas para el desarrollo de nuevas terapias paliativas de la ototoxicidad es de gran interés. En la segunda parte de la tesis doctoral aquí presentada, se describe, por primera vez, la presencia de receptores CB_2 en la cóclea de rata Wistar adulta mediante inmunohistoquímica y RT-qPCR, así como su sobreexpresión génica en animales tratados con cisplatino. Estos resultados sugieren el provechoso potencial de los receptores CB_2 como diana terapéutica de la ototoxicidad provocada por el cisplatino, abriendo una interesante línea de investigación para desarrollar tratamientos dirigidos específicamente a CB_2 empleando agonistas o antagonistas del mismo con el fin de conocer más a fondo su posible efecto en la protección de las células cocleares tras el tratamiento con el antitumoral.

ABSTRACT

Cisplatin is a cytostatic agent widely used in the treatment of many solid tumors. However, its use as an antitumor implies serious adverse effects, including ototoxicity due to its high cytotoxicity. The treatment of cisplatin-induced hearing loss, irreversible when high doses of the drug are employed, remains a big challenge.

In this thesis a total of 26 systems of polymeric nanoparticles were developed and tested, *in vitro* and *in vivo*, in order to palliate the ototoxic effect of cisplatin. Nanoparticulated systems are based on amphiphilic copolymers derived from vitamin E or α-TOS developed in our group. Three hydrophobic molecules with otoprotective potential were loaded within the nanoparticles: 6α-methylprednisolone, dexamethasone and α-TOS. Likewise, nanoparticles based on a blend of the aforementioned copolymers and others based on a methacrylic derivative of ibuprofen were obtained, in order to achieve pH-sensitive behavior and the ability of release its cargo in inflammatory environments, with mild acidosis. The promising results obtained during this thesis, both *in vitro* and *in vivo*, with several of the multiple tested formulations, support the potential of copolymeric nanoparticles as a valuable clinical alternative to treat cisplatin promoted ototoxicity.

Similarly, the study of overexpressed receptors in the inner ear after treatment with cisplatin, whose may serve as therapeutic target for the development of new therapies against cisplatin-induced ototoxicity, is of great interest. In the second part of the doctoral thesis presented here we described, for the first time, the presence of CB_2 receptors by immunohistochemistry and RT-qPCR. Up-regulation of gene expression in animals treated with cisplatin was also reported. These results suggest the potential of CB_2 receptor as a profitable therapeutic target of cisplatin-induced ototoxicity. This fact opens an interesting body of research to develop specific treatments able to target CB_2 using agonists or antagonists in order to explore its possible therapeutic effect in the protection of cochlear cells after cisplatin treatment.

INDICE

CLAVE DE ABREVIATURAS

α-TOS	α-tocopheryl succinate/ succinato de α-tocoferilo
ABR	auditory brainsteam response/ respuesta auditiva del tronco cerebral
ASSR	auditory steady state response/ potenciales evocados de estado estable
C-6	coumarin 6/ cumarina 6
CDDP	cisplatin/cisplatino
cDNA / ADNc	complementary DNA / ADN complementario
CHO	chinese hamster ovary cells / células de ovario de hamster chino
COX-2	cicleoxigenase-2 / ciclooxigenasa-2
dB	decibels/ decibelios
DLS	dynamic light scattering/ dispersión de luz dinámica
DNA/ADN	desoxirribonucleic acid / ácido desoxirribonucléico
Dx	dexamethasone/ dexametasona
EDTA	Ethylenediaminetetraacetic acid / Ácido etilendiaminotetraacético
HEI-OC1	house of ear institute-organ of Corti cell / células del órgano de Corti
HPLC	high performance liquid chromatography / cromatografía líquida de alta resolución
IL-1β	interleukin-1β / interleuquina-1β
IL-6	interleukin-6 / interleuquina-6

IHC	inner hair cell / célula ciliada interna
MP	methylprednisolone / metilprednisolona
MVE	methacrylic derivative of vitamin E / derivado metacrílico de la vitamina E
MTOS	methacrylic derivative of α-tcopheryl succinate / derivado metacrílico del succinato de α-tocoferilo
NF-kappa B	nuclear factor kappa-light-chain-enhancer of activated B cells / factor nuclear potenciador de las cadenas ligeras kappa de las células B activadas
nm	nanometer / nanómetro
NOS-2	nitric oxide synthase/ óxido nítrico sintasa
NPs	nanoparticles / nanopartículas
OHC	outer hair cell / célula ciliada externa
PBS	phosphate buffer saline / tampón fosfato salino
PCR	polymerase chain reaction / reacción en cadena de la polimerasa
PDI	polidispersity index/ índice de polidispersidad
RNA / ARN	ácido ribonucléico/ ribonucleic acid
mRNA / RNAm	messenger RNA / ARN mensajero
ROS	reactive oxigen species / especies reactivas de oxígeno
RT-PCR	reverse transcripted polymerase chain reaction / reacción en cadena de la polimerasa con transcriptasa inversa
RWM	round window membrane / membrana de la ventana redonda
SEM	scanning electron microscopy / microscopía electronic de barrido
SOD	superoxide dismutase / superóxido dismutasa

TEM	transmission electron microscopy / microscopía electrónica de transmisión
THC	tetrahidrocannabinol / tetrahidrocanabinol
TNF-α	tumor necrosis factor α / factor de necrosis tumoral α
VI	1-vinilimidazole / vinilimidazol
VP	N-vinilpirrolidone / vinilpirrolidona
δ	zeta potential / potencial zeta

1 *Introducción*

2

3

4

5

INTRODUCCIÓN

HIPOACUSIA

La hipoacusia o pérdida de audición afecta a más del 5% de la población mundial (360 millones de personas en todo el mundo). Un tercio de las personas mayores de 65 años se ven afectadas por pérdida de audición asociada a la edad o presbiacusia. La pérdida de audición, produce un gran impacto en la calidad de vida de las personas afectadas por la pérdida de la capacidad de comunicación, pudiendo provocar incluso angustia emocional (World Health Organization, 2015). Las causas de la pérdida de la audición y sordera pueden ser:

- **Congénitas**, tales como algunas infecciones durante el embarazo, bajo peso o asfixia al nacer, el uso inadecuado de algunos fármacos durante la gestación, o ictericia severa en el período neonatal.
- **Adquiridas**, tales como enfermedades infecciosas, infecciones crónicas del oído, otitis media, lesión en la cabeza o el oído, el envejecimiento, la cera o cuerpos extraños que bloquean el conducto auditivo externo, la exposición al ruido, y el uso de ciertos fármacos.

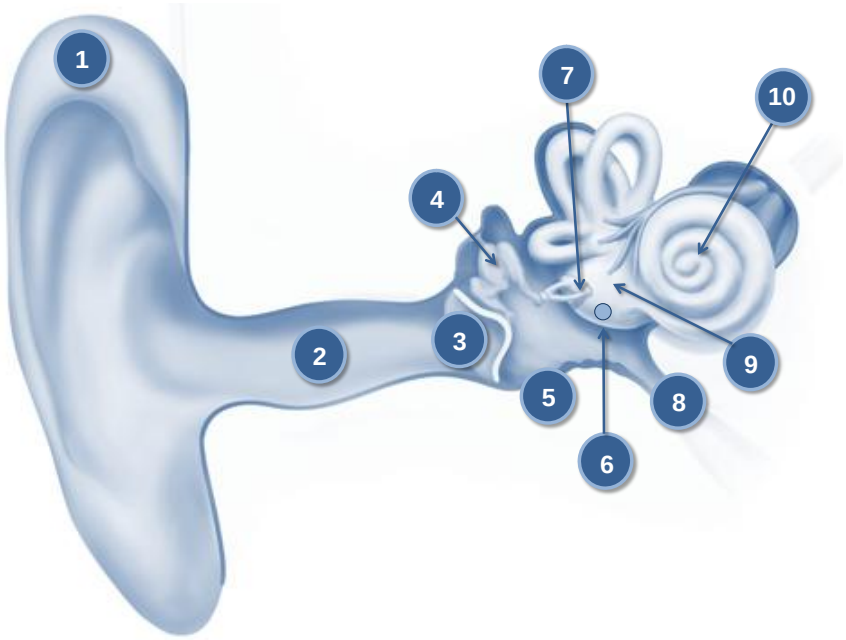

Figura 1: Anatomía del oído. Oído externo: pabellón auricular (1); canal auditivo (2). Oído medio: membrana timpánica (3); martillo, yunque y estribo (4); bulla timpánica (5); ventana redonda (6); ventana oval (7); trompa de Eustaquio (8). Oído interno: vestíbulo (9); cóclea (10).

HIPOACUSIA NEUROSENSORIAL (SNHL)

El oído interno es una estructura aislada de difícil acceso debido a la presencia de numerosas barreras anatómicas (**Figura 1**). Se considera una región hiper-especializada del sistema nervioso periférico (Osen et al., 2011) formado por la cóclea y el vestíbulo, órganos de la audición y el equilibrio respectivamente. La cóclea es una estructura compleja encargada de la transducción de ondas sonoras complejas en actividad neuronal eléctrica a través del nervio auditivo por medio de las células ciliadas del órgano de Corti (**Figura 2**). Existen dos tipos de células ciliadas en la cóclea: células ciliadas internas, que realizan la transducción e inician la despolarización de las neuronas del ganglio espiral, y las células ciliadas externas que mejoran la sensibilidad y la selectividad de la cóclea. La hipoacusia neurosensorial (SNHL, del inglés sensorineural hearing loss) es causada por la degeneración o el deterioro de las células ciliadas o por daños en el nervio auditivo.

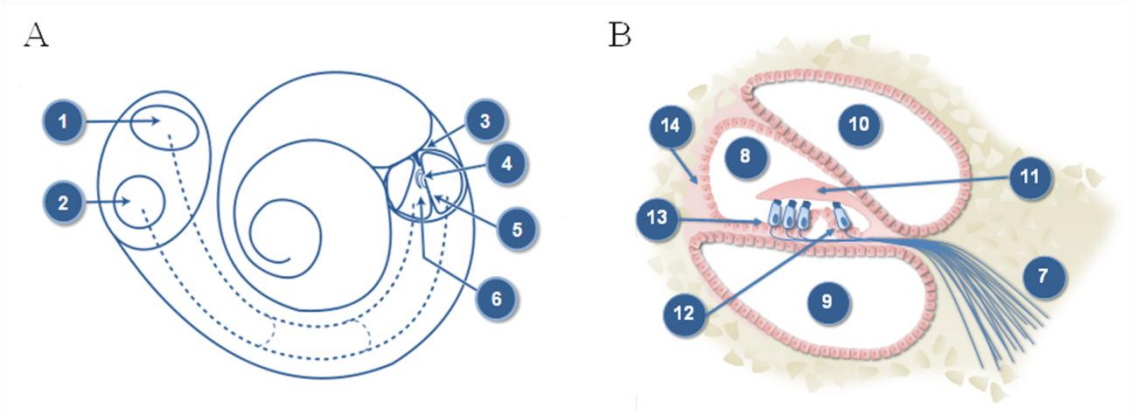

Figura 2: Estructura de la cóclea (A): Ventana oval (1); ventana redonda (2); ganglio espiral (3); órgano de Corti (4); membrana basilar (5) y escala media (6). Sección transversal del conducto coclear (B): ganglio espiral (7); escala media (8); escala timpánica (9); escala vestibular (10); membrana tectoria (11); célula ciliada interna (12); células ciliadas externas (13) y estría vascular (14).

OTOTOXICIDAD INDUCIDA POR CISPLATINO

Una de las causas más importantes de SNHL es la ototoxicidad, definida como el deterioro funcional y la degradación celular de los tejidos del oído interno debido a la utilización de agentes terapéuticos como por ejemplo, antibióticos aminoglicósidos, diuréticos del asa, antimaláricos y agentes quimioterapéuticos basados en platino (Rybak and Ramkumar, 2007).

El cis-diaminodicloroplatino (II) o cisplatino (CDDP) fue el primer fármaco con base de platino en ser empleado en tratamientos antitumorales y hoy en día es utilizado ampliamente en el tratamiento de algunas neoplasias tales como cabeza y cuello, ovario, vejiga, pulmón o cerebro. Sin embargo, presenta graves efectos secundarios (**Figura 3**) tales como toxicidad del sistema nervioso, nefrotoxicidad y ototoxicidad, debido al tropismo selectivo del fármaco (Ekborn et al., 2003). La mayoría de estos efectos adversos pueden prevenirse y tratarse. Sin embargo la ototoxicidad inducida por CDDP implica la pérdida irreversible de la audición, tinnitus y mareos debido al daño coclear, siendo una de las principales razones para interrumpir la quimioterapia.

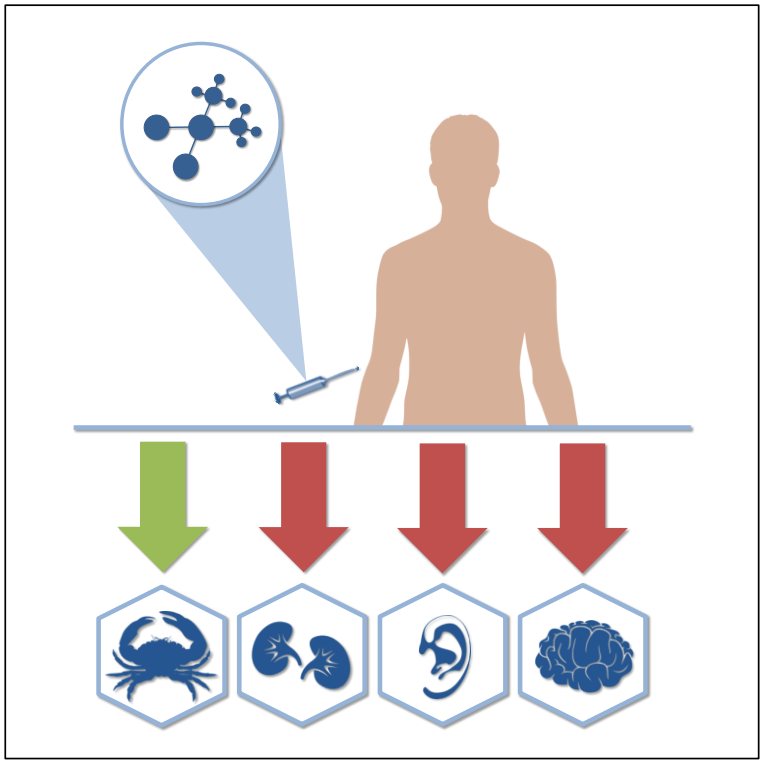

Figura 3. Tropismo selectivo del CDDP por el tejido tumoral (flecha verde), riñón, oído interno y sistema nervioso central (flechas rojas).

El CDDP induce la apoptosis de las células del oído interno mediante diferentes mecanismos (**Figura 4**): la unión del fármaco a bases de guanina en el ADN y la formación de uniones intra e intercatenarias, la generación de especies reactivas de oxígeno (ROS) con aumento de la peroxidación de lípidos y afluencia de Ca^{2+} y, por último, eventos proinflamatorios (Casares et al., 2012). La fuerte variabilidad en la susceptibilidad a los efectos ototóxicos derivados del CDDP está ampliamente estudiada. La pérdida auditiva aparece cuando las dosis usadas son mayores de 100

mg/m^2 afectando en primer lugar a las frecuencias altas y progresando a las de rango medio. Los pacientes que reciben dosis ultra-altas de CDDP (16mg/kg), presentan pérdida de audición en frecuencias ultra altas y altas en el 100% de los casos (Rybak et al., 2009). Sin embargo, pacientes con cáncer testicular tratados con dosis acumulativas bajas de CDDP demostraron presentar una probabilidad casi del 50% de reversibilidad completa de los síntomas (Bokemeyer et al., 1998).

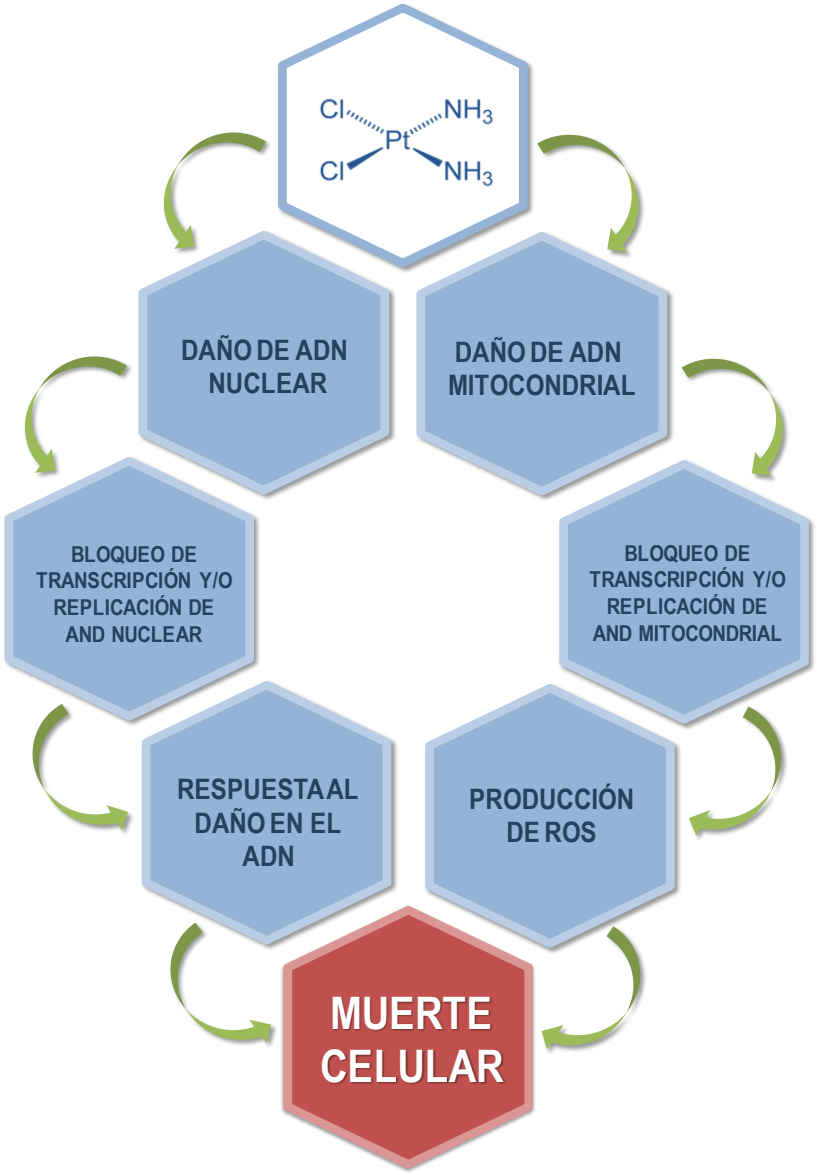

Figura 4: Mecanismo de acción del CDDP (modificado de Marullo et al.2013)

OTOPROTECCIÓN

La otoprotección se puede definir como el conjunto de estrategias de intervención química o física que intentan prevenir y/o tratar el daño auditivo producido por diversas agresiones al oído interno. En el sentido que nos atañe, este término se refiere al empleo de sustancias químicas (fármacos, moléculas antioxidantes o antiinflamatorias, proteínas, material genético etc.) involucradas en la interrupción de rutas o eventos intracelulares provocados por el CDDP que conducen a la apoptosis de las células sensoriales auditivas.

Vías de administración

Existen distintas vías de administración de sustancias con potencial otoprotector para alcanzar la diana terapéutica en el oído interno. Pueden dividirse en vías de administración sistémica, y vías de administración local.

Administración sistémica

Las vías de administración sistémica son aquellas que permiten llegar a la molécula con potencial ototoprotector al oído interno a través del torrente sanguíneo. Existen dos subdivisiones dentro de las estrategias de administración sistémica de moléculas con potencial otoprotector:

- *Vías de administración enteral*. Es el método más común de administración de fármacos. También el más seguro, cómodo y económico. La vías de administración enteral más habitual para utilizar en el dolor es la vía oral .Se pueden utilizar diferentes formas farmacéuticas para disimular el sabor o para facilitar la dosificación .Los fármacos que se administran a través de estas vías se absorben gastrointestinalmente y no evitan el primer paso hepático.
- *Vías de administración parenteral*. Son aquellas que introducen el fármaco en el organismo gracias a la ruptura de la barrera mediante un mecanismo que habitualmente es una aguja hueca en su interior. Dentro de las vías de administración parenteral se incluyen la vía intravenosa, la vía intramuscular, administración transdérmica y subcutánea.

Administración local

La administración local se basa en la administración directa del tratamiento en la zona a tratar. Permite una protección selectiva del oído interno, ejerciendo el efecto del agente protector a nivel local. Además, permite alcanzar concentraciones en el oído interno mucho más altas empleando dosis menores de fármaco que las estrategias de administración sistémica. Sin embargo, la administración local de fármacos supone una serie de procedimientos mucho más invasivos para el paciente, y la concentración del fármaco que accede a la cóclea tras su aplicación es poco estandarizable debida a la absorción de parte del inóculo por parte de los tejidos circundantes, y la pérdida a través de la trompa de Eustaquio, pasando al torrente sanguíneo. Actualmente se aplican varias estrategias de administración local en el oído:

- *Administración transtimpánica*. Ésta vía de administración consiste en la inoculación del fármaco mediante la perforación de la membrana timpánica con una aguja de pequeño tamaño, quedando el fármaco alojado en la cavidad del oído medio, para su posterior difusión a través de la membrana de la ventana redonda (RWM, del inglés round window membrane) al oído interno.
- *Administración mediante bullostomía*. Ésta estrategia, utilizada ampliamente en modelos animales, consiste en realizar una pequeña hendidura en la bulla timpánica (prolongación del hueso temporal) a través de la cual se inocula el fármaco al oído medio para su posterior difusión a través de la RWM al oído interno (Pinilla et al., 2001).
- *Administración mediante cocleostomía*. La cocleostomía es probablemente la intervención más invasiva para la administración de fármacos al oído interno, basándose en la realización de un pequeño orificio en la cápsula ótica coclear a través del cual se inocula el fármaco directamente al interior de la cóclea.

TRATAMIENTO DE LA OTOTOXICIDAD DERIVADA DEL CDDP

Terapias tradicionales

La ototoxicidad inducida por CDDP ha sido tratada tradicionalmente mediante corticoesteroides, antioxidantes o inhibidores de caspasas. Sin embargo, éste tipo de terapias no son lo suficientemente eficientes debido a la dificultad para llegar al oído

interno. Para conseguir concentraciones adecuadas de fármaco en esta parte del oído se siguen dos vías fundamentales de administración: administración sistémica, a través de la arteria laberíntica que suministra la cóclea y el vestíbulo, y la administración local, en el oído medio, con objeto de que el fármaco pase a través de la membrana de la ventana redonda (RWM), la barrera anatómica entre el oído medio y el oído interno. Todas estas estructuras suponen un reto anatómico para la administración de fármacos al oído interno.

Administración sistémica

Las afecciones del oído interno han sido tratadas tradicionalmente mediante la administración sistémica de fármacos, pero la llegada de fármaco al oído interno es muy variable debido a la barrera sangre-cóclea. Las terapias sistémicas se basan por lo general en el uso de corticoesteroides, antioxidantes o inhibidores de caspasas, pero existe un alto riesgo de efectos secundarios asociados e interacción sistémica entre el agente otoprotector y el CDDP, reduciendo la eficacia de la quimioterapia.

Con el fin de evitar eventos proinflamatorios en la cóclea asociados al tratamiento con CDDP el uso de corticosteroides tales como hidrocortisona, 6α-metilprednisolona (MP), y dexametasona (Dx) está ampliamente extendido. Sin embargo, éste tipo de fármacos muestran pobres ratios de acumulación en el oído interno cuando son administrados sistémicamente, y se hacen necesarias altas dosis para conseguir concentraciones terapéuticas (Parnes et al., 1999), lo que está asociado a graves efectos secundarios incluyendo hiperglucemia, úlceras, hipertensión y osteoporosis. Por otra parte, los corticoesteroides son capaces de reducir la apoptosis en las células tumorales, lo que supone una disminución de la eficacia de las propiedades antitumorales del CDDP (Waissbluth et al., 2013).

La administración de antioxidantes, capaces de inhibir la producción de ROS inducida por CDDP, puede evitar la apoptosis de las células de la cóclea y proteger así de la pérdida de audición derivada del tratamiento antitumoral. Recientes estudios están basados en el uso de moléculas con propiedades antioxidantes, tales como ginkolide b (Ma et al., 2015), un componente importante de los extractos de *Ginkgo biloba*, que muestran una disminución significativa en la pérdida de audición inducida por CDDP debido a una disminución en la generación de ROS resultando en la reducción del efecto ototóxico del CDDP en ratas Sprague-Dawley mediante la subregulación de hemo-

oxigenasa-1. La hesperidina, un flavonoide con propiedades antioxidantes, fue testado por Kara *et al*. (Kara et al., 2016) en rata Wistar llegando a la conclusión de que puede prevenir la ototoxicidad al provocar un aumento de enzimas antioxidantes y la reducción de ROS. Yumusakhuylu *et al*. administraron sistémicamente resveratrol (Yumusakhuylu et al., 2012) con efectos prometedores 72h después de administrar una dosis concomitantemente de 10 mg/kg de CDDP en un modelo animal de cobaya.

Administración local

La administración intratimpánica presenta grandes mejoras con respecto a la administración sistémica para evitar la interacción en tejidos no deseados entre el fármaco con potencial otoprotector y el CDDP, ya que ofrece la posibilidad de concentrar el fármaco en el oído interno minimizando los efectos secundarios asociados.

El principal reto de éste tipo de administración es lograr la concentración suficiente de fármaco en la cóclea pasando a través de la RWM. La permeabilidad del fármaco a través de esta membrana semipermeable de tres capas depende del tamaño, la concentración, la solubilidad, la estructura y la carga del fármaco, así como de factores físicos de la propia RWM, tales como el estado y forma de la misma (Bowe and Jacob, 2010).

Existen multitud de estudios recientes que eligen esta forma de administración para aminorar la pérdida de audición inducida por CDDP. En un reciente estudio Özel *et al*. (Özel et al., 2016) compararon el efecto de la administración intratimpánica de MP y Dx en ratas de mediana edad, tratadas con dosis de 8 mg/kg de CDDP, concluyendo que la Dx presenta un efecto más beneficioso en la ototoxicidad provocada por CDDP.

El uso de oxitocina, hormona secretada durante el embarazo con propiedades antioxidantes y antiinflamatorias, fue evaluada por Bilmez *et al*. (Bilmez et al., 2016) mostrando otoprotección frente al tratamiento con CDDP, especialmente mediante administración intratimpánica. Los autores hicieron hincapié en la importancia de esta forma de administración para evitar el efecto negativo en el potencial quimioterápico derivado de la interacción sistémica con el CDDP.

NANOTECNOLOGÍA COMO ALTERNATIVA PARA LA DISPENSACIÓN DE FÁRMACOS EN EL OÍDO INTERNO

En su hoja de datos, la FDA (U.S. Food and Drug Administration) habla de la nanotecnología como una tecnología emergente que tiene el potencial para ser utilizada en una amplia gama de productos ya regulados por la FDA, incluyendo productos médicos, alimenticios y cosméticos (U. S Food and Drug Administration, Fact Sheet: Nanotechnology, April 2012). Los nanomateriales se miden en nanómetros (nm; equivalente a una mil millonésima parte de un metro) y sus propiedades físicas, químicas y biológicas pueden variar con respecto a su contraparte macrométrica con la misma composición química. Aún cuando en general el término "nano" se utiliza para hacer referencia a partículas con tamaños entre 1 y 100 nm; no podemos aferrarnos a esta definición estrictamente ya que las partículas submicrónicas (de 10 a 1000 nm) también muestran propiedades especiales con respecto a los materiales orginales y son denominadas comúnmente como nanopartículas (NPs) en el campo de la farmacia y la medicina.

La aplicación de la nanotecnología con el fin de alcanzar los objetivos de la medicina se define como "nanomedicina" (Moghimi et al., 2005). Es un área ampliamente explorada de la investigación, y también se ha convertido en un importante área de desarrollo en clínica en los últimos años desde la notable producción de sistemas de administración de fármacos de tamaño nanométrico. Desde 1990, las entidades reguladoras han aprobado varios productos para uso clínico y, entre ellos, es fácil de identificar diferentes sistemas nanométricos que la nanociencia ha ido introduciendo en la clínica (Duncan, 2005).

La aplicación de la nanotecnología en el campo de la medicina ha emergido como un área de gran interés para la mejora del tratamiento de distintas enfermedades en la última década, incluida la administración de fármacos en el oído interno (Pritz et al., 2013b). La liberación controlada de fármacos es una de las aplicaciones más relevantes y con mayor proyección de la nanomedicina. La mayoría de los sistemas convencionales de administración de fármacos presentan enormes limitaciones asociadas fundamentalmente a la solubilidad y toxicidad de los principios activos (Williams et al., 2013).

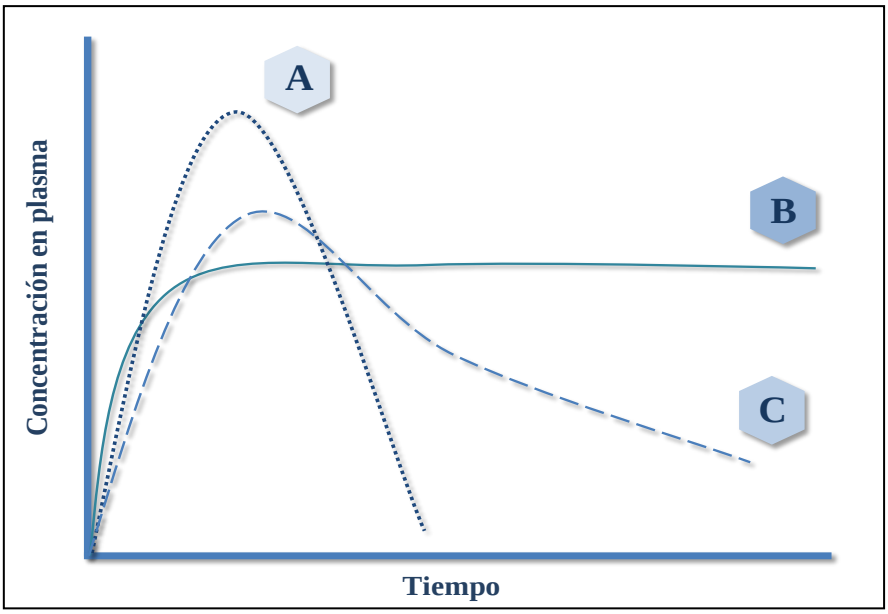

Figura 5: Modelos de cinética de liberación de fármacos. (A) Liberación de fármacos convencional; (B) Liberación sostenida con cinética de orden cero; (C) Liberación sostenida.

La administración convencional provoca que la concentración del principio activo alcance un valor máximo para después caer a un valor mínimo, haciendo necesaria la aplicación de nuevas dosis para mantenerse en un intervalo terapéutico adecuado. Los sistemas de liberación controlada de fármacos, por el contrario, permiten mantener la concentración de fármaco dentro del intervalo terapéutico de manera sostenida durante un tiempo prolongado con una única dosis, además de permitir dirigir el tratamiento a una diana terapéutica concreta (**Figura 5**). Así pues, el uso de vehículos nanométricos surge como una vía de administración con grandes ventajas para la dosificación continua y sostenida de fármacos en el órgano o tejido donde debe realizar su función (Bamrungsap et al., 2012, Uchegbu and Siew, 2013).

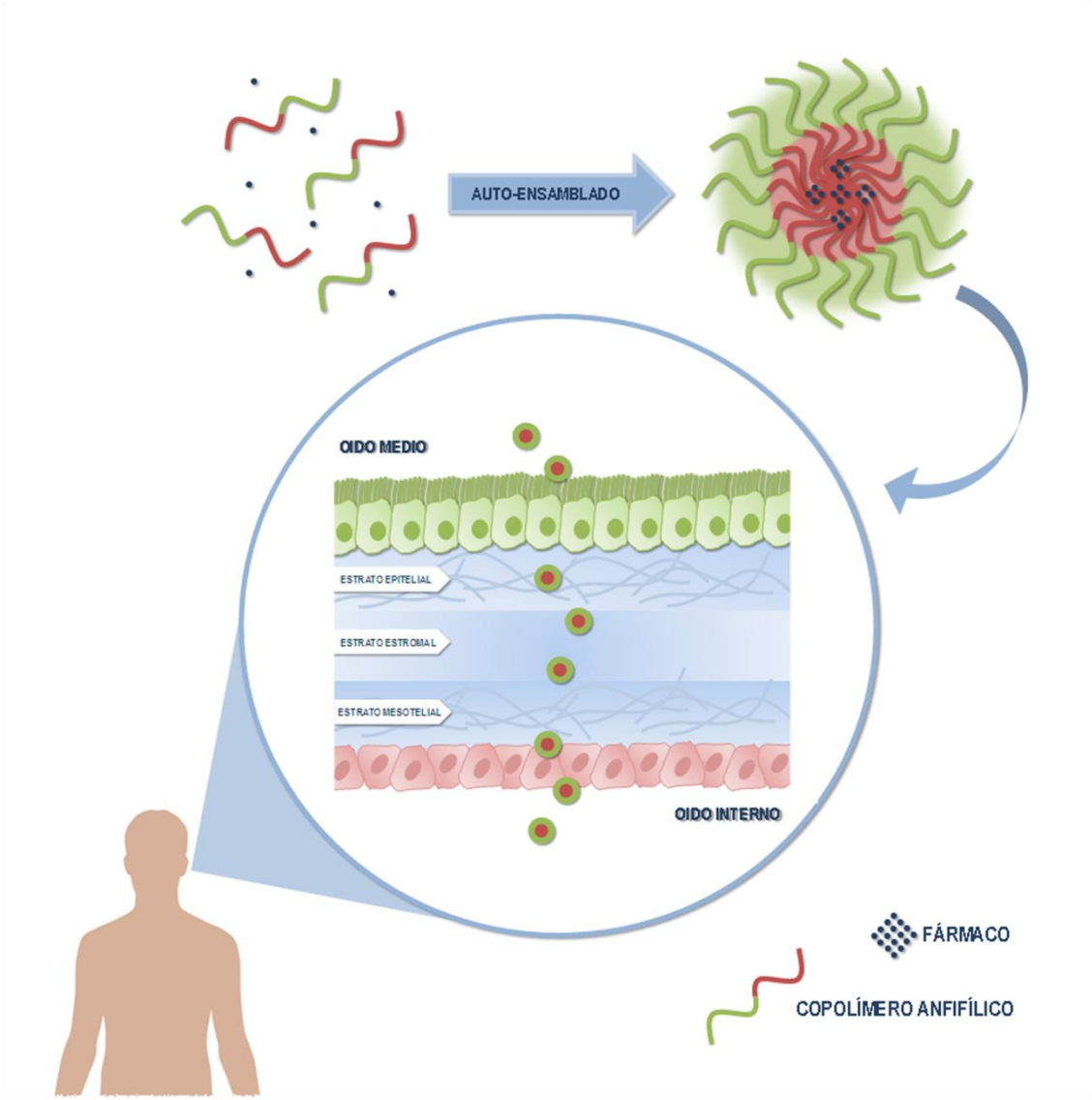

Figura 6: Paso por difusión de NPs poliméricas anfifilicas a través de la RWM.

El uso de la nanotecnología y, concretamente, el uso de NPs para liberación controlada de moléculas potencialmente activas, podría contribuir a paliar las limitaciones actuales de los tratamientos tradicionales tales como, baja solubilidad y estabilidad del fármaco, tamaño molecular, efectos secundarios asociados. El tamaño de las NPs es un factor limitante para pasar a través de la RWM al oído interno debido a que éstas necesitan penetrar a través de la RWM, formada por dos capas de células epiteliales y una capa de tejido conectivo central (**Figura 6**). Los estudios realizados hasta la fecha demuestran que el uso de NPs con tamaños de 200 nm o menos en la administración de fármacos al oído interno presentan buenos resultados (Hornyak, 2005).

Tabla 1: Nanovehículos testados en ensayos experimentales para la administración de fármacos en el oído interno.

TIPO DE NPs	MOLÉCULA ENCAPSULADA	TAMAÑO (nm)	*in vitro*	*in vivo*	REFERENCIA
Ag NP	---	---	BALB/c 3T3	Rata	(Zou et al., 2014)
Ag NP	---	21 ± 8	---	Rata	(Zou et al., 2015)
NP de silica	---	50 a 100	HEI-OC1	---	(Pritz et al., 2013a)
NP lipídica	---	50	L929 y cultivo primario coclear	Rata	(Zhang et al., 2011b)
NP lipídica	edaravona	93	---	Cobaya	(Gao et al., 2015)
Liposoma	GD-Dota	95; 130 y 240	---	Rata	(Zou et al., 2012)
Liposoma	Pro-fármaco de dexametasona	≥140	---	Cobaya	(El Kechai et al., 2016)
Dendrímero de PLL	Genes no virales		Explante y cultivo primario	Rata	(Zhang et al., 2011a)
PLGA	C-6 y distintos fármacos	135	---	Cobaya	(Cai et al., 2014)
PHEA	Rojo Nilo	27.4±16.2	---	Ratones C57/BL6	(Kim et al., 2015)
PCL-*b*-PEG	A665-A666	---	Explante coclear	---	(Surovtseva et al., 2012)
PHEA	Transgen	35 a 103	HEI-OC1y HMEECs	Ratones C57/BL6	(Yoon et al., 2015)

En el último lustro, han sido desarrollados múltiples nanovehículos para la administración de fármacos en el oído interno (**Tabla 1**) y probados tanto en modelos *in vitro* como *in vivo*.

FÁRMACOS NANOVECTORIZADOS PARA EL TRATAMIENTO DE LA OTOTOXICIDAD PROVOCADA POR CDDP

El uso de tratamientos basados en NPs podría ofrecer una nueva solución contra la ototoxicidad inducida por CDDP respondiendo a algunos de los factores limitantes de la administración sistémica o local de medicamentos libres.

Glueckert *et al*. (Glueckert et al., 2015) testaron recientemente varios tipos de NPs como NPs lipídicas, quantum dots, y NPs de silica como vehículos de fármacos *in vitro*

en HEI-OC1 con una modificación de la superficie dirigida a los receptores TrkB. Los autores también probaron a encapsular rolipram (inhibidor selectivo de la fosfodiesterasa-4) en las NPs lipídicas para evitar la apoptosis inducida por CDDP. En explantes de cóclea de ratón, las neuronas del ganglio espiral y las células del ligamento espiral de los animales tratados con CDDP y NPs cargadas con rolipram exhibían una expresión menor de caspasa-3 que los controles tratados exclusivamente con CDDP. Los autores concluyeron que estos sistemas nanométricos pueden actuar como un sistema de administración de fármaco óptimo, necesitando dosis bajas para alcanzar la liberación sostenida adecuada en el oído interno.

Sun et al. (Sun et al., 2015, Sun et al., 2016) realizaron ensayos para determinar las propiedades de liberación controlada y efecto otoprotector de NPs basadas en polietilenglicol y ácido poliláctico (PEG-PLA) cargadas con Dx administradas intratimpánicamente (10 mg / ml de NP) y mediante administración sistémica intraperitoneal (10 mg / kg) en animales tratados con 12 mg/kg de CDDP. Los autores prepararon las NPs mediante la técnica de emulsión y evaporación y obtuvieron NPs con un diámetro hidrodinámico de 130 nm, y un potencial zeta de -26 mV. La liberación sostenida de Dx durante más de 24 días se logró en solución salina tamponada con fosfato (pH 7,4), durante 5 días en perilinfa artificial (pH 7,4), y 1 día en plasma de rata. Así mismo, NPs cargadas con cumarina-6 se utilizaron para detectar la acumulación de NPs mediante microscopía confocal, siendo detectadas en el ganglio espiral, estría vascular y el órgano de Corti, 1 hora después de la administración intratimpánica. Los autores también informaron de una mejora de la biodisponibilidad de dexametasona en el oído interno en los animales tratados con NPs con respecto a los tratados con el fármaco libre. La respuesta auditiva del tronco cerebral (ABR) se midió a cuatro frecuencias (4, 8, 16, y 24 kHz) 1 día antes y tres días después del tratamiento con CDDP, mostrando protección de las células cocleares y preservando la audición de manera parcial, a 4 kHz y 8 kHz, tras el tratamiento con CDDP en cobayas tratadas con las NPs (Sun et al., 2015). El mismo sistema también fue probado por los autores por vía intraperitoneal 1 hora después de la administración de CDDP. Los autores informaron que las NPs eran capaces de conservar significativamente las propiedades funcionales y estructurales de la cóclea, mostrando potencial como tratamiento terapéutico para mejorar la administración de corticosteroides al oído interno para paliar la pérdida de audición inducida por CDDP (Sun et al., 2016).

Las NPs poliméricas pueden mejorar problemas asociados a la administración de fármacos, tales como la solubilidad de los mismos, problemas de estabilidad en medio biológico y especificidad del tratamiento, pero es importante recordar siempre que la eficiencia de encapsulación de fármacos y el perfil de liberación de nano-vehículos poliméricos dependerán de la pareja de polímero-fármaco con la que vamos a trabajar acorde a las necesidades del tratamiento (Torchilin, 2006). Por esta razón, con el fin de sintetizar NPs poliméricas cargadas con el fármaco deseado, se requiere un estudio anterior de cada componente de la formulación (Rao and Geckeler, 2011). La elección de un polímero particular se basará principalmente en el objetivo terapéutico y, ya que hay gran variedad de polímeros utilizados hoy en día en el campo de la biomedicina, las posibilidades aumentan cada día.

En este sentido, el uso de copolímeros anfifílicos bioactivos abre la posibilidad de ejercer un efecto dual entre la actividad propia de las NPs, basadas en el copolímero, y la molécula encapsulada que puedan ejercer un efecto terapéutico sobre la ototoxicidad provocada por el tratamiento con CDDP. Los copolímeros basados en la Vitamina E (MVE) o el succinato de α-tocopherol (MTOS) sintetizados previamente en el grupo de Biomateriales del Instituto de Ciencia y Tecnología de Polímeros del CSIC, han mostrado ser capaces de formar, mediante el método de nanoprecipitación, NPs con actividad antitumoral, así como tener la capacidad de encapsular eficientemente fármacos hidrofóbicos (Palao-Suay et al., 2015, Palao-Suay et al., 2015). El potencial antioxidante de la Vitamina E y sus derivados, así como éstos antecedentes de bioactividad de las NPs basadas en ambos copolímeros, es un indicio de la potencialidad de estos nanovehículos para el tratamiento de la ototoxicidad inducida por el CDDP, y la encapsulación de fármacos ya utilizados en clínica con este fin.

RECEPTORES DE CANABINOIDES COMO NUEVA DIANA TERAPÉUTICA EN EL OÍDO INTERNO

Con el fin de definir nuevas dianas terapéuticas en el oído interno para conseguir tratamientos más específicos y dirigidos a tipos celulares concretos, el estudio de la expresión de el receptor de canabinoides 2 (CB_2) en el órgano de la audición es de gran interés. Los receptores de canabinoides modulan un gran número de funciones cerebrales y corporales normales y se ha descrito su posible implicación como blancos terapéuticos en una amplia variedad de enfermedades tales como el cáncer (Pérez-Gómez et al., 2015) o trastornos neurodegenerativos (Fernández-Ruiz et al., 2015).

Sistema endocanabinoide

Los canabinoides son sustancias psicoactivas presentes en la resina de la planta *Cannabis sativa.* Dada su elevada liposolubilidad se asoció inicialmente su actividad a una posible interacción inespecífica con lípidos de membrana, pero estudios posteriores, demostraron que el mecanismo responsable de dichos efectos estaba mediado por receptores específicos de membrana. Éstos estudios iniciales vinieron a definir el denominado sistema endocanabinoide, un sistema de comunicación celular que se compone de dos receptores, CB_1 y CB_2, sus ligandos endógenos (anandamida y 2-AG), y las enzimas que producen y metabolizan dichos ligandos (Pertwee et al., 2010). Los canabinoides ejercen un amplio espectro de efectos terapéuticos a través de los receptores CB_1 y CB_2 (Mukherjee et al., 2004). De igual modo, existe la sospecha de que existan otros receptores de canabinoides debido a las acciones de compuestos que producen efectos similares a canabinoides sin activar CB_1 o CB_2 (McHugh et al., 2008). El receptor CB_1 se expresa principalmente en el cerebro (Devane et al., 1988), pulmón (Shire et al., 1995), el hígado (Mallat et al., 2011) y los riñones (Deutsch et al., 1997) mientras que el receptor CB_2 se expresa en las células T del sistema inmune, en macrófagos y en células B, en células hematopoyéticas, en los queratinocitos, los terminales de los nervios periféricos, y en la microglía cerebral, y se cree que desempeñan un papel en las respuestas inflamatorias e inmunes (Berdyshev, 2000).

Desde el punto de vista molecular, los receptores de canabinoides presentan los dominios estructurales característicos de los receptores acoplados a proteína G, siendo éstos un dominio amino-terminal extracelular, dominio carboxi-terminal intracelular y siete dominios transmembrana (**Figura 7**). La transducción de señales a través de los

receptores de canabinoides ocurre fundamentalmente mediante interacción con proteínas G. La activación del receptor CB_2 media la inactivación de la adenilato ciclasa y la activación de la vía de MAP quinasas, pero no modifica las corrientes de Ca^{2+} y K^+ como lo hace el receptor CB_1, lo que implica que el receptor CB_2 no tenga los efectos psicoactivos asociados a CB_1 (Pertwee, 1997).

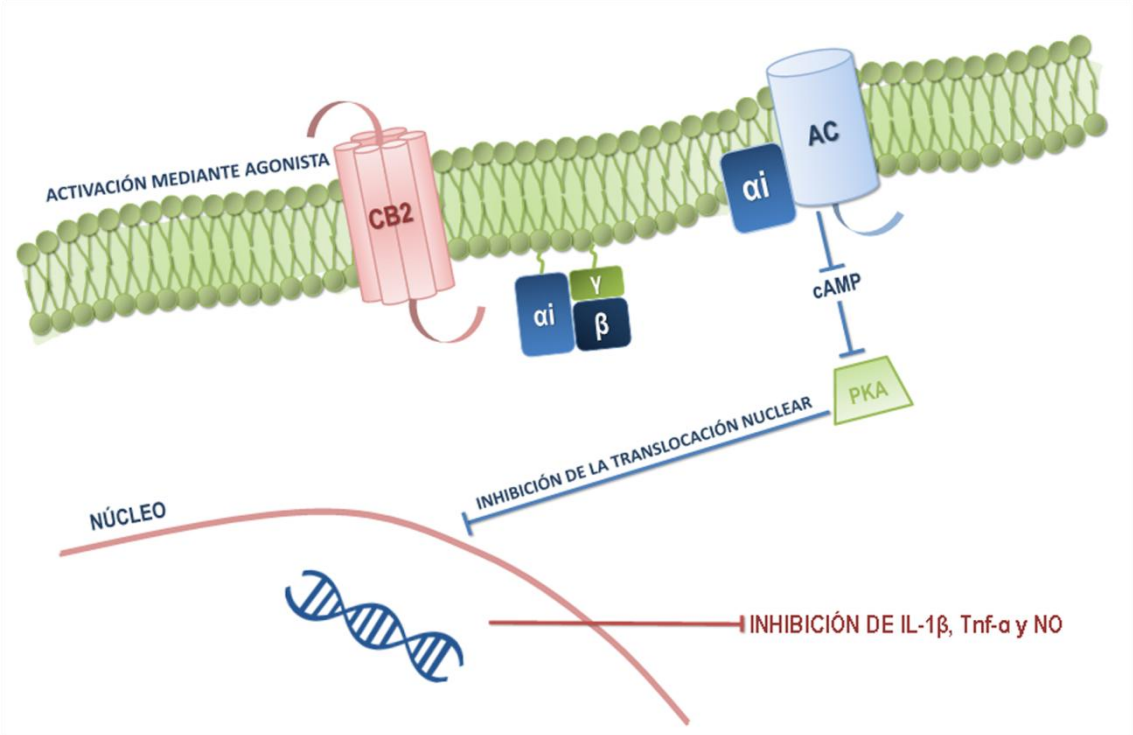

Figura 7: Estructura y mecanismo de acción de los receptores de CB_2 activados mediante agonistas con resultado de la inhibición de la síntesis de citoquinas pro-inflamatorias (CB2: receptor de canabinoides 2; AC: adenilato ciclasa; PKA: protein quinasa A).

Inflamación y CB_2

La inflamación juega un papel importante en la apoptosis inducida por CDDP de las células cocleares, y es el principal mecanismo involucrado en la pérdida de audición inmunomediada (García-Berrocal et al., 2006), y es por ello que la implicación del sistema endocanabioide en la modulación de la respuesta en diversos tejidos, ampliamente reportada, es de gran interés. De igual modo, numerosos estudios demuestran que los ratones que carecen del receptor CB_2 presentan un exacerbado fenotipo inflamatorio (Karsak et al., 2007, Duerr et al., 2015, Amenta et al., 2014). Este hecho sugiere que las estrategias terapéuticas destinadas a la modulación de la

señalización de CB_2 podrían ser prometedoras para el tratamiento de diversas condiciones inflamatorias.

En éste sentido, el uso de agonistas de CB_2, ha demostrado ser eficaz atenuando efectos derivados de la inflamación en diferentes patologías. La proliferación y la migración provocada por estímulos inflamatorios de células de músculo liso vascular participan en el desarrollo y progresión de la aterosclerosis y la restenosis, y el uso de agonistas de CB_2, como JWH-133 y HU-308, demostró atenuar dichos efectos en un modelo *in vitro* de estimulación mediante TNF-α (Rajesh et al., 2008). El uso de JWH-133 ha demostrado tener efectos beneficiosos en el tratamiento de otros procesos inflamatorios tales como el edema pulmonar inducido por herbicidas, mostrando que después pre tratar a los animales con el agonista de CB_2, tanto el edema como los cambios histopatológicos producidos por la exposición al herbicida fueron significativamente atenuados reduciendo la producción de TNF-α y la secreción de IL-1β (Liu et al., 2014).

De igual manera, se ha observado el efecto modulador de inflamación mediado por CB_2 mediante el uso de canabinoides naturales como el tetrahidrocanabinol (THC), canabionoide primario presente en la planta de marihuana, que produce un aumento en la expresión proteíca de CB_2 e inhibe la regulación al alza de NF-kB y de la cofilina-1 en células MG-63 (cultivo celular de osteosarcoma) en un modelo de inducción de la inflamaciónmediante LPS. Sin embargo, la administración de antagonistas de CB_2 como AM630 o el silenciamento de CB_2 mediante siRNA revierten parcialmente los efectos anti-inflamatorios inducidos por THC, mientras que antagonistas de CB_1 como AM251 no revertían dicho efecto, lo cual confirmaba el papel preponderante de CB_2 en la modulación de la respuesta inflamatoria (Yang et al., 2015).

El efecto regulador de CB_2 y el sistema endocanabinoide en la inflamación inducida por una lesión cerebral traumática fue estudiado por Amenta *et al.* mediante el uso de agonistas de CB_2 y animales knockout del receptor. Los resultados demuestran que el sistema canabinoide endógeno y el receptor CB_2 juegan un papel importante en la regulación de la inflamación y las respuestas neurovasculares en la lesión cerebral. La estimulación del receptor CB_2 mediante dos agonistas (0-1966 y JWH-133) así como la supresión, en el caso de los animales knockout, de CB_2 empeoró la inflamación (Amenta et al., 2014). Estudios recientes demuestran también el potencial de CB_2 en el tratamiento de fenómenos tales como la neuroinflamación derivada del estrés. Mediante

el agonista de CB_2 JWH-133, se evita el aumento de citoquinas pro inflamatorias (TNF-α y CCL2), de NF-kappa B, NOS-2 y COX-2, y el consecuente estrés oxidativo y nitrosativo (peroxidación lipídica). Así mismo, la falta de CB_2 exacerbó la neuroinflamación confirmando que los efectos de JWH-133 estaban mediados a través de receptores CB_2 (Zoppi et al., 2014).

Existe un consenso general acerca de la importancia del papel que el receptor de CB_2 juega de forma endógena contra los fenómenos inflamatorios propios de trastornos neurodegenerativos, así como sobre las posibilidades de un tratamiento farmacológico de esta función. Gómez-Gálvez *et al*. describieron el potencial como diana terapéutica del receptor CB_2 en el tratamiento de la enfermedad de Parkinson en un modelo murino tratado con LPS. Los autores observaron una reducción en la expresión génica de TNF-α e IL-1β (drásticamente elevados tras el tratamiento con LPS) tras la activación de los receptores CB_2 mediante el agonista selectivo HU-308 en el modelo animal, y proporcionaron la primera evidencia de la regulación al alza de los receptores CB_2 en elementos gliales en los tejidos postmortem de pacientes con Parkinson (Gómez-Gálvez et al., 2016).

Estrés oxidativo y CB_2

El estrés oxidativo es otro factor importante en el mecanismo de acción del CDDP, dado que el citoestático regula al alza la producción de ROS, fundamentalmente debida a su interacción con el DNA mitocondrial, alterando la función de las mismas, lo que desencadena fenómenos pro apoptóticos que conducen a la muerte celular (Marullo et al., 2013). El estrés oxidativo es por tanto otro factor a tener en cuenta a la hora de intentar paliar su toxicidad en zonas no deseadas.

Hay evidencias de que la activación de los receptores CB_2 mediante agonistas como HU-910 (Horváth et al., 2012) o el análogo sintético del Δ9-tetrahydrocannabivarin, Δ8-Tetrahidrocannabivarin (Δ8-THCV) (Bátkai et al., 2012), previenen del daño hepático por isquemia-reperfusión reduciendo notablemente el estrés oxidativo, así como los eventos inflamatorios y la muerte celular, en un modelo animal murino y en cultivo celular CHO tranfectadas con cDNA codificando receptores CB_2 humanos, respectivamente.

De igual manera, en un modelo animal de enfermedad de Parkinson mediante la inyección IP de rotenona, se observó una clara reducción en la peroxidación lipídica y aumento de la síntesis de enzimas antiinflamatorias con superóxido dismutasa (SOD) y catalasas, así como una disminución en la secreción de citokinas, tras la administración de β-cariofileno, un agonista natural de CB_2 (Javed et al., 2016).

Estos trabajos previos demuestran el potencial de CB_2 como modulador de algunos de los principales mecanismos responsables de la citotoxicidad del CDDP, indicando la importancia que podría tener en el tratamiento de la ototoxicidad.

Efectos de CB_2 en la nefrotoxicidad inducida por CDDP

El efecto de la activación de CB_2 mediante agonistas selectivos en la modulación de la inflamación, estrés oxidativo y apoptosis derivados del CDDP en modelos de nefrotoxicidad ha sido estudiado en los últimos años en modelos animales, con buenos resultados, lo que sugiere, en paralelo, también el potencial de la modulación de CB_2 en el tratamiento de la hipoacusia derivada del CDDP.

El uso del canabinoide no psicoactivo canabidiol (Pan et al., 2009), así como el tratamiento con agonistas selectivos como HU-308 (Mukhopadhyay et al., 2010) o LEI-101(Mukhopadhyay et al., 2016) administrados sistémicamente en modelos de ratón C57BL/6J, también demostró atenuar la respuesta inflamatoria, el estrés oxidativo/nitrosativo, y la muerte celular en el riñón y mejorar la función renal, demostrado en los estudios de Mukhopadhyay *et al* mediante el estudio de knockouts CB_2 , que desarrollaron una mayor inflamación y lesión tisular.

El uso del agonista no selectivo de CB_2, WIN-55,212-2, en modelo crónico de administración de CDDP en ratas Wistar (dosis de 1-2 mg/kg de CDDP), demostró también tener un efecto positivo sobre los efectos citotoxicos en el riñón, pero no impedir la anorexia o pérdida de peso relativa a la quimioterapia. Además, el tratamiento con WIN-55,212-2 demostró agravar la alteración de la motilidad gástrica inducida por CDDP (Abalo et al., 2013).

Estudios previos sobre CB_2 en el oído

Existe solo un estudio preliminar sobre la expresión de CB_2 en el oído interno *in vitro* en la línea HEI-OC1, en el cual los investigadores demostraron la capacidad de JWH-

015 (un agonista sintético de CB_2) para inhibir la apoptosis inducida por CDDP (Jeong et al., 2007). Mediante MTT, los autores detectaron una disminución de la citotoxicidad inducida por CDDP tras el uso de JWH-015, así como un descenso en la actividad de las caspasas 3, 8 y 9, notablemente aumentadas tras el tratamiento con CDDP. Además, el tratamiento con el agonista de CB_2 provocaba un descenso en la producción de ROS y Tnf-α. Los resultados obtenidos, en conjunto, mostraban el bloqueo en la apoptosis mediante el uso de JWH-015, lo que podría ser una estrategia útil para prevenir los efectos secundarios nocivos para la audición del CDDP en pacientes que tienen que someterse a quimioterapia.

Se ha relacionado además el receptor CB_2 con procesos inflamatorios en el oído externo (Mimura et al., 2012) y el oído medio (Oka et al., 2005) *in vivo*, pero no existen informes sobre la expresión del receptor o función de CB_2 en el oído interno, lo que podría tener implicaciones importantes como diana terapéutica en pacientes afectados por pérdida de audición inducida por CDDP y otras enfermedades inflamatorias del oído interno. En éste sentido, el estudio de la expresión de CB_2 en la cóclea, y su regulación tras eventos ototóxicos como el tratamiento con CDDP, podría ser de gran interés para el tratamiento paliativo de la hipoacusia neurosensorial provocada por el citostático.

1

2 *Hipótesis y Objetivos*

3

4

5

HIPÓTESIS

1. Es posible implementar los resultados de la prevención y el tratamiento de la ototoxicidad por cisplatino mediante la introducción de nuevos mecanismos de transporte de fármacos.
2. En el oído interno existen marcadores relacionados con la apoptosis de la célula ciliada susceptibles de responder ante terapéuticas locales.
3. Como en otros tejidos, sobre todo en los derivados ectodérmicos, en el oído interno pueden existir receptores de cannabinoides (CB_2) de acción antiinflamatoria, susceptibles de ser estimulados o inhibidos mediante tratamiento.

OBJETIVOS

1. Creación de sistemas nanoparticulados basados en fármacos poliméricos autoensamblables capaces de transportar de fármacos hasta el interior del órgano de Corti, obviando las resistencias físico-químicas a la difusión de medicamentos hasta el oído interno.
2. Valoración *in vitro* del efecto de los nanosistemas obtenidos, en una línea derivada del órgano de Corti (HEI-OC1).
3. Localización de los sistemas de nanopartículas en la cóclea de un modelo animal de experimentación, tras su aplicación en la bulla timpánica.
4. Estudio de la función auditiva de animales tratados con nanopartículas poliméricas encapsulando diferentes moléculas activas en una bulla timpánica, utilizando la contraria como control interno en cada sujeto.
5. Comparación del efecto otoprotector de sistemas nanoparticulados que encapsulen 6-metilprednisolona, dexametasona y del succinato de α-tocoferol.
6. Identificación y localización de expresión de CB_2 en el oído interno del animal de experimentación.
7. Estudio de las variaciones en la expresión de CB_2 tras la administración intraperitoneal de cisplatino.

1

2

3 *Publicaciones*

4

5

Otoprotective properties of 6a-methylprednisolone-loaded nanoparticles against cisplatin: in vitro and in vivo correlation

Nanomedicine, 2016

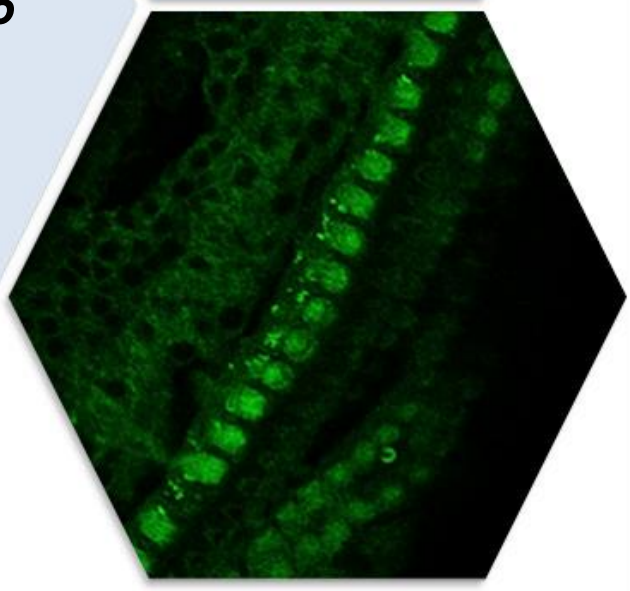

Resumen

En éste primer trabajo se puso a punto un modelo *in vitro* en línea celular HEI-OC1 y un modelo *in vivo* de administración de fármacos nanoencapsulados mediante bullostomía para tratar de paliar localmente la toxicidad del CDDP en las células del oído interno.

Se desarrollaron NPs, exentas de tensioactivos, para tratar de disminuir el efecto ototóxico derivado del tratamiento con CDDP. Las NPs estaban basadas en dos copolímeros anfifílicos de pseudo-bloque diferentes, obtenidos por polimerización radical libre. Éstos copolímeros se basan en N-vinilpirrolidona (segmento hidrofílico) y el derivado metacrílico de succinato de α-tocoferol (MTOS), o la vitamina E o α-tocoferol (MVE) (segmento hidrofóbico), por lo que se pretendía demostrar si éstas NPs podían tener actividad *per se*, sumada a la del fármaco que pudiera otorgar una mejora terapéutica. Así mismo, se quería comprobar si estos sistemas nanométricos, eran capaces de atravesar la membrana de la ventana redonda (RWM) y llegar de manera eficiente a las células de la cóclea en el oído interno. Para ello, se escogió la 6α-metilprednisolona como fármaco a encapsular, dado su amplio uso en clínica para revertir la sordera neurosensorial.

Ambos copolímeros presentaron la capacidad de formar NPs pseudo-esféricas mediante el método de nanoprecipitation en un medio acuoso. Así mismo, se consiguió vehiculizar de manera eficiente 6α-metilprednisolona en su núcleo interno.

Los nanovehículos obtenidos se testaron *in vitro* usando células HEI-OC1, e *in vivo* en un modelo murino en rata Wistar. Las NPs vacías demostraron tanto *in vitro* como *in vivo* no tener un efecto citotóxico salvo a altas concentraciones en la línea celular. Sin embargo, éstas NPs vacías, no fueron capaces de reducir significativamente la ototoxicidad provocada por el CDDP *in vivo*.

Se testaron, además, NPs basadas en ambos copolímeros cargadas con distintas cantidades de 6α-metilprednisolona, siendo varias de ellas capaces de reducir el efecto citotóxico *in vitro* del CDDP, siendo más activos los basados en el derivado metacrílico de la vitamina E (MVE), debido a su mayor eficacia de encapsulación. Esta formulación fue capaz de proteger a las células ciliadas en la base de la cóclea (frecuencias más altas donde afecta principalmente el CDDP), teniendo un efecto positivo en el frecuencias

auditivas más altas en el modelo murino. Se encontró una buena correlación entre los resultados obtenidos *in vitro* e *in vivo*.

Otoprotective properties of 6α-methylprednisolone-loaded nanoparticles against cisplatin: in vitro and in vivo correlation

Sergio Martín-Saldaña[1], Raquel Palao-Suay[2, 3], AlmudenaTrinidad[1], María Rosa Aguilar[2], Rafael Ramírez-Camacho[1,4], Julio San Román[2,3]*

[1] Department of Otorhinolaryngology, Puerta de Hierro University Hospital, C/ Manuel de Falla, 1, 28222 Majadahonda
[2]Group of Biomaterials, Department of Polymeric Nanomaterials and Biomaterials, Institute of Polymer Science and Technology, CSIC, C/ Juan de la Cierva, 3, 28006 Madrid, Spain
[3]Networking Biomedical Research Centre in Bioengineering, Biomaterials and Nanomedicine, CIBER-BBN, Spain
[4] Universidad Autónoma de Madrid, Cantoblanco Campus University, 28049 Madrid

Corresponding author (*): Dra. María Rosa Aguilar
Email: mraguilar@ictp.csic.es
Telephone: +34 91561 88 06 (ext.212)
Fax: +34 91 564 48 53

KEYWORDS: Cisplatin, otoprotection, Vitamin E, α-tocopheryl succinate, nanoparticles, HEI-OC1.

Funded institutions

This work was funded by the Spanish Ministry of Economy and Competitiveness (MAT2014-51918-C2-1-R), Spanish FIS Grant PI 11/00742, CIBER BBN-ECO Foundation project and the Autonoma University of Madrid Foundation. The authors declare that there are no conflicts of interest

ABSTRACT

6α-methylprednisolone-loaded surfactant-free nanoparticles have been developed to palliate cisplatin ototoxicity. Nanoparticles were based on two different amphiphilic pseudo-block copolymers obtained by free radical polymerization and based on *N*-vinyl pyrrolidone and a methacrylic derivative of α-tocopheryl succinate or α-tocopherol. Copolymers formed spherical nanoparticles by nanoprecipitation in aqueous media that were able to encapsulate 6α-methylprednisolone in their inner core. The obtained nanovehicles were tested *in vitro* using HEI-OC1 cells and *in vivo* in a murine model.

Unloaded nanoparticles were not able to significantly reduce the cisplatin ototoxicity. Loaded nanoparticles reduced cisplatin-ototoxicity *in vitro* being more active those based on the methacrylic derivative of vitamin E, due to their higher encapsulation efficiency. This formulation was able to protect hair cells in the base of the cochlea, having a positive effect in the highest frequencies tested in a murine model.

A good correlation between the *in vitro* and the *in vivo* experiments was found.

BACKGROUND

Cisplatin (CDDP) is a highly effective chemotherapeutic agent against a variety of solid tumors including head and neck, lungs, ovary, bladder and testicles, however, it presents severe side-effects. Marullo et al. (Marullo et al., 2013) described a double way of CDDP-induced cytotoxicity: CDDP binding to guanine bases on nuclear DNA and the formation of inter- and intra-strand chain crosslinking triggers cell apoptosis because of replication and transcription blockage; CDDP also has a direct effect on mitochondrial DNA resulting in the impairment of electron transport chain protein synthesis leading to ROS generation.

Increasing doses incorporated into protocols, with the aim of increasing cure rates, are related with serious adverse effects that affect kidney function, nervous system and hearing. CDDP induces apoptosis of inner ear cell by binding to DNA, reactive oxygen species (ROS) generation, increased lipid peroxidation and Ca^{2+} influx, and inflammation events (Casares et al., 2012). Hearing impairment begins in the high frequencies and progresses to midrange when the patient receives doses higher than 100 mg/m^2. Patients who receive ultrahigh doses of CDDP (150-225 mg/m^2), show hearing loss in the high and extended high frequencies in 100% of cases (Rybak et al., 2009). There is substantial variability in susceptibility to the ototoxic effects of CDDP. Rapid intravenous bolus injections, high cumulative doses, pre-existing hearing loss, renal insufficiency, anemia, hypoalbuminemia, and prior cranial irradiation are some of the factors that can play a role in CCDP toxicity. The incidence and severity of hearing loss after CDDP treatment varies considerably, and 40–80% of patients develop an elevated hearing threshold following CDDP treatment being a limiting factor in antineoplasic treatments (Kim et al., 2015a).

The molecular mechanism of CDDP ototoxicity has not been fully elucidated; however ROS accumulation plays a key role in it. González-García *et al*. found a significant increase in total superoxide dismutase (SOD) activity and caspase-3/7 and caspase-9 expression in whole cochlear extracts that relates to an antioxidant response against platinum accumulation on the seventh day after a single dose of 5 mg/kg CDDP (González-García et al., 2010). A depletation in endogenous antioxidants enzymes like SOD, catalase or glutathione peroxidase and glutathione reductase was observed in animals that have received ototoxic doses of CDDP (16 mg/kg), leading to ROS

accumulation and resulting in apoptosis (Rybak et al., 2007). CDDP inhibition of antioxidant enzymes after early antioxidant cell response, promotes ROS accumulation in the cochlea that brings on the entry of Ca^{2+} in the inner ear cells triggering apoptosis. Thus, activation and redistribution of bcl-2-like protein 4 (Bax) in the cytosol promotes the release of cytochrome c from damaged mitochondria. Caspases 3 and 9 are activated by cytochrome c causing DNA damage mediated by activation of DNAase with loss of outer hair cells (OHC) and spiral ganglia (Lee et al., 2004). Furthermore, some studies showed that CDDP induced apoptosis in inner hair cells (IHC) in a caspase independent way too (García-Berrocal et al., 2007, Li et al., 2006).

Utricle hair cells, with a common embryological origin with cochlea hair cells, minimizes oxidative stress by endogenous mechanisms and protective molecules such as glutathione, heat shock proteins (HSPs), heme oxigenase and adenosine A1 receptors that are proved to reduce CDDP-induced apoptosis *in vitro* (Cunningham and Brandon, 2006). HSP-70 is over expressed in CDDP treated animals over 14 days (Ramirez-Camacho et al., 2007), showing a correlation between its concentration and a decrease in caspase activity at the cochlea (García-Berrocal et al., 2010). Nevertheless, up-regulation of these protective molecules is not enough to settle CDDP-induced oxidative stress being necessary the systemic or local administration of protective drugs (Rybak et al., 2007) such as caspase inhibitors (caspase-3 inhibitor z-DEVD-fmk and caspase-9 inhibitor z-LEHD-fmk (Wang et al., 2004), cannabinoid receptor 2 JWH-15 (Jeong et al., 2007), antioxidants Bucillamine (Kim et al., 2015b), caffeic acid (Choi et al., 2014), metformin (Chang et al., 2014) *Ginkgo biloba* extract (Ma et al., 2015) or corticoids (dexamethasone (Waissbluth et al., 2013), 6α-methylprednisolone (Parnes et al., 1999).

The systemic administration of drugs is related to variable penetration into the inner ear due to the presence of a blood-cochlea barrier and undesired side effects. Hydrocortisone, 6α-methylprednisolone (MP), and dexamethasone showed poor delivery to inner ear, and the systemic administration of higher doses of corticoids would be necessary to achieve otoprotective therapeutic concentrations (Parnes et al., 1999). However, high concentrations of corticoids are accompanied by severe side-effects that need to be avoided, such as hyperglycemia, hypertension, hypokalemia, peptic ulcer disease, osteoporosis and immunosuppression (McCall et al., 2010, Waissbluth et al., 2013).

Intratympanic treatment presents several advantages if compared with systemic administration. It is possible to reach higher concentrations of drug in the inner ear, the target is locally treated minimizing the drug side effects, and CDDP antitumor activity is not affected. However, it is not patient friendly. The main challenge in intratympanic treatments is still to achieve sufficient concentration of drug in contact with the sensory auditory cells as any drug delivered through the middle ear has to cross the three-layered round window membrane (RWM), diffuse through the labyrinth fluids and finally enter the inner ear cells. RWM behaves like a semipermeable membrane and its permeability depends on the size, concentration, structure, solubility and charge of the crossing molecule, enable agents and RWM thickness (Bowe and Jacob, 2010).

In the last years, nanoparticles (NPs) have emerged as promising vehicles to transport drugs to specific tissues or even a particular cell or organelle. NPs with diameters between 100 nm and 1 µm have been used in drug delivery to the inner ear with good results (Hornyak, 2005).

Different NPs based on silica (unloaded NPs), polyethylene glycol (PEG) loaded with resveratrol or copolymers like poly-ε-caprolactone-PEG (PCL-PEG) loaded with furosemide were tested *in vitro* showing good internalization by auditory cells (Pritz et al., 2013a, Musazzi et al., 2014, Youm and Youan, 2013).

Different types of nanocarriers have been used *in vivo* to ameliorate sensorineural hearing loss. Lipid NPs showed a high capacity to incorporate hydrophobic or hydrophilic drugs, and improve stability of encapsulated drugs. Liposomes encapsulating gadolinium-tetra-azacyclo-dodecane-tetra-acetic acid (LPS+Gd-DOTA) showed an efficient diffusion through RWM (Zou et al., 2012), and Solid Lipid NPs (SLNs) edaravone-loaded had certain protective effects against noise‑induced hearing loss (Gao et al., 2015). NPs based on copolymers like polyethylene glycol (PEG) provided immunologic benefits and remained longer in plasma (Pritz et al., 2013b). Poly(D,L-lactide-*co*-glycolide acid) (PLGA) NPs were used for carrying single or multiple drugs through the RWM showing a significant improvement in drug distribution within the inner ear (Cai et al., 2014).

The aim of this work was the development of a new therapy against CDDP-induced ototoxicity based on MP-loaded self-assembled polymeric NPs. The NPs were designed not only to be MP nanocarriers, but also to be active as were based on methacrylic

derivatives of α-tocopherol (vitamin E), a very well-known free radical scavenger that protects the cochlea from CDDP damage and prevents hearing loss.

Our group has recently described the preparation, characterization and biological activity of surfactant-free NPs based on amphiphilic copolymeric drugs that self-assembled in aqueous media during nanoprecipitation giving rise to multimicellar nanoaggregates (Palao-Suay et al., 2015). The hydrophilic segment of the copolymers was mainly based on *N*-vinyl pyrrolidone (VP), that was selected because of its hydrophilicity, biocompatibility and capability to avoid the reticuloendothelial system (Knop et al., 2010). The hydrophobic segment was mainly formed by a methacrylic derivative of vitamin E (MVE) or a methacrylic derivative of α-tocopheryl succinate (MTOS). Surfactant-free polymeric micelles nanoaggregates with hydrodynamic diameters between 96 and 220 nm were formed by self-assembling in aqueous media due to the appropriate hydrophilic/hydrophobic balance of these amphiphilic polymers. The hydrophobic core allowed the encapsulation of poorly water-soluble molecules, such as coumarin-6 (C6) or additional α-TOS.

Our aim in this work was the encapsulation of hydrophobic MP in the inner core of these NPs to be administered intratympanically in order to reach higher concentrations of MP in the inner ear, improve MP stability, avoid the MP side effects, and prevent the systemic interaction with CDDP.

MATERIAL AND METHODS

CDDP (1 mg/ml) and MP were purchased from Accord Healthcare and Sigma-Aldrich, respectively.

Amphiphilic copolymers

A methacrylic derivative of α-TOS (MTOS) and a methacrylic derivative of Vitamin E (MVE), and the copolymers poly(VP-*co*-MTOS) (89:11) (from now on CO-MTOS) and poly(VP-*co*-MVE) (60:40) (from now on CO-MVE) were synthesized as recently described by our group (Palao-Suay et al., 2015).

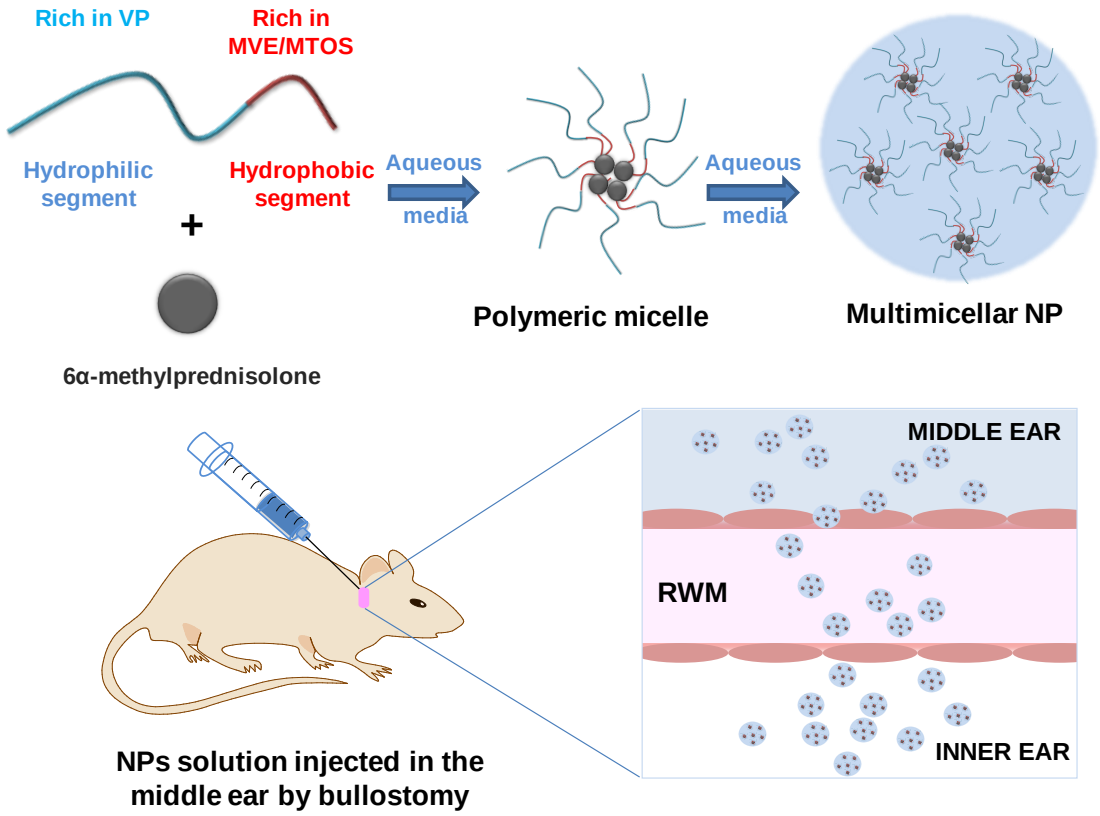

Figure 1: Formation of multimicellar NPs based on amphiphilic copolymer drugs and passive diffusion through round window membrane (RWM) from middle ear to inner ear after administration in the bulla.

Preparation of loaded nanoparticles

MP-loaded NPs were prepared by nanoprecipitation as previously published (Fessi et al., 1989). Briefly, CO-MVE and CO-MTOS were dissolved in dioxane (50 mg/ml) containing an appropriate amount of MP (NP-MVE-10 and NP-MTOS-10, with 10%

w/w of drug respect to the polymer, and NP-MVE-15 and NP-MTOS-15 with 15% w/w of drug respect to the polymer). The resulting solution was added drop-wise to PBS (10 ml) with constant mechanical stirring (650 rpm) (**Figure 1**).

C6-loaded NPs were also obtained by nanoprecipitation. C6 (1% w/w respect to the polymer) and the corresponding polymer (10 mg/mL) were dissolved in dioxane and added dropwise to PBS under magnetic stirring. The final NPs concentration was 2.0 mg/mL.

The obtained NPs were dialyzed during 72 h, sterilized by filtration through 0.22 µm polyethersulfone membranes (Millipore Express®, Millex GP), and stored at 4^{o}C until used.

Characterization of NPs

The particle size distribution of the NPs suspensions was determined by dynamic light scattering (DLS) using a Malvern Nanosizer NanoZS, at 25 °C. Zeta potential of the NPs was determined using laser Doppler electrophoresis (LDE). The measurements were obtained for 0.2 mg/ml NPs suspension containing 10 mM NaCl. The zeta potentials were automatically calculated from the electrophoretic mobility using the Smoluchowski´s approximation. The statistical average and standard deviation of data were calculated from 8 measurements of 20 runs each one.

SEM and TEM analysis were performed with a Hitachi SU8000 TED, cold-emission FE-SEM microscope working with an accelerating voltage between 15 and 50 kV. Samples were prepared by deposition of one drop of the corresponding NPs suspension (0.02 mg/ml) over a small glass disk (12 mm diameter) or poly(vinyl formal)-coated copper TEM grid, and evaporation at room temperature. SEM samples were coated with gold palladium alloy (80:20). An additional drop of Brilliant Black dye (Sigma-Aldrich, 1 mg/ml) was deposited on the grid and the excess was removed with filter paper and the grid was allowed to dry before TEM observation.

Encapsulation efficiency

MP-loaded NP-MVE and NP-MTOS were freeze dried and an amorphous powder was obtained with a yield higher than 90 % in all cases. The powder was dissolved in chloroform and the solvent was evaporated at room temperature for 24 hours. Ethanol (2

ml) was added to dissolve MP or C6, and stirred during 24 hours. Samples were centrifuged at 10.000 rpm and supernatant was analyzed by UV or fluorescence spectroscopy (λ_{abs}= 244 nm for MP, and λ_{exc}= 485 nm, λ_{emis}= 528 for C6). The encapsulation efficiency (EE%) was calculated as follows:

Encapsulation efficiency (EE%)= ([loaded molecule]$_i$/[loaded molecules]$_0$)×100

Being [loaded molecule]$_i$ the concentration of MP or C6 encapsulated and detected experimentally, and [loaded molecule]$_0$ the concentration of MP or C6 added in the nanoprecipitation process.

Esterase-mediated MP release

5 mL of MP-loaded NPs (NP-MVE-15 or NP-MTOS-15) with 15 u/mL of esterase from porcine liver (Sigma-Aldrich) were dialyzed against 10 mL of PBS at 37 °C using a 3.5-5 kDa MWCO membrane (Spectrum Laboratories). After certain periods, 1 mL of the dialyzing medium was withdrawn and the same volume (1 mL) of PBS was replenished. MP concentration was measured by HPLC (Shimadzu). The separation was performed on a C18-column (4.6 mm × 250 mm, Agela Technologies) at 30°C. The mobile phase was a mixture of acetonitrile, and distillated water (80:20, v/v) pumped at a rate of 1 mL/min. The UV detector was set at λ_{abs} =244 nm. The experiment was carried out in triplicate.

Cell culture experiments

The HEI-OC1 cell line was a kind gift from Dr. Federico Kalinec (House Ear Institute, Los Angeles, CA). HEI-OC1 cells were maintained under permissive conditions: high-glucose Dulbecco's modified Eagle's medium (DMEM, Sigma-Aldrich) supplemented with 10% fetal bovine serum (FBS, Gibco), 5% L-Glutamine (Sigma-Aldrich) and Penicillin-G (Sigma-Aldrich) at 33 °C and 10% CO_2 (Kalinec et al., 2003).

Toxicity of CDDP

To assess the impact of CDDP on cell viability, the cells ($3x10^4$ cells/ml) were exposed to 10, 20, 30, 40, 50 and 100 µM of CDDP in DMEM/PBS for 24 hours. DMEM without FBS was used to avoid uncontrolled cell growth.

Apoptosis

Apoptotic cell death was qualitatively evaluated by Hoechst 33258 nuclear staining. Cells were incubated with 2 µg/ml of the Hoechst 33258 (Sigma-Aldrich) for 20 min. After washing twice with PBS, cells were fixed with 4% paraformaldehyde for 10 min at room temperature. Cells were washed twice with distilled water and evaluated under a Nikon Eclipse TE 2000-S fluorescence microscope with a DS-U2 camera controller (Nikon).

NPs toxicity and protection assay

HEI-OC1 ($3x10^4$ cells/ml) were exposed to different concentrations of NPs solution (2.00, 1.00, 0.50, 0.25, 0.13, 0.06, 0.03, 0.02 and 0.01 mg/ml) in order to assess their impact on cell viability.

NPs were added to HEI-OC1 and 4 hours later 20 or 30 µM CDDP was added to the cultures in DMEM without FBS to avoid uncontrolled cell growth for 24 h, in order to study the protection effect of the NPs against CDDP.

AlamarBlue® (Invitrogen) was carried out to determine cell viability using a Multi-Detection Microplate Reader Synergy HT (BioTek Instruments; λ_{abs} = 570 nm).

***In vivo* experiments**

Thirty six healthy female Wistar rats weighting 180-280 g were used. All animals were housed in plastic cages with water and food available *ad libitum*, and maintained on a 12 h light/dark cycle. Rats with signs of present or past middle ear infection were discarded. Animals were randomly assigned to different groups (**Table 1**).

Table 1: Experimental groups (IP; intraperitoneal administration).

NPs name	N	Encapsulated MP (% w/w)	CDDP IP (10 mg/kg)
NP-MVE-0	2	-	-
NP-MTOS-0	2	-	-
NP-MVE-0	4	-	+
NP-MTOS-0	4	-	+
NP-MVE-10	4	10	+
NP-MTOS-10	4	10	+
NP-MVE-15	12	15	+
NP-MTOS-15	4	15	+

The animals were handled according to the guidelines of the Spanish law for Laboratory animals care registered in the "Real Decreto 53/2013" and the European Directive 2010/63/EU. The study was approved by the Clinical Research and Ethics Committee of the University Hospital Puerta de Hierro (dossier No. 013/2012).

Experimental procedure

Animals were anesthetized with intraperitoneal ketamine (100 mg/kg) and diazepam (0.1 mg/kg). An initial auditory steady-state responses (ASSR) test was performed on all animals. An insert earphone (Etymotic Research ER-2) was placed directly into the external auditory canal. Subcutaneous electrodes were placed over the vertex (active) and in the pinna of each ear (reference). Ground electrodes were placed in the right leg muscles. ASSR were recorded using an evoked potential averaging system (Intelligent Hearing System Smart-EP) in an electrically shielded, double-walled, sound-treated booth in response to 100 ms clicks or tone burst at 0.5, 1, 2, 4, 8, 12 and 16 kHz with 10 ms plateau and 1 ms rise/fall time. Intensity was expressed as decibels sound pressure level (dB SPL) peak equivalent. Intensity series were recorded, and an ASSR threshold was defined by the lowest intensity able to induce a replicable visual detectable response.

Following the ASSR measurements the right ear bulla was surgically approached and opened (Pinilla et al., 2001) and 50 µl of NPs solution were injected in the middle ear by bullostomy using a spinal needle (BD Whitecare 27G). Left ear was injected with PBS through the bullostomy as a control. After injection the anesthetized animals remained in lateral decubitus for 30 min to maximize the solution's contact time with the RWM and to prevent its leakage into the pharynx through the Eustachian tube.

After surgery, enrofloxacin and morphine (Braun 20 mg/ml) were administered subcutaneously for prevention of infection and postoperative analgesia, respectively.

CDDP-treated groups: after NPs administration in the right ear, an intraperitoneal slow infusion of CDDP (10 mg/kg) was carried out for 30 min. After CDDP infusion, animals were housed in individual cages with *ad libitum* access to water and food.

ASSR were tested after 3 days, and rats were euthanized by CO_2 suffocation.

In vivo distribution of coumarin-6-loaded NP

NP-MVE-C6 and NP-MTOS-C6 were administered *in vivo* as described in the previous section. However, these animals were euthanized after 2 h. Cochlea was extracted and fixed in paraformaldehyde over 24 h and decalcified in 1 % ethylenediaminetetraacetic acid (EDTA) at room temperature (with daily changes) for 10–12 days. Once the bone was completely decalcified, the cochlea was dissected in PBS, and cochlear surface extracts were visualized using an inverted microscope (Nikon Eclipse TE 2000-S) and a confocal laser fluorescence microscope (CLFM; Leica TCS-SP5 RS AOBS).

Statistical analysis

One-way ANOVA was used to analyze for statistical significance of all *in vitro* and *in vivo* results. Tukey test was used to identify significant differences between the paired treatments. $p<0.05$ was considered statistically significant.

RESULTS

NPs characterization

Unloaded and MP-loaded NPs were obtained by nanoprecipitation in PBS of the corresponding polymer solutions in dioxane and their principal characteristics are described in **Table 2**. EE% was higher for NP-MVE (48% for NP-MVE-10 and 53% for NP-MVE-15) than NP-MTOS (19% for NP-MTOS-10 and 26% for NP-MTOS-15).

Table 2: Hydrodynamic diameter (Dh), Polydispersity Index (PDI), zeta potential (ζ), and encapsulation efficiency (EE) of unloaded (NP-MVE-0 and NP-MTOS-0),MP-loaded (NP-MVE-10, NP-MVE-15 and NP-MTOS-10 and NP-MTOS-15),and C6-loaded NPs.

NPs	Load (w/w %)	EE (%)	D_h (nm)	PDI	ζ (mV)
NP-MVE-0	-	-	120.8 ± 9.6	0.139 ± 0.038	-3.12 ± 0.94
NP-MVE-10	10	48	124.8 ± 7.0	0.162 ± 0.021	-4.07 ± 0.32
NP-MVE-15	15	53	128.1 ± 7.4	0.134 ± 0.032	-3.25 ± 0.80
NP-MTOS-0	-	-	123.2 ± 7.0	0.302 ± 0.016	-5.11 ± 0.84
NP-MTOS-10	10	19	125.8 ± 9.7	0.313 ± 0.099	-3.74 ± 0.47
NP-MTOS-15	15	26	127 ± 13.55	0.318 ± 0.071	-4.73 ± 1.05
NP-MVE-C6	1	91	158.8 ± 44.77	0.239 ± 0.072	-3.78 ± 0.23
NP-MTOS-C6	1	85	159.9 ± 15.57	0.332 ± 0.024	-3.52 ± 0.29

All the synthesized NPs presented unimodal size distributions with apparent hydrodynamic diameters (by intensity, D_h) between 120 and 128 nm, with low PDI values. D_h slightly increased with the MP content in both families of NPs. All NPs presented slightly negative zeta potential.

SEM and TEM micrographs showed that both NP-MVE (**Figure 2A** and **2C**) and NP-MTOS (**Figure 2B** and **2D**) presented well-defined spherical morphology.

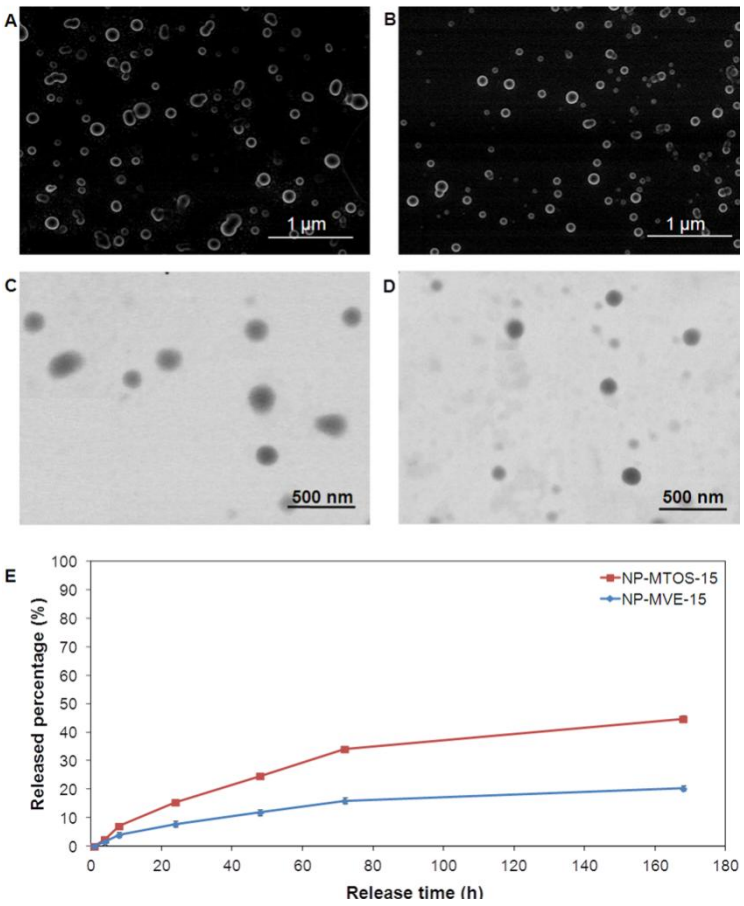

Figure 2: SEM (A and B) and TEM (C and D) micrographs of NP-MVE-15 (A, C) and NP-MTOS-15 (C, D) NPs. (E) *In vitro* release profile of MP loaded NPs in PBS at 37 °C.

Esterase-mediated *in vitro* MP release

In vitro release of MP was studied by an esterase-mediated dialysis diffusion method. Figure **2E** shows the *in vitro* MP release profile at 37 °C during one week. About 20% of the loaded MP is released from the NP-MVE-15 and more than 40% from NP-MVE-15 within seven days.

In vitro experiments

HEI-OC1 auditory cell line is very sensitive to ototoxic drugs and expresses specific markers of Organ of Corti (Kalinec et al., 2003). HEI-OC1 viability decreased with the concentration of CDDP in a dose dependent manner (**see supplementary data Figure S2A**).

Cytotoxicity of unloaded and loaded-NPs were also tested using HEI-OC1 and the results demonstrated that only the highest concentration (2.0 mg/ml) of both NP-MVE

and NP-MTOS was cytotoxic (viability <70%; ISO 10993−5:2009). Viability of cells treated with MVE formulations was reduced near to 40%, while MTOS formulations reduced viability near to 70%.

MVE formulations (**Figure 3A**) resulted to be more cytotoxic than MTOS formulations (**Figure 3B**) because MVE at 1.0 mg/ml also reduced cell viability more than 20% and in a corticoid loading dependent manner (HEI-OC1 viability NP-MVE-0 > NP-MVE-10 > NP-MVE-15 at 1.0 mg/ml). However, no statistically significant differences were found between the formulations.

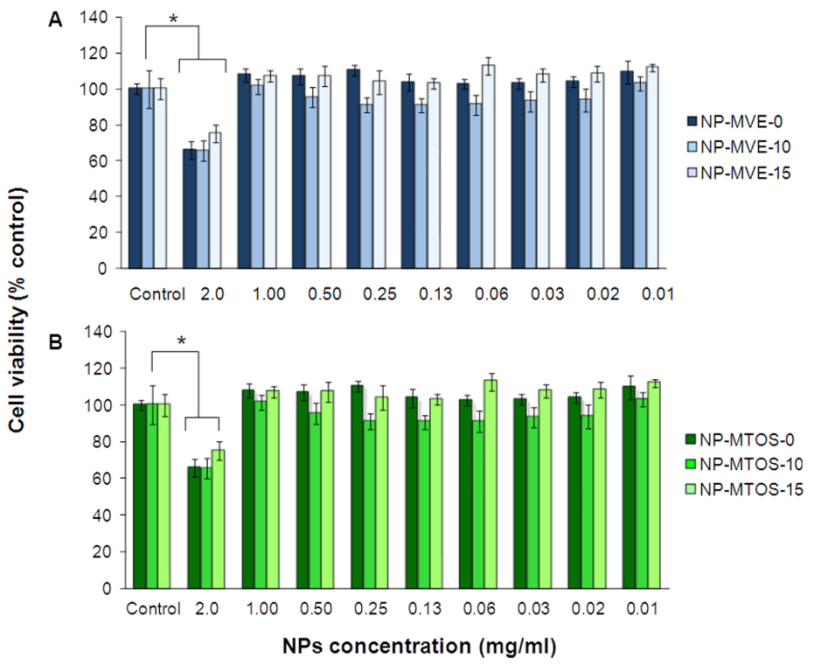

Figure 3: Cell viability of HEI-OC1 treated with different concentrations of NP-MVE (A) and NP-MTOS (B) at 24 hours. The diagrams include the mean, the standard deviation (n = 8), and the ANOVA results (*p < 0.05).

NP-MVE and NP-MTOS ameliorates CDDP-induced cytotoxicity in HEI-OC1

NPs were added to HEI-OC1, and 4 h later 20 or 30 µM CDDP was added for 24 h. Cell viability approximately decreased till 60%, and till 50% when 20 µM CDDP (**Figure 4A** and **5A**), and 30 µM CDDP was added to the cells (**Figure 4B** and **5B**), respectively.

MP-loaded NP-MVE (NP-MVE-10 and NP-MVE-15) at concentrations between 0.5 and 0.13 mg/ml significantly reduced CDDP-induced cytotoxicity of 20 and 30 µM

CDDP. NP-MVE concentrations of 2 and 1 mg/ml resulted to be cytotoxic *per se*, as shown in **Figures 3A** and **B** and were not able to ameliorate CDDP cytotoxic effect even if cells were treated with MP-loaded NPs. NP-MVE-15 was apparently the most effective formulation although there were no statistically significant differences with NP-MVE-10.

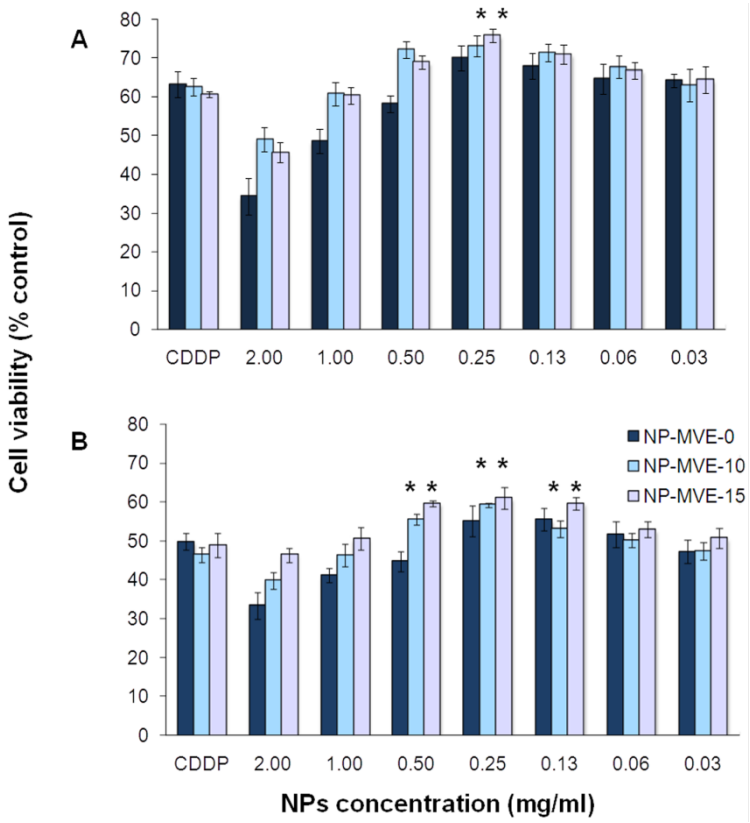

Figure 4: Cell viability of HEI-OC1 treated with different concentrations of NP-MVE and exposed to 20 (A) or 30 µM (B) CDDP after 4 hours of NPs administration, at 24 hours. The diagrams include the mean, the standard deviation (n = 8), and the ANOVA results (*p < 0.05).

2 mg/ml concentration of NP-MTOS resulted to be cytotoxic, but 1 mg/ml significantly protected HEI-OC1 from CDDP effects. No significant differences between NP-MTOS-0, NP-TOS-10 and NP-MTOS-15 were observed that could be explained due to the poor MP EE% with this copolymer.

NP-MVE-10, NP-MVE-15 and NP-MTOS-10 and NP-MTOS-15 significantly reduced CDDP cytotoxicity in a certain range of concentrations, being the most active MVE formulations. NP-MTOS-0 slightly increased cell viability of CDDP-treated cells.

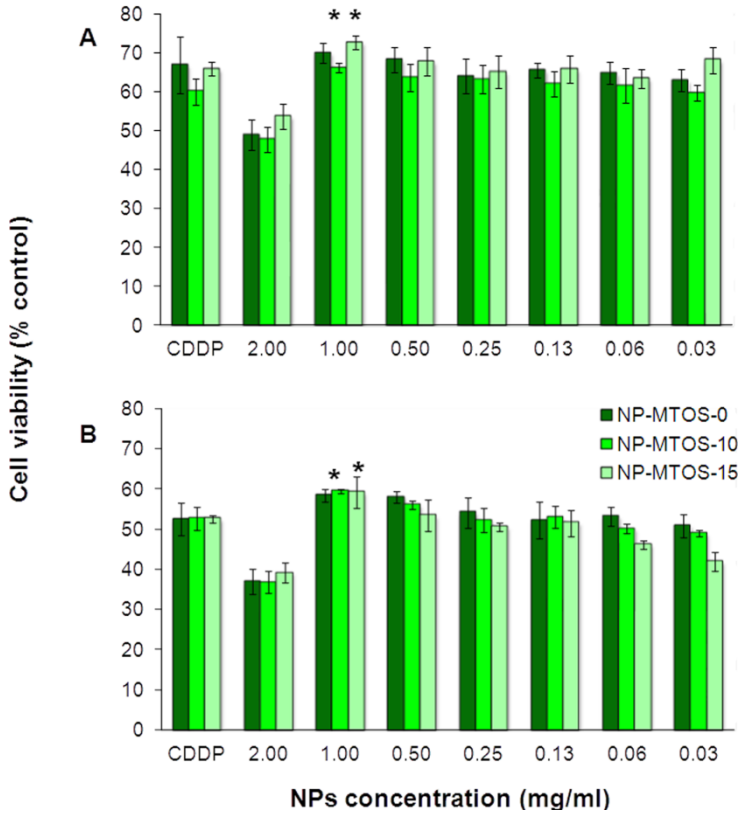

Figure 5: Cell viability of HEI-OC1 treated with different concentrations of NP-MTOS and exposed to 20 (A) or 30 µM (B) CDDP after 4 hours of NPs administration, at 24 hours. The diagrams include the mean, the standard deviation (n = 8), and the ANOVA results (*p < 0.05).

In vivo experiments

Young adult animals were selected to test the possible protective effect of the synthesized NPs as CDDP ototoxicity is also related to the age of the patient and both elderly and pediatric patients are reportedly more sensitive to CDDP ototoxicity.

In order to maximize NPs delivery to inner ear, the highest dose of NPs (2 mg/ml) was used even though it was toxic in the *in vitro* tests. Empty NPs were inoculated through a bullostomy in the right ear of 2 animals per formulation (NP-MVE-0 and NP-MTOS-0). These animals were not treated with CDDP after surgery although they did get the same palliative cares than the animals that received the chemotherapeutic treatment. After 72 hours of NPs exposure, no significant differences were observed between the auditory thresholds of the right ear and the left ear at all frequencies (**see supplementary data Figure S3**).

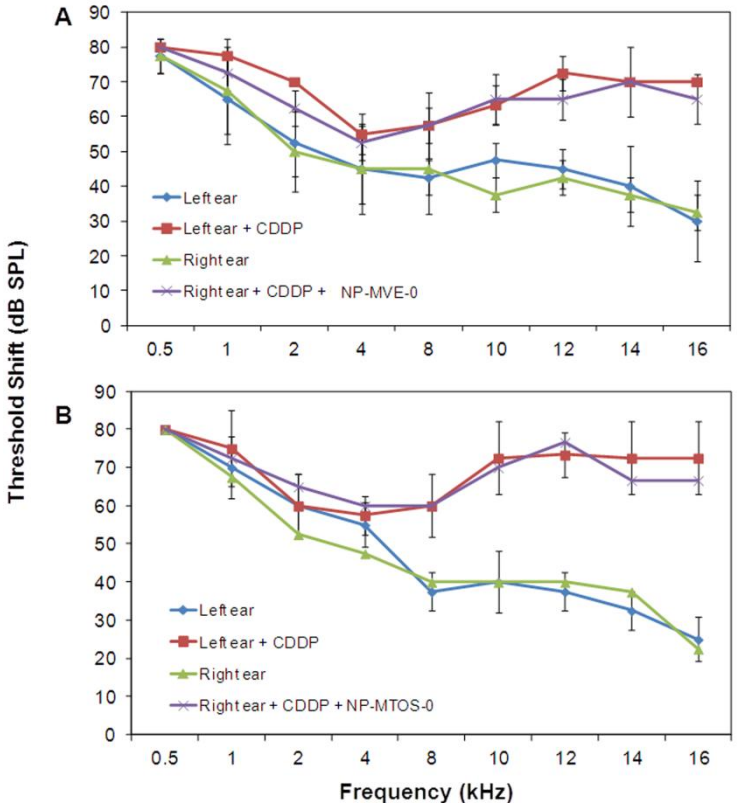

Figure 6: Hearing thresholds before and after local administration by bullostomy in right ear of NP-MVE-0 (A) and NP-MTOS-0 (B) solution and intraperitoneal 10 mg/kg dose of CDDP. The diagrams include the mean, the standard deviation (n = 4), and the independent TUKEY results (*p < 0.05).

NP-MVE-15 decreased CDDP-induced hearing loss in an *in vivo* model

NP-MVE-0 and NP-MTOS-0 were not able to decrease CDDP-induced ototoxicity. Auditory thresholds 72 hours after CDDP treatment increased in the same way in both ears (**Figure 6**).

NP-MVE-10 and NP-MTOS-10 showed no otoprotection (**data not shown**). However, NP-MTOS-15 and NP-MVE-15 were active *in vivo* and showed protection against CDDP-induced hearing loss. NP-MTOS-15 protected in a significant way only in one medium frequency (**Figure 7A**), while NP-MVE-15 was able to decrease CDDP-induced ototoxicity in frequencies between 10 and 16 kHz, being statistically significant from 14 to 16 kHz. In view of the results, the size of the group was increased from 4 animals to 12 to corroborate the preliminary results. Animals that received this treatment showed that auditory thresholds in high frequencies (14 and 16 kHz) were significantly lower in the protected right ear (Right ear: CDDP+NP-MVE-15) when

compared with the auditory thresholds of the left ear (left ear: PBS + CDDP) (**Figure 8A**).

NP-MVE-C6 and NP-MTOS-C6 accumulation in IHC and OHC

NP-MTOS-C6 (Figure 7B, C and D) and NP-MVE-C6 (Figure 8B, C and D) were preferentially accumulated in the IHC than in OHC of the basal turn of the cochlea after 2 hours post-administration in the middle ear. Green fluorescence due to the accumulation of C6-loaded NP progressively decreased from the basal turn to the apical turn (**see supplementary data Figure S4**).

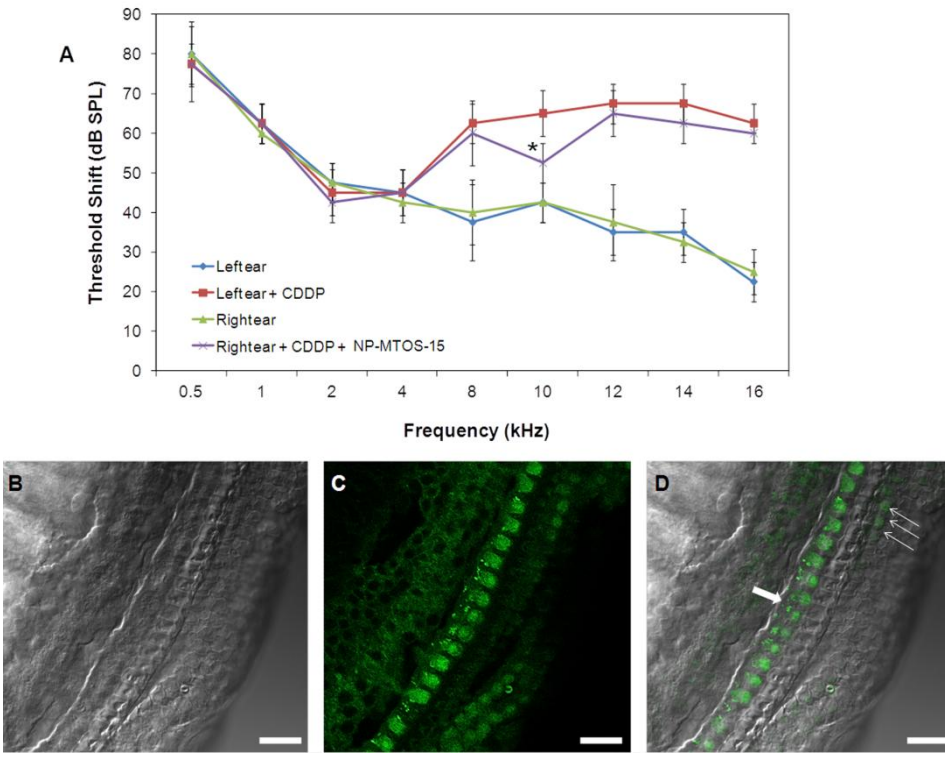

Figure 7: (A) Hearing thresholds before and after local administration by bullostomy in right ear of NP-MTOS-15 solution and intraperitoneal 10 mg/kg dose of CDDP. The diagrams include the mean, the standard deviation (n = 4), and the independent TUKEY results (*p < 0.05). Right ear basal turn of the cochlea of an animal treated with NP-MTOS-C6; phase contrast image (B), coumarin-6 fluorescence image (C) and merged image (D) (triple arrow correspond to OHC and single arrow to IHC; Scale bar= 25 µm).

DISCUSSION

CO-MVE and CO-MTOS are amphiphilic copolymers that present an appropriate hydrophilic/hydrophobic balance to self-organize in aqueous media forming spherical NPs with a hydrophilic shell (mainly VP sequences) and a hydrophobic core (mainly MVE or MTOS monomer, respectively) (Palao-Suay et al., 2015).

MP was incorporated in the core of the NPs in order to locally deliver the corticoid in the inner ear at appropriate concentrations and to increase its activity and decrease its undesired side effects. Encapsulation efficiency was higher for NP-MVE than NP-MTOS. This was probably due to a different hydrophobic/hydrophilic balance (MVE system is poly(VP-*co*-MVE)(60:40) and MTOS system is poly(VP-*co*-MTOS)(89:11)). CO-MVE has a higher content in the hydrophobic monomer MVE that could favor the encapsulation of MP.

Bowe et al. (Bowe and Jacob, 2010) studied the RWM perfusion dynamics and stated that NPs with sizes lower than 200 nm were able to pass through this membrane by rapid diffusion making them ideal candidates for drug delivery across the RWM. Cai et al. (Cai et al., 2014) demonstrated the potential of PLGA-based NPs with sizes between 135 and 154 nm for carrying drugs and crossing the RWM in guinea pigs. Sizes measured by DLS were between 120 and 128 nm and therefore were adequate for this purpose.

All NPs presented slightly negative zeta potential, indicating an almost neutral charge surface. These values have been previously described for other authors and were also corroborated by our group with α-TOS-loaded NPs based on CO-MVE and CO-MTOS. This fact indicates that the shell of the NPs is constituted by VP-rich hydrophilic domains.

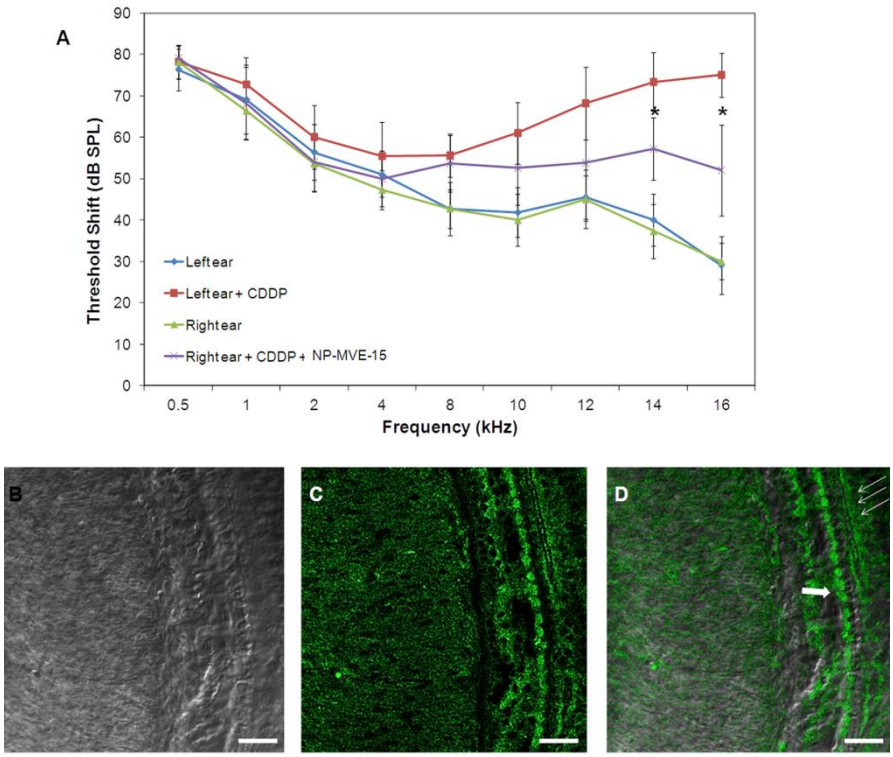

Figure 8: (A) Hearing thresholds before and after local administration by bullostomy in right ear of NP-MVE-15 solution and intraperitoneal 10 mg/kg dose of CDDP. The diagrams include the mean, the standard deviation (n = 12), and the independent TUKEY results (*p < 0.05). Right ear basal turn of the cochlea of an animal treated with NP-MVE-C6; phase contrast image (B), coumarin-6 fluorescence image (C) and merged image (D) (triple arrow correspond to OHC and single arrow to IHC; Scale bar= 25 µm).

Esterase-mediated MP release profiles of both systems followed a zero order kinetic during the first 80 hours, followed by a non-linear period (**Figure 2E**). The experimental conditions are far from the *in vivo* environment, however, this experiment probes that MP release takes place in the presence of esterase in a sustained manner during, at least, one week. The biological half-life of MP in the inner ear is around 24 hours (Parnes et al., 1999) and therefore, its protection and sustained release are of great interest to its application as otoprotector of CDDP-induced toxicity.

Non-loaded NPs (CO-MTOS and CO-MVE) were tested in order to check if they could effectively reduce ROS in CDDP treated HEI-OC1 cells as they incorporate α-tocopherol or α-tocopheryl succinate derivatives covalently attached to their macromolecular chain (Wang and Quinn, 1999).

Kruspig et al. (Kruspig et al., 2013) studied the effects of the combinatorial administration of α-TOS and other antiproliferative molecules, and demonstrated the

antagonic effects of low concentrations of α-TOS and CDDP. Therefore, NP-MTOS were tested in order to check if the α-TOS of the copolymer could effectively reduce the pro-apoptotic effect of CDDP in HEI-OC1 cells. NPs based on both MVE and MTOS with concentrations between 1 and 0.01 mg/ml resulted to be non-cytotoxic to HEI-OC1.

NP-MVE-15 was the most effective formulation *in vitro,* although there was not statistically significant difference with NP-MVE-10 (**Figure 4A** and **B**). NP-MTOS had less protector effect against CDDP-induced cytotoxicity than NP-MVE treated group (**Figure 5A** and **B**). NP-MTOS-0 slightly increased cell viability of CDDP-treated cells. This could indicate certain activity of the polymer although this effect was not statistically significant. Therefore, NP-MVE-0 and NP-MTOS-0 cannot be considered active against CDDP cytotoxicity *in vitro*, but are good nanocarriers to encapsulate and transport MP. As it has been commented before, the differences between both systems could be ascribed to the different composition of the copolymers better than the chemical structure of both MVE and MTOS components.

Despite the development of new regimens and dosage limits, the ototoxic effect of CDDP treatment is still unavoidable. A single injection of high doses of CDDP rapidly causes ototoxicity with a high incidence. CDDP-induced hearing loss firstly affects the high frequencies and continues to medium frequencies so an increase in auditory threshold is shown for frequencies from 8 to 16 kHz.

NP-MVE-0 and NP-MTOS-0 were not able to decrease CDDP-induced ototoxicity (**Figure 6**). This fact could be related to the high doses that were used in this experiment to simulate aggressive CDDP-based therapies used in clinical patients.

Corticoids have been systemically administered to protect against sensorineural hearing loss with good results (Wilson et al., 1980). However, some authors have called into question the efficacy of systemic steroids due to the controversial results in clinical studies because of the side effects. Other problem associated with corticoid systemic administration has been the wide range of pharmacokinetic factors that influence the concentration of the drug inside the inner ear including: difference in distribution, variability to cross the blood-labyrinth barrier, different drug metabolic pathways and varied routes of excretion (Paulson et al., 2008). Due to these related problems intratympanic administration is an accepted alternative to systemic administration in

patients with contraindications for systemic corticoids (Parnes et al., 1999, Haynes et al., 2007).

A good correlation between the *in vitro* and *in vivo* experiments was found when unloaded and MP-loaded nanoparticles were tested to palliate the ototoxicity of CDDP. Unloaded-NP reduced the ototoxicity of the CDDP but this effect was not statistically significant, although both copolymers incorporated vitamin E or α-TOS in their structure. Loaded-NPs were active and their activity mainly depended on the encapsulation efficiency. NP-MVE-15 was the most active formulation both *in vitro* and *in vivo*. In the *in vitro* experiments, concentrations between 0.13 and 0.50 mg/mL significantly reduced cytotoxicity of CDDP on HEI-OC1 cells. In the *in vivo* experiments, high frequencies (14-16 kHz) were protected by the addition of the NP suspension intratympanically by bullostomy (**Figure 8A**). In addition, NP-MVE-C6 (Figure 8B, C and D) and NP-MTOS-C6 (Figure 8B,C and D) were accumulated in the area of sensory auditory cells by crossing the three-layered RWM after 2 hours of the administration. Accumulation preferentially occurred in IHC in the basal turn of the cochlea associated with higher frequency hearing.

In conclusion, these results indicate that NP-MVE-15 could be a good candidate to deliver MP in the inner ear to palliate, at least in part, the CDDP ototoxicity. Moreover, both kinds of polymers could also be used to encapsulate and deliver other hydrophobic drugs (antioxidants, anti-inflammatory agent, or anticaspase drugs) as both NP crossed the round window membrane and enter the inner ear.

ACKNOWLEDGMENTS

Authors acknowledge David Gómez, Rosa Ana Ramírez and Carlos Vargas for their help in SEM/TEM, cell culture and histology experiments, respectively. Authors also thank Dr. Kalinec for providing HEI-OC1 cells for the experiments.

SUPPORTING INFORMATION

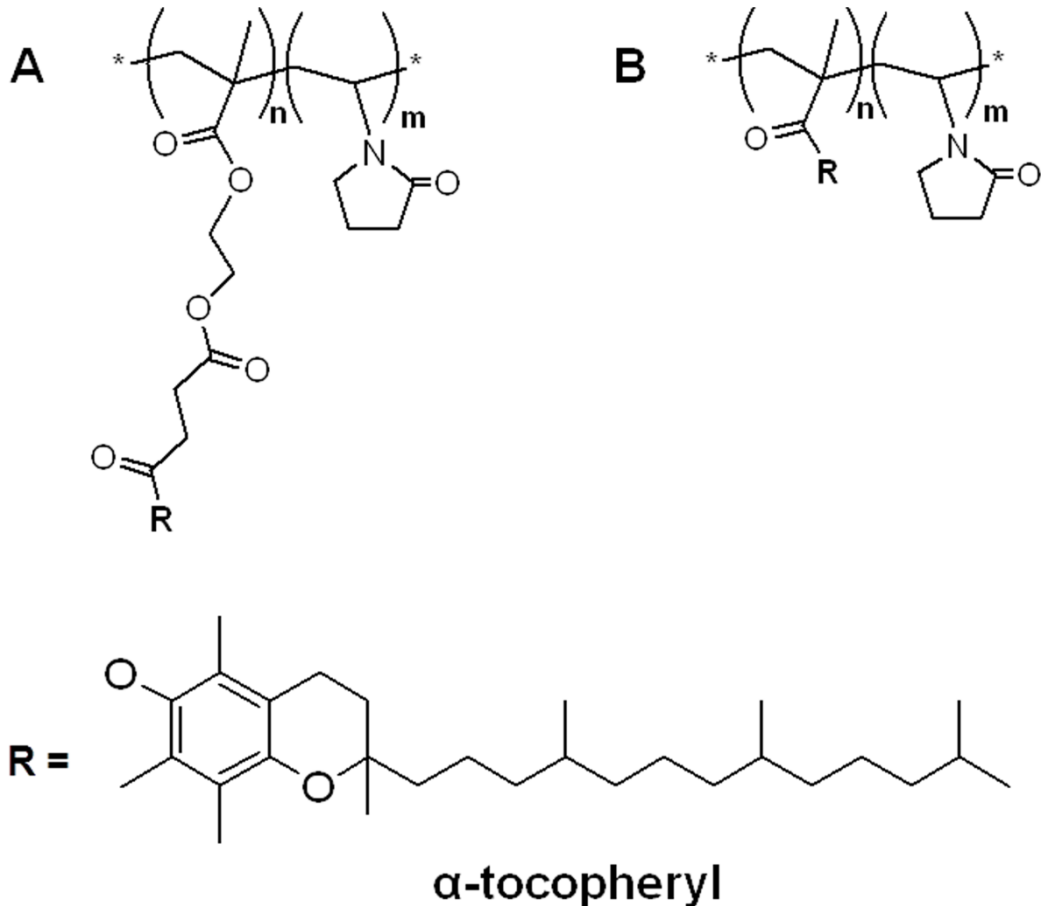

Figure S1: Chemical structure of (A) poly(VP-co-MTOS) and (B) poly(VP-co-MVE).

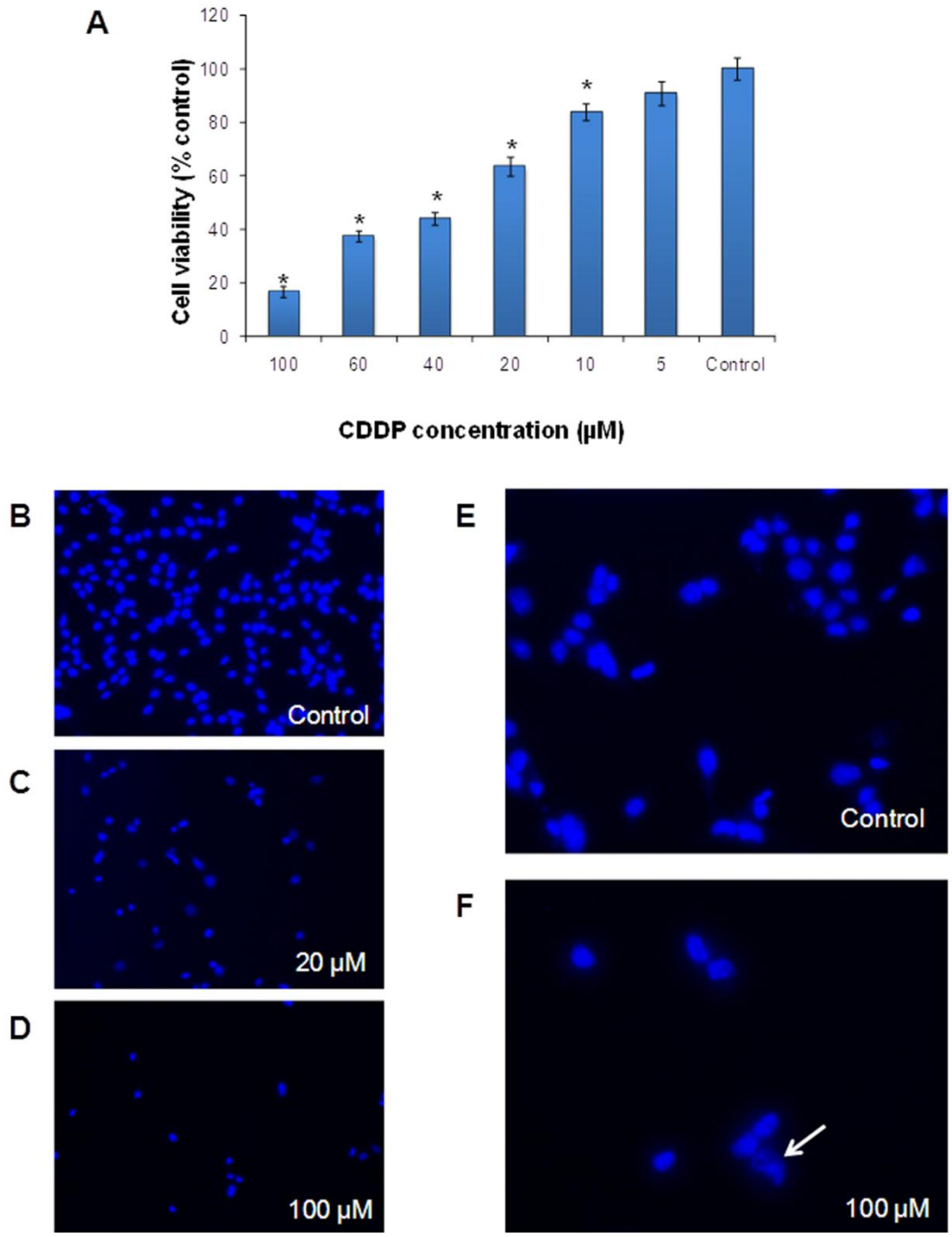

Figure S2: HEI-OC1 viability as a function of CDD concentration. The diagram include the mean (n=8), the standard deviation, and the ANOVA results at a significance level of *$p<0.05$ (A). Fluorescent micrographs of HEI-OC1 cells in 2D culture with Hoechst 33258 staining after treatment (B) with PBS, as a control, (C) 20 µM CDDP and (D) 100 µM CDDP. Fluorescent micrographs of HEI-OC1 cells with Hoechst 33258 staining to show differences between healthy nuclei (E) and pro-apoptotic nuclei (F). Apoptotic nuclei marked with an arrow.

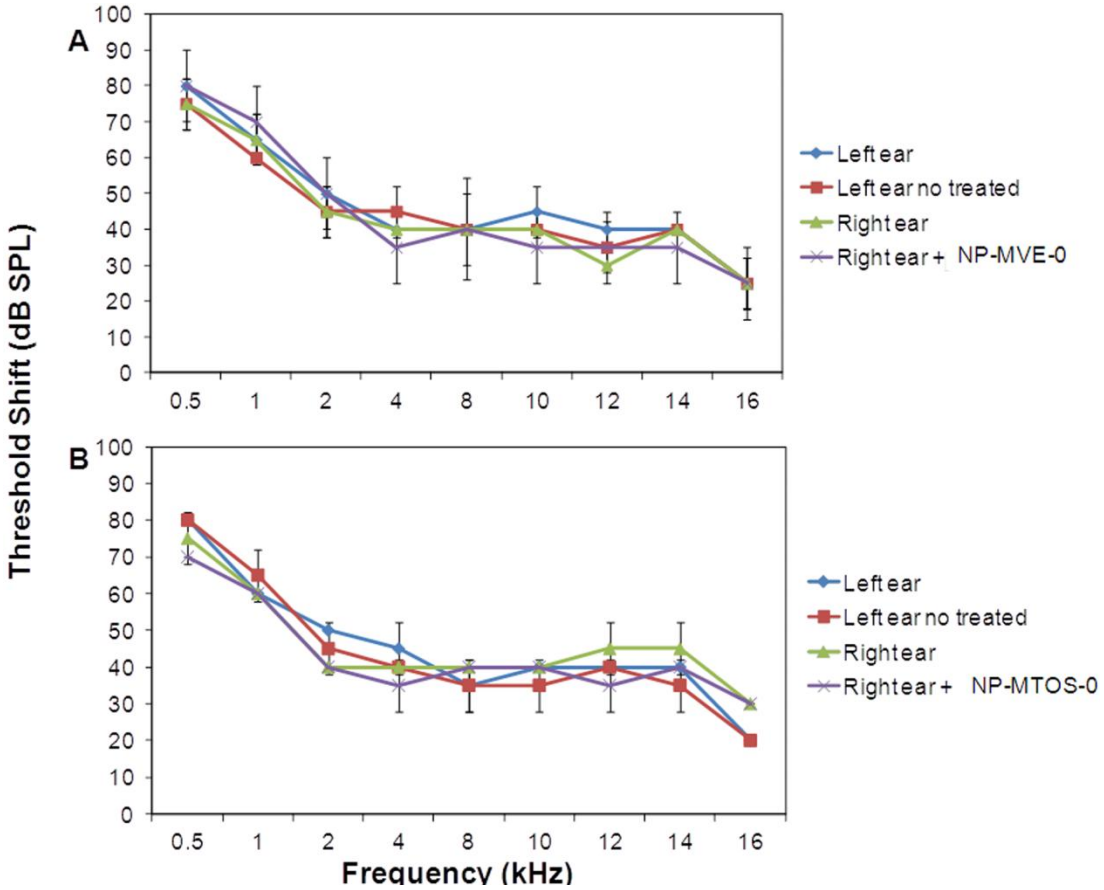

Figure S3: Hearing thresholds before and after local administration by bullostomy in right ear of NP-MVE-0 (A) and NP-MTOS-0 (B) solution. The diagrams include the mean, the standard deviation (n = 2), and the independent TUKEY results at a significance level of *p < 0.05.

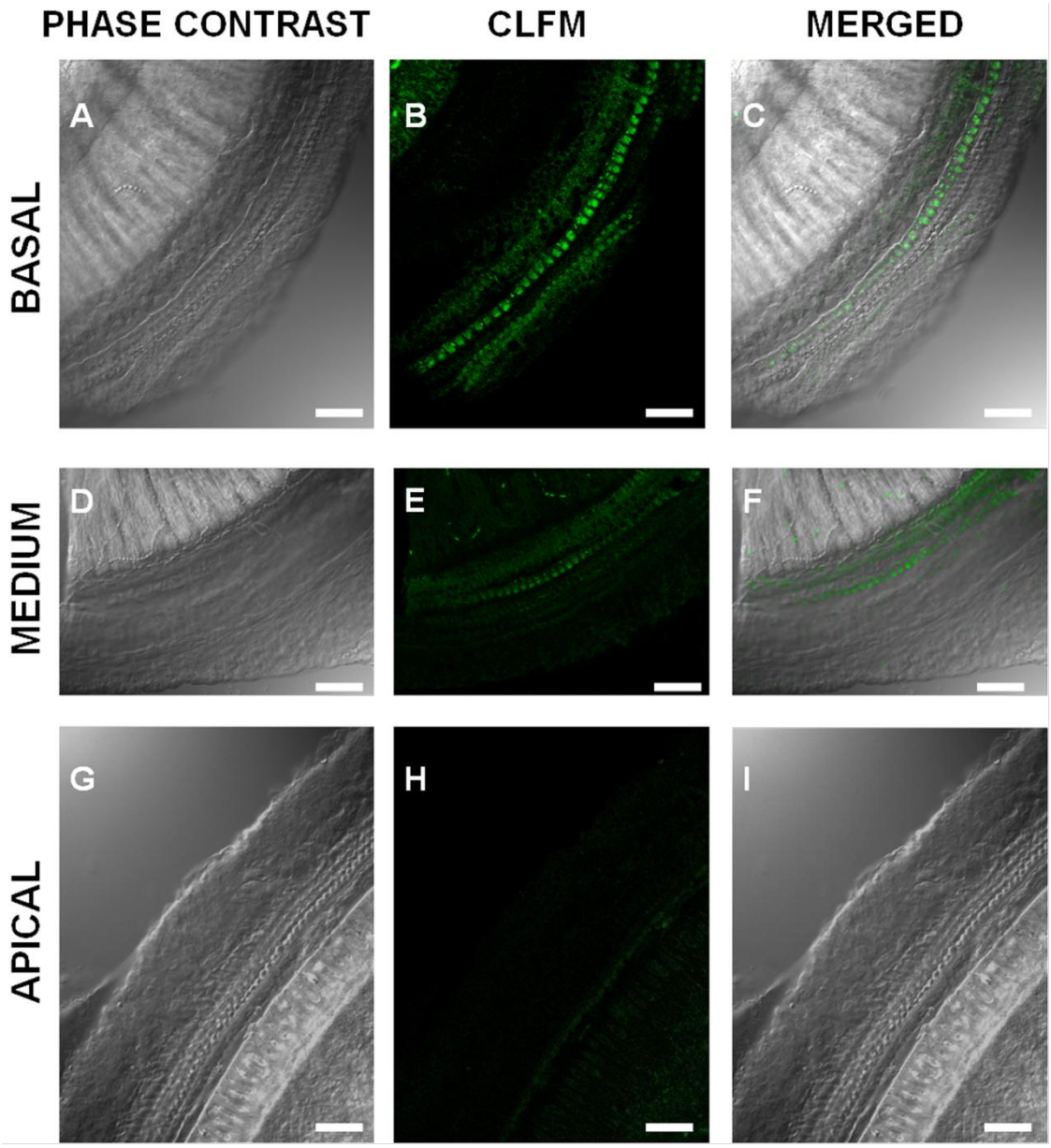

Figure S4: Right ear cochlea of an animal treated with NP-MTOS-C6: Basal turn (A, B, C), medium turn (D, E, F) and apical turn (G, H, I). Images were obtained by phase contrast microscopy (A, D, G), confocal laser fluorescence microscopy (B, E, H), and merged images (C, F, I). Scale bar = 25 µm.

Polymeric nanoparticles loaded with dexamethasone or a-tocopheryl succinate to ameliorate cisplatin-induced ototoxicity: study of caspase and proinflammatory dependent pathways

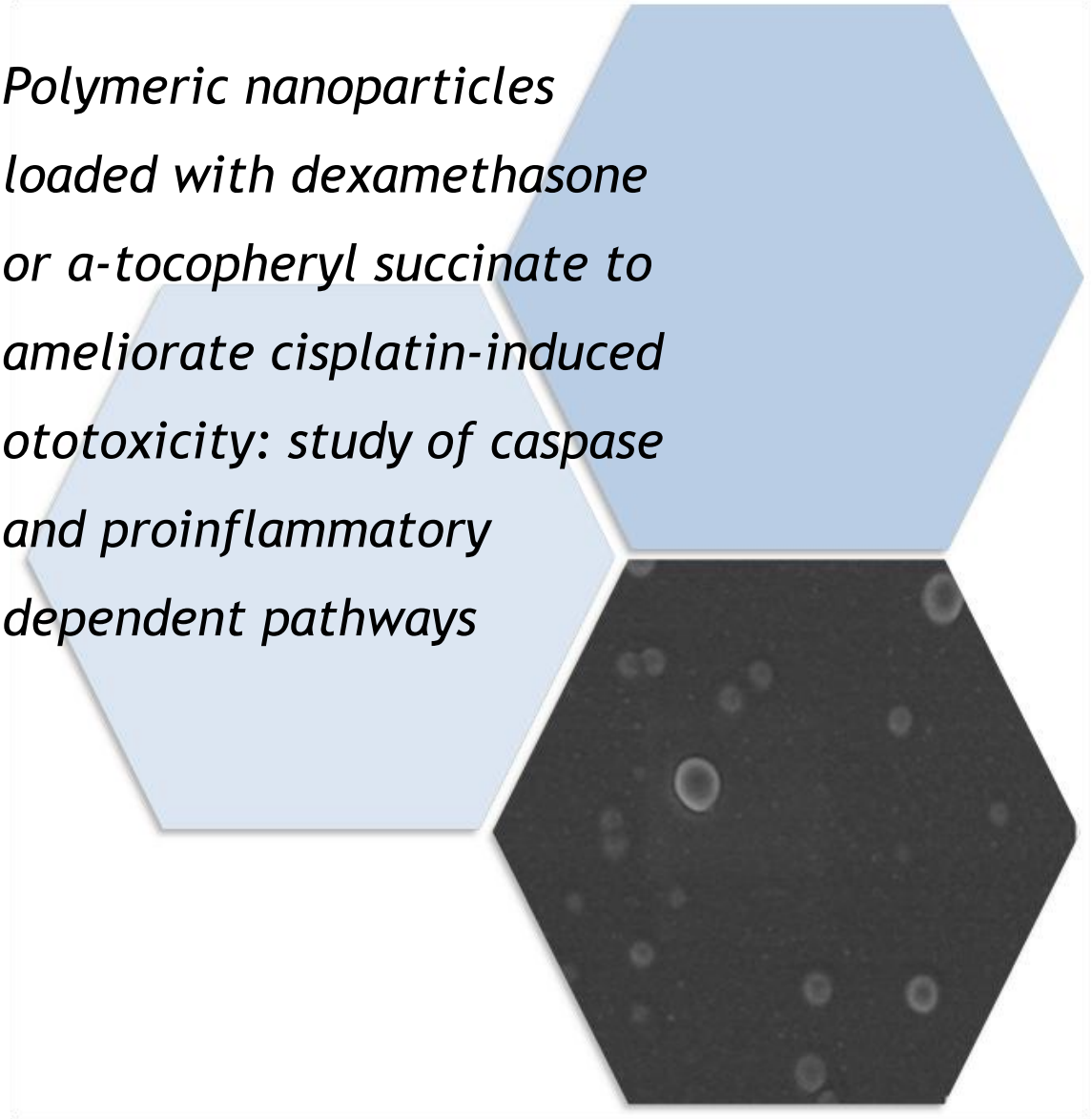

Resumen

Tras la puesta a punto de los modelos *in vitro* e *in vivo* con las NPs de metilprednisolona, en éste trabajo se prepararon NPs vehiculizando dexametasona, al ser un corticoide mucho más activo, y el succinato de la vitamina E (α-TOS), como molécula con capacidad antioxidante para mejorar el efecto terapéutico de las NPs contra la ototoxicidad provocada por el CDDP.

El objetivo de este segundo trabajo es el desarrollo de agentes altamente protectores que, administrados localmente en el oído medio, reduzcan la ototoxicidad inducida por CDDP. Los sistemas desarrollados se basan en NPs poliméricas cargadas con dexametasona o α-TOS, como modelos de molécula con capacidad anti-inflamatoria y anti-apoptótica.

Tanto la dexametasona como el α-TOS, son moléculas poco solubles en agua y pueden presentar graves efectos secundarios al ser administradas sistémicamente durante largos períodos de tiempo en dosis múltiples. Su incorporación en el núcleo hidrofóbico de las NPs con las propiedades hidrodinámicas apropiadas, proporciona los efectos deseados *in vitro* e *in vivo*.

Estos sistemas, se estudiaron más a fondo *in vitro*, para observar su efecto en marcadores moleculares sobre-expresados tras el tratamiento con el citostático. Además de los ensayos de citotoxicidad de las NPs y de protección de las mismas frente al CDDP, se estudió la expresión de caspasa 3/7, como modelo de marcador de apoptosis, así como la liberación de citoquina IL-1β, ambos sobre-expresados en HEI-OC1 tras el tratamiento con CDDP, dada la respuesta pro-apoptótica y pro- inflamatoria de las células tratadas con el antitumoral. En ambos casos se registraron buenos resultados. Así mismo, la protección *in vitro* registrada con éstos sistemas fue mayor que en el caso de los sistemas cargados con metilprednisolona.

De igual modo, la administración local de las NPs mediante bullostomía arrojó resultados mejores que los anteriormente mostrados con la 6α-metilprednisolona. Dichos resultados *in vivo* mostraron la protección parcial obtenida por las NPs, siendo ésta estadísticamente significativa para varias frecuencias altas en los mejores sistemas testados.

Polymeric Nanoparticles loaded with dexamethasone or α-tocopheryl succinate to ameliorate cisplatin-induced ototoxicity: study of caspase and proinflammatory dependent pathways

Sergio Martín-Saldaña[1,2], Raquel Palao-Suay[2,3], María Rosa Aguilar[2], Rafael Ramírez-Camacho[1,4], Julio San Román[2,3]*

[1] Department of Otorhinolaryngology, Puerta de Hierro Majadahonda University Hospital, C/ Manuel de Falla, 1, 28222 Majadahonda
[2]Group of Biomaterials, Department of Polymeric Nanomaterials and Biomaterials, Institute of Polymer Science and Technology, CSIC, C/ Juan de la Cierva, 3, 28006 Madrid, Spain
[3]Networking Biomedical Research Centre in Bioengineering, Biomaterials and Nanomedicine, CIBER-BBN, Spain
[4] Universidad Autónoma de Madrid, Cantoblanco Campus University, 28049 Madrid

Corresponding author (*): Dra. María Rosa Aguilar
Instituto of Polymer Science and Technology
C/ Juan de la Cierva, 3
28006 Madrid
SPAIN
Email: mraguilar@ictp.csic.es
Telephone: +34 91561 88 06 (ext.212)
Fax: +34 91 564 48 53

ABSTRACT

The aim of this work is the development of highly protective agents to be administered locally within the middle ear to avoid cisplatin-induced ototoxicity, which affects to 100% of the clinical patients at ultra-high concentrations (16 mg/kg). The protective agents are based on polymeric nanoparticles loaded with dexamethasone or α-tocopheryl succinate as anti-inflammarory and anti-apoptotic molecules. Dexamethasone and α-tocopheryl succinate are poorly soluble in water and present severe side effects when systemic administered during long periods of time. Their incorporation in the hydrophobic core of nanoparticles with the appropriate hydrodynamic properties provides the desired effects *in vitro* (lower cisplatin-induced toxicity, downregulation of caspase 3/7 expression, and lower IL-1β release) and *in vivo* (reducing the hearing loss at the local level). The local administration of the nanoparticles by bullostomy provides an adequate dose of drug without systemic interference with the chemotherapeutic effect of cisplatin.

Graphical Abstract

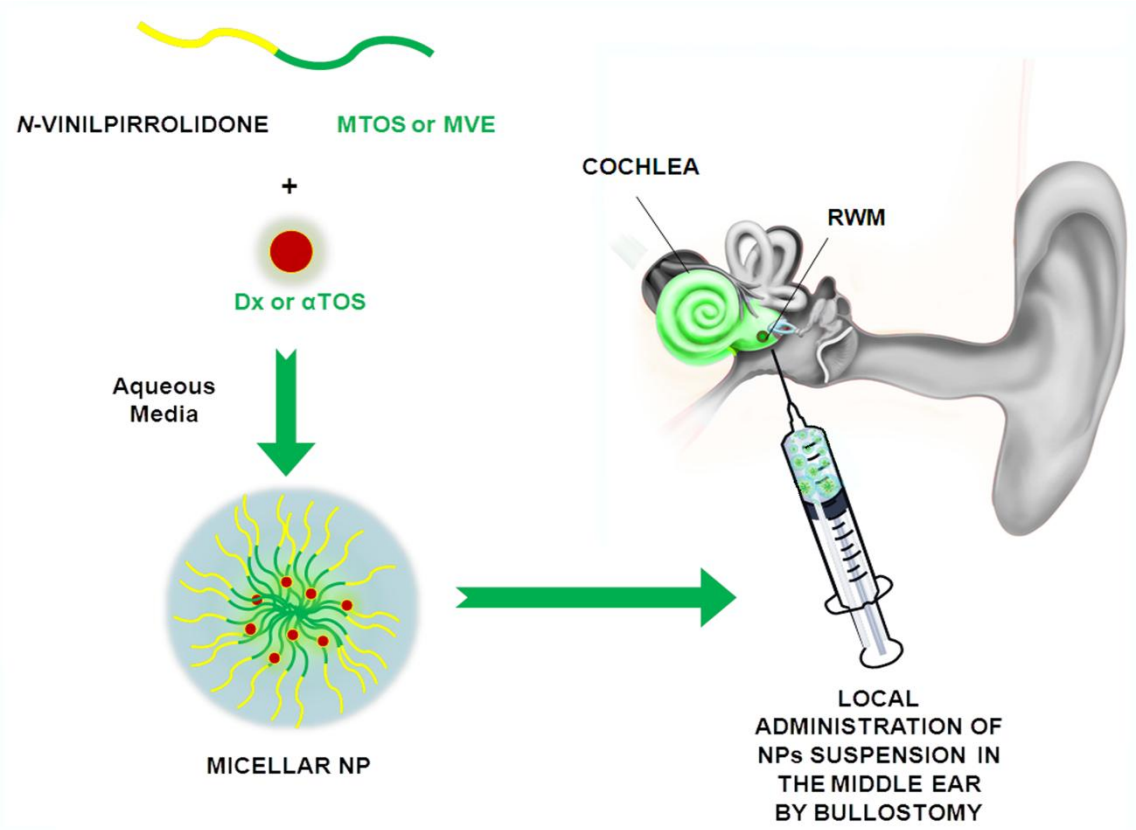

Graphical abstract: Schematic diagram of the procedure done (MTOS and MVE: methacrylic derivatives of α-TOS, and Vitamin E, respectively).

KEYWORDS: Cisplatin, otoprotection, dexamethasone, α-tocopheryl succinate, nanoparticles.

Introduction

Cisplatin (CDDP) administration induces apoptosis in the inner ear by different mechanisms related to caspase and pro-inflammatory dependent pathways. Specifically, CDDP induces the formation of adducts in the structure of nuclear DNA (nDNA) and mitochondrial DNA (mDNA) (Casares et al., 2012). CDDP-induced sensorineural hearing loss is due to the loss of auditory hair cells of the Organ of Corti, mainly outer hair cells (OHC), but also inner hair cell (IHC) via apoptosis and necrosis. CDDP-induced apoptosis of hair cells involves the caspase and MAPK/JNK dependent pathways which are activated by oxidative stress (Lee et al., 2004) and the secretion of inflammatory cytokines in response to the damage (Kim et al., 2008). So *et al.* (So et al., 2007) demonstrated that the secretion and expression of proinflammatory cytokines like TNF-α, IL-1β, and IL-6 were increased *in vitro* and *in vivo* after the peritoneal injection of CDDP and are directly involved in the apoptosis of the cells of the cochlea. The identification of these pathways that lead to apoptosis provides therapeutic targets for the preservation of hearing.

Corticosteroid therapy reduced CDDP-related inflammation and inhibited apoptosis while activating pro-survival pathways in the Organ of Corti (N Abi-Hachem et al., 2010). Corticoids were usually administered systematically (Waissbluth et al., 2013), but the high doses needed to reach therapeutic concentrations in the inner ear due to its short half-life result in many undesirable side effects (Parnes et al., 1999). Due to that, local administration of hydrocortisone, methylprednisolone (MP) or dexamethasone (Dx) is an accepted alternative in patients with contraindications for systemic corticoids (Haynes et al., 2007).

Antioxidants ameliorate CDDP-induced ototoxicity by the reduction of ROS levels generated by oxidative stress in response to platinum-based drugs. ROS are produced during cellular metabolism and are reduced by the intrinsic cell's scavengers system (superoxide dismutase, catalase, glutathione peroxidase and glutathione reductase). Nevertheless CDDP treatment produced ROS that exceed the capability of the intrinsic defense of the cell. Marullo *et al* (Marullo et al., 2013) showed that CDDP induces a mitochondrial-dependent ROS response that significantly enhances the cytotoxic effect caused by nDNA damage. These ROS generation is independent of the nuclear damage

and occurs in the mitochondria affecting to DNA integrity and the bioenergetic cellular function. Several drugs with the capability to scavenge ROS like bucillamine (Kim et al., 2015), N-L-acetylcysteine (Yoo et al., 2014) or Ginkgolide B (Ma et al., 2015) were tested recently *in vitro* and *in vivo* with promising results, but total protection against CDDP is still pending.

Vitamin E (α-tocopherol) is an antioxidant agent with ability in protecting biologic membranes by inhibition of the peroxidation of polysaturated fatty acids, in preventing CDDP-induced neurotoxicity as it was confirmed in a Phase III clinical trials by Kottschade *et al* (Kottschade et al., 2011). α-tocopheryl succinate (α-TOS), the succinate derivative of vitamin E, is a well-known mitocan which induces apoptosis by targeting ubiquinone-binding sites in mitochondrial respiratory complex II of cancer cells (Dong et al., 2008). When is used at low concentrations, α-TOS can suppress apoptosis induced by CDDP when it was cleaved by cellular esterases due to its mitocan properties and its capability to monopolize the mitochondria respiratory chain regulating ROS production (Kruspig et al., 2013).

Most of the drugs used to ameliorate CDDP-induced ototoxicity are poorly water-soluble small molecule with poor biodistribution and a short half-life *in vivo*. To palliate these troubles nanotechnology-based systems has generated considerable interest in the past several years. Recent studies, used Dx-loaded polymer-based NPs (Sun et al., 2015) to ameliorate CDDP-induced hearing loss following RWM administration showing attenuation in CDDP-induced hearing loss only in medium frequencies. However, only partial protection against CDDP-induced ototoxicity was shown but total hearing protection of the treated animals was not achieved (Zou et al., 2015).

Our group has recently described the preparation, characterization and biological activity *in vitro* and *in vivo* of surfactant-free MP-loaded NPs (Martín-Saldaña et al., 2015) with promising results as drug carrier to the Organ of Corti cells. The aim of this work was the development of more effective NPs to ameliorate CDDP-induced hearing loss with Dx or α-TOS-loaded self-assembled polymeric NPs in order to reach higher concentrations of the drugs (with short half lifes) in the inner ear, improve drug stability, avoid the related side effects, and prevent the systemic interaction with CDDP. These two drugs were chosen in order to effectively reduce CDDP-induced toxicity in the inner ear via pro inflammatory and caspase dependent pathways. The NPs were

based on two amphiphilic copolymers of *N*-vinylpyrrolidone (hydrophilic monomer) and a methacrylic derivative of α-TOS (MTOS) or vitamin E (MVE) (hydrophobic monomers). Poly(VP-*co*-MTOS)(90:10) and poly(VP-*co*-MVE)(85:15), from now on CO-MTOS and CO-MVE, respectively were previously synthesized and optimized by our group in terms of physic-chemical, and biological characteristics. The copolymers presented an adequate distribution of monomers that allowed self-assembling in aqueous medium. The hydrophilic monomer (VP) was mainly placed in the surface of the NP and MVE or MTOS were placed in the inner-core of the NP. These NP were able to encapsulate and transport different hydrophobic molecules including 6α-methylprednisolone (Martín-Saldaña et al., 2015), coumarin-6 and α-TOS (Palao-Suay et al., 2015).

Methods

Chemicals

CDDP (1 mg/ml) was purchased from Accord Healthcare (Barcelona, Spain). Dx and α-TOS were purchased from Sigma-Aldrich (Sigma-Aldrich; St.Louis, USA).

Description of polymeric vehicles MVE, MTOS

The methacrylic derivative of α-TOS (MTOS) and methacrylic derivative of Vitamin E (MVE), and the copolymers poly(VP-*co*-MTOS) (89:11) (from now on CO-MTOS) and poly(VP-*co*-MVE) (60:40) (from now on CO-MVE) were synthesized as recently described by our group (Palao-Suay et al., 2015). Briefly, the copolymer was obtained by free radical polymerization of VP and MTOS or MVE in 1,4-dioxane (total monomer concentration, 0.25M CO-MTOS and 1M CO-MVE), using AIBN (1.5×10^{-2}M) as radical initiator, at 60ºC, for 24 hours. Copolymers were purified by dialysis against distilled water for 72 hours, and isolated by freeze-drying.

Preparation of Dx and α-TOS loaded NPs

Eight formulations of self-assembled NPs (**Table 1**) were prepared by nanoprecipitation technique adapted from previously published method (Fessi et al., 1989). CO-MVE and CO-MTOS were dissolved in dioxane (50 mg/ml) containing an appropriate amount of α-TOS or Dx (NP-MVE-5α-TOS and NP-MTOS-5α-TOS, with 5% w/w of α-TOS respect to the polymer; NP-MVE-10Dx, NP-MTOS-10Dx, NP-MVE-10α-TOS and NP-MTOS-10α-TOS, with 10% w/w of Dx or α-TOS respect to the polymer; and NP-MVE-15Dx and NP-MTOS-15Dx with 15% w/w of Dx respect to the polymer). The resulting solution was added drop-wise to an aqueous phase (10 ml of PBS) without surfactant with constant mechanical stirring (650 rpm). Then, the organic phase was eliminated by dialysis over three days. Final NPs suspension was stored at 4^{o}C and sterilized by filtration through 0.22 µM polyethersulfone membranes (PES, Millipore Express®, Millex GP) until used.

Table 1: Hydrodynamic diameter (D_h), polydispersity index (PDI), zeta potential (ζ), and encapsulation efficiency (EE) of Dx-loaded NPs, α-TOS loaded NPs and C6-loaded NPs.

NPs	**Load (w/w %)**	**EE (%)**	**D_h (nm)**	**PDI**	**ζ (mV)**
NP-MVE-10Dx	10	52	138.2 ± 7.17	0.227± 0.050	-3.69 ± 0.88
NP-MTOS-10Dx	10	20	127.4 ± 5.23	0.275± 0.008	-4.82 ± 0.21
NP-MVE-15Dx	15	55	135.2 ± 11.01	0.111± 0.067	-3.23 ± 0.63
NP-MTOS-15Dx	15	25	124.1 ± 7.60	0.130± 0.054	-3.27 ± 1.03
NP-MVE-5α-TOS	5	76	130.9 ± 2.88	0.146± 0.047	-4.10 ± 0.61
NP-MTOS-5α-TOS	5	61	131.5 ± 2.46	0.220± 0.041	-5.28 ± 0.46
NP-MVE-10α-TOS	10	82	137.7 ± 5.16	0.164± 0.042	-4.03 ± 0.38
NP-MTOS-10α-TOS	10	72	122.3 ± 5.98	0.095± 0.040	-7.23 ± 4.05
NP-MVE-C6	1	91	164.9 ± 47.18	0.255 ± 0.067	-3.83 ± 0.31
NP-MTOS-C6	1	85	163.3 ± 20.44	0.320 ± 0.018	-3.36 ± 0.08

Preparation of coumarin 6-loaded NPs

Coumarin-6 (C6) loaded NPs were also obtained by nanoprecipitation. C6 (1 % w/w respect to the polymer) and CO-MTOS or CO-MVE (10 mg/ml) were dissolved in 1,4-dioxane and added drop-wise to PBS under magnetic stirring. The final polymer concentration was 2.0 mg/ml. The suspension was dialyzed against PBS for 72 hours in order to eliminate the organic solvent and non-encapsulated C6.

Characterization of Dx-loaded and α-TOS-loaded NPs

Particles mean diameter, polydispersity index and zeta potential measurements

The particle size distribution of the NPs suspensions was determined by dynamic light scattering (DLS) using a Malvern Nanosizer. Measurements of NPs dispersions were performed in square polystyrene cuvettes (SARSTEDT) and the temperature was kept constant at 25 °C.

Evolution of mean diameter with temperature from 24 to 42ºC was also evaluated in the same apparatus.

The zeta potential (ζ) was determined for NPs formulations at 2.0 mg/ml concentration containing 100 mM NaCl and using laser Doppler electrophoresis (LDE). The zeta potentials were automatically calculated from the electrophoretic mobility using the Smoluchowski´s approximation.

For each sample, the statistical average and standard deviation of data were calculated from 6 different samples (3 measurements of 20 runs each one).

Scanning Electron Microscopy NPs morphology characterization

SEM analysis was performed with a Hitachi SU8000 TED, cold-emission FE-SEM microscope working with an accelerating voltage between 15 and 50 kV. Samples were prepared by deposition of one drop of the corresponding NPs suspension (0.02 mg/ml) over a small glass disk (12 mm diameter) and evaporation at room temperature. The samples were coated with gold palladium alloy (80:20) prior to examination by SEM.

Entrapment efficiency (EE%)

Dx and α-TOS loaded NP-MVE and NP-MTOS were freeze dried in order to eliminate aqueous phase. White amorphous powder was obtained in all types of NPs with a yield higher than 90 %. The freeze-dried NPs were dissolved in 2 ml of chloroform over 24 hours. After that, ethanol was added in agitation over 24 hours to precipitate the polymer. Samples were centrifuged at 10.000 rpm and supernatant was analyzed by UV (Dx λ= 239 nm; α-TOS λ= 285 nm).

Esterase-mediated Dx and α-TOS release

High performance liquid chromatography

5 mL of Dx-loaded or α-TOS-loaded NPs (NP-MVE-15Dx, NP-MTOS-15Dx, NP-MVE-10α-TOS or NP-MTOS-10α-TOS) with 15 u/mL of esterase from porcine liver (Sigma-Aldrich) were dialyzed against 10 mL of PBS at 37 °C using a 3.5-5 kDa MWCO membrane (Spectrum Laboratories). After certain periods, 1 mL of the dialyzing medium was withdrawn and the same volume (1 mL) of PBS was replenished. Dx concentration was measured by HPLC (Shimadzu). The separation was performed on a C18-column (4.6 mm × 250 mm, Agela Technologies) at 30°C. The mobile phase was a mixture of acetonitrile, and distillated water (80:20, v/v) pumped at a rate of 1 mL/min. The UV detector was set at λ_{abs} =239 nm for Dx. The experiment was carried out in triplicate.

α-TOS release was measured by various techniques. Firstly we tried to determine α-TOS concentration by HPLC (Shimadzu). The separation was performed on a C18-column (4.6 mm × 250 mm, Agela Technologies) at 30°C. Different mobile phase was tested and all were pumped at a rate of 1 mL/min: A mixture of acetonitrile, and distillated water (80:20, v/v); a mixture of methanol and distilled water (98:2 v/v); a mixture of acetonitrile and methanol (60:40 v/v); a mixture of methanol, distilled water (90:10 v/v) with 0.1% of trifluoroacetic acid. The UV detector was set at λ_{abs} =285 nm. The experiment was carried out in triplicate. Even in the calibrate curve, quantification of the drug was too low with each mobile phase tested.

Gas chromatography

Gas chromatography was also tested to measure α-TOS release with similar results. The separation of the additives was carried out using a Hewlett Packard 6890 HRGC high resolution gas chromatograph equipped with a 5973 mass spectrometer detector. A DB-5 fused silica capillary column (30m x 250µm and 0.25µm film thickness) was used. The carrier gas is helium pumped at a rate of 1 mL/min, with a trend of temperature (10°C/min) from 80 to 300 °C.

Cell culture

The HEI-OC1 cell line was a kind gift from Dr. Federico Kalinec (House Ear Institute, Los Angeles, CA). HEI-OC1 cells were maintained over permissive conditions in high-glucose Dulbecco's modified Eagle's medium (DMEM; Sigma, Saint Louis, MO, USA)

supplemented with 10% fetal bovine serum (FBS; Gibco, BRL), 5% L-Glutamine (Sigma, Saint Louis, MO, USA) and Penicillin-G (Sigma, Saint Louis, MO, USA) at 33 °C in a humidified incubator with 10% CO_2.

Endocytosis of C6 loaded NPs

C6-loaded NPs were used as a model of endocytosis of the NPs in cell culture. HEI-OC1 cells were seeded into 6 well plates at $1x10^5$cells/mL, in complete DMEM. The cells were incubated overnight at 33ºC and 10% CO_2. The medium was replaced with the corresponding NP suspension in PBS (1 ml of the NP suspension and 1 ml of DMEM) and incubated over different times from 1 hour to 8 hours at 33 ºC. Cells were harvested (and counted to normalize fluorescence/cell) at 1, 2, 4, 6 and 8 hours after NPs addition, and were washed with cold PBS and centrifugate at 10.000 rpm. Supernatant was discarded and cell's pellet was lysate with ethanol to free endocyted C6. Fluorescence of supernatant at 458/540 nm (excitation/ emission) was measured on a Multi-Detection Microplate Reader Synergy HT (BioTek Instruments; Vermont, USA).

NPs toxicity and otoprotection Assay

3000 live cells/well were seeded in a 96 well-plate under permissive conditions. Cells were exposed to different concentrations of NPs suspension (2.00, 1.00, 0.50, 0.25 and 0.12 mg/ml) and viability was determined.

To measure NPs cell protection against CDDP, cells were treated under the same concentrations of NPs and 30 µM CDDP for the period of 24 hours in DMEM without FBS to avoid uncontrolled cell growth. CDDP was added 4 hours after NPs administration to allow for NPs endocytosis by cells.

AlamarBlue® (Invitrogen) was used to determine cell viability. Absorbance at 570 nm was measured on a Multi-Detection Microplate Reader Synergy HT (BioTek Instruments; Vermont, USA). The treatments were done in replicates (n=8). Results of the experiments are expressed as percentage of relative cell viability (% with respect of control).

Caspase-3/7 activity measurement

HEI-OC1 cells were incubated with 20 µM CDDP dose over different times between 1 and 24 hours to determine the maximum caspase 3/7 activity. 0.25 mg/ml of NPs were added and after 4 hours 20 µM CDDP dose was added to each well. CDDP-induced Caspase-3 activation were estimated 16 hours after CDDP addition with the colorimetric assay EnzChek® Caspase-3 Assay Kit #2 (Molecular Probes, Inc) following the manufacturers protocol.

Interleukin IL-1β release

HEI-OC1 cells were incubated with 20 µM CDDP dose over 24 hours. Then, cells were exposed to CDDP and different NPs formulations at 0.25 mg/ml (added after 4 hours of CDDP addition) and CDDP-induced IL-1β release was measured by ELISA IL-1β mouse kit (BioSource International, Camarillo, CA) following the manufacturers protocol.

***In vivo* experiments**

Thirty two healthy Wistar rats weighting 180-280 g were used. All animals were housed in plastic cages with water and food available *ad libitum*, and maintained on a 12 h light/dark cycle. Rats with signs of present or past middle ear infection were discarded. Animals were randomly assigned to different groups (**Table 2**).

Table 2: Experimental groups (IP; intraperitoneal administration)

NPs name	**N**	**Encapsulated Dx (% w/w)**	**Encapsulated α-TOS (% w/w)**	**CDDP IP (10 mg/kg)**
NP-MVE-15Dx	2	15	-	-
NP-MTOS-15Dx	2	15	-	-
NP-MVE- 10α-TOS	2	-	10	-
NP-MTOS- 10α-TOS	2	-	10	-
NP-MVE-15Dx	6	15	-	+
NP-MTOS-15Dx	6	15	-	+
NP-MVE- 10α-TOS	6	-	10	+
NP-MTOS- 10α-TOS	6	-	10	+

The animals were handled according to the guidelines of the Spanish law for Laboratory animals care registered in the "Real Decreto 53/2013" and the European Directive 2010/63/EU. The study was approved by the Clinical Research and Ethics Committee of the University Hospital Puerta de Hierro (PROEX 022/16).

Experimental procedure

An initial auditory steady-state responses (ASSR) test was performed on all anesthetized animals. An insert earphone (Etymotic Research ER-2) was placed directly into the external auditory canal. Subcutaneous electrodes were placed over the vertex (active) and in the pinna of each ear (reference). Ground electrodes were placed in the right leg muscles. ASSR were recorded using an evoked potential averaging system (Intelligent Hearing System Smart-EP) in an electrically shielded, double-walled, sound-treated booth in response to 100 ms clicks or tone burst at 8, 12, 16, 20, 24, 28, 32 kHz with 10 ms plateau and 1 ms rise/fall time. Intensity was expressed as decibels sound pressure level (dB SPL) peak equivalent. Intensity series were recorded, and an ASSR threshold was defined by the lowest intensity able to induce a replicable visual detectable response.

Following the ASSR measurements the right ear bulla was surgically approached and opened (Pinilla et al., 2001) and 50 µl of NPs suspension were injected in the middle ear by bullostomy using a spinal needle (BD Whitecare 27G). Left ear was injected with

PBS through the bullostomy as a control. After injection the anesthetized animals remained in lateral decubitus for 30 min to maximize the suspension's contact time with the RWM and to prevent its leakage into the pharynx through the Eustachian tube.

After surgery, enrofloxacin and morphine (Braun 20 mg/ml) were administered subcutaneously for prevention of infection and postoperative analgesia, respectively.

CDDP-treated groups: after NPs administration in the right ear, an intraperitoneal slow infusion of CDDP (10 mg/kg) was carried out for 30 min. After CDDP infusion, animals were housed in individual cages with *ad libitum* access to water and food.

ASSR were tested after 3 days, and rats were euthanized by CO_2 suffocation.

In vivo distribution of C6-loaded NP

NP-MVE-C6 and NP-MTOS-C6 were administered *in vivo* as described in the previous section. However, these animals were euthanized after 2h. Cochlea was extracted and fixed in paraformaldehyde over 24h and decalcified in 1 % ethylenediaminetetraacetic acid (EDTA) at room temperature (with daily changes) for 10–12 days. Once the bone was completely decalcified, the cochlea was dissected in PBS, and cochlear surface extracts were visualized using an inverted microscope (Nikon Eclipse TE 2000-S) and a confocal laser fluorescence microscope (CLFM; Leica TCS-SP5 RS AOBS).

Statistical analysis

One-way ANOVA was used to analyze for statistical significance of all *in vitro* and *in vivo* results. Tukey test was used to identify significant differences between the paired treatments. $p<0.05$ was considered statistically significant.

Results

NPs characterization

Dx-loaded and α-TOS-loaded NPs were obtained by nanoprecipitation in PBS of the corresponding polymer solutions in dioxane and their principal characteristics are described in **Table 1**. EE% was higher for NP-MVE (52% for NP-MVE-10Dx, 55% for NP-MVE-15Dx, 76% for NP-MVE-5α-TOS and 82% for NP-MVE-10α-TOS) than NP-MTOS (20% for NP-MTOS-10Dx, 25% for NP-MTOS-15Dx, 61% for NP-MTOS-5α-TOS and 72% for NP-MTOS-10α-TOS).

All the synthesized NPs were spherical (**Figure 1A-D**) and presented unimodal size distributions with apparent hydrodynamic diameters (by intensity, D_h) between 122 and 165 nm, with low PDI values and slightly negative zeta potential. Dh and PDI were stable as a function of temperature (from 24 to 42ºC (**Figure 1E-H**).

Esterase-mediated *in vitro* drug release

In vitro release of Dx and α-TOS was studied by an esterase-mediated dialysis diffusion method. **Figure 2A** shows the *in vitro* Dx and α-TOS release profile of NP-MVE 15-Dx. NP-MTOS-15Dx, NP-MVE-10α-TOS and NP-MTOS-10α-TOS at 37 °C during 15 days. About 52% of the loaded Dx is released from the NP-MVE-15Dx and more than 83% from NP-MTOS-15Dx within fifteen days. α-TOS release could not be monitored in PBS at 37ºC in the presence of esterases to stimulate α-TOS release, however, these NPs presented higher biological activity than non-loaded NPs (Martín-Saldaña et al., 2015) as will be shown in the following section. Therefore, α-TOS release was not detectable in the reported experimental conditions, but took place in the biological system during the first 24 hours.

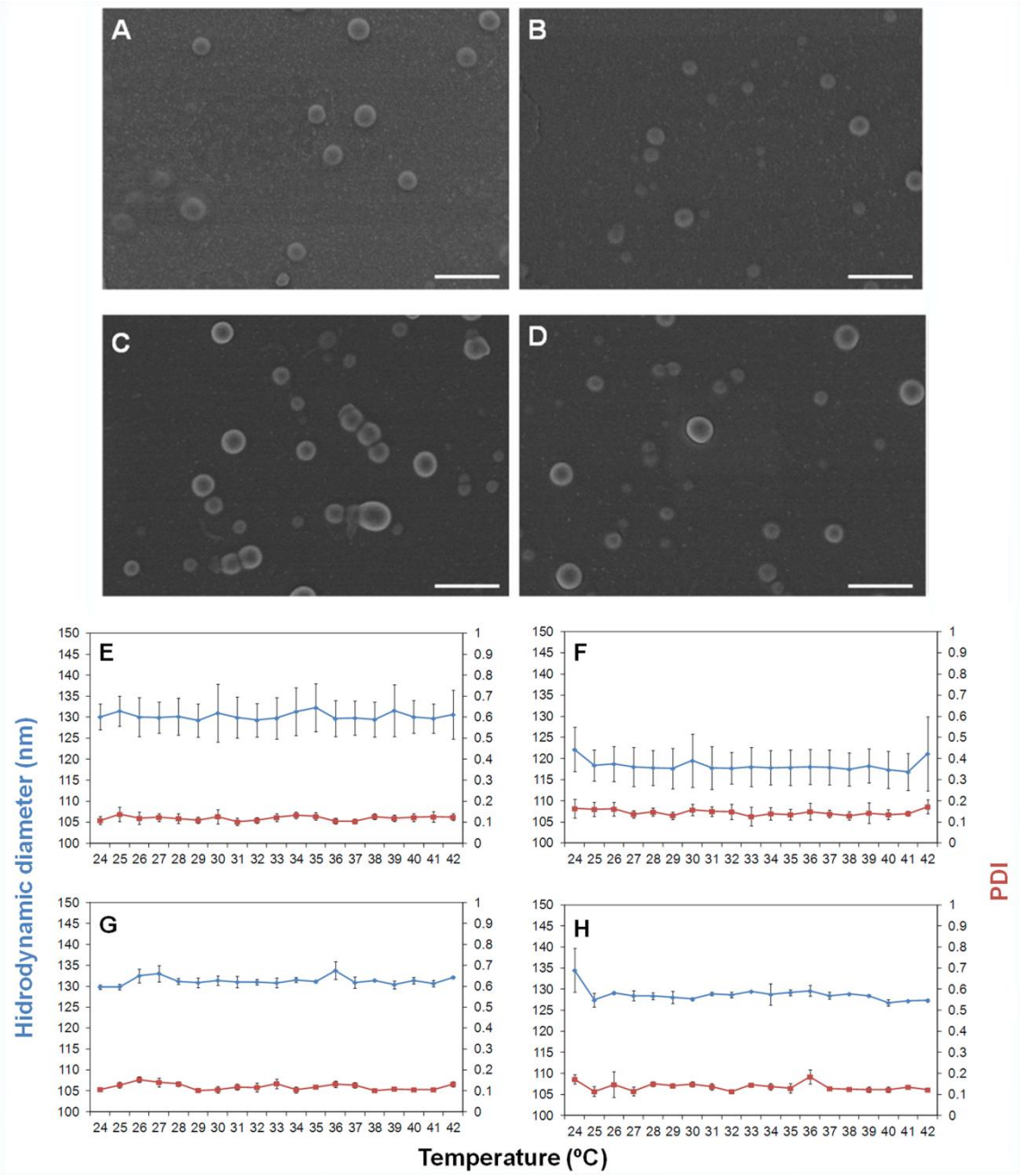

Figure 1: SEM micrographs of NP-MVE-15Dx (A), NP-MTOS-15Dx (B), NP-MVE-10α-TOS (C) and NP-MTOS-10α-TOS (D) NPs (Scale bar= 500 nm). NPs mean diameter variation of NP-MVE-15Dx (E), NP-MTOS-15Dx (F), NP-MVE-10α-TOS (G) and NP-MTOS-10α-TOS (H) with a temperature trend from 24 to 42ºC.

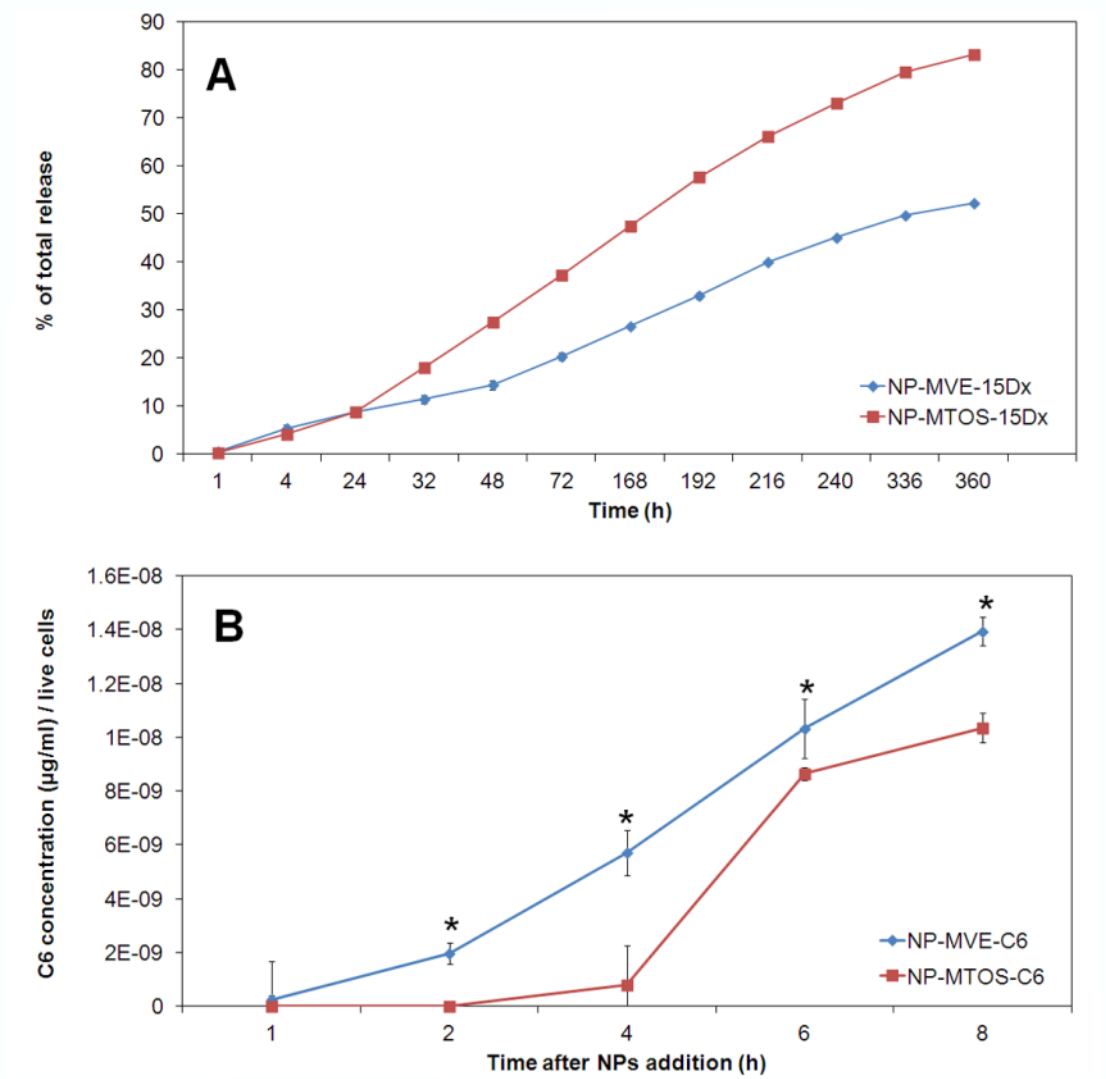

Figure 2: (A) *In vitro* release profile of Dx loaded NPs in PBS at 37 °C. (B) C6-loaded NPs endocytosis by HEI-OC1 cells over 8 hours. The diagram include the mean, the standard deviation (n = 8), and the ANOVA results (*$p < 0.05$).

In vitro experiments

C6- loaded NPs uptake in vitro

C6 fluorescent probe was efficiently encapsulated in both NP-MVE and NP-MTOS. The fluorescent NPs were used to monitor the cellular uptake process when added to HEI-OC1 cell culture. HEI-OC1 cells were exposed to NP-MVE-C6 and NP-MTOS-C6 over 8 hours. **Figure 2B** shows that the uptake by HEI-OC1 cells of NP-MVE-C6 was significantly higher after two hours of exposure than the NP-MTOS-C6 uptake (**Table 2**).

NPs toxicity assay in HEI-OC1

Cytotoxicity of Dx-loaded and α-TOS-loaded NPs were tested using HEI-OC1 and the results demonstrated that only the highest concentration (2.0 mg/ml) of NP-MVE-10Dx and NP-MVE-15Dx was cytotoxic after 24 hours (viability <70%; ISO 10993−5:2009). α-TOS-loaded formulations were more cytotoxic (2.0 mg/ml and 1.0 mg/ml) than Dx formulations, especially the 10% w/w loaded formulations. NP-MVE-15Dx reduced viability over 50% (**Figure 3A**) while α-TOS-loaded formulations reduced viability under 30% for the highest concentration, and over 50% when treated with 1.0 mg/ml of NP-MVE-10α-TOS and NP-MTOS-10α-TOS (**Figure 3B**).

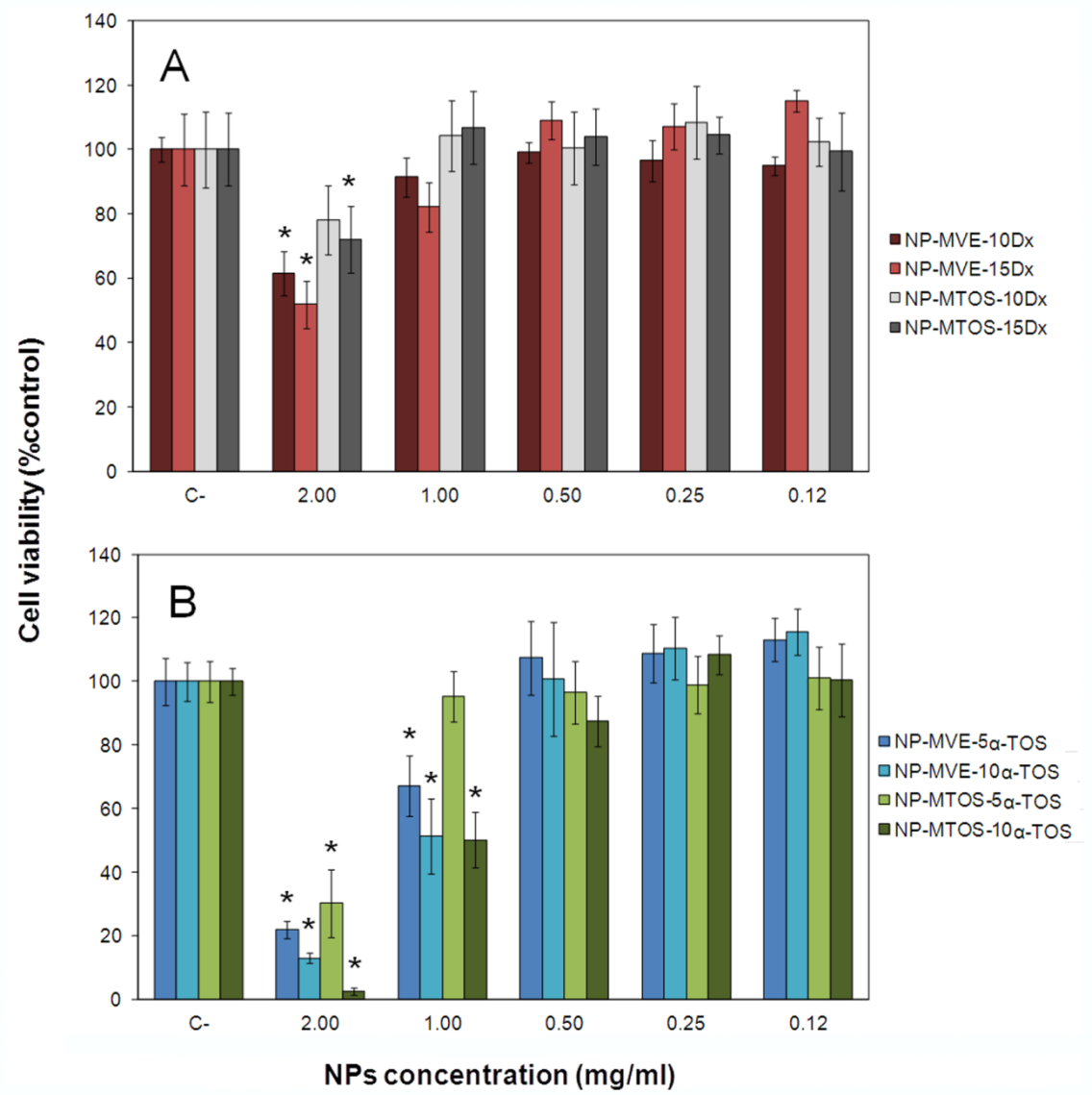

Figure 3: Cell viability of HEI-OC1 treated with different concentrations of Dx-loaded NPs (A) and α-TOS-loaded NPs (B) over 24 hours. The diagrams include the mean, the standard deviation (n = 8), and the ANOVA results (*p < 0.05).

Protection of CDDP-induced cytotoxicity in HEI-OC1 with high loading NPs formulations

After 4h of NPs exposure to HEI-OC1, 30 µM CDDP was added and kept in the cell culture over 24 h. Cell viability decreased between 40 and 50% when 30 µM CDDP was added to the cells (**Figure 4A** and **4B**).

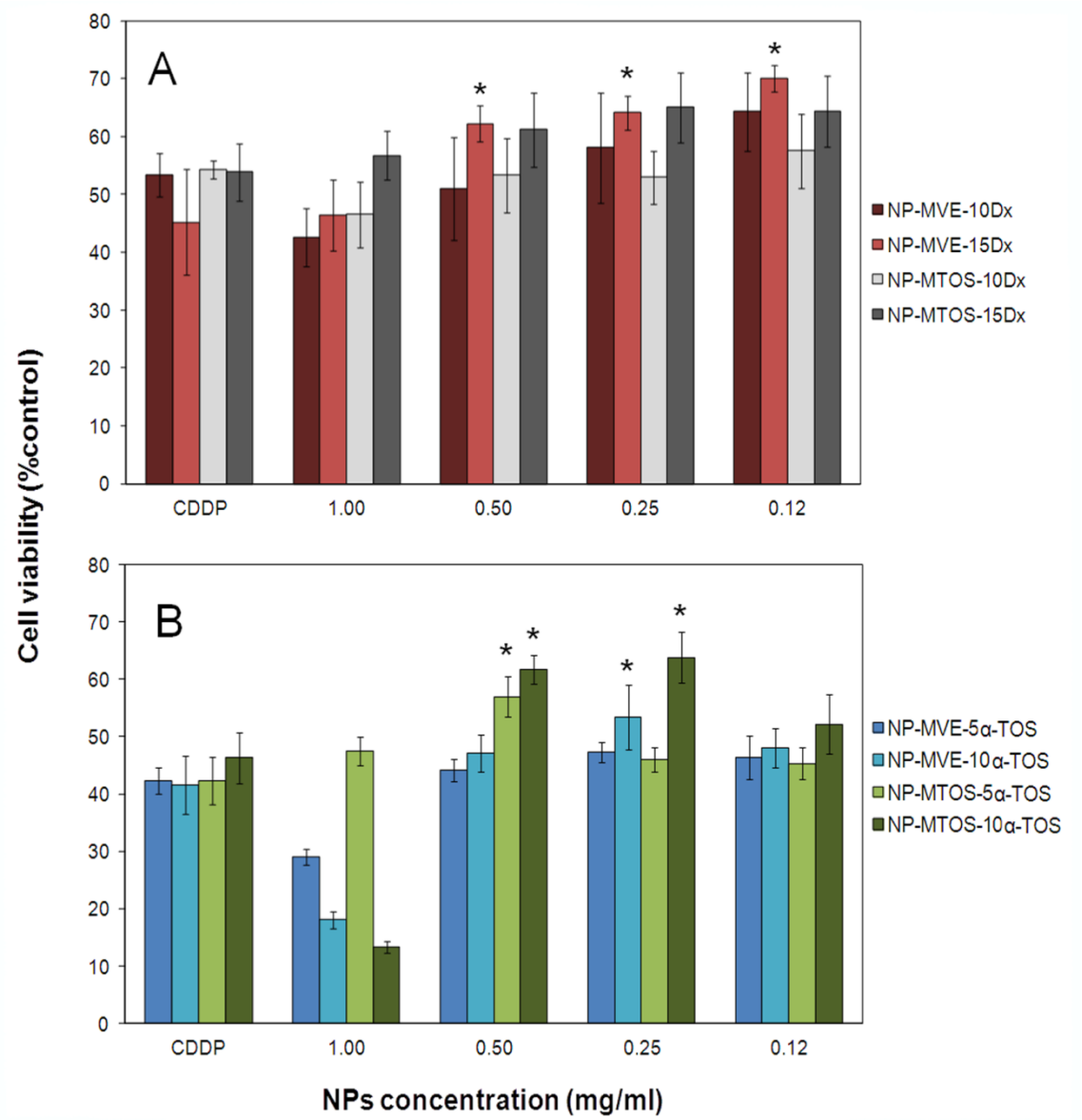

Figure 4: Cell viability of HEI-OC1 treated with different concentrations of Dx-loaded NPs (A) and α-TOS-loaded NPs (B) to inhibit the cytotoxic effect of 30 µM CDDP at 24 hours. The diagrams include the mean, the standard deviation (n = 8), and the ANOVA results (*$p < 0.05$).

Concentrations between 0.5 and 0.12 mg/ml NP-MVE-15Dx significantly reduced CDDP-induced cytotoxicity of 30 μM CDDP. NP-MTOS-15Dx slightly reduced CDDP-induced cytotoxicity although there were no statistically significant differences with CDDP-treated control. NP-MVE-10Dx and NP-MTOS-10Dx did not show statistically differences with only CDDP treated cells.

NP-MVE-10α-TOS and NP-MTOS-10α-TOS significantly protected HEI-OC1 from CDDP effects at 0.50 and 0.25 mg/ml. No significant differences between NP-MTOS-5α-TOS and NP-MTOS-10α-TOS at 0.50 mg/ml concentration were found.

NP-MVE-15Dx and NP-MTOS-10α-TOS significantly reduced CDDP cytotoxicity in a certain range of concentrations (20% when treated with NP-MVE-15Dx and 17% when treated with NP-MTOS-10α-TOS), being the most active formulations *in vitro*. NP-MVE-15Dx and NP-MTOS-10α-TOS were the most effective formulations *in vitro* against 30 μM CDDP (**Figure 4A** and **B** respectively). NP-MVE-10α-TOS also has a cytoprotector effect on HEI-OC1 and NP-MTOS-15Dx slightly increased cell viability of CDDP-treated cells but not in statistically significant way.

Down-regulation of CDDP-induction of caspase 3/7 activity after the treatment with NP

CDDP-induced caspase 3 expression was measured over 24 h (see **supplementary information Figure S1**). There was no difference between 16 and 24 hours in the expression, so the following assays were done at 16h. NP-MVE-15Dx, NP-MTOS-15Dx, NP-MVE-10α-TOS and NP-MTOS-10α-TOS ameliorate CDDP-induced caspase 3 expression in a statistically significant way with respect CDDP treated cells after 16 h of CDDP exposure. There is no statistically significant difference between formulations except NP-MTOS-10α-TOS that presents best down regulation of caspase 3/7 activity and has no difference with the negative control (**Figure 5A**).

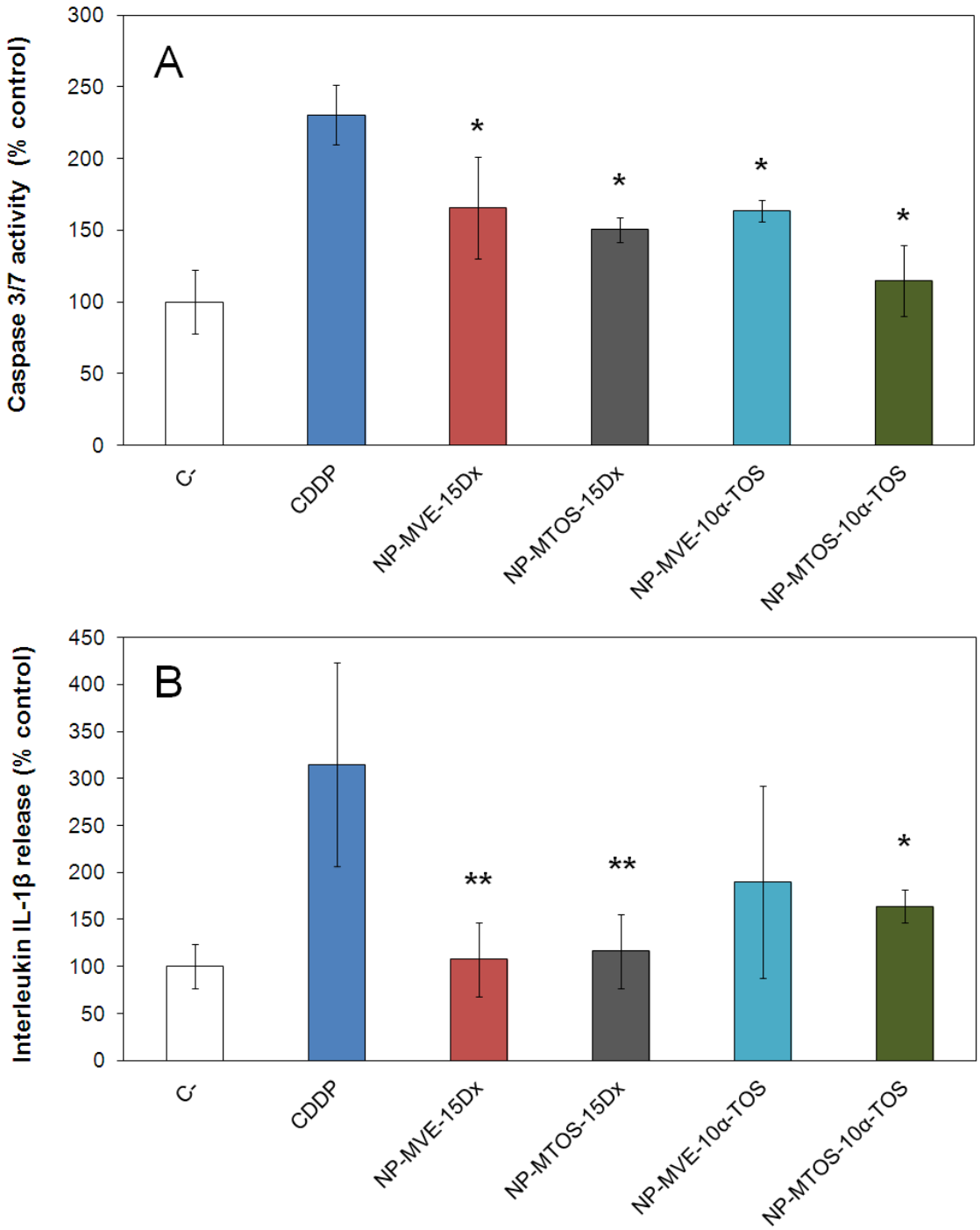

Figure 5: Caspase-3/7 expression when cells were treated with 20 µM CDDP and 0.25 mg/ml NP suspension at 16 hours (A). IL-1β release after treatment with 20 µM CDDP and 0.25 mg/ml NP suspension over 24 hours (B). The diagrams include the mean, the standard deviation (n = 8), and the ANOVA results (* $p< 0.05$ and ** $p< 0.01$ statistically significant with CDDP)

Down regulation of CDDP-induced IL-1β release after NP treatment

CDDP-induced IL-1β release was measured after 24 h of CDDP administration. NP-MVE-15Dx, NP-MTOS-15Dx and NP-MTOS-10α-TOS ameliorate CDDP-induced IL-1β release in a statistically significant way with respect CDDP treated cells after 24 h of CDDP exposure. There is no statistically significant difference between NP-MVE-10α-TOS formulation and CDDP treated cells, but this formulation slightly down regulate IL-1β release. Dx-loaded formulations present the best down regulation of IL-1β release (**Figure 5B**).

***In vivo* assay**

NP-MVE-C6 and NP-MTOS-C6 accumulation in IHC and OHC

NP-MTOS-C6 and NP-MVE-C6 were preferentially accumulated in the IHC than in OHC of the basal turn of the cochlea 2 hours after administration in the middle ear (**see supplementary data Figure S2**) as previously described by our group (Martín-Saldaña et al., 2015). Green fluorescence due to the accumulation of C6-loaded NP progressively decreased from the basal turn to the apical turn.

Control of NPs ototoxicity

In order to maximize NPs delivery to inner ear, the highest dose of NPs (2 mg/ml) was used even though it was toxic in the *in vitro* tests. NP formulations with best results *in vitro* were selected to *in vivo* assays. Two animals per formulation (NP-MVE-15Dx, NP-MTOS-15Dx, NP-MVE-10α-TOS and NP-MTOS-10α-TOS) were inoculated through a bullostomy in the right ear. These animals were not treated with CDDP after surgery although they did get the same palliative cares than the animals that received the chemotherapeutic treatment. After 72 hours of NPs exposure, no significant differences were observed between the auditory thresholds of the right ear and the left ear at all frequencies (**see supplementary information Figure S3**).

NP-MVE-15Dx and NP-MTOS-10α-TOS protects from CDDP-induced hearing loss in vivo

NP-MVE-15Dx and NP-MTOS-10α-TOS were active *in vivo* and showed protection against CDDP-induced hearing loss. NP-MVE-15Dx protected in a significant way in two frequencies (**Figure 6A**). The total protection in animals treated with this formulation was higher than the others, being statistically significant difference for 16 and 32 kHz.

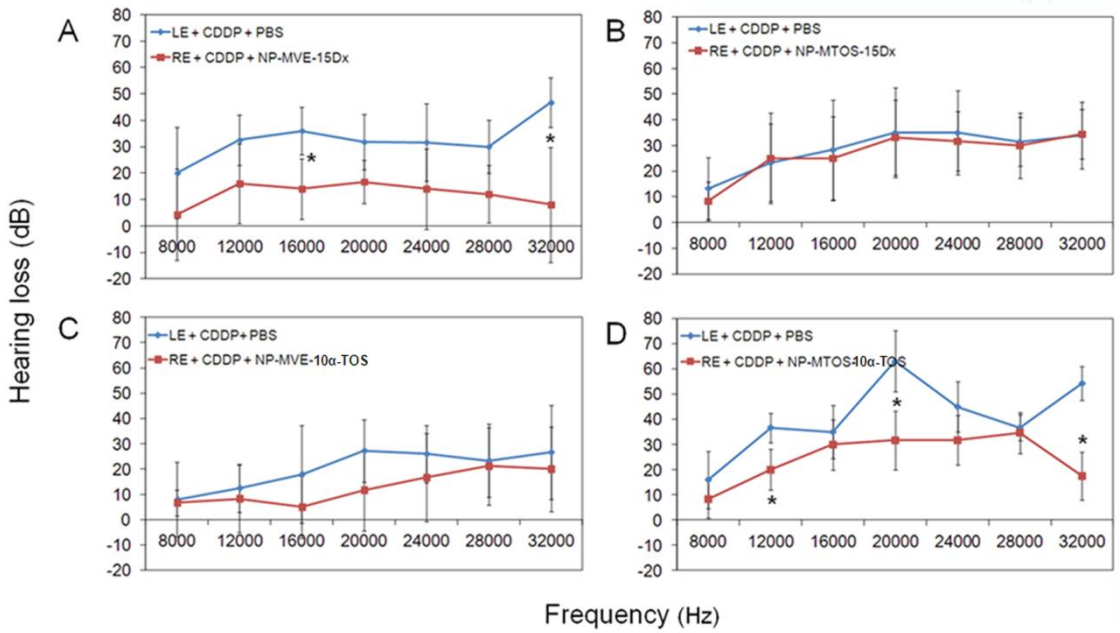

Figure 6: Hearing loss after local administration by bullostomy in right ear of NP-MVE-15Dx (A), NP-MTOS-15Dx (B), NP-MVE-10α-TOS (C) and NP-MTOS-10α-TOS (D) suspensions and intraperitoneal 10 mg/kg dose of CDDP (LE: left ear; RE: right ear). The diagrams represents the difference between hearing threshold after CDDP-administration and before treatment with the NP suspension (in the right ear) and CDDP-administration after 24 hours. Diagrams include the mean, the standard deviation (n = 6), and the independent TUKEY results (*$p < 0.05$).

NP-MTOS-15Dx and NP-MVE-10α-TOS showed no difference between the non treated left ear and NP treated right ear (**Figure 6B and 6C respectively**).

Animals that received NP-MTOS-10α-TOS treatment showed that auditory thresholds in sound frequencies of 12, 20 and 32 kHz were significantly lower in the protected right ear when compared with the auditory thresholds of the left ear (**Figure 6D**).

Discussion

A lot of experimental studies have attempted to find an ideal otoprotector against CDDP-induced ototoxicity. Different approaches have been assayed with several problems like: short half life of potential drugs, difficulties to cross biological barriers to the inner ear and interaction between the antitumor activity of CDDP and the treatment in the neoplasm. Nanotechnology is an appropriate approach to palliate all these issues and develop more efficient treatments to ameliorate CDDP-induced hearing loss because allows hydrophobic drugs to pass through biological barriers, and increases drug half-life.

Dx and α-TOS were incorporated in the core of the NPs in order to locally deliver the drug into the inner ear at appropriate concentrations and to increase its local activity and decrease its undesired side effects. Encapsulation efficiency of both drugs was higher for NP-MVE than NP-MTOS with each drug. CO-MVE has a higher content in the hydrophobic monomer MVE that could favor the encapsulation of the drugs (Martín-Saldaña et al., 2015, Palao-Suay et al., 2015). Better EE% was seen in α-TOS-loaded and C6-loaded NPs probably due to higher hydrophobicity of these molecules and the structural similarities of α-TOS and C6.

NPs with size lower than 200 nm efficiently pass through round window membrane in *in vivo* models (Bowe and Jacob, 2010), so all NPs synthesized in this research were adequate for this purpose, with diameters between 122 and 165 nm. This size was measured by DLS and corroborated by SEM. NPs size was constant when they were exposed to temperature trend from 24 to 42ºC. This fact suggests that the physical properties of the NPs do not changed when placed at physiological temperature.

As previously described by our group with NPs based on CO-MVE and CO-MTOS (Palao-Suay et al., 2015) all NPs presented an almost neutral charge surface, with slightly negative zeta potential between -7.23 to -3.23, indicating that NPs shell is constituted by VP-rich hydrophilic domains.

Esterase mediated drug release profiles of the systems followed a zero order kinetic during the first 2 weeks, followed by a non-linear period for longer periods of time (**Figure 2E**). The biological half-life of Dx in the inner ear is around 8 hours (Parnes et

al., 1999) and therefore, Dx sustained release is of great interest to its application as otoprotector of CDDP-induced toxicity. (Teng et al., 2005).

NPs were able to encapsulate C6 and were used to follow the cellular uptake process when added to a HEI-OC1 cell culture. The fluorescence of C6 entrapped NPs was quantified in cell culture over 8 h after the NP incubation and the accumulation in the cells gradually increased over time in both formulations (**Figure 2F**). After 2 hours, accumulation of C6 in cells treated with NP-MVE-C6 was significantly higher than cells treated with as NP-MTOS-C6. That is probably related in part with better EE% in MVE formulations. These results showed that both formulations entered in HEI-OC1 cells.

Dx and α-tocopherol (Niki, 2014) are two slow-acting free radical scavengers, and they have been shown to ameliorate ototoxicity in animals receiving CDDP (Paksoy et al., 2011). α-TOS was shown to selectively kill malignant cells at concentrations that are non-toxic for normal cells. In non-malignant cells α-TOS is hydrolyzed by means of esterases (Dong et al., 2008). As a result of the hydrolysis, Vitamin E is gradually released to prevent membrane oxidative damage. All the NPs formulations derived from Vitamin E or α-TOS were tested in HEI-OC1 in order to check its cytotoxicity, resulting no cytotoxic at concentrations lower than 1.0 mg/ml of NPs in Dx-loaded formulations and lower than 0.5 mg/ml of NPs in α-TOS-loaded formulations. *In vitro* test showed that at 2.0 mg/ml NP-MTOS-10α-TOS was significantly the most cytotoxic formulation probably due to the higher amount of α-TOS loaded in this formulation if considering the entrapped drug and the α-TOS conjugated to the copolymer (**Figure 3**).

Supporting these results NP-MVE-15Dx and NP-MTOS-15Dx at 0.5 mg/ml were able to significantly reduce caspase-3/7 activity in cells treated with CDDP during 16 hours (**Figure 5B**). The use of corticoids like Dx when use as co-treatment causes resistance to CDDP-induced apoptosis in carcinoma cells (Herr et al., 2003) and other tumor cells from bone, brain, breast, cervix, melanoma and neuroblastoma (Zhang et al., 2006) with a significant reduce in caspase-3 expression. NP-MVE-10α-TOS and NP-MTOS-10α-TOS also reduced caspase-3 expression. NP-MTOS-10α-TOS was the best formulation ameliorating this pro-apoptotic way, even showing no statistically significant difference with negative control (**Figure 5B**). Kruspig *et al* (Kruspig et al., 2013) showed a contrasting effect against CDDP-induced cytotoxicity when cells were treated with

relatively low concentrations of α-TOS, below 40 μM, when the drug was supposedly cleaved by cellular esterases and regulate ROS production. García-Berrocal *et al*. (García-Berrocal et al., 2007) previously described that cochlear cells like the interdental cells of the spiral limbus, inner sulcus cells, IHCs and OHCs and Hensen's cells presented significant expression of the executioner caspase-3 after CDDP injection. In the same way Wang *et al* (Wang et al., 2004) demonstrated that the intracochlear perfusion of caspase-3 inhibitor (z-DEVD-fmk) drastically reduced the ototoxic effects of CDDP. Kalinec *et al* (Kalinec et al., 2016) recently described the potential of HEI-OC1 cells as a model to investigate biological responses associated with auditory cells. Due to that fact, the down regulation of pro-apoptotic biomarkers like caspase-3 and IL-1β of Dx and α-TOS-loaded NPs, and the protection against CDDP-induced cytotoxicity *in vitro* suggested that these formulations could reduce ototoxicity in an *in vivo* model.

CDDP rapidly causes ototoxicity with a high incidence, affecting the apical turn of the cochlea and consequently the high frequencies. Due to that toxicity an increase in auditory threshold is shown for frequencies located in the apical turn of the cochlea corresponding to higher frequencies. CDDP entry into OHC results in cell death, which appears to be primarily caspase-dependent (Rybak and Ramkumar, 2007). CDDP-induced apoptosis in the inner ear could be due to the activation of different pathways. Caspase dependent pathway that culminates in the activation of caspase 3 which cleaves several substrates resulting in chromosomal DNA fragmentation and cellular morphologic changes characteristic of apoptosis.

Another pathway that could trigger to CDDP-induced apoptosis is due to inflammatory mechanisms that contribute to the cell destruction by up regulation of proinflammatory cytokines like TNFα, IL-1β and IL-6 (Casares et al., 2012). Inflammation plays an important role in CDDP-induced apoptosis in the cochlea. Corticosteroid therapy reduces inflammation and inhibits apoptosis while activating pro-survival pathways in the organ of Corti following exposure to CDDP or other ototoxic events like gentamicin treatment (Bas et al., 2012). The literature on administration of Dx against CDDP-induced ototoxicity presents a big variability of protective effects in animal models in a dose dependent manner and related with the way of administration. Hargunani *et al* (Hargunani et al., 2006) studied the time of diffusion of Dx 21-phosphate from middle

to inner ear and showed it in the inner ear within 15 minutes by inmunohistochemistry, reaching their highest staining intensity at 1 hour. The strongest staining occurred in the spiral ligament, Organ of Corti, spiral ganglion, and vestibular sensory epithelia. Administration of NP-MVE-15Dx, with the highest loading of corticoid, ameliorates CDDP-induced hearing loss in all the frequencies measured probably due to its better EE% of corticoid. However, only for 16 kHz and 32 kHz the protection was statistically significant (**Figure 6A**) but total hearing protection was the best in all the formulations tested (**see supplementary data Figure S4**).

CDDP significantly increased intracellular ROS accumulation especially dependent of the mitochondria that significantly contributes to cell death (Marullo et al., 2013). Antioxidants like flunarizine (So et al., 2006), metformin (Chang et al., 2014) or bucillamide (Kim et al., 2015) could reduce the level of ROS generated by oxidative stress ameliorating cell death induced by CDDP. α-TOS was used in the present work as a drug with specific target in the mitochondria treating to reduce the CDDP-induced ROS generation as consequence of its direct effect on mDNA. α-TOS effect on CDDP-induced ototoxicity can be due to its ability to monopolize the respiratory chain of mitochondria by targeting ubiquinone-binding sites in mitochondrial respiratory complex II (Dong et al., 2008) exerting a regulatory effect on ROS production decreasing oxidative stress induced by CDDP. Teranishi *et al* (Teranishi et al., 2001) showed that the CDDP-induced ototoxicity and nephrotoxicity were suppressed by a combined treatment of intraperitoneal vitamin E that is present in CO-MVE. α-TOS when used at low concentrations can suppress apoptosis induced by CDDP. Of the two cleavage products of α-TOS, α-tocopherol (Vitamin E) and succinate, the most protective was succinate (Kruspig et al., 2013). That fact could explain that NP-MTOS-10α-TOS, with only 10% less EE% than NP-MVE-10α-TOS formulation, with the presence of the methacrylic derivative of α-TOS in the polymer CO-MTOS, showed great results protecting against hearing loss *in vivo* (**Figure 6D**). Protection of CDDP-induced hearing loss was statistically significant in 12, 20 and 32 kHz frequencies. Auditory thresholds in the protected right ear for these frequencies decreased more than 10dB than in the non protected left ear, so the protection was higher.

Conclusions

New protective agents based on bioactive polymeric nanoparticles loaded with Dx or α-TOS as anti-inflammarory and anti-apoptotic molecules were successfully developed. The drugs were incorporated in the hydrophobic core of nanoparticles and presented appropriate hydrodynamic properties. In vitro biological test showed lower CDDP-induced toxicity, downregulation of caspase 3/7 expression, and lower IL-1β release, while in vivo experiments demonstrated a reduced hearing loss. The local administration of the nanoparticles by bullostomy provided an adequate biological activity locally, without systemic interference with the quimiotherapeutic effect of CDDP.

Acknowledgments

Authors acknowledge David Gómez, Rosa Ana Ramírez, Carlos Vargas, and Enrique Blazquez and Isabel Quijada for their help in SEM, cell culture, histology experiments, and gas chromatography experiments respectively. Authors also thank Dr. Kalinec for providing HEI-OC1 cells for the experiments.

Funding sources

This work was funded by the Spanish Ministry of Economy and Competitiveness (MAT2014-51918-C2-1-R), Spanish FIS Grant PI 11/00742, CIBER BBN-ECO Foundation project, and the Autonoma University of Madrid Research Foundation.

pH-sensitive nanoparticles with antioxidant and anti-inflammatory properties against cisplatin-induced hearing loss

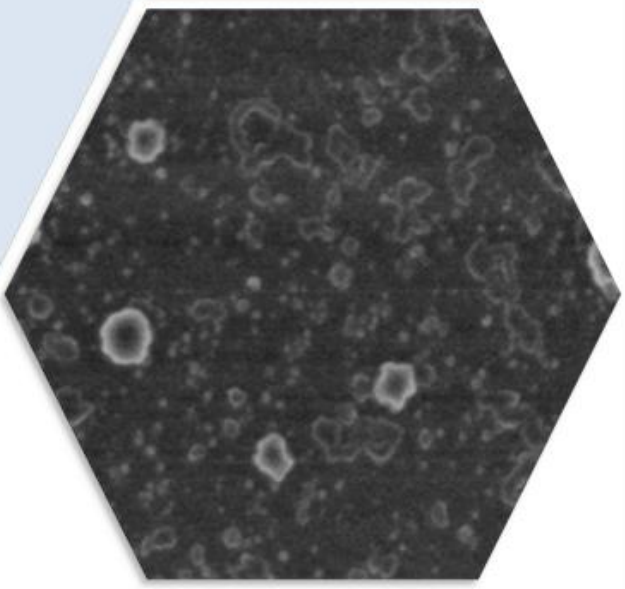

Resumen

Dado los buenos resultados obtenidos con las NPs poliméricas basadas en los copolímeros anfifílicos derivados de la vitamina E y el α-TOS, se planteó la posibilidad de desarrollar sistemas nanoparticulados basados en una mezcla de copolímeros anfifílicos capaces de formar NPs mediante el método de nanoprecipitación, de manera que se otorgara a las mismas nuevas propiedades que optimizaran la liberación de los fármacos en micro ambientes pro inflamatorios, tales como el generado en el oído interno tras el tratamiento con CDDP.

Para ello, se utilizaron, además de los copolímeros previamente utilizados en los trabajos de la tesis, copolímeros basados en el derivado metacrílico de ibuprofeno (HEI), como segmento hidrofóbico, y en 1-vinilimidazol (VI), como segmento hidrofílico. Estos copolímeros fueron previamente sintetizados en el grupo, y mostraron tener capacidad anti-inflamatoria, lo que podría suponer un efecto positivo añadido a los sistemas nanoparticulados para tratar de paliar el efecto del CDDP en las células auditivas. Además de esto el VI presenta sensibilidad a pH, con un pKa en torno a 6, lo que podía suponer una ventaja a la hora de liberar el fármaco en un entorno inflamatorio, en el que pH decrece con respecto al de un tejido sano.

En base a esto, se desarrollaron nuevos sistemas poliméricos basados en HEI-VI combinado correctamente con CO-MTOS o CO-MVE con el fin de obtener NPs autoensambladas, con propiedades adecuadas con respecto a su tamaño, carga y punto isoeléctrico (pI) con el fin de favorecer la ionización de VI en el entorno ligeramente ácido del tejido inflamado debido al aumento de ROS y a la liberación de citoquinas tras el tratamiento con CDDP, y favorecer así la liberación del compuesto activo encapsulado en el oído interno.

El resultado fue la obtención de NPs que presentaban diámetros hidrodinámicos adecuados para ser utilizados como nanovehículos al oído interno, y con capacidad de vehiculizar moléculas hidrófobas pequeñas como cumarina-6 (sonda fluorescente para determinar el pI) o dexametasona (como compuesto bioactivo) que aumentaran la posible actividad biológica de las NPs frente al efecto ototóxico del CDDP.

pH-sensitive nanoparticles with antioxidant and anti-inflammatory properties against cisplatin-induced hearing loss

Sergio Martín-Saldaña[1, 2], Raquel Palao-Suay[2,3], Humberto Arévalo[4], María Rosa Aguilar[2,3*], Luis García-Fernández[2], Rafael Ramírez-Camacho[1§], Julio San Román[2,3§]

[1]Ear Research Group, Universitary Hospital Puerta de Hierro Majadahonda- Health Research Institute Puerta de Hierro, Madrid, Spain

[2]Group of Biomaterials, Department of Polymeric Nanomaterials and Biomaterials, Institute of Polymer Science and Technology, CSIC, C/ Juan de la Cierva, 3, 28006 Madrid, Spain

[3]Networking Biomedical Research Centre in Bioengineering, Biomaterials and Nanomedicine,
CIBER-BBN, Spain

[4]Simón Bolivar University, Caracas, Venezuela

KEYWORDS: anti-inflammatory, anti-oxidant, ototoxicity, cisplatin, nanoparticles, dexamethasone, ibuprofen

INTRODUCTION

Nanomedicine represents one of the most attractive tools to develop new therapies to effectively reach the inner ear (Pritz et al., 2013). In this sense, polymer therapeutics, and more specifically polymer drugs (a polymer where a drug has been covalently attached), offer the opportunity to obtain bioactive macromolecules with improved pharmacological properties and can be designed with amphiphilic properties that give rise to the formation of micelles or vesicles through self-assembled mechanisms.

These polymeric nano-assemblies have several advantages if compared to other traditional treatments. Particularly, the core of the polymeric nanoparticles (NPs) can be used to encapsulate hydrophobic drugs, improving their bioavailability, decreasing their toxicity and protecting them from degradation processes (Martín-Saldaña et al., 2016).

However, one of the most relevant limitations of NPs drug delivery systems is their poor cellular internalization that significantly reduces the intracellular dosages of drugs to the level below the therapeutic window (Du et al., 2011). In this sense, intelligent-responsive delivery systems have opened the possibility to counteract this limitation, (Traitel et al., 2008, Aguilar and Roman, 2014).

Among the different types of stimuli, pH-responsiveness is one of the most frequently used to design nano-system for drug delivery for the treatment of inflamed tissues where the pH is ranged from 5.5 to 6.8 as a result of the high rate of glycolysis and an increase in lactic acid concentration in affected cells, averaging 0.2– 0.6 units lower than mean extracellular pH of normal tissues (Lardner, 2001). Additionally, significant differences can be also found in the pH into different cellular organelles. For instance, pH of endosome and lysosome are even lower than 5.5. This is particularly relevant in the case of polymeric NPs, that are frequently uptaken by endocytosis within endosomal and lysosomal compartments (Liu et al., 2014, Pyykkö et al., 2015).

Inflammation and reactive oxidative species (ROS) accumulation are closely related to cisplatin (CDDP) induced apoptosis of cochlear cells, wich leads to a severe hearing loss (Marullo et al., 2013, Casares et al., 2012, Rybak et al., 2009). In spite of serious side effects related to the treatment with high doses (up to 80 mg/m^2) of CDDP, the

platinum-based cytostatic is still being used due to its high efficacy in the treatment of several solid tumors, such as non-small cell lung cancer (Fennell et al., 2016) or testicular cancers (Einhorn, 2002). Over 60% of pediatric patients developed irreversible hearing loss when treated with CDDP, which delays educational and psychosocial development (Karasawa and Steyger, 2015).

CDDP efficacy against tumor cells is principally due to DNA damage which leads to apoptosis. Although, cochlear and stria vascularis cells have low rates of proliferation and they are prone to CDDP-induced apoptosis. One of the major causes of CDDP-induced ototoxicity is related to reactive oxygen species (ROS) generation (Marullo et al., 2013). Although, the mechanism which describes ROS-induced cytotoxicity of cochlear cells remains unclear, all the mechanisms previously described of CDDP-induced ototoxicity involves oxidative stress. For example, NADPH oxidase 3 (NOX3), which is highly expressed in cochlear cells is a major source of ROS and leads to inflammation and cell death when after CDDP treatment, which results in hearing loss (Mukherjea et al., 2011).

The design of an effective pH sensitive drug delivery system for the effective treatment of associated inflammatory process related to CDDP-induced ototoxicity is an important goal of our society. In this sense, our group has extensive experience in the preparation of nanovehicles to transport toxic and hydrophobic anticancer and anti-inflammatory drugs (Donaire et al., 2009, García-Fernández et al., 2010, Reyes-Ortega et al., 2013).

On the one hand, α-tocopheryl succinate (α-TOS) is a well-known mitocan (mitochondially targeted anticancer compound) with demonstrated anticancer and antiangiogenic properties (Neuzil et al., 2001, Duhem et al., 2014). α-TOS selectively induces apoptosis of cancer cells and apoptosis of proliferating endothelial cells by the increase of ROS levels and induction of the intrinsic pathway of apoptosis (Dong et al., 2008). Our group has recently described the synthesis and biological activity of bioactive NP based on α-TOS-bearing copolymer drugs (Palao-Suay et al., 2015). Specifically, *N*-vinylpyrrolidone (VP) was copolymerized with a methacrylic derivative of α-TOS or vitamin E (MTOS and MVE, respectively) and formed pseudo-block copolymers due to the marked difference in their reactivity ratios and hydrophilicity. This copolymers (in particular, poly(VP-*co*-MTOS)(89:11) and poly(VP-*co*-MVE)(60:40)) demonstrated their potential as nanocarriers for drug delivery to the inner

ear, reducing CDDP-induced ototoxicity *in vitro* and *in vivo* by the encapsulation of 6α-methylprednisolone in the inner core of the NPs (Martín-Saldaña et al., 2016). Moreover, recent studies by Kim et al. (Kim et al., 2016) support the effectiveness of α-TOS acting as ROS scavenger in CDDP-induced cytotoxicity in the auditory cell line HEI-OC1 resulting in a significant reduce of apoptosis.

Alternatively, ibuprofen is one of the most commonly used non-steroidal anti-inflammatory drug (NSAIDs) for the treatment of inflammatory diseases in our society. Due to its quite hydrophobicity and therefore its difficult effective administration, Suarez et al. synthesized amphiphilic copolymer based on a methacrylic derivative of ibuprofen HEI and 1-vinylimidazol (VI) (Suárez et al., 2013). In fact, VI was selected due to its hydrophilicity, pH sensitivity (pKa of VI is around 6) (Velasco et al., 2012). However, the pKa of synthesized copolymers was too low for their application in an inflammatory microenviroment.

For that reason, the aim of this work was the synthesis, characterization, *in vitro* and *in vivo* evaluation of pH-sensitive NP with antioxidant and anti-inflammatory properties by the combination of amphiphilic bioactive copolymers with the mentioned properties and the formation of surfactant-free self-assembled NPs by nanoprecipitation which could ameliorate CDDP-induced apoptosis in the inner ear. For this purpose, new poly(VI-*co*-HEI) (94:6) or (86:14) were synthesized by free radical copolymerization using the methodology that was previously described by our group.

New HEI-based polymeric systems were properly combined with poly(VP-*co*-MTOS)(89:11) or poly(VP-*co*-MVE)(60:40) in order to obtain self-assembled NPs with optimal properties regarding to size, charge and isoelectric point (pI), in order to favor VI ionization in the slightly acid environment of the tissue due to ROS increase and inflammation generated by CDDP treatment and induce the release of the encapsulated active compound in the inner ear. In fact, the resulted NP presented appropriate hydrodynamic diameters to be used as nanovehicles and were able to encapsulate hydrophobic small molecules, as coumarin-6 (fluorescent probe) or Dx (bioactive compound) that enhanced the biological activity of the NP.

MATERIALS AND METHODS

Reagents

Dimethylsulfoxide (DMSO, Scharlau) was used without further purification and 2,2'-azobisisobutyronitrile (AIBN, Merck) was recrystallized from ethanol for the preparation of amphiphilic copolymers. Deuteraded DMSO (DMSO_d_6, Merck) and chromatographic grade dimethylformamide (DMF, Scharlab) were used without further purification to characterize polymeric systems. Additionally, 1,4-dioxane (Panreac), tetrahydrofuran (THF, Scharlau), ethanol (EtOH, Merck), phosphate buffered solution at pH 7.4 (PBS, Sigma-Aldrich), coumarin-6 (Sigma-Aldrich) and α-tocopheryl succinate (α-TOS, Sigma-Aldrich) were used without further purification to prepare self-assembled NP.

Monomers

N-vinyl pyrrolidone (VP, Sigma-Aldrich) was purified by distillation under reduced pressure and 1-vinylimidazole (VI, Sigma-Aldrich) was used without further purification. The methacrylic derivatives of ibuprofen (HEI) (Suárez et al., 2013), α-tocopherol (MVE) and α-tocopheryl succinate (MTOS) (Palao-Suay et al., 2015)were synthesized as described by our group elsewhere.

Poly(VP-co-MVE) and poly(VP-co-MTOS)

Poly(VP-co-MVE) and poly(VP-*co*-MTOS) with a copolymer molar composition of VP:MVE 60:40 and VP:MTOS 89:11 (from now on MVE-40 and MTOS-11, respectively) were synthesized as recently described by our group (Palao-Suay et al., 2015).

Poly(VI-co-HEI)

Two copolymers based on VI and HEI were obtained by free radical polymerization with copolymer molar compositions of VI:HEI (94:6) and (86:14) (from now on HEI-6 and HEI-14), according to the procedure previously described by our group (Palao-Suay et al., 2015).

Synthesis of unloaded, Dx and coumarin-6 loaded NP

Self-assembled NPs were synthesized by nanoprecipitation as previously described (Fessi et al., 1989).

NP based on poly(VP-co-MTOS) or poly(VP-co-MVE) and poly(VI-co-HEI)

MTOS-11 or MVE-40 and HEI-6 or HEI-14 (10 or 20 % w/w) were dissolved in THF:EtOH (50:50 v/v) at a concentration of 50 mg/mL. In the case of loaded NP, Dx or coumarin-6 (10 % and 1% w/w respect to the polymer) was dissolved in THF and added to polymer solution. Afterwards, the organic solution was added drop by drop over PBS under constant magnetic stirring to obtain a final polymer concentration of 2.0 mg/mL.

After the nanoprecipitation, milky NP dispersions were dialyzed against PBS during 72 h in order to remove the organic solvent and unloaded Dx or coumarin-6. NP suspension was sterilized by filtration through 0.22 µM polyethersulfone membranes (PES, Millipore Express®, Millex GP) and stored at 4 ºC before biological studies.

Dx and coumarin-6 encapsulation efficiency (EE)

Dx and coumarin-6 loaded NP were freeze dried in order to eliminate the aqueous phase, obtaining an amorphous powder in both types of NP. Afterwards, Dx and coumarin-6 entrapped in self-assembled NP was measured by absorbance and fluorescence spectroscopy, respectively. For this purpose, Dx (2.5 mg/mL) or coumarin-6 (2 mg/mL) loaded NPs were dissolved in EtOH at room temperature for 24 h. On the one hand, Dx absorbance was measured with an excitation wavelength of 239 nm using a Perkin Elmer Lambda 35 UV/VIS spectrophotometer. On the other hand, fluorescence of coumarin-6 was quantified with an excitation wavelength of 485 nm and a maximum emission of 528 nm using a Biotek SYNERGY-HT plate reader. In both cases, the absorbance or fluorescence was correlated with drug concentration using a calibration curve that was previously obtained using a range of drug concentrations between 1 – 0.001 mg/mL in ethanol.

The encapsulation efficiency (EE) was defined as the ratio of calculated and original amount of coumarin-6 or Dx encapsulated in the NP. The calculation equation is as follows:

[1]

Being $[\text{loaded molecule}]_i$ the concentration of the molecule (coumarin-6 or α-TOS) encapsulated in the inner core of the NP and detected experimentally, and $[\text{loaded molecule}]_0$ the concentration of the molecule added in the nanoprecipitation process.

Characterization of the NPs

Scanning electron microscopy (SEM)

The morphology of NPs was observed using scanning electron microscopy (SEM) SEM analysis was performed with a Hitachi SU8000 TED, cold-emission FE-SEM microscope working with an accelerating voltage between 15 and 25 kV. Samples were prepared by deposition of one drop of the corresponding NP suspension over small glass disks (12 mm diameter and 1 mm thickness), and evaporation at room temperature. Finally, the samples were coated with gold palladium alloy.

Particle Size Distribution

The particle size distribution of the NP suspensions was determined by dymanic light scattering (DLS) using a Malvern Nanosizer NanoZS Instrument equipped with a 4mW He-Ne laser (λ=633 nm) at a scattering angle of 173°. Measurements of NP dispersions were performed in square polystyrene cuvettes (SARSTEDT), and the temperature was kept constant at 25 ºC. The autocorrelation function was converted in an intensity particle size distribution with ZetaSizer Software 7.10 version, to get the mean hydrodynamic diameter (D_h) and the particle dispersion index (PDI) between 0 (monodisperse particles) and 1 (polydisperse particles) based on the Stokes-Einstein equation, assuming the particle to be spherical. For each sample, the statistical average and standard deviation of data were calculated from 8 measurements of 20 runs each one.

Zeta potential measurements: determination of isoelectric point (pI)

The zeta potential of NP dispersions was measured by laser Dopper electrophoresis (LDE) using a Malvern Nanosizer NanoZS Instrument. Particularly, NP formulations were prepared at 0.4 mg/mL in a saline solution (NaCl 100 mM). The zeta potentials were automatically calculated from the electrophoretic mobility at an applied voltage of 30 mV, using the Smoluchowski´s approximation. The pI values of different NP formulations were calculated when their zeta potential is zero. The pH of NP dispersions was changed by acid-base titration. Specifically, HCl (1M) was used to change the pH of NP dispersion between 2 and 10 and NaOH (0.1 M) was used as a titrant.

In vitro coumarin-6 release

Coumarin-6 loaded NPs were prepared in 10 mL of saline solution (NaCl, 100 mM), obtaining a neutral pH. Afterwards, pH was varied with HCl and NaOH (0.1 N) under magnetic stirring at room temperature. At desired pH values, the fluorescence intensity of coumarin-6 was quantified by fluorescence spectroscopy ($\lambda_{excitation}$ = 485 nm and $\lambda_{emission}$ = 528 nm) using a Biotek SYNERGY-HT plate reader and the size of NPs was evaluated by DLS as it was previously described.

Entrapment efficiency (EE%)

Dx loaded NP-MVEH14 and NP-MTOSH14 were freeze dried in order to eliminate aqueous phase. White amorphous powder was obtained in all types of NPs with a yield higher than 90 %. The freeze-dried NPs were dissolved in 2 ml of chloroform over 24 hours. After that, ethanol was added in agitation over 24 hours to precipitate the polymer. Samples were centrifuged at 10.000 rpm and supernatant was analyzed by UV (Dx λ= 239 nm).

Esterase-mediated Dx release

High performance liquid chromatography

5 mL of Dx-loaded NPs (NP-MVEH14-10Dx, NP-MTOSH14-10Dx) with 15 u/mL of esterase from porcine liver (Sigma-Aldrich) were dialyzed against 10 mL of PBS at 37 °C using a 3.5-5 kDa MWCO membrane (Spectrum Laboratories). After certain periods, 1 mL of the dialyzing medium was withdrawn and the same volume (1 mL) of PBS was replenished. Dx concentration was measured by HPLC (Shimadzu). The separation was performed on a C18-column (4.6 mm × 250 mm, Agela Technologies) at 30°C. The mobile phase was a mixture of acetonitrile, and distillated water (80:20, v/v) pumped at a rate of 1 mL/min. The UV detector was set at λ_{abs} =239 nm for Dx. The experiment was carried out in triplicate.

In vitro biological activity

Cell culture

The HEI-OC1 cell line was a kind gift from Dr. Federico Kalinec (House Ear Institute, Los Angeles, CA). HEI-OC1 cells were maintained over permissive conditions in high-

glucose Dulbecco's modified Eagle's medium (DMEM; Sigma, Saint Louis, MO, USA) supplemented with 10% fetal bovine serum (FBS; Gibco, BRL), 5% L-Glutamine (Sigma, Saint Louis, MO, USA) and Penicillin-G (Sigma, Saint Louis, MO, USA) at 33 °C in a humidified incubator with 10% CO_2.

Endocytosis of C6 loaded NPs

C6-loaded NPs were used as a model of endocytosis of the NPs in cell culture. HEI-OC1 cells were seeded into 6 well plates at $1x10^5$cells/mL, in complete DMEM. The cells were incubated overnight at 33ºC and 10% CO_2. The medium was replaced with the corresponding NP suspension in PBS (1 ml of the NP suspension and 1 ml of DMEM) and incubated over different times from 1 hour to 8 hours at 33 ºC. Cells were harvested (and counted to normalize fluorescence/cell) at 1, 2, 4, 6 and 8 hours after NPs addition, and were washed with cold PBS and centrifugate at 10.000 rpm. Supernatant was discarded and cell's pellet was lysate with ethanol to free endocyted C6. Fluorescence of supernatant at 458/540 nm (excitation/ emission) was measured on a Multi-Detection Microplate Reader Synergy HT (BioTek Instruments; Vermont, USA).

NPs toxicity and otoprotection assay

3000 live cells/well were seeded in a 96 well-plate under permissive conditions. Cells were exposed to different concentrations of NPs suspension (2.00, 1.00, 0.50, 0.25 and 0.12 mg/ml) and viability was determined.

To measure NPs cell protection against CDDP, cells were treated under the same concentrations of NPs and 30 µM CDDP for the period of 24 hours in DMEM without FBS to avoid uncontrolled cell growth. CDDP was added 4 hours after NPs administration to allow for NPs endocytosis by cells.

AlamarBlue® (Invitrogen) was used to determine cell viability. Absorbance at 570 nm was measured on a Multi-Detection Microplate Reader Synergy HT (BioTek Instruments; Vermont, USA). The treatments were done in replicates (n=8). Results of the experiments are expressed as percentage of relative cell viability (% with respect of control).

Caspase-3/7 activity measurement

HEI-OC1 cells were incubated with 20 µM CDDP dose over different times between 1 and 24 hours to determine the maximum caspase 3/7 activity. 0.25 mg/ml of NPs were added and after 4 hours 20 µM CDDP dose was added to each well. CDDP-induced Caspase-3 activation were estimated 16 hours after CDDP addition with the colorimetric assay EnzChek® Caspase-3 Assay Kit #2 (Molecular Probes, Inc) following the manufacturers protocol.

Interleukin IL-1β release

HEI-OC1 cells were incubated with 20 µM CDDP dose over 24 hours. Then, cells were exposed to CDDP and different NPs formulations at 0.25 mg/ml (added after 4 hours of CDDP addition) and CDDP-induced IL-1β release was measured by ELISA IL-1β mouse kit (BioSource International, Camarillo, CA) following the manufacturers protocol.

Reactive Species Quantification (Total ROS/RNS)

Total ROS/RNS free radical activity was measured by the OxiSelect In Vitro ROS/RNS Assay Kit. The assay employs a dichlorodihydrofluorescein DiOxyQ (DCFH-DiOxyQ), which is a specific ROS/RNS probe. For this purpose, supernatants of HEI-OC1 cultures, after being in contact with PBS, NPs, or NPs and CDDP (50 µL each), were added to the wells with 50 µL of a catalyst included in the kit (diluted in PBS at 1:250) in order to accelerate the oxidative reaction. After a brief incubation, 100 µL of the prepared DCFH probe was added to each well. The samples were measured fluorometrically against DCF standard and free radical content was determined by comparison with the predetermined DCF curve. Relative fluorescence was Multi-Detection Microplate Reader Synergy HT (BioTek Instruments; Vermont, USA) at 480 nm excitation/530 nm emission.

***In vivo* experiments**

Thirty two healthy Wistar rats weighting 180-280 g were used. All animals were housed in plastic cages with water and food available *ad libitum*, and maintained on a 12 h light/dark cycle. Rats with signs of present or past middle ear infection were discarded. Animals were randomly assigned to different groups (**Table 1**).

Table 1: Experimental groups (IP; intraperitoneal administration)

NPs name	N	Encapsulated Dx (% w/w)	CDDP IP (10 mg/kg)
NP-MVE HEIcoVI10-10Dx	2	10	-
NP-MTOS HEIcoVI10-10Dx	2	10	-
NP-MVE HEIcoVI10-10Dx	2	10	+
NP-MTOS HEIcoVI10-10Dx	6	10	+

The animals were handled according to the guidelines of the Spanish law for Laboratory animals care registered in the "Real Decreto 53/2013" and the European Directive 2010/63/EU. The study was approved by the Clinical Research and Ethics Committee of the University Hospital Puerta de Hierro (PROEX 022/16).

Experimental procedure

An initial auditory steady-state responses (ASSR) test was performed on all anesthetized animals. An insert earphone (Etymotic Research ER-2) was placed directly into the external auditory canal. Subcutaneous electrodes were placed over the vertex (active) and in the pinna of each ear (reference). Ground electrodes were placed in the right leg muscles. ASSR were recorded using an evoked potential averaging system (Intelligent Hearing System Smart-EP) in an electrically shielded, double-walled, sound-treated booth in response to 100 ms clicks or tone burst at 8, 12, 16, 20, 24, 28, 32 kHz with 10 ms plateau and 1 ms rise/fall time. Intensity was expressed as decibels sound pressure level (dB SPL) peak equivalent. Intensity series were recorded, and an ASSR threshold was defined by the lowest intensity able to induce a replicable visual detectable response.

Following the ASSR measurements the right ear bulla was surgically approached and opened and 50 µl of NPs suspension were injected in the middle ear by bullostomy using a spinal needle (BD Whitecare 27G). Left ear was injected with PBS through the bullostomy as a control. After injection the anesthetized animals remained in lateral decubitus for 30 min to maximize the suspension's contact time with the RWM and to prevent its leakage into the pharynx through the Eustachian tube.

After surgery, enrofloxacin and morphine (Braun 20 mg/ml) were administered subcutaneously for prevention of infection and postoperative analgesia, respectively.

CDDP-treated groups: after NPs administration in the right ear, an intraperitoneal slow infusion of CDDP (10 mg/kg) was carried out for 30 min. After CDDP infusion, animals were housed in individual cages with *ad libitum* access to water and food.

ASSR were tested after 3 days, and rats were euthanized by CO_2 suffocation.

Statistical analysis

One-way ANOVA was used to analyze for statistical significance of all *in vitro* and *in vivo* results. Tukey test was used to identify significant differences between the paired treatments. $p<0.05$ was considered statistically significant.

RESULTS AND DISCUSSION

NPs characterization

NP-based on poly(VP-co-MTOS) or poly(VP-co-MVE) and poly(VI-co-HEI)

New NP were synthesized by the combination of MTOS-11 or MVE-40 and HEI-6 or HEI-14. **Table 2** includes the most relevant characteristics of these NP. D_h varied between 108 and 184 nm with relatively low PDI values, according to the unimodal and narrow size distributions. In particular, these combined NP presented a lower size in comparison to HEI based NP, improving their application as drug delivery systems in cancer therapy and associated inflammatory diseases. On the one hand, NP had a size lower than 200 nm that improves their uptake by cells. On the other hand, NP presented a D_h higher than 100 nm avoiding their elimination by the RES systems (Danhier et al., 2010).

Table 2. Hydrodynamic diameter (D_h), polydispersity index (PDI), zeta potential values (ζ) and Isoelectric point (pI) of the NP based on the combination of poly(VP-*co*-MTOS)(89:11) or poly(VP-*co*-MVE)(60:40) and poly(VI-*co*-HEI)(94:6) or (86:14).

Copol A	Copol B	B (wt-%)	D_h (nm)	PDI	ζ (mV)	pI (pH)
MTOS-11	HEI-6	10	121.6 ± 8.4	0.172 ± 0.045	-2.76	5.4
		20	141.2 ± 3.4	0.131 ± 0.040	- 3.30	5.8
	HEI-14	10	156.6 ± 10.3	0.241 ± 0.061	-2.10	4.9
		20	179.9 ± 16.7	0.173 ± 0.038	-2.20	5.2
MVE-40	HEI-6	10	108.0 ± 6.8	0.090 ± 0.020	-2.11	5.0
		20	161.3 ± 11.4	0.093 ± 0.013	-0.52	6.5
	HEI-14	10	134.7 ± 9.5	0.232 ± 0.062	-3.22	5.9
		20	184.0 ± 11.2	0.106 ± 0.074	-2.75	6.5

The size of NP significantly increased with the HEI content in the copolymer and in the mixture with MTOS-11 and MVE 40. As an example, the size of MVE-40 and HEI-6 based NP varied from 108 to 161 nm when the feed molar ratio of these different copolymers was modified (10 or 20 % w/w, respectively). At a same feed molar ratio of 90:10, the hydrodynamic diameter also increased as a function of the HEI content in the copolymer, ranging between 108 and 135 nm for HEI-6 and HEI-14 respectively.

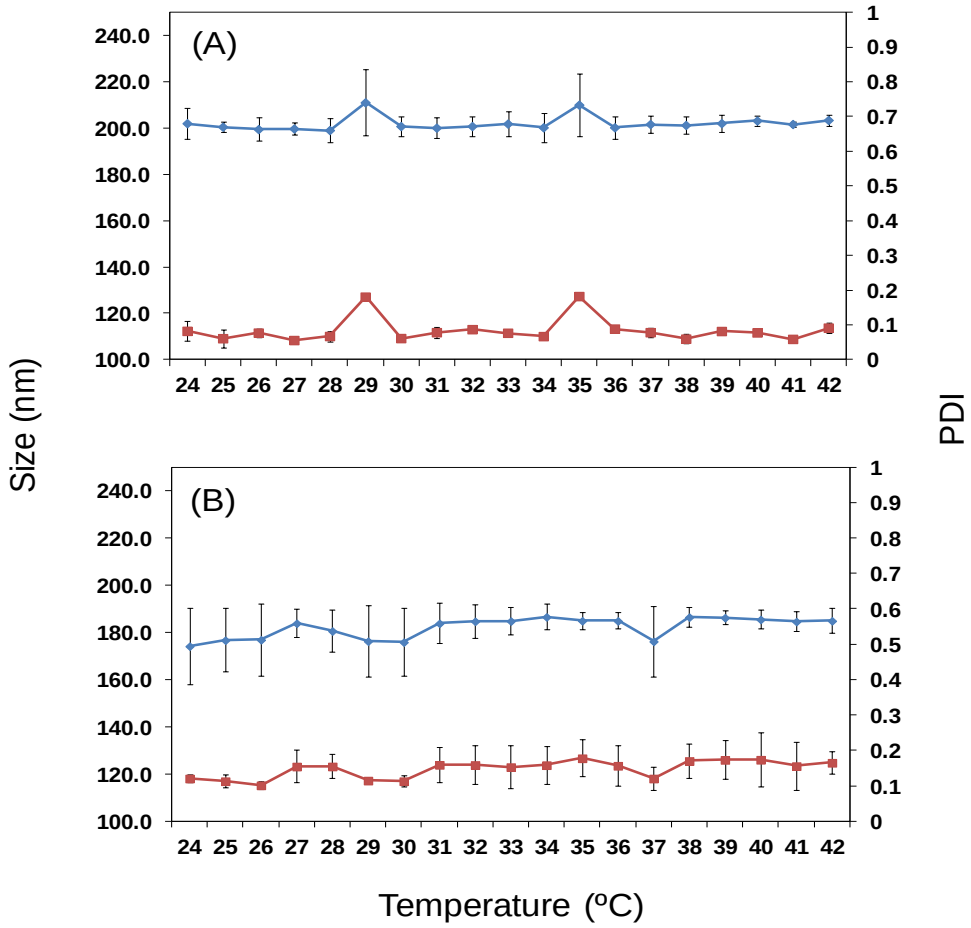

Figure 1: NPs mean diameter variation of NP-MVEH14-10Dx (A) and NP-MTOSH14-10Dx (B) with a temperature trend from 24 to 42ºC.

As opposed to the positive charge of HEI-6 and HEI-14 based NP, zeta potential of combined NP were slightly negative. These results indicate the almost neutral charge of the NP surface as a result of the reduction of the number of VI units that are probably intercalated with a majority number of VP units with the absence of charged groups. These results are in the same magnitude order described for other VP nano-assemblies.

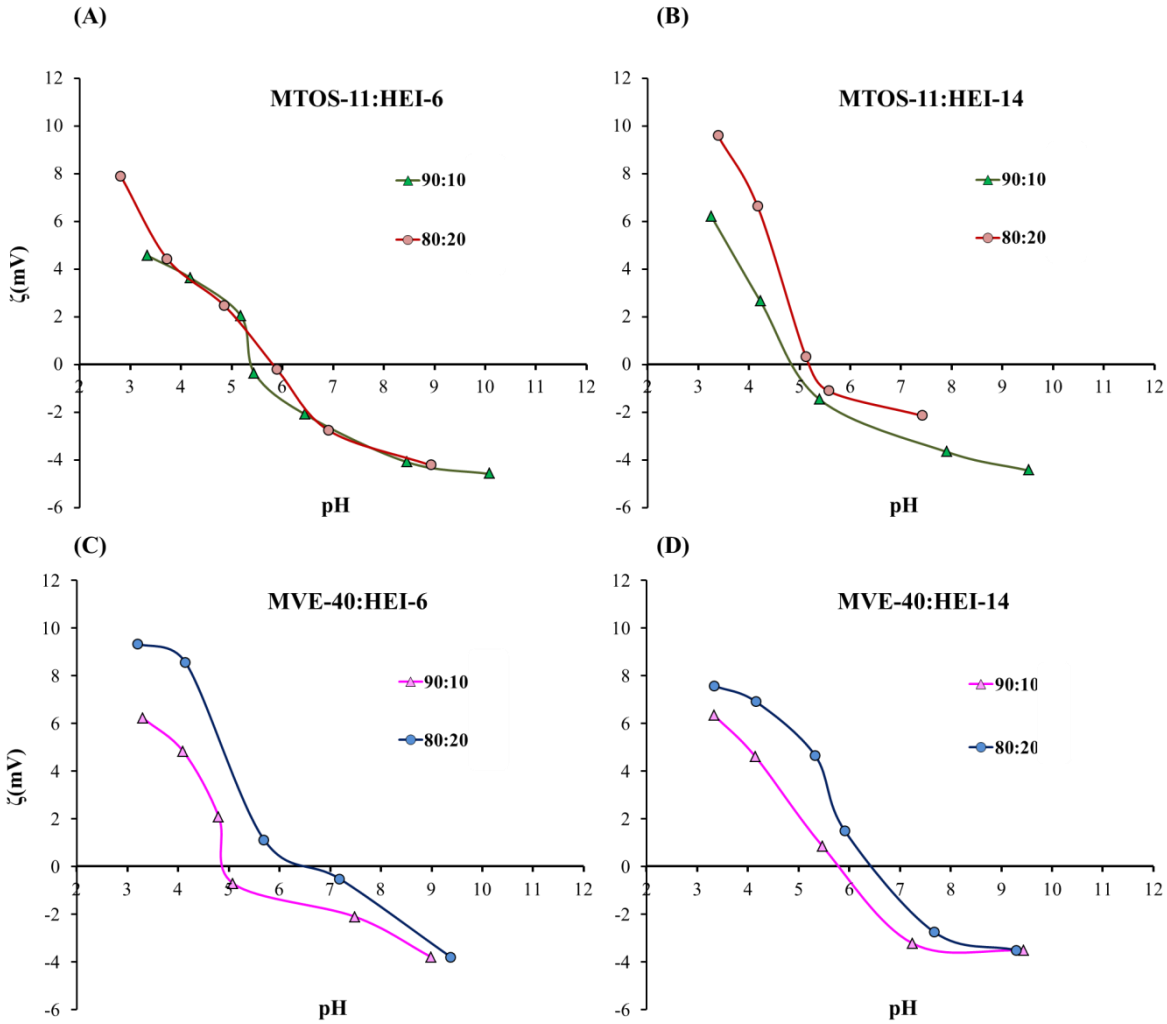

Figure 2. Variation of zeta potential values of NP based on (A) MTOS-11:HEI-6, (B) MTOS-11:HEI-14, (C) MVE-40:HEI-6 and (D) MVE-40:HEI-14 as a function of pH.

The pH sensitivity of these combined NP was proved by the measurement of their isoelectric point that was defined as the pH where zeta potential is zero, or the surface charge of the NP is zero. In this case, the determination of their pKa values was not feasible due to the low sensitivity of the titration curves obtained. **Figure 2** shows the variation of the zeta potential as a function of pH for NP based on MTOS-11 or MVE-40 and HEI-6 or HEI-14, including the effect to vary the weight percentage of these different copolymers (90:10 or 80:20 w:w). It is noteworthy that ζ significantly decreased with the increasing of pH as a result of the conversion of protonated to deprotonated form of VI units that are located into the NP surface. This effect produced a destabilization of self-assembled NPs at basic pH with a strong tendency to their aggregation (Lee et al., 2005).

pI of the NP slightly increased with the content in HEI copolymer, ranging from 5.0 to 6.5. The most appropriate pI values were obtained from the combination of MTOS-11 or MVE-40 with a 20 wt. % of HEI-based copolymers. In these conditions, pI of combined NP were very close to the slightly acid environment of the inner ear exposed to an ototoxic event like CDDP treatment, which enhances the inflammation (Watanabe et al., 2001, So et al., 2008). For that reason, these NP were selected to encapsulate Dx and coumarin-6 in their inner core. The most characteristic properties of these loaded NP are summarized in the **table 3**.

Both hydrophobic molecules were successfully entrapped in the core of the nano-assemblies with EE higher than 24 % in all copolymeric systems. All size distributions were unimodal with D_h between 158 and 230 nm and low PDI values. These results confirmed that these combined NP are good candidates for their use as drug delivery systems for the controlled administration of otoprotective drugs or other hydrophobic molecules that are quite toxic and also problematic for its effective administration.

Additionally, the size of loaded NPs significantly increased as a function of HEI content into macromolecular chains. As an example, the size of Dx loaded NPs based on MTOS-11 and MVE-40 increased from 140 nm to 180 nm when they were mixed with HEI-6 and HEI-14, respectively.

In vitro coumarin-6 release

As it was previously demonstrated, the pI of the self-assembled NP was adjusted to 5.0-6.0 with the aim to promote the VI ionization and therefore the preferential release of the entrapped hydrophobic molecules in the acidic environment promoted by an ototoxic event. Coumarin-6 loaded NP were successfully prepared and used as fluorescence probe to check the influence of pH on their fluorescence emission intensity. Results of fluorescence titration of different coumarin-6 loaded NP as a function of pH is shown in the **figure 3**. Additionally, the effect of pH on the particle size of these different formulations is also represented.

Table 3. Hydrodynamic diameter (D_h), polydispersity index (PDI), zeta potential values (ζ) and EE (%) of the Dx and coumarin-6 loaded NP based on the combination of poly(VP-*co*-MTOS)(89:11) or poly(VP-*co*-MVE)(60:40) and poly(VI-*co*-HEI)(94:6) or (86:14).

Drug	**Copol A**	**Copol B**	**Dx (wt-%)**	**EE (%)**	**D_h (nm)**	**ζ (mV)**	**PDI**
Dx	MTOS-11	HEI-6	10	26	158.90±12.32	-6.49	0.125 ± 0.016
		HEI-14	10	33	181.40±11.41	-5.23	0.138 ± 0.020
		HEI-6	15	24	180.60±18.47	-3.80	0.114±0.055
		HEI-14	15	25	187.30±2.93	-3.44	0.102±0.028
	MVE-40	HEI-6	10	59	178.80±3.79	-2.59	0.040±0.014
		HEI-14	10	53	211.20±36.39	-0.53	0.108±0.074
		HEI-6	15	36	201.40±13.05	-2.53	0.068±0.022
		HEI-14	15	41	230.10±24.29	-3.91	0.186±0.068
Coumarin-6	MTOS-11	HEI-14	20	----	175.5 ± 10.1	- 1.80	0.232 ± 0.046
	MVE-40	HEI-14	20	----	175.2 ± 13.7	- 3.27	0.189 ± 0.028

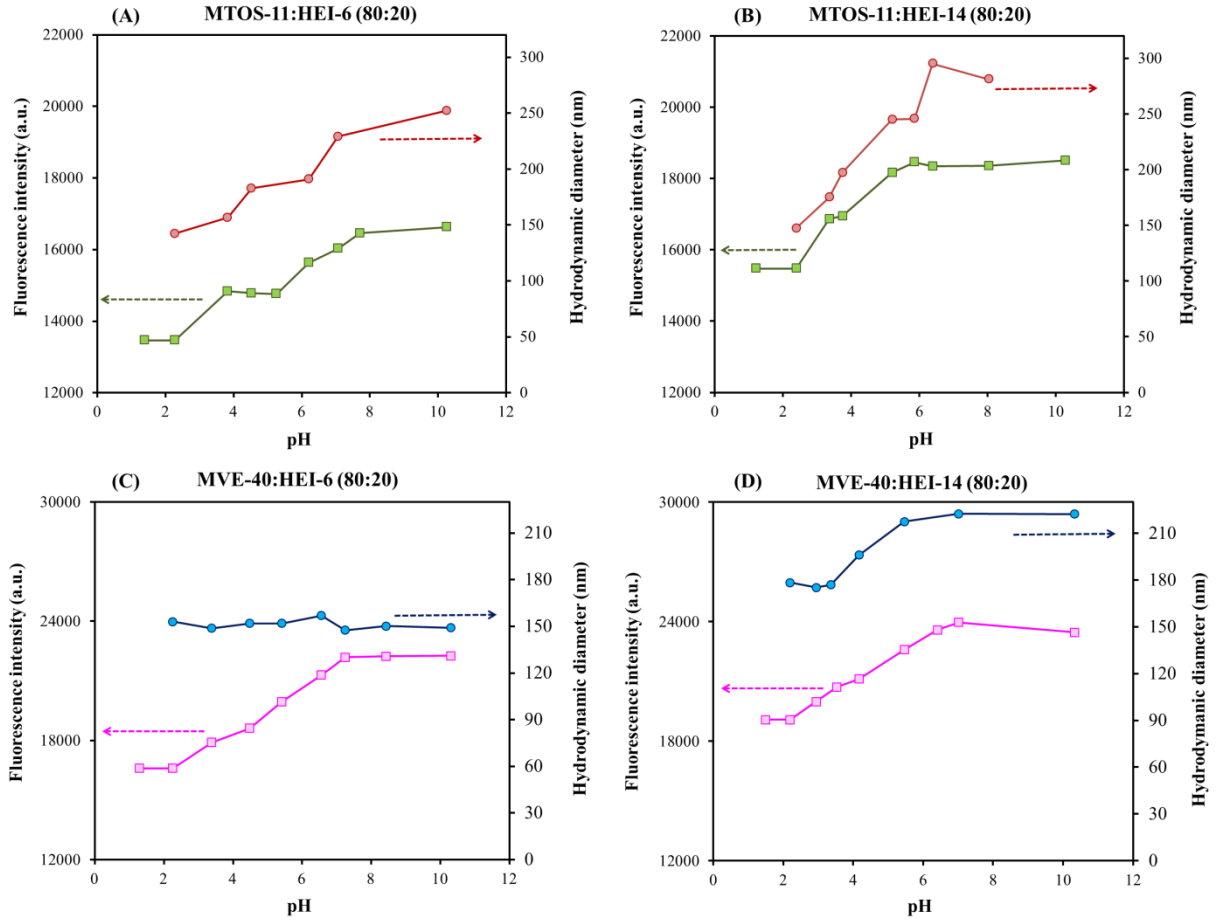

Figure 3. Fluorescence titration and D_h of coumarin-6 loaded NP based on (A) MTOS-11:HEI-6, (B) MTOS-11:HEI-14, (C) MVE-40:HEI-6 and (D) MVE-40:HEI-14 (80:20) copolymeric formulations as a function of pH.

In all cases, the fluorescence emission intensity of coumarin-6 significantly varied as a function as pH due to the protonation of VI units that are localized into the NP surface. At very acid pH (lower than pKa of each NP formulation), protonation of VI units decreased the emission fluorescence intensity. At increasing pH, this emission of coumarin-6 fluorescence significantly enhanced due to the progressive deprotonation of VI. In all cases, the transition of emission fluorescence was equivalent to the pI values that were obtained from titration curves. Furthermore, the change of fluorescence was also accompanied by the increasing of particle size. As it was previously demonstrated, ζ decreased with the increment of pH, producing a destabilization effect that favored the aggregation and therefore the increase of particle size. Additionally, the modification of coumarin-6 entrapped into the NP as a result of pH change also produced a direct effect on the particle size of the copolymeric formulations. These results suggest that these

pH sensitive NP significantly enhance the preferential release of hydrophobic molecules in “acidic” tumor tissues in comparison to normal tissues.

Esterase-mediated in vitro drug release

In vitro release of Dx was studied by an esterase-mediated dialysis diffusion method. **Figure 4** shows the *in vitro* Dx release profile of NP-MVE-HEI14-10-Dx and NP-MTOS-HEI14-10Dx at 37 °C during 15 days. About 20% of the loaded Dx is released from the NP-MVE-HEI14-10-Dx and more than 45% from NP-MTOS-HEI14-10Dx within fifteen days. Esterase mediated drug release profiles of the systems followed a zero order kinetic during the first 2 weeks, followed by a non-linear period for longer periods of time (**Figure 4**). The biological half-life of Dx in the inner ear is around 8 hours (Parnes et al., 1999) and therefore, Dx sustained release is of great interest to its application as otoprotector of CDDP-induced toxicity (Teng et al., 2005). Degradation of the NPs could be seen after 15 days of exposure to esterase, and their size were higher than in the first day (**Figure 4C and E**).

***In vitro* biological activity**

In vitro biological activity of Dx-loaded NP based on MTOS-11 or MVE-40 and HEI-6 (80:20) was tested using HEI-OC1 in order to evaluate their otoprotection activity against CDDP. The aim of these experiments was to optimize the most appropriate concentration of Dx entrapped NPs that allows combining an optimal anti-apoptotic, antioxidant and anti-inflammatory activity in a same pH-sensitive drug delivery system for otoprotection.

NPs toxicity assay in HEI-OC1

Cytotoxicity of Dx-loaded NPs were tested using HEI-OC1 and the results demonstrated that any concentration was cytotoxic after 24 hours (viability <70%; ISO 10993−5:2009) (**Figure 5**).

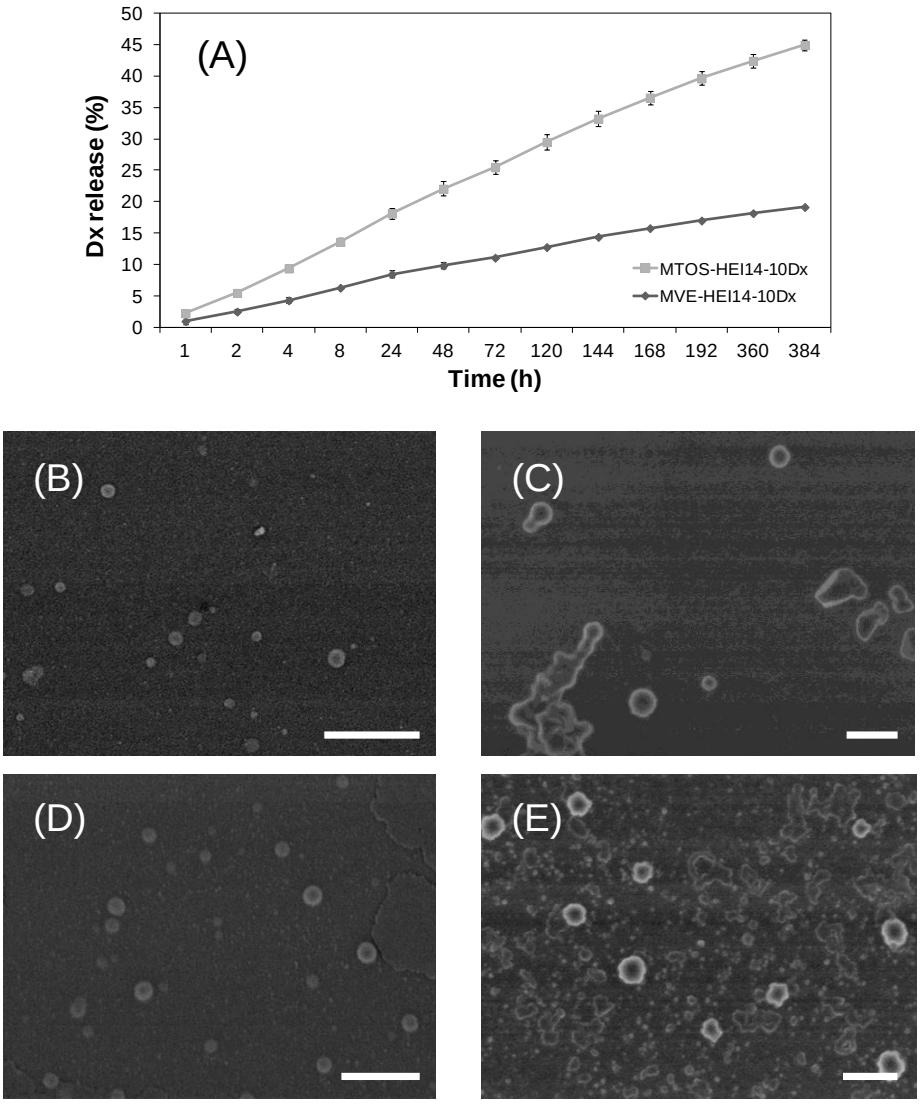

Figure 4: (A) *In vitro* release profile of Dx loaded NPs in PBS at 37 °C. SEM micrographs of NP-MVEH14-10Dx (B) and NP-MTOSH14-10Dx before release (D) and after 15 days of esterase degradation under physiological conditions (C and E respectively).

Protection of CDDP-induced cytotoxicity in HEI-OC1 with high loading NPs formulations

After 4h of NPs exposure to HEI-OC1, 30 µM CDDP was added and kept in the cell culture over 24 h. Cell viability decreased between 40 and 50% when 30 µM CDDP was added to the cells (**Figure 6**).

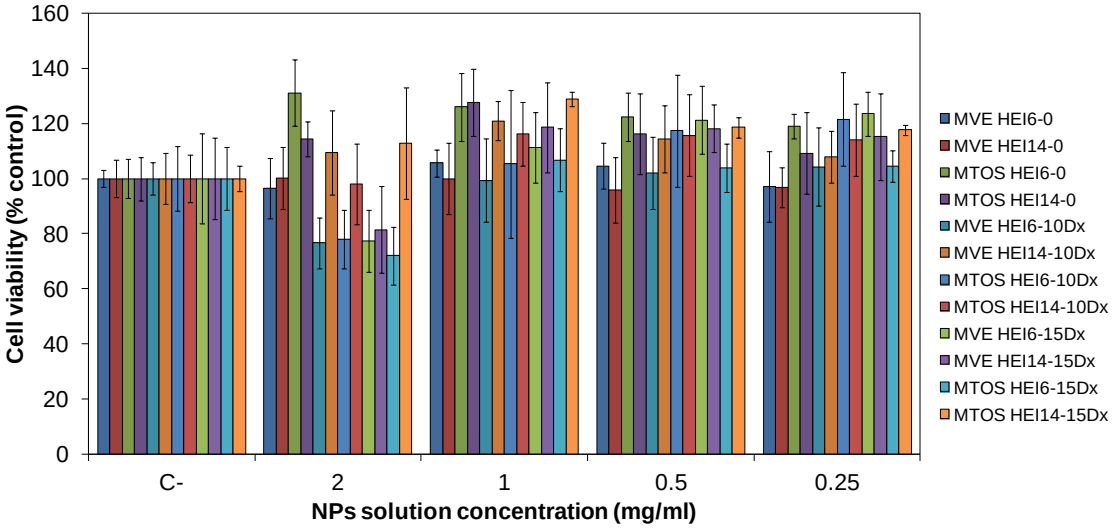

Figure 5: Cell viability of HEI-OC1 treated with different concentrations of Dx-loaded NPs over 24 hours. The diagrams include the mean, the standard deviation (n = 8), and the ANOVA results (*p < 0.05).

MVE HEI14 (**Figure 6B**) and MTOS HEI14 (**Figure 6D**) NPs loaded with 10% w/w of Dx were the best formulations protecting against CDDP cytotoxicity *in vitro* in good range of concentrations (over 20% when treated with MTOS HEI14 NPs and 15% when treated with MVE HEI14). Between 2 and 0.25 mg/ml both formulations significantly reduced CDDP-induced cytotoxicity of 30 µM CDDP. MTOS HEI6 NPs also reduced CDDP-induced cytotoxicity (almost 10%) but only with a dose of 2.0 mg/ml the difference with CDDP-treated control was statistically significant (**Figure 6C**). MVE HEI6 NPs did not show statistically differences with only CDDP treated cells (**Figure 6A**). The combination of an adequate size and good EE% could be related with the great results obtained with MTOS HEI14 systems in relation with the other tested. However, MVE HEI14 demonstrated good protection against 30µM CDDP dose, even if their size was slightly higher than the optimus diameter to this application (Hornyak, 2005). The pI of the systems probably allow the sustained release of Dx when cells were exposed to CDDP which induced inflammation and ROS generation due to the decreased of the pH related to inflammatory tissues (Punnia-Moorthy, 1987).

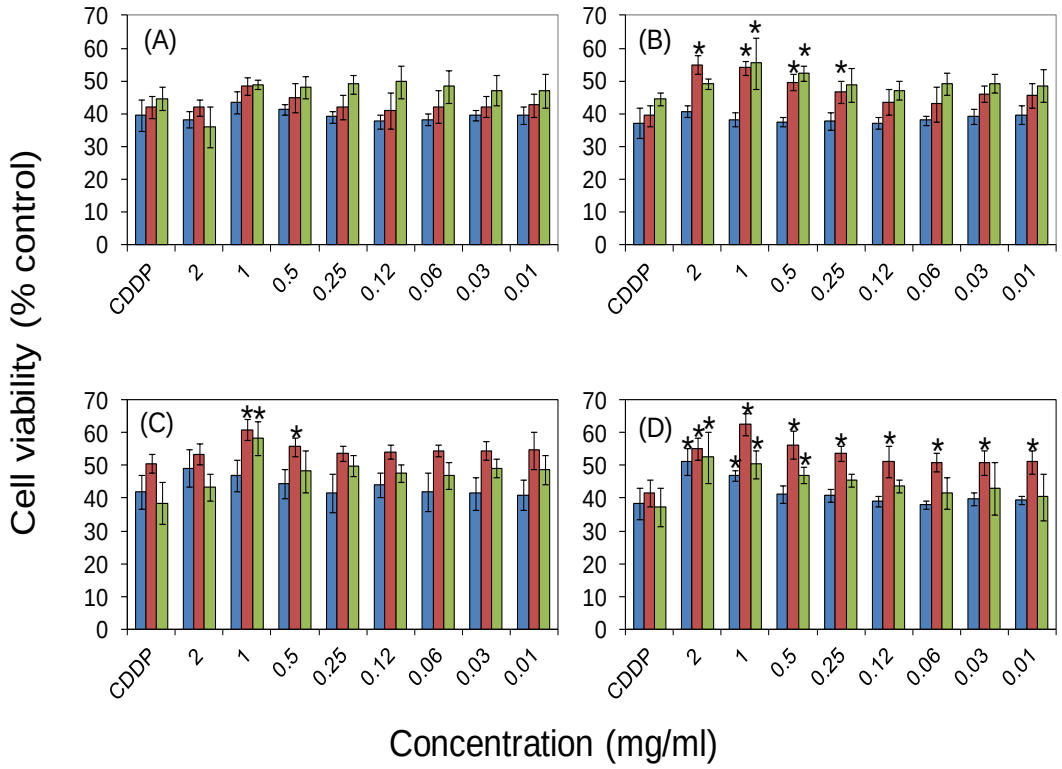

Figure 6: Cell viability of HEI-OC1 treated with different concentrations of MVE HEI6 NPs (A), MVE HEI14 NPs (B), MTOS HEI6 NPs (C) and MTOS HEI14 NPs (D) to inhibit the cytotoxic effect of 30 μM CDDP at 24 hours. The diagrams include the mean, the standard deviation (n = 8), and the ANOVA results (*p < 0.05) (legend: unloaded NPs in blue; 10% w/w of Dx in red and 15% w/w od Dx in green).

NP-MVE HEI14-10Dx and NP-MTOS HEI14-10Dx reduced caspase 3/7 activity in vitro

Supporting these results NP-MTOS HEI14-10Dx at 1 mg/ml were able to significantly reduce caspase-3/7 activity in cells treated with CDDP during 16 hours (**Figure 7A**). NP-MVE HEI14-10Dx slightly reduced caspase 3/7 activity but not in a statistically significant way. The use of corticoids like Dx when use as co-treatment causes resistance to CDDP-induced apoptosis in carcinoma cells (Herr et al., 2003) and other tumor cells from bone, brain, breast, cervix, melanoma and neuroblastoma (Zhang et al., 2006) with a significant reduce in caspase-3 expression. Even when the EE% was higher in NP-MVE HEI14-10Dx system, the higher size with respect to NP-MTOS HEI14-10Dx, and their slow release of Dx showed *in vitro* could be related with this lower inhibition effect on the caspase activity.

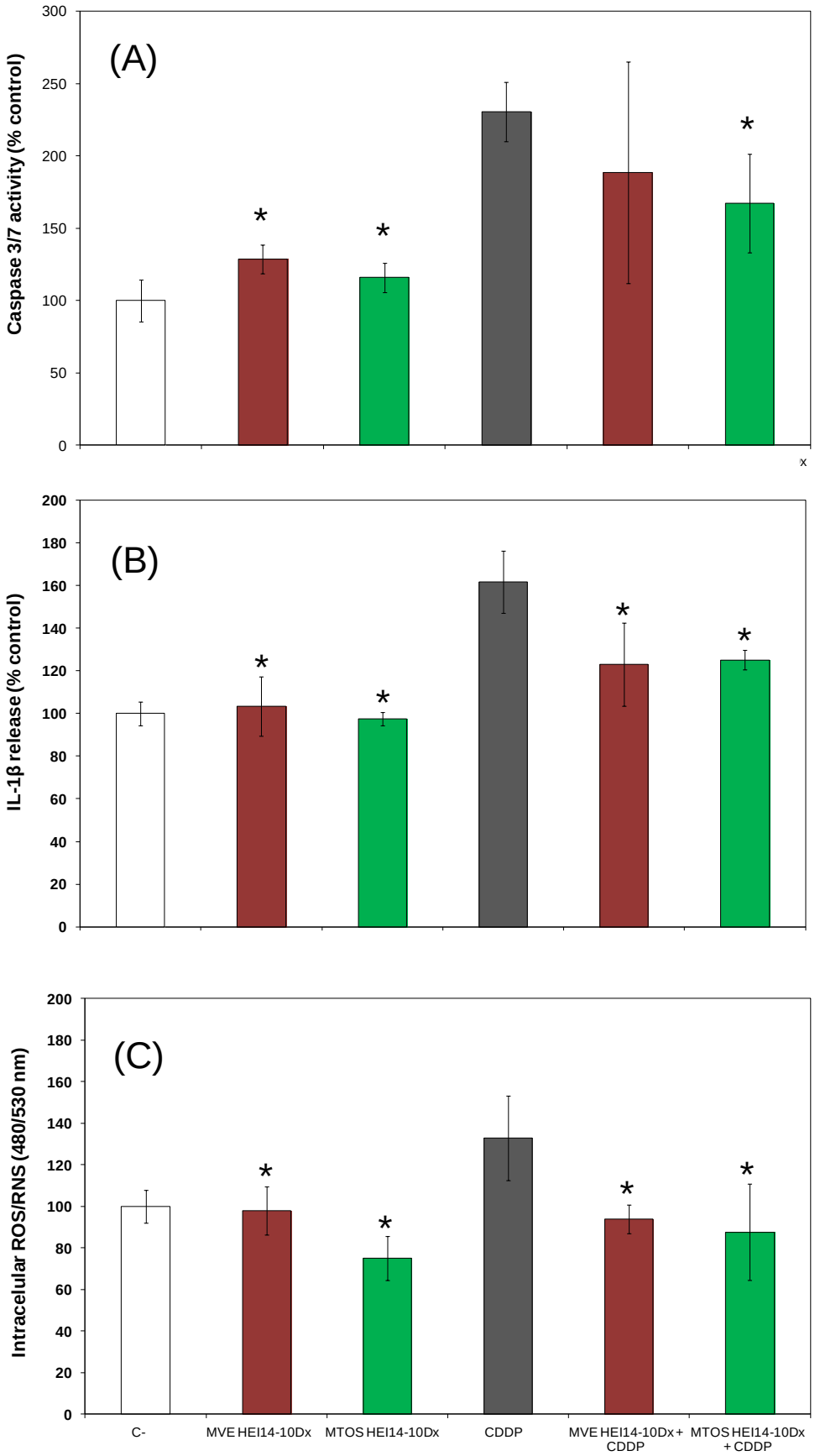

Figure 7: Caspase-3/7 expression when cells were treated with 20 μM CDDP and 0.25 mg/ml NP suspension at 16 hours (A). IL-1β release after treatment with 20 μM CDDP and 0.25 mg/ml NP suspension over 24 hours (B). Inracellular ROS measure after treatment with 20 μM CDDP

and 0.25 mg/ml NP suspension over 24 hours (C). The diagrams include the mean, the standard deviation (n = 4), and the ANOVA results (* p< 0.05 statistically significant with CDDP).

NP-MVE HEI14-10Dx and NP-MTOS HEI14-10Dx reduced IL-1β release and intracellular ROS with respect with CDDP treated cells

Dx could act as free radical scavenger (Niki, 2014), and it has been shown to ameliorate ototoxicity in animals receiving CDDP (Paksoy et al., 2011), so the effect shown on the IL-1β release of both formulations was expected in that sense (**Figure 7B**). Both systems contain in the co-polymeric blend a 20% of HEIcoVI14 copolymer with demonstrated anti inflammatory properties (Suárez et al., 2013). The combined action of the entrapped corticoid and ibuprofen released from the polymer inhibited IL-1β in statistically significant way. Downregulation of pro-inflammatory cytokines such as Tnf-α, Il-6 and IL-1β, which play a critical role in CDDP ototoxicity, resulted in the attenuation of CDDP-induced cochlear damage (So et al., 2008)

In this sense, it is known that CDDP increased ROS generation in the cochlea in a dose dependent way (Marullo et al., 2013). CDDP-induced ototoxicity is closely related to the increased production of ROS and that intracellular oxidative stress, could overwhelm the antioxidant defense mechanisms within the cochlea, activating the apoptotic pathway causing the death of cochlear cells (Rybak and Ramkumar, 2007). Both NPs systems efficiently reduced intracellular ROS production respect to CDDP treated cells *in vitro*, even not showing difference with untreated cells (**Figure 7C**).

In vivo assays

Control of NPs ototoxicity

In order to maximize NPs delivery to inner ear, the highest dose of NPs (2 mg/ml) was used due to its non toxic effect *in vitro*. NP formulations with best results *in vitro* were selected to *in vivo* assays. Two animals per formulation (NP-MVEH14-10Dx, NP- S and NP-MTOSH14-10Dx) were inoculated through bullostomy in the right ear. These animals were not treated with CDDP after surgery although they did get the same palliative cares than the animals that received the chemotherapeutic treatment. After 72

hours of both NPs exposure, no significant differences were observed between the auditory thresholds of the right ear and the left ear at all frequencies (**Figure 8**).

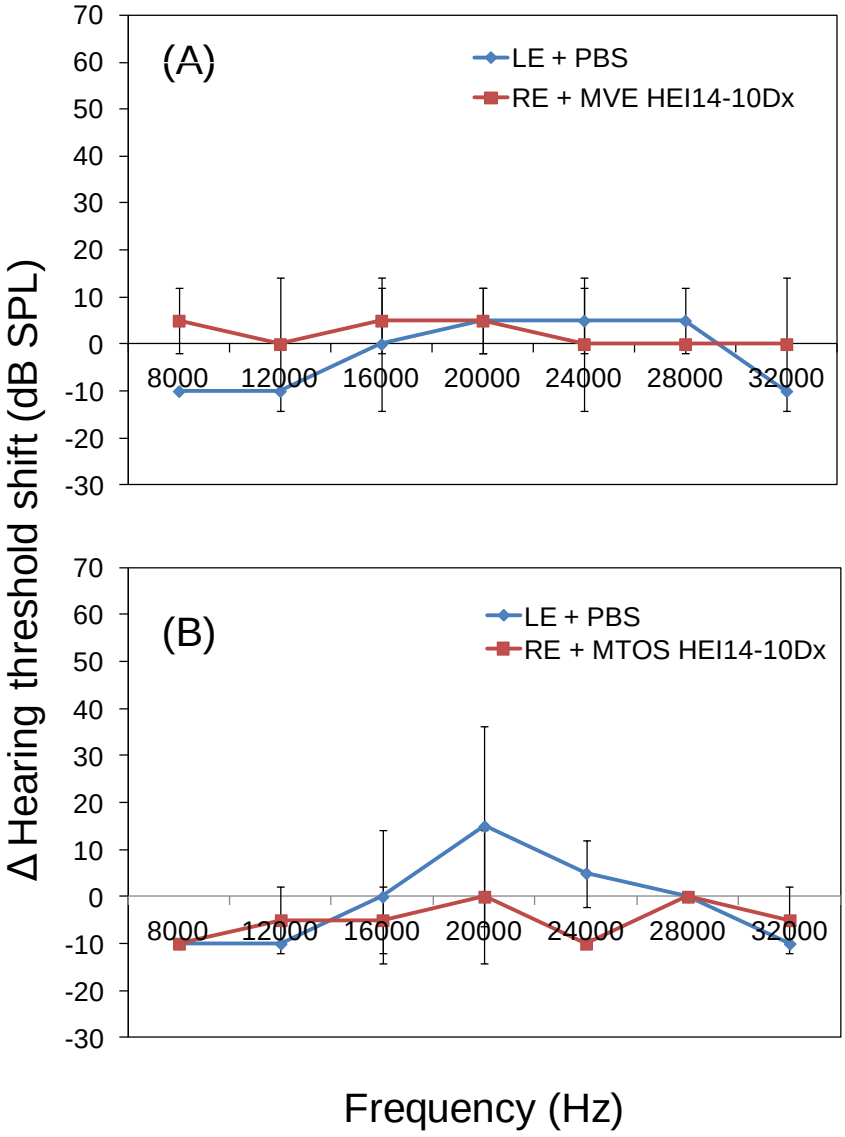

Figure 8: Δ of hearing threshold after local administration by bullostomy in right ear of NP-MVEH14-10Dx (A) and NP-MTOSH14-1oDx (B) (LE: left ear; RE: right ear). The diagrams represents the difference between hearing threshold after CDDP-administration and before treatment with the NP suspension (in the right ear) and CDDP-administration after 72 hours. Diagrams include the mean, the standard deviation (n = 2), and the independent TUKEY results (*p < 0.05).

NP-MTOSH10-10Dx protects from CDDP-induced hearing loss in vivo

A potential problem with the administration of antioxidants and corticoids is a reduction in antitumor efficacy of CDDP. That fact was resolved by the bullostomy approach, improving the Dx delivery to the inner ear without systemic interaction in other tissues. Due to CDDp-induced ototoxicity an increase in auditory threshold is shown for frequencies located in the apical turn of the cochlea corresponding to higher frequencies. CDDP entry into cochlear cells results in cell death, which appears to be primarily caspase-dependent (Rybak and Ramkumar, 2007). Several mechanism pathways that could trigger to CDDP-induced apoptosis included ROS accumulation which triggers to inflammatory mechanisms that contribute to the cell destruction by up regulation of pro-inflammatory cytokines like TNFα, IL-1β and IL-6 (Casares et al., 2012).

Results obtained *in vitro* suggested the potential of both systems to ameliorate CDDP-induced ototoxicity in a murine model. NP-MVEH10-10Dx (**Figure 9A**) and NP-MTOS14-10Dx (**Figure 9B**) were tested *in vivo* and only the second one showed protection against CDDP-induced hearing loss. NP-MTOSH14-10Dx protected in a significant way for 24 kHz frequency (**Figure 9B**). NP-MVEH14-10Dx showed no difference between the non treated left ear and NP treated right ear (**Figure 9A**).

EE% of Dx in NP-MVEH10-10Dx was substantially higher than in NP-MTOS14-10Dx. However, NP-MVEH10-10Dx did not protect from CDDP-induced hearing loss *in vivo*. These results could be due to the medium size of this system which is higher than NP-MTOS14-10Dx, and was near to the optimal D_h (≥200nm) previously described to cross through RWM (Hornyak, 2005). This factor was described as a *must* to properly deliver of NPs system to cochlear cells from middle ear. Better medium size of NP-MTOS14-

10Dx allowed it to cross RWM and effectively deliver Dx into cochlear cells resulting in the ameliorating of CDDP-induced hearing loss in all the frequencies measured. However this NP system only in 24 kHz the protection was statistically significant (**Figure 9B**). In spite of the lower EE% showed by NP-MTOS14-10Dx, the physical properties of this system allowed it to a efficient drug delivery to the inner ear

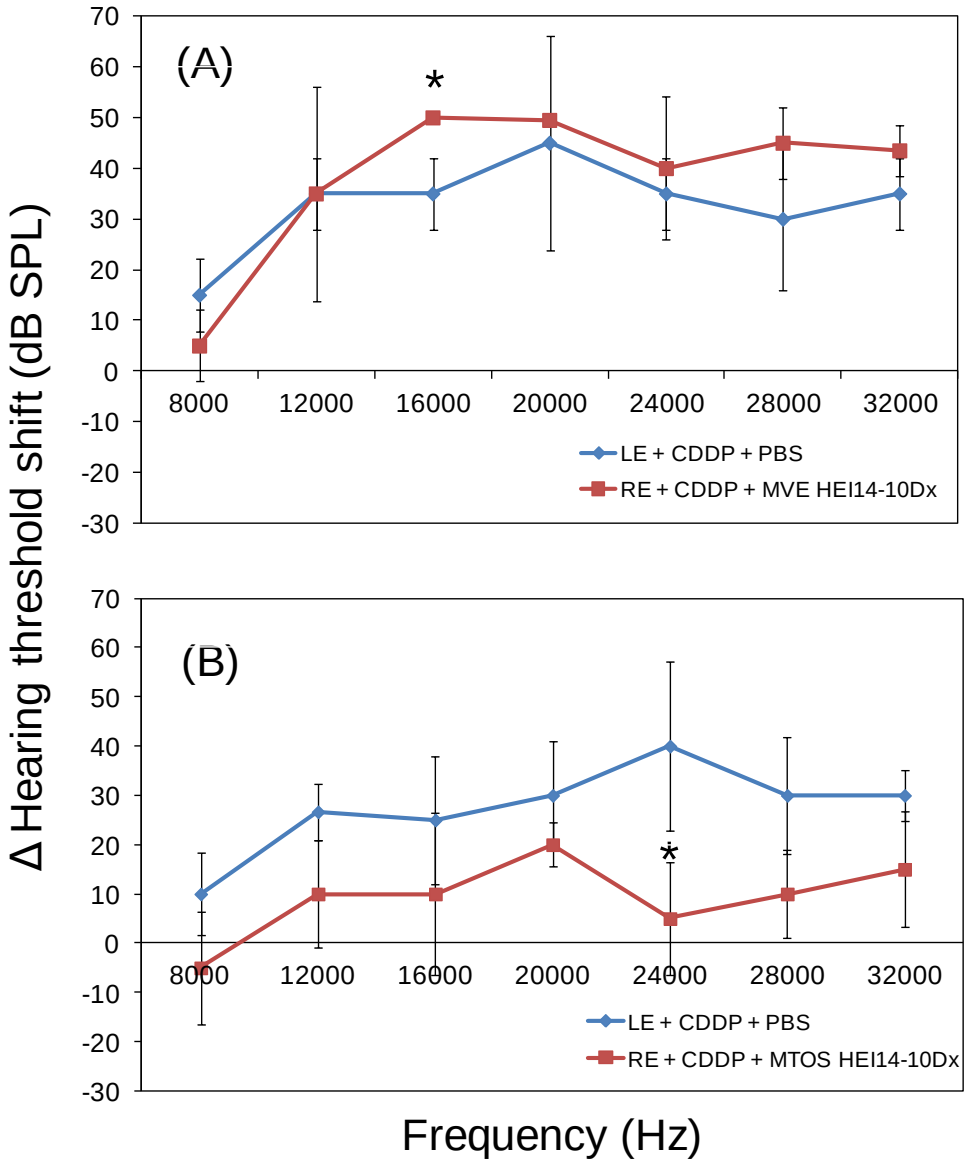

Figure 9: Δ of hearing threshold after local administration by bullostomy in right ear of NP-MVEH14-10Dx (A) and NP-MTOSH14-1oDx (B) and intraperitoneal 10 mg/kg dose of CDDP (LE: left ear; RE: right ear). The diagrams represents the difference between hearing threshold after CDDP-administration and before treatment with the NP suspension (in the right ear) and CDDP-administration after 72 hours. Diagrams include the mean, the standard deviation (n = 6), and the independent TUKEY results (*p < 0.05).

Conclusions

The combination of copolymeric drugs obtained by free radical polymerization forming surfactant-free NPs is described for the first time. These nanocarriers were used to efficiently entrapped Dx as anti-inflammarory and anti-apoptotic molecule. The drug was incorporated in the hydrophobic core of NPs and presented good properties *in vitro*. *In vitro* biological test showed lower CDDP-induced toxicity, down-regulation of caspase 3/7 expression, and lower IL-1β release and intracellular ROS accumulation, while *in vivo* experiments demonstrated a reduced hearing loss when animals received NP-MTOS14-10Dx. Hydrodinamic diameter of NP-MVEH14-10Dx probably avoid it to cross trough RWM resulting in non protection of the auditory function after CDDP treatment. The local administration of the NPs by bullostomy provided an adequate biological activity locally, without systemic interference with the chemotherapeutic effect of CDDP.

AUTHOR INFORMATION

Corresponding Author

*****Telephone: +34915618806 (ext. 212); Fax: +34915644853; Email: **mraguilar@ictp.csic.es**

Author Contributions

The manuscript was written through contributions of all authors. All authors have given approval to the final version of the manuscript.

Funding Sources

This work was funded by the Spanish Ministry of Economy and Competitiveness (MAT2010-18155) and CIBER BBN-ECO Foundation project.

Acknowledgments

Authors would like to thank financial support from the Spanish Ministry of Economy and Competitiveness (MAT2010-18155) and CIBER BBN-ECO Foundation project. Authors also acknowledge David Gómez, and Rosa Ana Ramírez and Mar Fernández for their help in SEM, and cell culture experiments, respectively.

Spontaneous cannabinoid receptor 2 (CB_2 expression in the cochlea of adult albino rat and its up-regulation after cisplatin treatment

Plos One, 2016

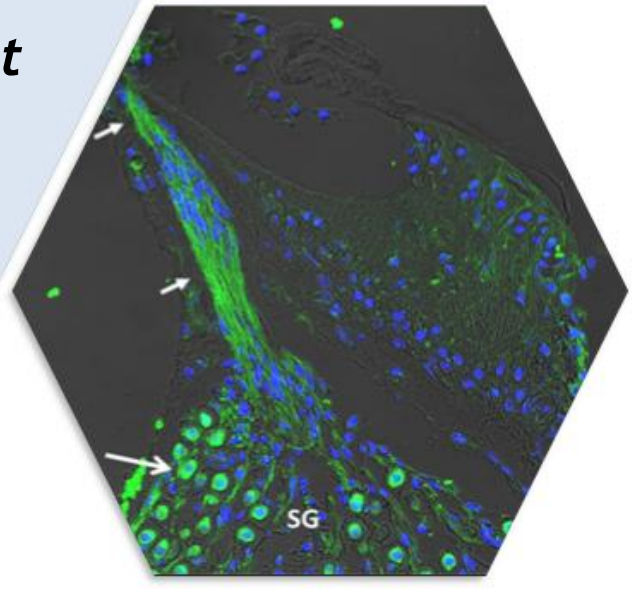

Resumen

En ésta segunda parte de la tesis, se planteó la posibilidad de estudiar la presencia de receptores de cannabinoides CB_2, en la cóclea de ratas Wistar. De igual manera, se quiso comprobar el efecto de un evento ototóxico, como el tratamiento con CDDP, en la expresión génica y proteica de estos receptores. Los cannabinoides y sus receptores son cada vez más estudiados debido a su alto potencial para su uso clínico. Como una parte hiperespecializados del sistema nervioso periférico, el estudio de la expresión y función de receptores de cannabinoides en el órgano de la audición es de gran interés.

Se observó la presencia de receptores CB_2 en algunos tipos celulares de la cóclea de rata adulta albino. Tanto la estría vascular como las células ciliadas internas, mostraron tener presencia de receptores CB_2 en ensayos de inmunohistoquímica. De igual manera se observó inmunomarcado en las células del ganglio espiral. En cambio, tipos celulares tales como células de sostén o las células ciliadas externas, en las que está ampliamente reportada la expresión de otros tipos de receptores funcionales, no se observó expresión proteica significativa de los receptores CB2 en este estudio. La intensidad de fluorescencia en animales que recibieron tratamiento con CDDP fue mayor, siendo estadísticamente significativa con respecto a los animales sanos, solo en el caso de la estría vascular.

Para tratar de apoyar éstos indicios de expresión de CB_2 en los ensayos de inmunohistoquímica, se estudió la expresión génica de CB_2 y CB_1 (como control de expresión, al ya haber sido reportada su expresión en la cóclea) mediante RT-qPCR.

Se detectó una sobre regulación de la expresión génica CB_2 después de un evento ototóxico como es el tratamiento con CDDP, probablemente debido a los eventos pro-inflamatorias provocados por el fármaco antitumoral.

Los resultados obtenidos, sugieren un prometedor potencial del receptor CB_2 como diana terapéutica para el desarrollo de nuevos tratamientos orientados a paliar la pérdida de audición inducida por el tratamiento con CDDP, y otros eventos ototóxicos que incluyan una respuesta inflamatoria importante.

SPONTANEOUS CANNABINOID RECEPTOR 2 (CB_2) EXPRESSION IN THE COCHLEA OF ADULT ALBINO RAT AND ITS UP-REGULATION AFTER CISPLATIN TREATMENT

Martín-Saldaña S[1*], Trinidad A[1], Ramil E[2], Sánchez-López AJ[3], Coronado MJ[4], Esther Martínez-Martínez[5], García JM[5], García-Berrocal JR[1], Ramírez-Camacho R[1].

[1]Ear Research Group, Universitary Hospital Puerta de Hierro Majadahonda- Health Research Institute Puerta de Hierro

[2]Sequencing and Molecular Biology Unit. Universitary Hospital Puerta de Hierro Majadahonda, Health Research Institute Puerta de Hierro

[3]Neuroimmunology Unit, Universitary Hospital Puerta de Hierro Majadahonda- Health Research Institute Puerta de Hierro

[4]Confocal Microscopy Unit. Universitary Hospital Puerta de Hierro Majadahonda, Health Research Institute Puerta de Hierro

[5]Department of Medical Oncology, Universitary Hospital Puerta de Hierro Majadahonda- Health Research Institute Puerta de Hierro

*Corresponding autor

smartinsaldana@gmail.com (SMS)

Abstract

We provide evidence for the presence of cannabinoid CB_2 receptors in some cellular types of the cochlea of the adult albino rat. Cannabinoids and their receptors are increasingly being studied because of their high potential for clinical use. As a hyperspecialized portion of the peripheral nervous system, study of the expression and function of cannabinoid receptors in the hearing organ is of high interest. Stria vascularis and inner hair cells express CB_2 receptor, as well as neurites and cell bodies of the spiral ganglion. Cellular types such as supporting cells and outer hair cells, in which the expression of other types of functional receptors has been reported, do not significantly express CB_2 receptors in this study. An up-regulation of CB_2 gene expression was detected after an ototoxic event such as cisplatin treatment, probably due to pro-inflammatory events triggered by the drug. That fact suggests promising potential of CB_2 receptor as a therapeutic target for new treatments to palliate cisplatin-induced hearing loss and other ototoxic events which triggers inflammatory pathways.

Introduction

There is an increasing body of research on molecular signalling in the cochlea with the expectation that a deeper understanding of cell damage and regeneration pathways could uncover potential targets for the treatment and prevention of auditory damageIn the context of searching for potential therapeutic targets against inner ear disorders, the study of cannabinoid receptors expression in the auditory organ is of great interest. Cannabinoid receptors modulate a large number of normal brain and bodily functions and have been implicated as potential drug targets in a wide variety of diseases from cancer (Pérez-Gómez et al., 2015) to neurodegenerative disorders (Fernández-Ruiz et al., 2015).The endocannabinoid system is increasingly being studied because of the high potential for clinical use of cannabinoids. The endocannabinoid system is a cell communication system which consists of two receptors, CB_1 and CB_2, their endogenous ligands (anandamide and 2-AG), and the enzymes that produce and metabolize these ligands (Pertwee et al., 2010). Cannabinoids exert a wide spectrum of therapeutic effects through CB_1 and CB_2 receptors (Mukherjee et al., 2004). Cannabinoid receptors are of a class of cell membrane receptors under the G protein-coupled receptor superfamily that contain seven transmembrane spanning domains (Pertwee et al., 2010). Also, the existence of other cannabinoid receptors is suspected due to the actions of compounds that produce cannabinoid-like effects without activating either CB_1 or CB_2 (McHugh et al., 2008). CB receptors signaling pathways include regulation of adenylyl cyclase, MAP kinase, intracellular Ca^{2+}, and ion channels (Demuth and Molleman, 2006). The first cannabinoid receptor (CB_1) was characterized in rat brain in 1988 (Devane et al., 1988) and is mainly expressed in lung (Shire et al., 1995), liver (Mallat et al., 2011) and kidneys (Deutsch et al., 1997). CB_2 was isolated in the rat spleen in 1993 (Munro et al., 1993). CB_2 receptor has been found to be 10-100 times more abundant than CB_1 in immune cells such as macrophages, B cells, “natural killer” (NK) cells, monocytes, neutrophills and T cells (Berdyshev, 2000). It has also been described in non-immunological cells such as gastrointestinal system cells (Storr et al., 2002); lung endotelium (Zoratti et al., 2003); osteocytes and osteoclasts of bone (Ofek et al., 2006) mouse spermatogenesis (Grimaldi et al., 2009) and other aspects of reproduction (Maccarrone, 2008); in trabecular meshwork cells of the eye (He and Song, 2007); in adipocytes (Roche et al., 2006); and in cells from cirrhotic liver (but not in the healthy organ) (Julien et al., 2005).

Cisplatin (CDDP) was the first platinum-based drug to be used and nowadays is widely employed in the treatment for some neoplastic entities such as head and neck, ovary, bladder, lung or brain. However, it presents severe side effects such as nephrotoxicity, bone marrow toxicity, gastrointestinal toxicity, liver toxicity, peripheral nervous system toxicity and ototoxicity (Bokemeyer et al., 1998). Most of these related effects can be treated. However, CDDP- induced ototoxicity, that implies several cochlear damage which evolves in hearing impairment, tinnitus and dizzines, is one of the main reasons to chemotherapy discontinue.Inflammation has been recently shown to play a role in auditory cells apoptosis induced by CDDP, and is the main mechanism involved in immune-mediated hearing loss (Berrocal and Ramírez-Camacho, 2000). The inflammatory mediator inducible nitric oxide synthase (iNOS), is activated through nuclear factor-kB (NF-kB) and is related with cochlear wound by increasing cytokine expression and apoptosis in the cochlea (Watanabe et al., 2001). Therefore, CDDP induce an over expression of COX-2, iNOS and TNF-α, that are regulated in cell nucleus by STAT1. STAT1 has an important role in inflammation and apoptosis in the cochlea like Kaur *et al*. demonstrated when used short interfering RNA against STAT1 to ameliorate CDDP-induced ototoxicity reducing the inflammation (Kaur et al., 2011).

There is a report on the expression of CB_2 receptors in the auditory HEI-OC1 (House Ear Institute-Organ of Corti) cell line (Jeong et al., 2007). In this study, researchers were able to demonstrate that JWH-015 (a synthetic CB_2 agonist) could inhibit CDDP-induced apoptosis in HEI-OC1 cells.

Up to our knowledge, CB_2 receptor has been studied *in vivo* in relation to inflammatory processes in the outer ear (Mimura et al., 2012) and the middle ear (Oka et al., 2005), but there are no reports on CB_2 receptor expression or function in the inner ear.

The aim of this study was to explore the expression of CB_2 receptors in the mature inner ear of the Wistar rat by means of immunohistochemical staining in post-mortem tissue sections of the cochlea. CB_2 gene expression was also measured by RT-qPCR in healthy and CDDP treated animals, using a well-established murine model of CDDP-induced ototoxicity, in order to study if an ototoxic event triggers an up- or down-transcriptional modulation of this receptor in the cochlea. These results may have important preliminary implications for the therapy of CDDP-induced hearing loss and other

inflammatory inner ear diseases using CB_2 receptor as a therapeutic target to ameliorate ototoxicity events.

Material and Methods

Animals

Thirty three female Wistar rats (14-16 weeks old) weighting between 200 and 280 g were used in the present study. Animals were breaded and handled at the animal facility of the Health Research Institute Puerta de Hierro in controlled temperature rooms, with light–dark cycles, and with free access to food and water. Rats with signs of present of past middle ear infection were discarded.

The animals were handled according to Spain Royal Law 53/2013 and the European Directive 2010/63/EU. The study was approved by the Clinical Research and Ethics Committee of Hospital Universitario Puerta de Hierro and the Autonomic Community of Madrid (PROEX 022/16).

Auditory steady-state responses (ASSR)

The animals were randomly assigned in two different groups: one group (n=20; 10 for histology and 10 for RT-PCR analysis) was administered with phosphate buffered saline (PBS) as a control, and the other group (n=13; 3 for histology and 10 for RT-PCR) received 10 mg/kg of CDDP (Accord Healthcare, Barcelona, Spain) dose. After 72 hours animals were euthanized by CO inhalation and cochleae, spleen and kidneys of each animal were extracted. Animals were anesthetized with intraperitoneal ketamine (100 mg/kg) and diazepam (0.1 mg/kg) before the procedure.

Subcutaneous electrodes were placed over the vertex (active) and in the pinna of each ear (reference). An insert earphone (Etymotic ER-2) was placed directly into the external auditory canal. Ground electrodes were placed over the neck muscles. ASSR were recorded using an evoked potential averaging system (Intelligent Hearing System Smart-EP, FL, USA) in an electrically shielded, double-walled, sound-treated booth in response to 100 ms clicks or tone bursts, at 8, 12, 16, 20, 24, 28 and 32 kHz with 10 ms plateau and 1 ms rise/fall time. Intensity was expressed in decibels sound pressure level (dB SPL) peak equivalent. Intensity

series were recorded, and an ASSR threshold was defined by the lowest intensity able to induce a replicable visual detectable response.

ASSR was measured before treatments with PBS or CDDP, and 72 hours after the administration.

Tissue extraction, fixation and decalcification

Thirteen animals were euthanized by CO inhalation and subsequently decapitated. Temporal bones were removed and structures of middle ear dissected for isolation of the cochlear portion. Cochleae were fixed by intralabyrinthine perfusion with 4% paraformaldehyde (PFA) in phosphate buffer (pH=7) and then immersed for 24 hours in 4% PFA solution. Afterwards, cochleae were decalcified in 0.12 M Ethylenediaminetetracetic acid dipotassium salt dihydrate (Sigma-Aldrich, St.Louis, USA) for 7-10 days. Cochleae were finally maintained in 1% PFA in 0.1 M PBS.

Spleen and kidneys of each animal were extracted and submitted to the same protocol (except the decalcification step).

Histological processing

In order to obtain complementary images from the cellular structures of the organ of Corti, the two cochleae from one animal were each randomly processed by one of the following techniques:

Inner ear surface preparations

Cochleae were dissected following Liberman's technique. In short, cochlea was bisected along a mid-modiolar plane and the half-turns cut apart, ensuring that the spiral ligament and tectorial membrane were pulled off and the resulting pieces of tissue were mounted on a microscope slide for examination in a confocal laser scanning microscope**.**

Mid-modiolar sections

The cochleae were processed for paraffin embedding. Careful placement of the cochlear portion was performed to obtain transverse serial sections of 6 □m (Leica microtome RM 2235), which were orthogonal and complementary to the surface preparations.

Immunolabeling

CB_2 receptors were immunostained with the polyclonal anti-cannabinoid receptor II antibody (ab45942, Abcam, USA; dilution 1:50), using Alexa 488-conjugated anti-rabbit raised in goat (Molecular Probes–Invitrogen; dilution 1:400) as the secondary antibody. Antibodies were diluted in PBS supplemented with 1% bovine serum albumin (BSA) and 0.04% triton. All preparations were contrasted with TOPRO-3 iodide (Life Technologies, USA; dilution 1:500). Specificity was confirmed in separated experiments with additional negative controls, including tissue sections incubated with primary antibody pre-adsorbed to an excess of control peptide (ab45941, Abcam, USA; dilution 1:25).

Cochleae assigned to surface preparations were immunolabeled once bisected into two halves and before final dissection, by means of a "free floating" technique. Transversal sections were immunolabeled once mounted on the slide and conveniently dried.

As a positive control of the primary antibody used, spleen and kidneys (Barutta et al., 2011) of each animal were submitted to the same protocol.

Microscopic analysis

Samples were visualized by means of a confocal laser scanning microscope Nikon Eclipse C1 coupled to a Nikon 90i microscope with a camera DXM1200F (Nikon, Haarlem, Netherlands).

For validation of the specificity of the CB_2 immunolabelling, immunofluorescence patterns were compared to negative controls in which primary antibody was pre-adsorbed with blocking peptide, and kidney and spleen were used as a positive control.

Measurement of immunofluorescence intensity

For relative quantification of CB_2 fluorescence intensity, standardized settings for image acquisition and processing were used. To obtain values for CB_2 immunofluorescence intensity in cell types of the cochlear duct, morphological boundaries of each cell type were determined on phase contrast images. The cell type-specific outlines were plotted with the corresponding grey-scaled CB_2 immunofluorescence images. Single measurements of fluorescence intensity were performed using ImageJ software (version 1.40 g; National Institutes of Health, US). CB_2 fluorescence intensity values for each cell type of the cochlear duct were averaged from ten independent measurements of immunolabelled cochlear mounts and sections from ten specimens. The fluorescence intensity of CB_2 labelling was plotted using arbitrary units ranging from 0 to 2500.

Following the same protocol used to determine relative fluorescence intensity in cell types of the cochlea, effect of CDDP treatment in the immunofluorescence was compared in stria vascularis and IHC of three animals treated with CDDP and three animals treated with PBS.

Measurement of CB_2 gene expression by RT-qPCR in healthy and CDDP treated animals

Total RNA purification

Dissected cochleae obtained from CDDP-treated and control Wistar rats were embebed in RNA later overnight and kept at -80ºC until purification. Tissues were resuspended in Trizol and homogenized by the MagNA Lyser System (Roche). Total RNA was isolated by RNeasy kit (QIAGEN) including on-column DNAse Digestion, following protocol previously described (Patil et al., 2015).

RNA concentration was determined by spectrophotometry and each sample was reverse-transcripted to cDNA by using the First-Strand cDNA Synthesis Protocol (Agilent Technologies).

Relative Quantification of CB_2 and CB_1 gene expression

qPCR was performed in a LC480 (Roche) in order to quantify CB_2 and CB_1 levels of gene expression in relation to the level of the reference TATA-binding protein (TBP), in the cochlear tissue using Real Time Ready Single Assay (TBP Transcript ID ENSRNOT0000002038, amplicon length of 75 bps from 1029 to 110; CB_2 Transcript ID ENSRNOT00000012342, amplicon length of 65 bps from 344 to 408; CB_1 Transcipt ID ENSRNOT00000010850, amplicon length of 66 bps from 3244 to 3309; Roche). CB_1 gene expression was used as a control (**see supporting information Fig.S1**).

Statistical analysis

Statistical analysis was performed with GraphPad Prism6 (San Diego, USA). One-way ANOVA was used to analyze for statistical significance of the results. Tukey test was used to identify significant differences between the paired treatments. $p<0.05$ was considered statistically significant.

Results

Ototoxic effect of CDDP-treatment

Post-treatment ASSR recordings were found to be higher than pre-treatment ASSR recordings in the CDDP-treated animals, as it was previously described (Rybak et al., 2007). PBS-treated animals did not suffer hearing loss (**Fig.1**).

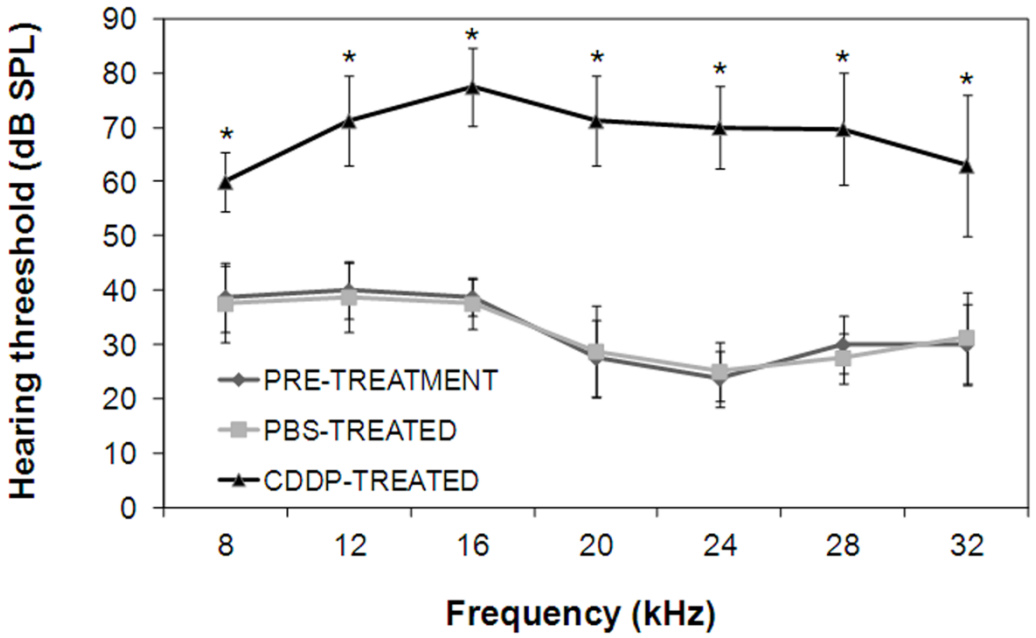

Fig 1. Hearing thresholds before and after intraperitoneal administration of 10 mg/kg dose of CDDP or PBS.
CDDP-induced hearing loss was statistically significant for all frequencies with respect to pre-treatment hearing. The diagrams include the mean, the standard deviation (n = 33), and the ANOVA results (difference statistically significant respect control *p<0.05).

CB_2 receptor detection in the cochlea by immunohistochemistry

CB_2 labeling was detected in the organ of Corti, specifically in inner hair cells (IHC) (**Fig. 2**).

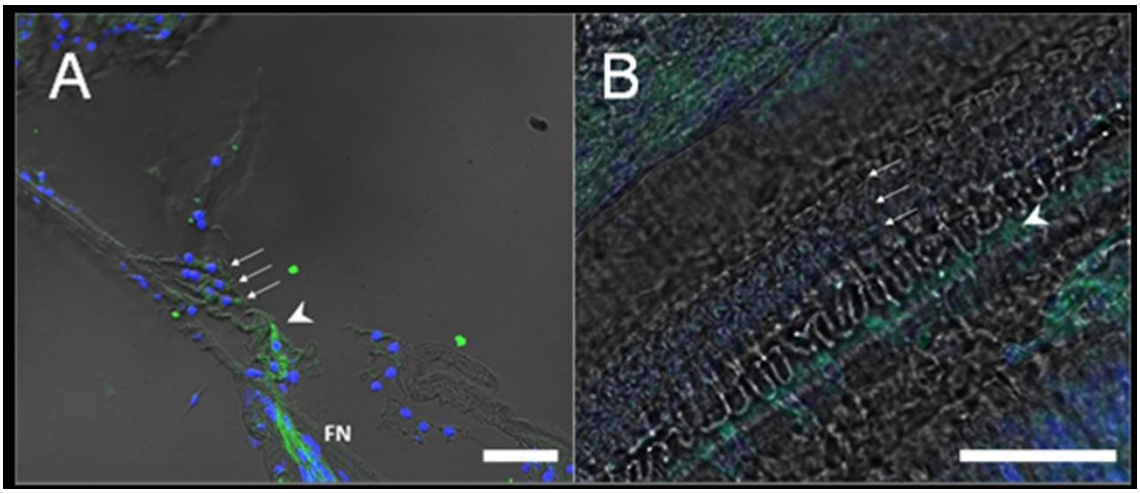

Fig 2. Detailed view of the sensory hair cells of the organ of Corti.
Detailed view of the 3 rows of OHC (arrows) and the single row of IHC (arrowhead). (A) Mid-modiolar section. (B) Cochlear whole mount. Immunofluorescence labeling of CB_2 receptors is shown in green. To-Pro (blue) stains nuclei of cells. Intense fluorescence is observed in IHC (arrowhead), but not in OHC. Labeling of nerve fibers can be seen at the bottom of the figure (FN). IHC: inner hair cell. OHC: outer hair cell.(Scale bar = 30μm)

In the stria vascularis, the CB_2 labeling pattern was mostly coincident with an intermediate region within the stria vascularis, although some of the clearly immunolabeled cells occupied a luminal position and also the basal region in some areas. This is compatible with the distribution of intermediate cells as well as at least some of the marginal and basal cells (**Fig. 3**).

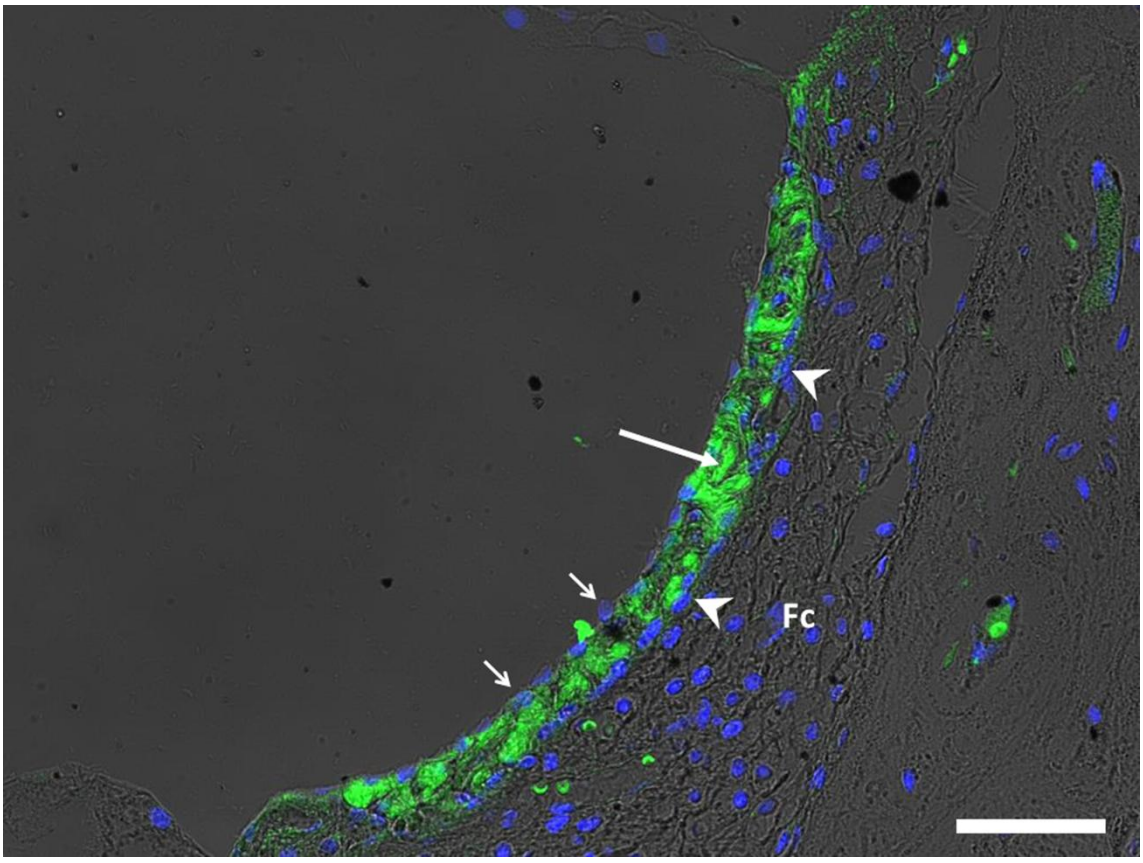

Fig 3. Image showing intense CB_2 immunolabeling in cellular types of the stria vascularis (SV).
Intermediate cells are indicated by long arrow. Marginal cells (short arrows); basal cells (arrowheads) might show labeling at some points. Fibrocytes of the spiral ligament (Fc) do not show expression of CB_2 receptors. (Scale bar = 30µm)

A strong CB_2 labeling was also observed in the soma and neurites of the spiral ganglion neurons (**Fig. 4**).

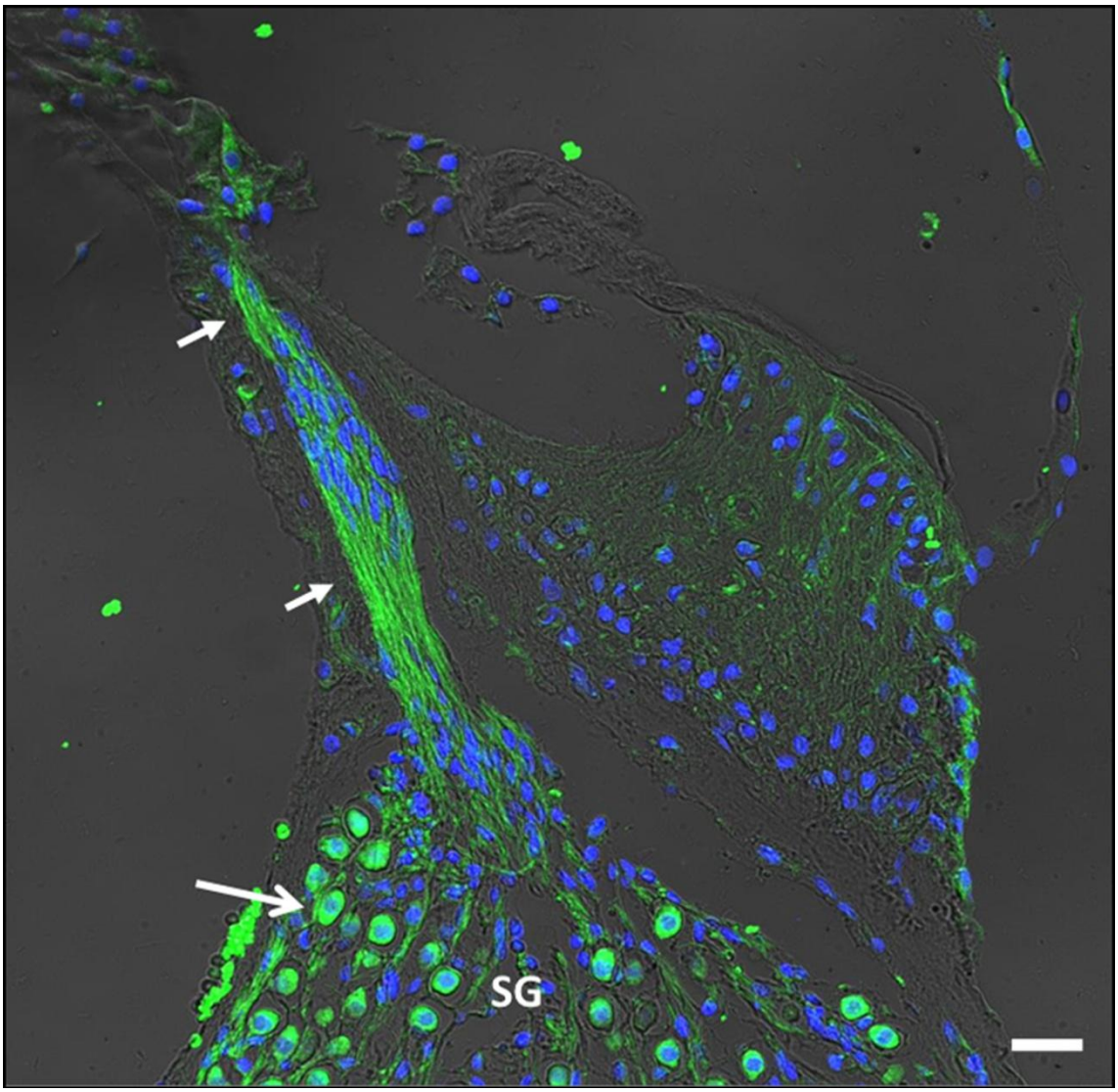

Fig 4. Close view of CB_2 immunolabeling of nerve fibers and spiral ganglion. Neurites are intensely labeled (short arrows), as well as the soma (long arrow) of the spiral ganglion (SG) neurons (Scale bar = 30µm).

As a control, the same protocol was assayed in the kidney and spleen. A strong marking was observed in the spleen related to the B cells (**Fig.5A**). A strong labeling of CB_2 receptor in the epithelial cells of renal tubules was observed in the kidney. A slightly marking in the glomerule was also detected and the pattern of staining was suggestive of podocyte labeling, as previously described by Barutta *et al*. (**Fig. 5B**).

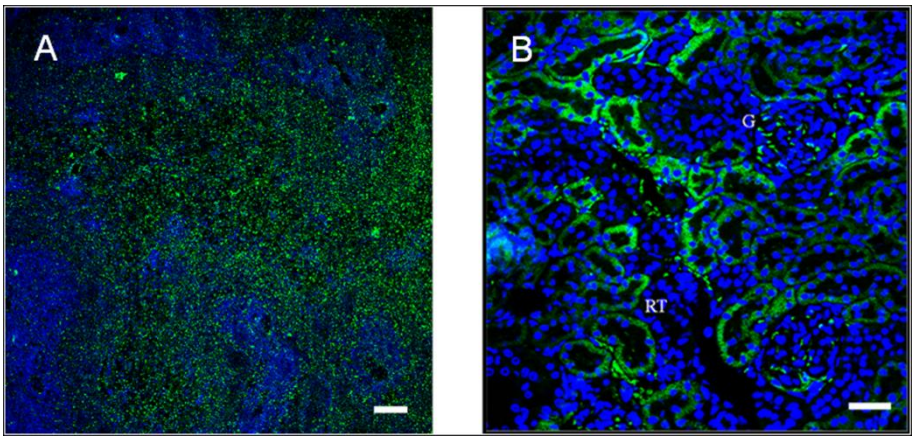

Fig 5. Detailed view of immunolabeling of CB_2 in the spleen and the kidney.
Detailed view of CB_2 immunolabeling in the spleen (A), used as a positive control of the primary antibody (Scale bar = 100µm) . Detailed view of CB_2 immunolabeling of epithelial cells of the renal tubules (RT) and the glomerule (G) of the kidney (B). (Scale bar = 30µm).

Tissue sections incubated with CB_2 primary antibody pre-adsorbed with control peptide did not show immunofluorescence, demonstrated the specificity of primary antibody used against the CB_2 receptor (**Fig.S1**).

Relative quantification of CB_2 immunofluorescence labeling intensity in the IHC and OHC, the stria vascularis, modiolus, Reissner and tectorial membranes and the supporting cells of the rat inner ear is presented in **Fig. 6**. OHC as well as supporting cells were almost completely devoid of CB_2 staining. Relative immunofluorescence of OHC was remarkably lower when compared to labeling of IHC and was not statistically significant (**Fig.6**). The same protocol was assayed to compare relative fluorescence in in the stria vascularis (**Fig.7A** and **7B**) and IHC (**Fig.7C** and **7D**) of healthy and CDDP-treated animals. CB_2 immunofluoresce was higher in the stria vascularis of CDDP-treated animals in a statistically significant way (**Fig.7E**). No difference between IHC of healthy and CDDP-treated animals was achieved.

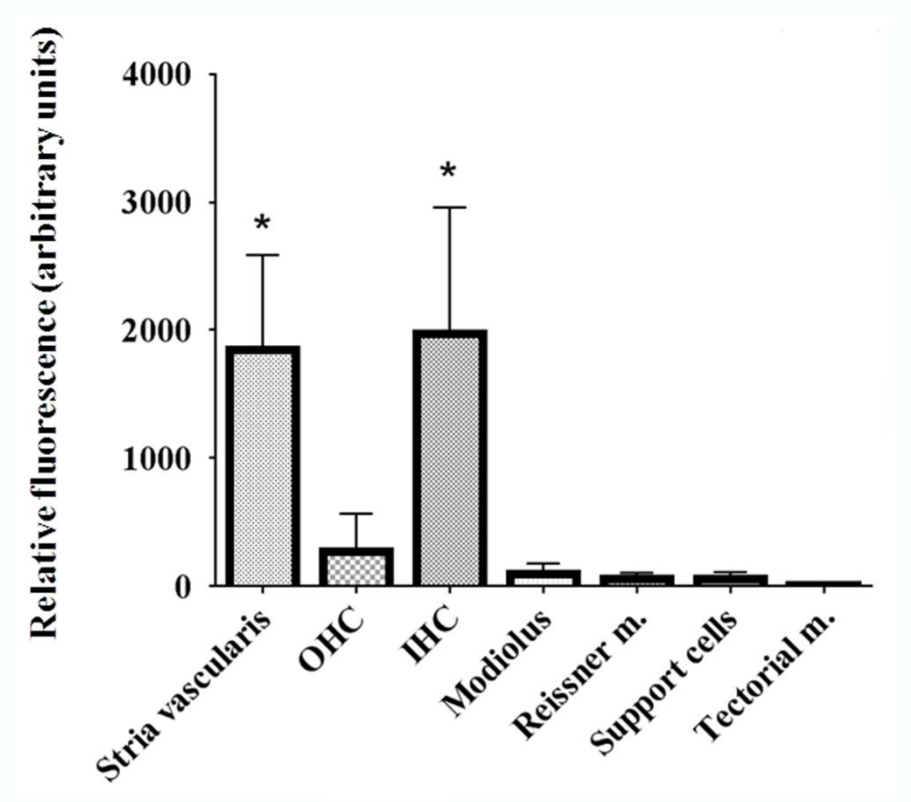

Fig 6. Relative quantification of CB_2 immunofluorescence labeling intensity in different structures of the cochlea by ImageJ.
Support cells: supporting cells (including Deiters', Hensen's, Claudius and pillar cells). Tectorial m: tectorial membrane (acellular). Reissner m.: Reissner membrane. OHC: outer hair cells. IHC: inner hair cells. Relative immunofluorescence in the IHC and in the stria vascularis was significantly than in the other cell types. The diagrams include the mean, the standard deviation (n = 10), and the ANOVA results (difference statistically significant respect tectorial membrane *$p<0.05$).

CB_2 gene expression in the cochlea and CDDP induced an up-regulation in their expression

Gene expression of CB_2 receptors was studied in the cochlea of healthy animals with respect to TBP reference gene. The relative levels of expression showed up-transcriptional regulation of CB_2 under CDDP treatment in a statistically significant way. Similar results were observed in kidney of animals untreated, an under CDDP treatment (**Fig. 8**).

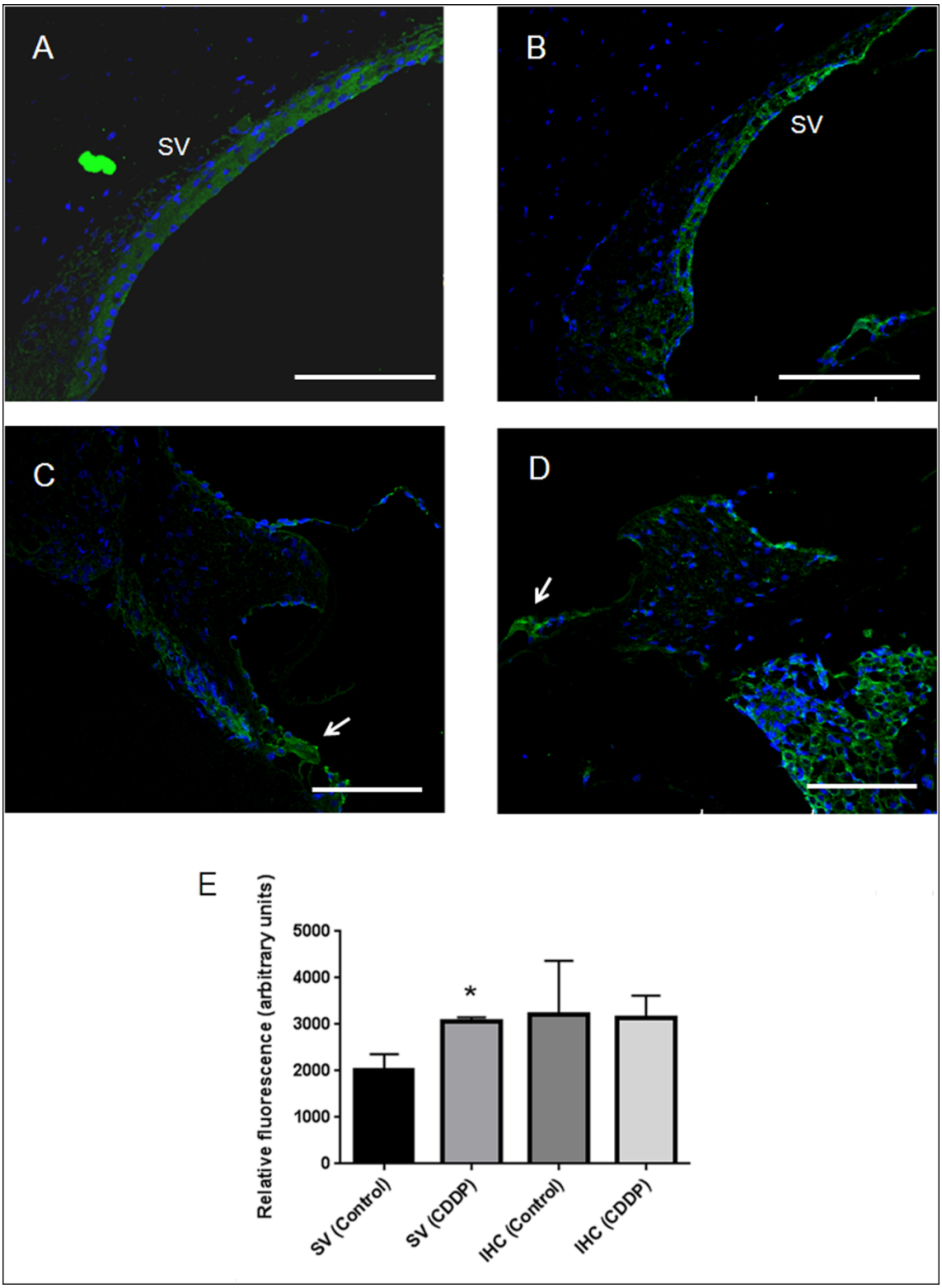

Fig 7. Relative quantification of CB_2 immunofluorescence labeling intensity in healthy and CDDP-treated animals by ImageJ.

Detailed view of the stria vascularis (SV) and the IHC (arrowhead) of healthy (A and C) and CDDP-treated animals (B and D) (Scale bar = 100μm). Relative immunofluorescence in the IHC and in the stria vascularis of healthy and CDDP-treated animals (E). CB_2 relative immunofluorescence was significantly higher only in the stria vascularis of animals treated with CDDP if compared with the control group. The diagram include the mean, the standard deviation (n = 6; 3 control and 3 CDDP-treated), and the ANOVA results (difference

statistically significant in each cellular structure between healthy and CDDP-treated animals *p<0.05).

Level of CB_1 gene expression in both organs was also measured as a control. CB_1 receptors expression was detected in the cochlea and in the kidney. A slightly down-transcriptional regulation in the CDDP treated animals was observed in the cochlea, but there was no statistically significant difference between control and CDDP-treated groups (**see supporting information Fig.S2)**.

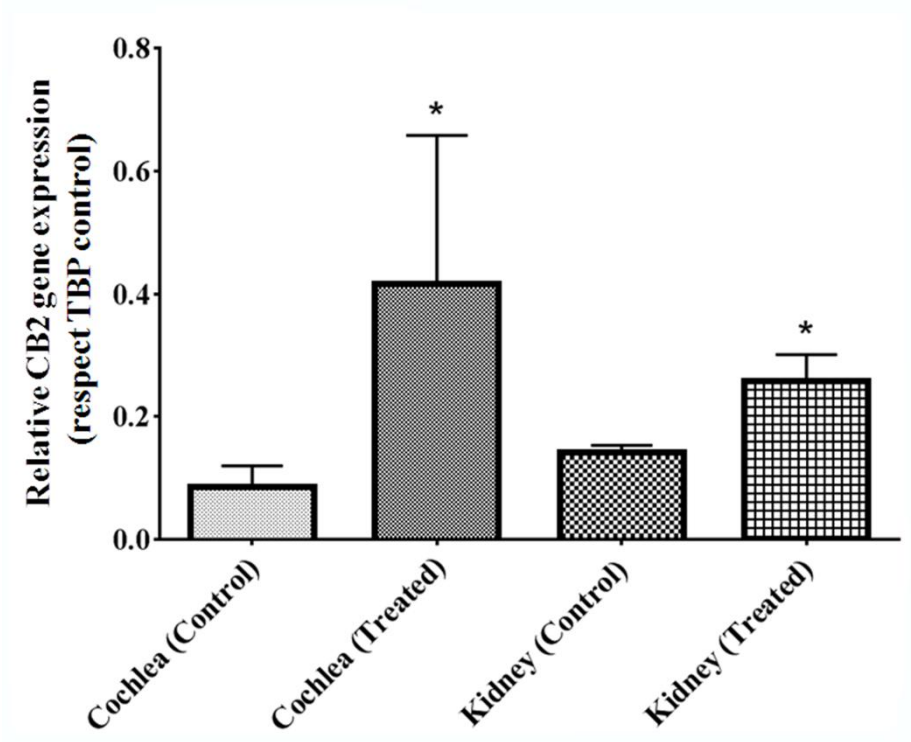

Fig 8. Measure of relative CB_2 gene expression by RT-qPCR.
Measure of CB_2 gene expression in the cochlea and kidney of healthy (control) and CDDP treated animals, respect TBP reference. CB_2 gene expression was significantly higher in animals treated with CDDP than those in control group. The diagrams include the mean, the standard deviation (n = 10), and the ANOVA results (difference statistically significant respect control *p<0.05).

Discussion

The expression of cannabinoid receptors in a specific tissue opens the door to potential treatments with agonists and antagonists that could trigger certain cell signaling pathways. Expression of CB_2 has also been described in astrocytes and some neuron subpopulations. Role of CB_2 receptor in the central nervous system is related to neuroinflammation and neurodegeneration (Fernández-Ruiz et al., 2007). In the peripheral nervous system, CB_2 agonists have analgesic effects by acting at dorsal root ganglia (as well as at spinal cord) (Hsieh et al., 2011). Other authors have reported CB_2 expression on human skin nerve fibers (Ständer et al., 2005). Baek *et al*. previously described expression of CB_2 protein receptor in the vestibular and cochlear nuclei of the brain in a rat model, suggesting that it could have an important role in the control of balance and hearing function (Baek et al., 2009). As part of the peripheral nervous system (Osen et al., 2011), it is not surprising to find such a remarkable immunolabelling of CB_2 receptor in organ of Corti cells, although its functional role has still to be ascertained. Immunolabeling to CB_2 receptor resulted to be higher in the stria vascular of animals which received the chemotherapeutic, but no difference could be appreciate in the IHC of healthy and CDDP-treated animals. Due to these limitations of immunohistochemistry to appreciate differences in the transcriptional up-regulation of CB_2 between healthy and CDDP-treated animals, which suffered big structural tissue degradation, RT-qPCR was assayed to determine the regulation of CB_2 gene expression.

In 2005 meeting of the Association for Research in Otolaryngology (ARO), Fauser *et al.* reported preliminary studies of the expression of CB_1 cannabinoid receptor in type I and type II spiral ganglion cells that was higher after intratympanic treatment with salicilate and glutamate in comparison with saline, with no specific stain in the organ of Corti or stria vascularis (Fauser, 2005). In this study high values of CB_1 gene expression was observed and used as a control of cannabinoid gene expression **(see supplementary data Fig.S2)**, probably due to the presence of the spiral ganglion in the dissected cochleae. A slightly down-regulation of CB_1 gene expression in the cochlea and in the kidney was observed when animals received CDDP treatment, being statistically significant in the kidney probably due to a primary down-regulation trying to ameliorate tissue damage promoted by CB_1 in nephropathy models (Mukhopadhyay et al., 2010a). Recent studies go deeper in the role of CB_1 receptor in hearing function**.**

Zheng *et al*. use CBD and Δ-9-THC, and concluded that their results suggest that cannabinoids, such as Δ-9-THC and CBD, may actually aggravate tinnitus, probably because of the net effect of activation of CB_1 receptors in the dorsal cochlear nucleus might be to increase the excitation of fusiform cells, thus exacerbating neuronal hyperactivity (Zheng et al., 2015). In a study published in Hearing Research, researchers showed in knockout CB_1 mice, the role of the cannabinoid receptor in hearing. Animals without CB_1 presents deficit in their audiograms for frequencies above 8 kHz, but they are still able to distinguished changes in frequencies as well as the wild type (Toal et al., 2016).

Up to our knowledge, this is the first *in vivo* report of the expression of CB_2 receptors in the inner ear of mammals. Expression of CB_2 gene had been previously described in the *in vitro* line HEI-OC1, by means of RT-qPCR (Jeong et al., 2007). The authors demonstrated that JWH-015 (a synthetic CB_2 agonist) and HU210 (CB_1 agonist), could inhibit CDDP-induced apoptosis in HEI-OC1 cells. Specifically, they found that JWH-015 inhibited CDDP-induced caspase-3 and caspase-8 activity; cytochrome c (proapoptotic molecule) release from the mitochondria; increased phosphorylation of ERK; blocked the increase of ROS produced by CDDP; and inhibited TNF-α production on HEI-OC1 cells. From this, they suggested that CB activation was important in CDDP-induced apoptosis of HEI-OC1 cells.

HEI-OC1 cells express several molecular markers characteristic of organ of Corti sensory cells and could be considered as precursors. CB_2 immunolabeling in our study was seen in inner hair cells, but not in outer hair cells. Previous studies suggested that hair cell types derived from different progenitor cells. Specifically, these studies suggest that IHC derive from the greater epithelial ridge and the OHC derive from the lesser epithelial ridge (Lim and Anniko, 1985, Lim, 1992). This difference during ontogenesis has been related to the lateral process of inhibition that avoid cells from follow the same developmental pathway (Zine and Romand, 1996). These differences in the development of IHC and OHC could explain the differential immunolabeling of CB_2 receptor in sensory cells reported in our assays.

Our study suggests the expression of CB_2 receptor mostly in the intermediate region of the stria vascularis, although luminal and basal labeling could also be seen. We consider this as a limitation of our study and further studies would be needed to ascertain what

cellular types are specifically expressing CB_2 receptor. Potential labeling of residual erythrocytes within the capillary vessels of stria vascularis was contemplated, but we consider that it small size is negligible in relation to strial cells. The fact that CB_2 immunolabeling is also located in the stria vascularis suggests that CB_2 receptors might play a role in generation and/or maintenance of endocochlear potential. Potential interaction with structures identified in stria vascularis that are related to water and ion transport, antioxidant defenses and other homeostatic mechanisms merit further research.

CDDP clinical use is limited due to the induced toxicity affecting nervous system, kidney function and hearing. CDDP induces apoptosis by binding to DNA, ROS accumulation, increased lipid peroxidation and Ca^{2+} influx and inflammation events (Casares et al., 2012). In the present study CDDP treated animals presents an up-regulation in the expression of CB_2 gene in cochleae and also in the kidney. Mukhopaday *et al*. used an agonist of CB_2 receptor and CB_2 knockout mice trying to understand the role of the endocannabinoid system in CDDP-induced kidney disease. They observed that treatment with CB_2 agonist HU-308 ameliorates many CDDP-induced events like: ROS and inflammation markers; inflammatory cell infiltration and chemokine production; leading to a marker improvement of the renal function in CDDP-treated animals that also receive HU-308. An increase in inflammation , oxidative stress and cell death in knockout mice CB_2 -/- when compared to wild type was also observed, suggesting the protective role of the CB_2 receptor activation (Mukhopadhyay et al., 2010b). More recently, Mukhopaday *et al*. characterized the partial CB_2 receptor agonist LEI-101 showing promising results. The partial agonist does not induce cannabimimetic in animals treated, and a considerable attenuation in CDDP-induced nephropathy, including inflammation and oxidative stress (Mukhopadhyay et al., 2016).

As shown in this study, CDDP treatment increased the gene expression levels of CB_2 in the cochlea and in kidney (control) (**Fig.8**). This up-regulation of the inflammatory microenvironment induced by the treatment with CDDP promotes the overexpression of endocannabinoid system (increased CB_2). CB_2 overexpression may represent an adaptive response to control a deregulated balance in the ear maybe trying to restore normal conditions. A deeper understanding of the functional role of CB_2 receptor in

sensory and non-sensory elements of the cochlea may help develop therapies using CB_2 as target for reducing damage to the hearing organ. That opens a big field of possibilities to the treatment of inner ear diseases which involves inflammation process, using drugs with non canabimimetic effects, because CB_2 is the lack of psychoactive side effects after stimulation.

Conclusions

In conclusion, evidence for the presence of cannabinoid CB_2 receptor by immunohystochemistry and by RT-qPCR was provided. An immunolabeling of CB_2 antibodies in four structures of the adult rat cochlea was found. That was, stria vascularis, inner hair cells, auditory afferent nerves and cell bodies of the spiral ganglion. Up-regulation of CB_2 gene expression in animals exposed to CDDP treatment was also detected, when compared with healthy animals. This fact was partially supported by the higher immunofluorescence observed in the stria vascularis of CDDP-treated animals if compared with the healthy ones. These results suggest a considerable promising potential of CB_2 receptor as a target of new treatments against CDDP-induced ototoxicity, and probably against other inflammatory diseases in the inner ear. Further research is needed to determine the functionality of CB_2 receptors in the organ of Corti and the potential therapeutic role of agonists and antagonists of these receptors.

Acknowledgements

Authors acknowledge Carlos Vargas for his help in histology experiments, and PhD. Martin Santos, Maria Dolores Molina and Aitor Martín for their help in the animal facilities.

Supporting Information

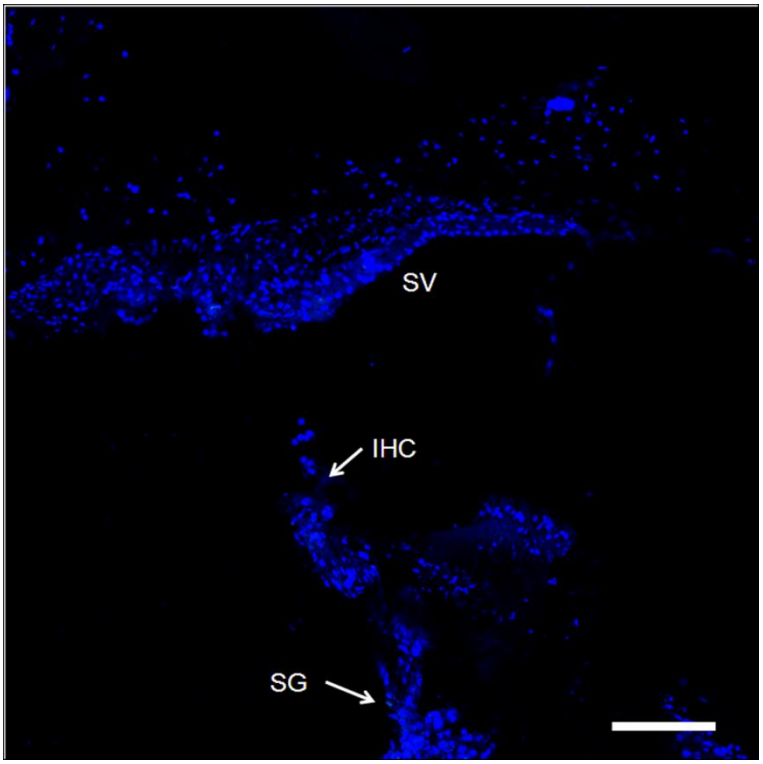

Fig S1: Detailed view of tissue sections pre adsorbed with CB_2 blocking peptide.
Detailed view of the cochlea pre adsoberd with CB_2 blocking peptide. No immunofluorescence was observed in the stria vascularis (SV), the IHC or the spiral ganglion (SG) (Scale bar = 100µm).

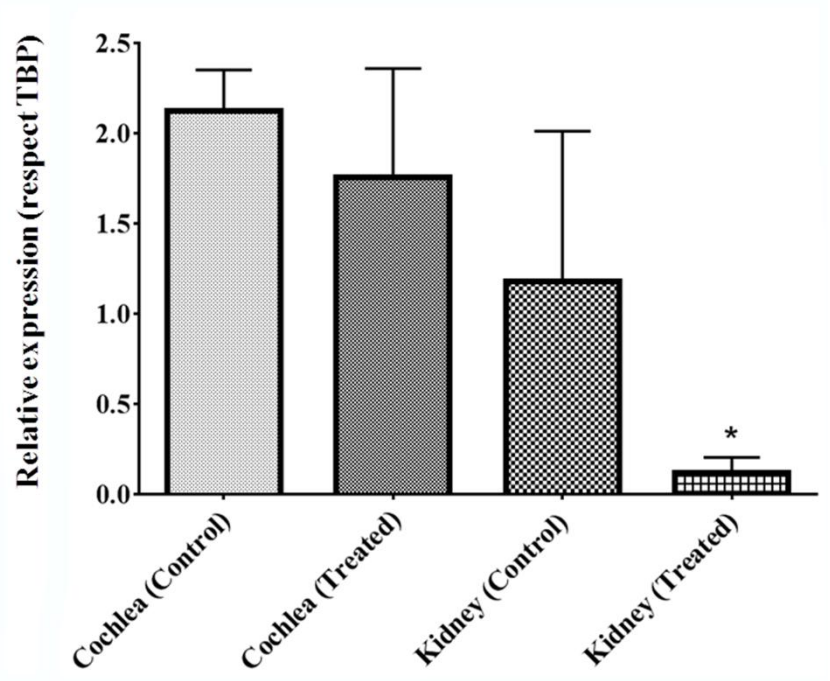

Fig S2: Measure of relative CB_1 gene expression by RT-qPCR.
Measure of relative CB_1 gene expression in the cochlea and kidney of healthy (control) and CDDP treated animals, respect TBP reference. The diagrams include the mean, the standard deviation (n = 10), and the ANOVA results (difference statistically significant respect control *$p<0.05$)

1

2

3

4 *Discusión General*

5

DISCUSIÓN GENERAL

Nanopartículas poliméricas basadas en derivados de la Vitamina E y el α-TOS para el tratamiento de la ototoxicidad inducida por CDDP

A pesar del desarrollo de nuevos regímenes de dosificación, el efecto ototóxico derivado del tratamiento con CDDP sigue siendo inevitable. Una sola inyección de CDDP en dosis elevadas tiene un rápido efecto ototóxico con una alta incidencia. La pérdida de audición inducida por el citostático afecta en primer lugar a las frecuencias altas y continúa a frecuencias medias, de modo que se muestra un aumento en el umbral auditivo para frecuencias a partir de 8 kHz. La entrada de CDDP en las células neurosensoriales del órgano de Corti tiene como resultado la muerte celular, que parece ser principalmente dependiente de caspasa (Rybak et al., 2007). La apoptosis inducida por el antitumoral en el oído interno podría ser debido a la activación de diferentes vías, siendo de especial importancia la ruta dependiente de caspasa que culmina en la activación de la caspasa-3 que escinde varios sustratos que resultan en la fragmentación del ADN cromosómico y provoca cambios morfológicos en la célula característicos de la apoptosis.

Tradicionalmente, el uso de corticoides administrados por vía sistémica para proteger contra la pérdida de audición neurosensorial ha arrojado buenos resultados (Wilson et al., 1980). Sin embargo, algunos autores han puesto en duda la eficacia de los esteroides sistémicos debido a los irregulares resultados en estudios clínicos debido a los efectos secundarios asociados. Otro problema derivado de la administración sistémica de corticoides ha sido la gran variedad de factores farmacocinéticos que influyen en la concentración del fármaco en el interior del oído interno, incluyendo: diferencia en la distribución, la variabilidad en la capacidad de cruzar la barrera sangre-perilinfa, diferentes vías metabólicas de los fármacos y la variabilidad en las vías de excreción (Paulson et al., 2008). Debido a estos problemas relacionados con la administración sistémica, la administración intratimpánica es una alternativa aceptada en pacientes con contraindicaciones para el tratamiento mediante corticoides sistémicos (Parnes et al., 1999, Haynes et al., 2007).

Una gran cantidad de estudios experimentales han intentado encontrar un otoprotector ideal contra la ototoxicidad inducida por CDDP. Se han desarrollado diversos abordajes

para enfrentarse a los múltiples problemas asociados a la llegada de fármacos al oído interno: la corta vida media de los potenciales fármacos, las dificultades para cruzar las barreras biológicas hasta el oído interno y la posible interacción entre la actividad antitumoral del CDDP y el tratamiento otoprotector. El uso de sistemas nanoparticulados para la encapsulación de fármacos podría ser un enfoque adecuado para paliar todos estos problemas y desarrollar tratamientos más eficaces para mejorar la pérdida de audición inducida por CDDP, dado que permite que fármacos hidrofóbicos atraviesen las barreras biológicas hasta la cóclea, y aumenta la vida media del fármaco.

En ésta primer parte de la tesis se trató de poner a punto un modelo *in vitro* e *in vivo* de tratamiento de la ototoxicidad provocada por CDDP mediante el uso de NPs poliméricas con capacidad de usar fármacos de uso común en clínica como la MP o la Dx. Para ello, se utilizaron los copolímeros CO-MVE y CO-MTOS, de carácter anfifílico, que presentan un adecuado equilibrio hidrófilo/hidrófobo para auto-organizarse en medios acuosos formando NPs pseudo esféricas con una envoltura hidrofílica (principalmente secuencias de VP) y un núcleo hidrofóbico (principalmente segmentos de MVE o MTOS, respectivamente) (Palao-Suay et al., 2015b). Éstas características hacen que presenten la capacidad de encapsular eficientemente fármacos hidrofóbicos en el interior de las NPs, mejorando la solubilidad intrínseca de los mismos.

Dos corticoides de uso habitual en clínica como la MP y la Dx fueron encapsulados de manera eficiente en el interior de las NPs copoliméricas descritas en éste trabajo. Tanto la MP como la Dx fueron incorporadas en el núcleo de los NPs con el fin de realizar una administración local de corticoide en el oído interno en concentraciones apropiadas y así aumentar su actividad a largo plazo, mejorar su biodisponibilidad, y disminuir los efectos secundarios no deseados. De igual manera, se testó la capacidad de las NPs para encapsular α-TOS, un derivado de la vitamina E con gran capacidad antioxidante, lo que podría reducir el estrés oxidativo intracelular generado tras el tratamiento con altas dosis de CDDP. La eficiencia de encapsulación de las tres moléculas testadas fue mayor para las NPs basadas en CO-MVE que para aquellos sistemas basados en CO-MTOS. Esto se debe probablemente a un equilibrio hidrófobo/hidrófilo diferente en ambos sistemas (sistema MVE es poli(VP-co-MVE) (60:40) y el sistema de MTOS es poli(VP-co-MTOS) (89:11)). CO-MVE tiene un contenido más alto en el monómero hidrófobo, MVE, que puede favorecer la encapsulación de MP, Dx o α-TOS [18, 20] (Palao-Suay

et al., 2015a, Palao-Suay et al., 2015). Así, se consiguieron EE% de más del 20% para las formulaciones de NP-MTOS que encapsulaban MP o Dx, aumentando por encima del 50% en los sistemas basados en MVE que encapsulaban cualquiera de los dos corticoides. La mayor EE% se observó en las NPs cargadas con α-TOS y C6, debido a la mayor hidrofobicidad de estas moléculas y las similitudes estructurales de α-TOS y C6. Como se ha comentado anteriormente, cuanto más hidrofóbica es la molécula, mayor es la EE%, y es por ello que la mayor eficiencia se registró en los sistemas que encapsulaban α-TOS como molécula con potencial otoprotector, siendo ésta mayor del 61% para las NP-MTOS y mayor de 72% para los sistemas NP-MVE.

Uno de los factores críticos a la hora de la administración de moléculas al oído medio a través de la RWM es el tamaño de las mismas. Bowe et al. (Bowe and Jacob, 2010) estudiaron la dinámica de perfusión a través de la RWM declarando que las NPs con tamaños inferiores a 200 nm eran capaces de pasar a través de esta membrana por difusión haciendo a éste tipo de sistemas candidatos ideales para la administración de fármacos a través de la RWM. Cai et al. (Cai et al., 2014) demostraron el potencial de las NPs basadas en PLGA con tamaños entre 135 y 154 nm para transportar fármacos y pasar a través de la RWM en cobayas. Los tamaños medios medidos por DLS fueron entre 120 y 128 nm en el caso de las NPs cargadas con MP, de entre 124 y 138 nm en aquellas cargadas con Dx y de 122 a 137 nm en los sistemas con α-TOS, cumpliendo todos ellos con los parámetros indicados anteriormente. Además, en el caso de las NPs cargadas con Dx y α-TOS se comprobó la estabilidad en el tamaño de las NPs en rangos de temperatura de 24 a 42ºC, lo que sugería que las propiedades físicas de las NPs no cambian en un rango de temperatura fisiológica. Estos resultados fueron corroborados por SEM, donde se observó además la morfología cuasi esférica de todas las preparaciones nanométricas.

Todos las NPs preparadas presentan valores de potencial zeta (δ) ligeramente negativos, siendo de entre -7 y -3 para todas las formulaciones ensayadas, lo que indica una superficie de carga prácticamente neutra. Estos valores se han descrito anteriormente por otros autores que trabajaban con NPs de corteza basada en VP (Zhu et al., 2010), e indica que la superficie externa de los sistemas NP está constituida por dominios hidrófilos ricos en VP.

Los perfiles de liberación de las distintas moléculas testadas fueron estudiados en condiciones fisiológicas (37ºC; PBS pH 7,4) para comprobar si mejoraban el perfil de liberación, ampliamente estudiado, de las moléculas libres. Los perfiles de liberación ambos corticoides siguieron una cinética de orden cero durante los primeros 80 horas, seguido de un período no lineal. En el caso de la Dx, ésta cinética se mantuvo durante dos semanas. Las condiciones experimentales están lejos de simular las condiciones *in vivo*, sin embargo, estos modelos experimentales *in vitro* sugieren que la liberación de MP y Dx tiene lugar en presencia de esterasas de manera sostenida durante, por lo menos, una semana. La vida media biológica de MP en el oído interno es de alrededor de 24 horas y la de la Dx de solo 8 horas (Parnes et al., 1999) y por lo tanto, su liberación sostenida es de gran interés para su aplicación como otoprotector de la toxicidad inducida por CDDP al reducir la dosis necesaria para obtener efecto terapéutico (Teng et al., 2005).

La C6 fue utilizada como modelo de fármaco hidrofóbico, encapsulándose con una alta eficiencia dado su alto carácter hidrofóbico. Éste fluorocromo se utilizó para seguir el proceso de captación celular de las NPs con el tiempo cuando éstas eran añadidas a un cultivo de células HEI-OC1. La fluorescencia de C6 se cuantificó en un cultivo celular durante 8 h tras la incubación NP y se observó que la acumulación intracelular de fluorescencia aumentaba gradualmente con el tiempo en ambas formulaciones. Después de 2 horas, la acumulación de C6 en las células tratadas con NP-MVE-C6 fue significativamente mayor que las células tratadas con NP-MTOS-C6, lo que probablemente está relacionado en parte con una mejor EE% en las formulaciones de MVE. Estos resultados mostraron que ambas formulaciones presentan la capacidad de ser internalizadas por las células HEI-OC1.

Demostrar la inocuidad de las NPs en la línea auditiva HEI-OC1 era el primer paso a tener en cuenta para corroborar si los sistemas podrían utilizarse como vehículo de fármacos al oído interno, dado que el cultivo HEI-OC1 es un modelo de ototoxicidad ampliamente utilizado al ser muy sensible a cualquier evento tóxico (Kalinec et al., 2002). Tanto las NPs basadas en MVE, como aquellas que lo estaban en MTOS resultaron no ser citotóxicas *in vitro* en concentraciones de entre 1 y 0,01 mg/ml, con la excepción de aquellas formulaciones que encapsulaban α-TOS que no lo eran a partir de 0,50 mg/ml. NP-MTOS-10αTOS fue la formulación con el efecto citotóxico más marcado probablemente debido a la mayor cantidad de α-TOS cargado en esta

formulación si se considera el fármaco atrapado y el α-TOS conjugado con el copolímero. Éstos resultados confirmaban la compatibilidad de todos los sistemas de NP-MVE y NP-MTOS con el cultivo de células del órgano de Corti.

Se testaron NPs no cargadas basadas en ambos copolímeros (CO-MTOS y CO-MVE) con el fin de comprobar si las propias NPs tenían la capacidad de reducir de forma efectiva la citotoxicidad derivada del tratamiento con CDDP en células auditivas HEI-OC1, ya que los copolímeros incorporan α-tocoferol (Vitamina E) o α-TOS unidos covalentemente a la cadena macromolecular (Palao-Suay et al., 2015a). En éste sentido, Kruspig et al. (Kruspig et al., 2013) estudiaron los efectos de la administración combinatoria de α-TOS y otras moléculas antiproliferativos, y demostraron el efecto antagónico de la administración de bajas concentraciones de α-TOS frente al tratamiento con CDDP. Por ello, las NPs vacías se pusieron a prueba con el fin de comprobar si el α-TOS o la Vitamina E, del copolímero podría reducir efectivamente el efecto pro-apoptótico de CDDP, pero los resultados demostraron que no existía dicha capacidad, probablemente debido a la pequeña cantidad de molécula activa en el copolímero y a la alta toxicidad del CDDP en HEI-OC1, al no existir diferencias significativas en la viabilidad celular de aquellos cultivos tratados solo con CDDP y aquellas que recibieron además el tratamiento con NP-MVE-0 y NP-MTOS-0.

NP-MVE-15MP (15% de MP w/w con respecto al copolímero) resultó ser la formulación más eficaz *in vitro* de aquellas que encapsulaban MP en los ensayos preliminares de la tésis, aunque no había diferencia estadísticamente significativa con NP-MVE-10MP en los mismos. Los sistemas de NP-MTOS presentaron un menor efecto protector contra la citotoxicidad inducida por CDDP que los basados en NP-MVE. El tratamiento con NP-MTOS-0 (sin MP encapsulada) consiguió aumentar ligeramente la viabilidad celular de las células tratadas con CDDP. Esto podría indicar cierta actividad del polímero aunque este efecto no fue estadísticamente significativo. Por lo tanto, tanto NP-MVE-0 como NP-MTOS-0 no pueden considerarse activos contra la citotoxicidad inducida por el tratamiento con CDDP *in vitro*, pero si resultaron ser buenos nanovehículos para encapsular y transportar MP.

La Dx y el α-tocoferol (Niki, 2014) son dos captadores de radicales libres de acción lenta, con reportado efecto positivo en la mejora de la ototoxicidad en animales tratados con CDDP (Paksoy et al., 2011). Ha sido demostrado el efecto apoptótico selectivo de

α-TOS en células tumorales en concentraciones que no son tóxicos para las células sanas. En las células no malignas α-TOS se hidroliza por medio de esterasas (Dong et al., 2008). Como resultado de la hidrólisis, la vitamina E se libera gradualmente para evitar el estrés oxidativo intracelular. NP-MVE-15Dx y NP-MTOS-10αTOS redujeron significativamente la citotoxicidad derivada del CDDP en un cierto rango de concentraciones (20% con NP-MVE-15Dx y 17% cuando son tratados con NP-MTOS-10αTOS), siendo las formulaciones más activas *in vitro* contra 30 µM CDDP, mejorando notablemente los resultados obtenidos con la mejor de las formulaciones que encapsulaban MP (10% de reducción de la citotoxicidad en NP-MVE-15). NP-MVE-10αTOS y NP-MTOS-15Dx también mostraron un ligero efecto citoprotector en HEI-OC1 con respecto a las células tratadas solo con CDDP, pero no de forma estadísticamente significativa.

Una vez puesto a punto el modelo in vitro mediante los sistemas que encapsulaban MP, se quiso ahondar en el posible efecto en distintos fenómenos desencadenados por el CDDP, tales como el aumento en la secreción de citoquinas pro-inflamatorias o el aumento en la actividad de caspasa 3 (Casares et al., 2012). De ésta manera, se observó que tanto NP-MVE-15Dx como NP-MTOS-15Dx fueron capaces de reducir significativamente la actividad de caspasa-3/7 en las células tratadas con CDDP durante 16 horas. El uso de corticoides como la Dx empleada en co-tratamientos con antitumorales como el CDDP causa resistencia a la apoptosis inducida por el citostático en células de carcinoma (Herr et al., 2003) y otras células tumorales de la médula, cerebro, mama, cuello uterino, melanoma y neuroblastoma (Zhang et al., 2006) con una reducción significativa de la expresión de caspasa-3. Así mismo, NP-MVE-10αTOS y NP-MTOS-10αTOS también redujeron la expresión de caspasa-3, siendo NP-MTOS-10αTOS la formulación que arrojó mejores resultados en el descenso de la expresión de éste marcador pro-apoptótico, incluso no mostrando ninguna diferencia estadísticamente significativa con respecto al control negativo. Como ha sido comentado anteriormente, α-TOS presenta un efecto protector frente a la toxicidad del CDDP a concentraciones relativamente bajas, por debajo de 40 µM, cuando el succinato es escindido por las esterasas celulares, mostrando la capacidad de regular la producción de ROS (Kruspig et al., 2013). García-Berrocal et al. (García-Berrocal et al., 2007) describieron previamente que las células cocleares tales como las células interdentales del limbo espiral, las células del surco interior, las células neurosensoriales (IHC y OHC), y las

células de Hensen presentan una expresión significativa de caspasa-3 tras la inyección de CDDP. De la misma manera Wang et al. (Wang et al., 2004) demostraron que la perfusión intracoclear del inhibidor de caspasa-3 (z-DEVD-fmk) provocaba una reducción drástica de los efectos ototóxicos de CDDP, demostrando la importancia de ésta proteína en los mecanismos de apoptosis desencadenados por el CDDP.

Otra vía que podría desencadenar mecanismos de apoptosis inducidos por el tratamiento con CDDP, se debe a los fenómenos inflamatorios que contribuyen a la muerte celular por la sobrerregulación de las citoquinas proinflamatorias tales como TNF-, IL-1β y IL-6 (Casares et al., 2012). La inflamación desempeña un papel importante en la apoptosis inducida por CDDP en la cóclea. La terapia con corticosteroides ha demostrado reducir la inflamación e inhibir la apoptosis en el órgano de Corti tras la exposición a CDDP u otros eventos ototóxicos como el tratamiento con antibióticos aminoglicósidos (Bas et al., 2012). Las formulaciones más efectivas cargadas con Dx y α-TOS (NP-MVE-15Dx, NP-MTOS-15Dx y NP-MTOS-10α-TOS) demostraron disminuir la liberación de IL-1β inducida por CDDP de una manera estadísticamente significativa con respecto a las células tratadas solo CDDP tras 24 horas de exposición al citostático.

La regulación a la baja de los biomarcadores pro-apoptóticos como la caspasa-3 e inflamatorios como IL-1β de los sistemas NP que encapsulan Dx y α-TOS, y la protección contra la citotoxicidad inducida por CDDP *in vitro* sugiere que estas formulaciones podrían reducir la ototoxicidad de manera eficiente en una modelo *in vivo*.

Se encontró una buena correlación entre los resultados obtenidos *in vitro* e *in vivo* tanto con las NPs vacías, como aquellas cargadas con cualquiera de las tres moléculas testadas. Los sistemas de NPs vacías, NP-MVE-0 y NP-MTOS-0, demostraron no ser capaces de disminuir la ototoxicidad inducida por CDDP. Las NPs vacías redujeron parcialmente la ototoxicidad derivada del CDDP, pero este efecto no fue estadísticamente significativo, aunque ambos copolímeros incorporaran moléculas activas como la vitamina E (MVE) o el α-TOS (MTOS) en su estructura. Este hecho podría estar relacionado con las altas dosis que se utilizaron en los experimentos para simular las terapias agresivas basadas en CDDP utilizadas en clínica.

Inicialmente, la formulación NP-MVE-15MP arrojó buenos resultados como otoprotector, mostrando que su actividad dependía principalmente de la eficiencia de

encapsulación, siendo ésta la formulación más activa tanto *in vitro* como *in vivo*. En los experimentos *in vitro*, las concentraciones entre 0,13 y 0,50 mg / ml redujeron significativamente la citotoxicidad de CDDP sobre las células HEI-OC1. Resultados confirmados *in vivo*, donde las frecuencias altas (14 a 16 kHz) presentaron una disminución significativa en el aumento del umbral de audición provocado por el CDDP tras ser administradas mediante bullostomía en el oído medio. Además, se comprobó la eficiencia de las NPs basadas en ambos copolímeros encapsulando el fluorocromo C6 (NP-MVE-C6 y NP-MTOS-C6) para atravesar la RWM hasta el oído interno y acumularse en el área de las células auditivas sensoriales cruzando 2 horas después de la administración. La acumulación se produjo fundamentalmente en las IHC en la región basal de la cóclea, asociada con la audición de altas frecuencias. Éstos resultados arrojaron la posibilidad de utilizar ambos tipos de polímeros para encapsular y dispensar de manera eficiente en el oído interno otros fármacos hidrófobos (antioxidantes, otros anti-inflamatorios, o fármacos anticaspasas) ya que ambos tipos de NPs fueron capaces de atravesar la membrana de la ventana redonda y entrar en el oído interno.

De esta manera, la administración de NP-MVE-15Dx demostró aminorar la pérdida de audición inducida por CDDP en todas las frecuencias medidas probablemente debido a su mejor EE% de corticoide. Sin embargo, sólo para sonidos de 16 kHz y 32 kHz, la protección fue estadísticamente significativa, pero la protección total de la audición fue el mejor en todas las formulaciones ensayadas.

El CDDP provoca un aumento significativo en la acumulación intracelular de ROS especialmente dependiente de la actividad mitocondrial, que contribuye significativamente a la muerte celular. Los antioxidantes como flunarizina (So et al., 2006), la metformina (Chang et al., 2014) o bucillamida (Kim et al., 2015) son capaces de reducir el nivel de ROS intracelular, protegiendo frente a la muerte celular inducida por CDDP. Por ello se utilizó el α-TOS para intentar aminorar los efectos nocivos del fármaco antitumoral, al ser una molécula con destino específico en las mitocondrias y con capacidad de reducir la generación de ROS inducida por CDDP como consecuencia de su efecto directo sobre mDNA (Marullo et al., 2013). El efecto de α-TOS sobre la ototoxicidad inducida por CDDP puede ser debido a su capacidad de monopolizar la cadena respiratoria de las mitocondrias por su unión a sitios de unión de ubiquinona en el complejo respiratorio II mitocondrial (Dong et al., 2008) ejerciendo un efecto regulador sobre la producción de ROS y disminuyendo así el estrés oxidativo inducido

por CDDP. Teranishi et al. (Teranishi et al., 2001) mostraron que la ototoxicidad y nefrotoxicidad inducidas por CDDP podían ser suprimidas mediante un tratamiento combinado de vitamina E intraperitoneal, que está presente en CO-MVE, sin embargo podría haber interferencias con la acción antitumoral del CDDP al ser administrada por ésta vía. Además, cuando α-TOS se usa a bajas concentraciones puede suprimir la apoptosis inducida por CDDP, dado que de los dos productos resultado de la degradación de la molécula tras la acción de las esterasas celulares, α-tocoferol (vitamina E) y succinato, la más protectora resultó ser el succinato (Kruspig et al., 2013). En nuestra experiencia, este hecho podría explicar que NP-MTOS-10α-TOS, con sólo un 10% menos de EE% que la formulación NP-MVE-10α-TOS, con la presencia del derivado metacrílico de α-TOS en el polímero CO-MTOS, mostrara grandes resultados que protegen contra la pérdida de audición *in vivo* (Figura 7D). La protección de la pérdida de audición inducida por CDDP fue estadísticamente significativa en frecuencias de 12, 20 y 32 kHz, reduciendo en más de 10 dB el umbral auditivo en el oído derecho protegido con respecto al oído izquierdo no protegido, demostrando tener un efecto parcialmente protector notablemente más alto que el mostrado por las formulaciones de MP, probablemente al ser moléculas más activas.

NPs sensibles a pH para paliar la ototoxicidad provocada por CDDP

Con el objetivo de obtener sistemas más complejos que pudieran aportar características adicionales a los sistemas de NPs poliméricas, se puso a punto la preparación de NPs basadas en la mezcla de los biopolímeros anteriormente descritos, basados en derivados metacrílicos de la vitamina E o el α-TOS (80-90% en peso) y copolímeros basados en un derivado metacrílico del ibuprofeno (10-20% en peso), HEI.

El tamaño de las NPs aumentaba significativamente con el aumento del contenido de HEI en la mezcla, con respecto a los sistemas basados solo en la CO-MTOS y CO-MVE. Como ejemplo, el tamaño de las NPs basadas MVE y HEI-6 varió desde 108 hasta 161 nm cuando se modificó la relación molar de estos diferentes copolímeros de (10 o 20% w / w, respectivamente). De igual manera, para una misma relación molar de 90:10, el D_h también aumentó en función de la cantidad de HEI en el copolímero, oscilando entre 108 y 135 nm para HEI-6 y HEI-14 respectivamente. A diferencia de los valores positivos de potencial zeta descritos previamente en NPs basadas en HEI (Suárez et al., 2013), en éste caso fueron ligeramente negativos. Estos resultados indican

la carga casi neutra de la superficie de las NPs como resultado de la menor cantidad de unidades de VI que probablemente se intercalan con un número mayoritario de las unidades de VP con la ausencia de grupos cargados.

La sensibilidad al pH de estos sistemas de NPs se demostró mediante la medición de su punto isoeléctrico, definido como el pH donde el potencial zeta es cero, o la carga superficial de la NP es cero. Es de destacar que el ζ disminuyó significativamente con el aumento de pH, como resultado de la conversión de VI de protonado a la forma desprotonada. Este efecto produce una desestabilización de las NPs a pH básico con una fuerte tendencia a agregarse. El pI de las NPs aumentó ligeramente con el contenido en copolímero de HEI, yendo desde 5,0 hasta 6,5. Los valores de pI más apropiados se obtienen a partir de la combinación de MTOS o MVE con un 20% en peso de copolímero HEI. En estas condiciones, el pI de las NPs combinadas, presentaba valores cercanos a los de un microambiente ligeramente ácido, como el que provoca el tratamiento con CDDP en el oído interno debido a la inflamación (Watanabe et al., 2001, So et al., 2008). Por esa razón, se seleccionaron estos sistemas de NPs basados en composiciones 80:20 de los copolímeros, para encapsular Dx y cumarina-6 en su núcleo interno.

La liberación *in vitro* de Dx fue estudiada a 37 °C durante 15 días. Alrededor del 20% de la carga Dx se libera de las NP-MVE-HEI14-10Dx y más del 45% de las NP-MTOS-HEI14-10Dx. Los perfiles de liberación de Dx de ambos sistemas siguieron una cinética de orden cero durante las primeras 2 semanas. La vida media biológica de Dx en el oído interno es de alrededor de 8 horas (Parnes et al., 1999) y por lo tanto, la liberación sostenida del fármaco es de gran interés para su aplicación como otoprotector de la toxicidad inducida por CDDP.

La actividad *in vitro* frente al CDDP de los sistemas de NPs basados en MTOS o MVE y HEI-6 o HEI14 (80:20) fue probada usando HEI-OC1. El objetivo de estos experimentos era optimizar la concentración más apropiada de NPs que permitiera la combinación de una actividad óptima anti-apoptótica, antioxidante y anti-inflamatoria en un mismo sistema de administración de fármacos sensible al pH.

Los mejores sistemas de todos los testados resultaron ser NP-MVEHEI14-10Dx y NP-MTOSHEI14-10Dx protegiendo contra la citotoxicidad provocada por CDDP en buen rango de concentraciones (más de 20% de protección con NP-MTOSHEI14-10Dx y 15

% cuando son tratados con NP-MVEHEI14-10Dx). La combinación de un tamaño adecuado y una buena EE% podría estar relacionado con los excelentes resultados obtenidos con los sistemas NP-MTOSHEI14-10Dx. Sin embargo, NP-MVEHEI14-10Dx también mostró buenos resultados contra dosis 30μM de CDDP, aunque su tamaño resultaba estar cerca del límite óptimo para una difusión adecuada hasta el oído interno (Hornyak, 2005). El pI de los sistemas probablemente permite la liberación sostenida de Dx tras la exposición de las células al CDDP, que induce la generación de ROS e inflamación, disminuyendo el valor del pH en relación con el de tejidos sanos(Punnia-Moorthy, 1987). El resto de ensayos realizados, se llevaron a cabo solo con éstos dos sistemas tras los resultados arrojados en el test de cito protección.

Apoyando estos resultados NP-MTOSHEI14-10Dx demostró reducir significativamente la actividad de caspasa-3/7 en las células tratadas con CDDP. En cambio, NP-MVE HEI14-10Dx reduce ligeramente la actividad de caspasa 3/7 pero no de una manera estadísticamente significativa. Está ampliamente reportado el efecto de el uso de corticoides como la Dx, causando resistencia a la apoptosis inducida por CDDP en células de carcinoma (Herr et al., 2003) y otras células tumorales de la médula, cerebro, mama, cuello uterino, melanoma y neuroblastoma (Zhang et al., 2006) con una importante reducción en la expresión de caspasa-3.

La Dx actúa como captador de ROS (Niki, 2014), y su efecto protector frente a la ototoxicidad provocada por CDDP en modelos animales ha sido estudiado (Paksoy et al., 2011). Los dos sistemas contienen en la mezcla un 20% de copolímero HEIcoVI14 con propiedades anti inflamatorias (Suárez et al., 2013), por lo que la acción combinada del corticoide encapsulado y el ibuprofeno liberado del polímero provocaba la inhibición de la liberación de IL-1β en forma estadísticamente significativa. La regulación a la baja de citoquinas pro-inflamatorias como TNF-α, IL-6 y IL-1β, que desempeñan un papel crítico en CDDP ototoxicidad, da como resultado la atenuación del daño coclear provocado por CDDP (So et al., 2008).

Así mismo, la ototoxicidad inducida por CDDP está estrechamente relacionada con el aumento de la producción de ROS y el estrés oxidativo intracelular (Rybak and Ramkumar, 2007). Ambos sistemas redujeron de manera eficiente la acumulación intracelular de ROS respecto a las células solo tratadas con CDDP.

No se observaron diferencias significativas entre los umbrales de audición entre el oído derecho (tratado con NPs) y el izquierdo (PBS) en ninguna de las frecuencias medidas, lo que demostraba la inocuidad de ambos sistemas.

Los resultados obtenidos *in vitro* sugerían el potencial de ambos sistemas como posibles otoprotectores frente a la pérdida de audición provocada por CDDP en el modelo murino. Tanto NP-MVEH10-10Dx, como NP-MTOS14-10Dx fueron testados *in vivo*, mostrando efecto otoprotector solamente el segundo de ellos de manera significativa para sonidos de 24 kHz. En cambio, NP-MVEH14-10Dx no mostró diferencias entre el oído izquierdo sin tratar y el oído derecho, tratado con NPs.

A pesar de que la EE% de Dx en NP-MVEH10-10Dx era sustancialmente más alta que en NP-MTOS14-10Dx, NP-MVEH10-10Dx no mostró ningún efecto protector frente a la ototoxicidad inducida por CDDP *in vivo*. Estos resultados podrían deberse al tamaño medio de este sistema, que es significativamente mayor que NP-MTOS14-10Dx, y estaba muy cerca del límte de tamaño óptimo (≥200nm) para cruzar a través RWM(Hornyak, 2005). Este factor está descrito como limitante para conseguir una dispensación eficiente del tratamiento a las células cocleares desde el oído medio. Las mejores características de tamaño medio de NP-MTOS14-10Dx le permitieron cruzar la RWM de manera eficiente y dispensar la Dx encapsulada en las células cocleares mejorando la pérdida de audición inducida por CDDP en todas las frecuencias medidas.

Nuevas dianas terapéuticas para el tratamiento de la ototoxicidad provocada por CDDP

La expresión de los receptores de canabinoides en un tejido específico abre la puerta a posibles tratamientos con agonistas y antagonistas que podrían desencadenar ciertas rutas de señalización celular. La expresión de CB_2 se ha descrito en los astrocitos y algunas subpoblaciones de neuronas, teniendo un papel en el sistema nervioso central relacionado con la neuroinflamación y la neurodegeneración (Fernández-Ruiz et al., 2007). Baek et al. describieron anteriormente la expresión proteica del receptor CB_2 en los núcleos coclear y vestibular del cerebro en un modelo de rata, lo que sugiere que podría tener un papel importante en el control del equilibrio y la función auditiva (Baek et al., 2009). Como parte del sistema nervioso periférico (Osen et al., 2011), no es sorprendente encontrar un notable inmunomarcado del receptor CB_2 en las células del órgano de Corti, aunque su papel funcional aún no se ha comprobado. El

inmunomarcado del receptor CB_2 resultó ser mayor en la estría vascular de animales que recibieron el tratamiento con el antitumoral, sin observarse diferencias significativas entre las IHC de animales sanos y tratados con CDDP. Debido a estas limitaciones de la inmunohistoquímica para apreciar diferencias en la regulación transcripcional de CB_2 entre animales sanos y tratados con CDDP, debido a la gran degradación estructural del tejido, se realizaron ensayos de RT-qPCR para determinar la regulación de la expresión del gen CB_2 ante un evento ototóxico.

En este estudio se observaron valores altos de la expresión del gen CB_1, utilizado como control de la expresión génica de canabinoides, probablemente debido a la presencia del ganglio espiral en las cócleas diseccionadas. Se observó una regulación a la baja de la expresión del gen CB_1 en la cóclea y en el riñón cuando los animales recibieron dosis de 10 mg/kg de CDDP, siendo estadísticamente significativa en el riñón probablemente debido a la sub-regulación primaria tratando de mejorar el daño tisular promovido por CB_1 en modelos de nefropatía (Mukhopadhyay et al., 2010a). Estudios recientes profundizan en el papel de los receptores CB_1 en la función auditiva. Zheng et al. utilizaron los canabinoides CBD y Δ-9-THC, sugiriendo que éstos pueden incluso agravar el tinnitus, probablemente debido al efecto neto de la activación de los receptores CB_1 en el núcleo coclear dorsal, lo que podría aumentar la excitación de las células fusiformes, exacerbando así la hiperactividad neuronal (Zheng et al., 2015). En un estudio publicado en Hearing Research recientemente, los investigadores demostraron en ratones knockout CB_1, el papel de los receptores de canabinoides en la audición. Los animales sin CB_1 presentaron déficit en sus audiogramas para frecuencias superiores a 8 kHz (Toal et al., 2016).

La expresión del gen CB_2 se había descrito previamente en la línea celular HEI-OC1, por medio de RT-qPCR (Jeong et al., 2007). Los autores demostraron que JWH-015 (un agonista sintético de CB_2) y HU210 (agonista de CB_1), podría inhibir la apoptosis inducida por CDDP en células HEI-OC1. Específicamente, encontraron que JWH-015 inhibió la actividad de la caspasa-3 y caspasa-8 inducida por CDDP; la liberación de citocromo c (molécula proapoptótico); aumento de la fosforilación de ERK; bloqueó el aumento de ROS producido por CDDP; e inhibió la producción de TNF-α en las células HEI-OC1. A partir de estos resultados, sugirieron el papel importante de la activación de CB en la apoptosis inducida por CDDP *in vitro*.

Las células HEI-OC1 expresan diversos marcadores moleculares característicos del órgano de Corti. El inmunomarcado de CB_2 en nuestro modelo experimental *in vivo* se observó en las células ciliadas internas, pero no en las células ciliadas externas. Los estudios anteriores sugirieron que los dos tipos de células ciliadas derivan de diferentes células progenitoras. Específicamente, estos estudios sugieren que las IHC derivan de la cresta mayor epitelial y la OHC de la cresta epitelial menor(Lim and Anniko, 1985, Lim, 1992). Esta diferencia durante la ontogénesis se ha relacionado con el proceso de inhibición lateral que evita que las células sigan la misma vía de desarrollo [42]. Estas diferencias en el desarrollo de IHC y OHC podrían explicar el marcado diferencial del receptor CB_2 en las células sensoriales reportado en nuestros ensayos.

El hecho de que se registrara también un importante inmunomarcado de CB_2 estría vascular sugiere que los receptores CB_2 podrían desempeñar un papel en la generación y/o mantenimiento del potencial endococlear.

El uso clínico del CDDP está limitado debido a la toxicidad inducida que afecta al sistema nervioso, la función renal y el oído. CDDP induce la apoptosis mediante la unión a ADN, la acumulación de ROS, el aumento de la peroxidación lipídica y eventos inflamatorios (Casares et al., 2012). En el presente estudio, los animales tartados con CDDP presentaron una sobre regulación de la expresión del gen CB_2 en la cóclea y también en el riñón. Mukhopadyay et al. estudiaron el papel de CB_2 en la enfermedad renal inducida por CDDP mediante el uso de agonistas de los receptores CB_2 y ratones knockout CB_2. Los autores observaron que el tratamiento con agonista el agonista selectivo de CB_2 HU-308, mejoró los eventos inducidos por CDDP, tales como: acumulación de ROS y la inflamación; la infiltración de células inflamatorias y la producción de citoquinas; conduciendo a una mejora marcada de la función renal en los animales tratados con CDDP que también recibieron HU-308. También se observó un marcado aumento de la inflamación, el estrés oxidativo y la apoptosis en los ratones knockout CB_2 -/-, lo que sugiere el papel protector de la activación del receptor CB_2 (Mukhopadhyay et al., 2010b). Más recientemente, Mukhopadyay et al. caracterizaron el agonista parcial de CB_2 LEI-101 mostrando resultados prometedores. El agonista parcial no indujo efectos canabimiméticos en los animales tratados, y provocaba una atenuación considerable en la nefropatía inducida por CDDP, incluyendo una notable reducción de la inflamación y el estrés oxidativo (Mukhopadhyay et al., 2016).

Como se muestra en este estudio, el tratamiento con CDDP aumentó los niveles de expresión génica de CB_2 en la cóclea y en el riñón. Los procesos pro inflamatorios inducidos por el tratamiento con CDDP promueven la sobreexpresión de sistema endocannabinoide (aumento de CB_2), lo que puede representar una respuesta adaptativa para controlar éste desequilibrio en el oído, tal vez tratando de restablecer las condiciones normales. Una comprensión más profunda del papel funcional de los receptores CB_2 en las céulas neurosensoriales y no sensoriales de la cóclea puede ayudar a desarrollar terapias que utilicen CB_2 como diana para la reducción de los daños en el órgano de la audición provocados por eventos ototóxicos, lo cual abre un gran campo de posibilidades para el tratamiento de enfermedades del oído interno que impliquen procesos inflamatorios.

1

2

3

4

5 *Conclusiones*

CONCLUSIONES

1. Se pusieron a punto modelos de otoxicidad derivada por el tratamiento con cisplatino *in vitro* e *in vivo*, para la aplicación de fármacos vehiculizados en sistemas nanométricos basados en copolímeros anfifílicos derivados de la Vitamina E y del succinato de α-tocoferilo (α-TOS), usando como modelo la 6α-metilprednisolona, ampliamente utilizada en clínica.
2. Se consiguió vehiculizar de manera eficiente distintos tipos de moléculas con capacidad antiinflamatoria, como la metilprednisolona y la dexametasona, o capacidad antioxidante, como el α-tocoferil succinato.
3. Mediante la encapsulación del fluorocromo cumarina-6, se comprobó que tanto las NP-MVE como NP-MTOS eran capaces de llegar al oído interno atravesando la membrana de la ventana redonda de manera eficiente, acumulándose preferentemente en las células ciliadas internas, y en menor medida en las externas.
4. Se desarrollaron sistemas de NPs sensibles a pH con una mezcla de copolímeros derivados de la vitamina E y el ibuprofeno, con el fin de liberar dexamtasona en el entorno pro-inflamatorio del oído tras el tratamiento con cisplatino.
5. Se describió la presencia de receptores de camabinoides CB_2 en la coclea de rata Wistar, así como su sobreexpresión génica tras el tratamiento con CDDP. Los resultados obtenidos sugieren el potencial de éstos receptores como dianas terapéuticas para el desarrollo de tratamientos contra la ototoxicidad provocada por CDDP.

Referencias

Referencias

Referencias

Referencias

ABALO, R., CABEZOS, P., VERA, G., LÓPEZ-PÉREZ, A. & MARTIN, M. 2013. Cannabinoids may worsen gastric dysmotility induced by chronic cisplatin in the rat. *Neurogastroenterology & Motility,* 25**,** 373-e292.

AGUILAR, M. R. & ROMAN, J. 2014. *Smart polymers and their applications*, Elsevier.

AMENTA, P. S., JALLO, J. I., TUMA, R. F., HOOPER, D. C. & ELLIOTT, M. B. 2014. Cannabinoid receptor type-2 stimulation, blockade, and deletion alter the vascular inflammatory responses to traumatic brain injury. *Journal of neuroinflammation,* 11**,** 1.

BAEK, J.-H., ZHENG, Y., DARLINGTON, C. L. & SMITH, P. F. 2009. Cannabinoid CB2 receptor expression in the rat brainstem cochlear and vestibular nuclei. *Acta oto-laryngologica,* 128**,** 961-967.

BAMRUNGSAP, S., ZHAO, Z., CHEN, T., WANG, L., LI, C., FU, T. & TAN, W. 2012. Nanotechnology in therapeutics: a focus on nanoparticles as a drug delivery system. *Nanomedicine,* 7**,** 1253-1271.

BARUTTA, F., PISCITELLI, F., PINACH, S., BRUNO, G., GAMBINO, R., RASTALDI, M. P., SALVIDIO, G., DI MARZO, V., PERIN, P. C. & GRUDEN, G. 2011. Protective role of cannabinoid receptor type 2 in a mouse model of diabetic nephropathy. *Diabetes,* 60**,** 2386-2396.

BAS, E., VAN DE WATER, T., GUPTA, C., DINH, J., VU, L., MARTÍNEZ-SORIANO, F., LAINEZ, J. & MARCO, J. 2012. Efficacy of three drugs for protecting against gentamicin-induced hair cell and hearing losses. *British journal of pharmacology,* 166**,** 1888-1904.

BÁTKAI, S., MUKHOPADHYAY, P., HORVÁTH, B., RAJESH, M., GAO, R. Y., MAHADEVAN, A., AMERE, M., BATTISTA, N., LICHTMAN, A. H. & GAUSON, L. A. 2012. Δ8-Tetrahydrocannabivarin prevents hepatic ischaemia/reperfusion injury by decreasing oxidative stress and inflammatory responses through cannabinoid CB2 receptors. *British journal of pharmacology,* 165**,** 2450-2461.

BERDYSHEV, E. 2000. Cannabinoid receptors and the regulation of immune response. *Chemistry and physics of lipids,* 108**,** 169-190.

BERROCAL, J. R. G. & RAMÍREZ-CAMACHO, R. 2000. Immune response and immunopathology of the inner ear: an update. *Journal of Laryngology & Otology,* 114**,** 101-107.

BILMEZ, Z. E. B., AYDIN, S., ŞANLI, A., ALTINTOPRAK, N., DEMIR, M. G., ERDOĞAN, B. A. & KÖSEMIHAL, E. 2016. Oxytocin as a protective agent in cisplatin-induced ototoxicity. *Cancer chemotherapy and pharmacology,* 77**,** 875-879.

BOKEMEYER, C., BERGER, C., HARTMANN, J., KOLLMANNSBERGER, C., SCHMOLL, H., KUCZYK, M. & KANZ, L. 1998. Analysis of risk factors for cisplatin-induced ototoxicity in patients with testicular cancer. *British journal of cancer,* 77**,** 1355.

BOWE, S. N. & JACOB, A. 2010. Round window perfusion dynamics: implications for intracochlear therapy. *Curr Opin Otolaryngol Head Neck Surg,* 18**,** 377-385.

CAI, H., WEN, X., WEN, L., TIRELLI, N., ZHANG, X., ZHANG, Y., SU, H., YANG, F. & CHEN, G. 2014. Enhanced local bioavailability of single or compound drugs delivery to the inner ear through application of PLGA nanoparticles via round window administration. *International journal of nanomedicine,* 9**,** 5591.

CASARES, C., RAMIREZ-CAMACHO, R., TRINIDAD, A., ROLDAN, A., JORGE, E. & GARCIA-BERROCAL, J. R. 2012a. Reactive oxygen species in apoptosis induced by cisplatin: review of physiopathological mechanisms in animal models. *Eur Arch Otorhinolaryngol,* 269**,** 2455-2459.

CUNNINGHAM, L. L. & BRANDON, C. S. 2006. Heat shock inhibits both aminoglycoside-and cisplatin-induced sensory hair cell death. *Journal of the Association for Research in Otolaryngology,* 7**,** 299-307.

CHANG, J., JUNG, H. H., YANG, J. Y., LEE, S., CHOI, J., IM, G. J. & CHAE, S. W. 2014. Protective effect of metformin against cisplatin-induced ototoxicity in an auditory cell line. *Journal of the Association for Research in Otolaryngology,* 15**,** 149-158.

CHELLAT, F., MERHI, Y., MOREAU, A. & YAHIA, L. H. 2005. Therapeutic potential of nanoparticulate systems for macrophage targeting. *Biomaterials,* 26**,** 7260-7275.

CHOI, J., KIM, S. H., RAH, Y. C., CHAE, S. W., LEE, J. D., MD, B. D. L. & PARK, M. K. 2014. Effects of caffeic acid on cisplatin-induced hair cell damage in HEI-OC1 auditory cells. *International journal of pediatric otorhinolaryngology*.

DANHIER, F., FERON, O. & PRÉAT, V. 2010. To exploit the tumor microenvironment: passive and active tumor targeting of nanocarriers for anti-cancer drug delivery. *Journal of Controlled Release,* 148**,** 135-146.

DEMUTH, D. G. & MOLLEMAN, A. 2006. Cannabinoid signalling. *Life sciences,* 78**,** 549-563.

DEUTSCH, D. G., GOLIGORSKY, M. S., SCHMID, P. C., KREBSBACH, R. J., SCHMID, H., DAS, S., DEY, S., ARREAZA, G., THORUP, C. & STEFANO, G. 1997. Production and physiological actions of anandamide in the vasculature of the rat kidney. *Journal of Clinical Investigation,* 100**,** 1538.

DEVANE, W. A., DYSARZ, F. R., JOHNSON, M. R., MELVIN, L. S. & HOWLETT, A. C. 1988. Determination and characterization of a cannabinoid receptor in rat brain. *Molecular pharmacology,* 34**,** 605-613.

DONAIRE, M. L., PARRA-CÁCERES, J., VÁZQUEZ-LASA, B., GARCÍA-ÁLVAREZ, I., FERNÁNDEZ-MAYORALAS, A., LÓPEZ-BRAVO, A. & SAN ROMÁN, J. 2009. Polymeric drugs based on bioactive glycosides for the treatment of brain tumours. *Biomaterials,* 30**,** 1613-1626.

DONG, L.-F., LOW, P., DYASON, J. C., WANG, X.-F., PROCHAZKA, L., WITTING, P. K., FREEMAN, R., SWETTENHAM, E., VALIS, K. & LIU, J. 2008. α-Tocopheryl succinate induces apoptosis by targeting ubiquinone-binding sites in mitochondrial respiratory complex II. *Oncogene*, 27**,** 4324-4335.

DU, J.-Z., DU, X.-J., MAO, C.-Q. & WANG, J. 2011. Tailor-made dual pH-sensitive polymer–doxorubicin nanoparticles for efficient anticancer drug delivery. *Journal of the American Chemical Society*, 133**,** 17560-17563.

DUERR, G. D., HEINEMANN, J. C., GESTRICH, C., HEUFT, T., KLAAS, T., KEPPEL, K., ROELL, W., KLEIN, A., ZIMMER, A. & VELTEN, M. 2015. Impaired border zone formation and adverse remodeling after reperfused myocardial infarction in cannabinoid CB2 receptor deficient mice. *Life sciences,* 138**,** 8-17.

DUHEM, N., DANHIER, F. & PRÉAT, V. 2014. Vitamin E-based nanomedicines for anti-cancer drug delivery. *Journal of Controlled Release,* 182**,** 33-44.

DUNCAN, R. 2005. Nanomedicine gets clinical. *Materials Today*, 8**,** 16-17.

EINHORN, L. H. 2002. Curing metastatic testicular cancer. *Proceedings of the National Academy of Sciences*, 99**,** 4592-4595.

EKBORN, A., LINDBERG, A., LAURELL, G., WALLIN, I., EKSBORG, S. & EHRSSON, H. 2003. Ototoxicity, nephrotoxicity and pharmacokinetics of cisplatin and its monohydrated complex in the guinea pig. *Cancer chemotherapy and pharmacology,* 51**,** 36-42.

EL KECHAI, N., MAMELLE, E., NGUYEN, Y., HUANG, N., NICOLAS, V., CHAMINADE, P., YEN-NICOLAŸ, S., GUEUTIN, C., GRANGER, B. & FERRARY, E. 2016. Hyaluronic acid liposomal gel sustains delivery of a corticoid to the inner ear. *Journal of Controlled Release,* 226**,** 248-257.

FAUSER, C. B., THORSTEN; NIEDERMEYER, HANS; OESTREICHER, ELMAR. CB1 cannabinoid receptor is expressed in the mammalian cochlea. *In:* SANTI, P. A., ed. ASSOCIATION FOR RESEARCH IN OTOLARYNGOLOGY, 2005.

FENNELL, D., SUMMERS, Y., CADRANEL, J., BENEPAL, T., CHRISTOPH, D., LAL, R., DAS, M., MAXWELL, F., VISSEREN-GRUL, C. & FERRY, D. 2016. Cisplatin in the modern era: The backbone of first-line chemotherapy for non-small cell lung cancer. *Cancer treatment reviews,* 44**,** 42-50.

FERNÁNDEZ-RUIZ, J., MORO, M. A. & MARTÍNEZ-ORGADO, J. 2015. Cannabinoids in Neurodegenerative Disorders and Stroke/Brain Trauma: From Preclinical Models to Clinical Applications. *Neurotherapeutics,* 12**,** 793-806.

FERNÁNDEZ-RUIZ, J., ROMERO, J., VELASCO, G., TOLÓN, R. M., RAMOS, J. A. & GUZMÁN, M. 2007. Cannabinoid CB 2 receptor: a new target for controlling neural cell survival? *Trends in pharmacological sciences,* 28**,** 39-45.

FESSI, H., PUISIEUX, F., DEVISSAGUET, J. P., AMMOURY, N. & BENITA, S. 1989. Nanocapsule formation by interfacial polymer deposition following solvent displacement. *International journal of pharmaceutics,* 55**,** R1-R4.

GAO, G., LIU, Y., ZHOU, C., JIANG, P. & SUN, J. 2015. Solid Lipid Nanoparticles Loaded with Edaravone for Inner Ear Protection After Noise Exposure. *Chinese medical journal,* 128**,** 203.

GARCÍA-BERROCAL, J., NEVADO, J., GONZÁLEZ-GARCÍA, J. Á., SÁNCHEZ-RODRÍGUEZ, C., SANZ, R., TRINIDAD, A., ESPAÑA, P., CITORES, M. & RAMÍREZ-CAMACHO, R. 2010. Heat shock protein 70 and cellular disturbances in cochlear cisplatin ototoxicity model. *The Journal of Laryngology & Otology,* 124**,** 599-609.

GARCÍA-BERROCAL, J. R., IBÁÑEZ, A., RODRÍGUEZ, A., GONZÁLEZ-GARCÍA, J. Á., VERDAGUER, J. M., TRINIDAD, A. & RAMÍREZ-

CAMACHO, R. 2006. Alternatives to systemic steroid therapy for refractory immune-mediated inner ear disease: a physiopathologic approach. *European Archives of Oto-Rhino-Laryngology and Head & Neck,* 263**,** 977-982.

GARCÍA-FERNÁNDEZ, L., HALSTENBERG, S., UNGER, R. E., AGUILAR, M. R., KIRKPATRICK, C. J. & SAN ROMÁN, J. 2010. Anti-angiogenic activity of heparin-like polysulfonated polymeric drugs in 3D human cell culture. *Biomaterials,* 31**,** 7863-7872.

GARCÍA-BERROCAL, J., NEVADO, J., RAMÍREZ-CAMACHO, R., SANZ, R., GONZÁLEZ-GARCÍA, J., SÁNCHEZ-RODRÍGUEZ, C., CANTOS, B., ESPANA, P., VERDAGUER, J. & TRINIDAD CABEZAS, A. 2007. The anticancer drug cisplatin induces an intrinsic apoptotic pathway inside the inner ear. *British journal of pharmacology,* 152**,** 1012-1020.

GLUECKERT, R., PRITZ, C. O., ROY, S., DUDAS, J. & SCHROTT-FISCHER, A. 2015. Nanoparticle mediated drug delivery of rolipram to tyrosine kinase B positive cells in the inner ear with targeting peptides and agonistic antibodies. *Frontiers in aging neuroscience,* 7.

GÓMEZ-GÁLVEZ, Y., PALOMO-GARO, C., FERNÁNDEZ-RUIZ, J. & GARCÍA, C. 2016. Potential of the cannabinoid CB 2 receptor as a pharmacological target against inflammation in Parkinson's disease. *Progress in Neuro-Psychopharmacology and Biological Psychiatry,* 64**,** 200-208.

GONZÁLEZ-GARCÍA, J. Á., NEVADO, J., GARCÍA-BERROCAL, J. R., SÁNCHEZ-RODRÍGUEZ, C., TRINIDAD, A., SANZ, R. & RAMÍREZ-CAMACHO, R. 2010. Endogenous protection against oxidative stress caused by cisplatin: role of superoxide dismutase. *Acta oto-laryngologica,* 130**,** 453-457.

GRIMALDI, P., ORLANDO, P., DI SIENA, S., LOLICATO, F., PETROSINO, S., BISOGNO, T., GEREMIA, R., DE PETROCELLIS, L. & DI MARZO, V. 2009. The endocannabinoid system and pivotal role of the CB2 receptor in mouse spermatogenesis. *Proceedings of the National Academy of Sciences,* 106**,** 11131-11136.

HARGUNANI, C. A., KEMPTON, J. B., DEGAGNE, J. M. & TRUNE, D. R. 2006. Intratympanic injection of dexamethasone: time course of inner ear distribution and conversion to its active form. *Otology & Neurotology,* 27**,** 564-569.

HAYNES, D. S., O'MALLEY, M., COHEN, S., WATFORD, K. & LABADIE, R. F. 2007. Intratympanic dexamethasone for sudden sensorineural hearing loss after failure of systemic therapy. *The Laryngoscope,* 117**,** 3-15.

HE, F. & SONG, Z.-H. 2007. Molecular and cellular changes induced by the activation of CB2 cannabinoid receptors in trabecular meshwork cells. *Molecular Vision,* 13**,** 1348-56.

HERR, I., UCUR, E., HERZER, K., OKOUOYO, S., RIDDER, R., KRAMMER, P. H., VON KNEBEL DOEBERITZ, M. & DEBATIN, K.-M. 2003. Glucocorticoid cotreatment induces apoptosis resistance toward cancer therapy in carcinomas. *Cancer research,* 63**,** 3112-3120.

HORNYAK, G. L. 2005. Nanotechnology in otolaryngology. *Otolaryngologic Clinics of North America,* 38**,** 273-293.

HORVÁTH, B., MAGID, L., MUKHOPADHYAY, P., BÁTKAI, S., RAJESH, M., PARK, O., TANCHIAN, G., GAO, R. Y., GOODFELLOW, C. E. & GLASS, M. 2012. A new cannabinoid CB2 receptor agonist HU-910 attenuates oxidative stress, inflammation and cell death associated with hepatic ischaemia/reperfusion injury. *British journal of pharmacology,* 165**,** 2462-2478.

HSIEH, G. C., PAI, M., CHANDRAN, P., HOOKER, B. A., ZHU, C. Z., SALYERS, A. K., WENSINK, E. J., ZHAN, C., CARROLL, W. A. & DART, M. J. 2011. Central and peripheral sites of action for CB2 receptor mediated analgesic activity in chronic inflammatory and neuropathic pain models in rats. *British journal of pharmacology,* 162**,** 428-440.

JAVED, H., AZIMULLAH, S., HAQUE, M. E. & OJHA, S. K. 2016. Cannabinoid Type 2 (CB2) Receptors Activation Protects against Oxidative Stress and Neuroinflammation Associated Dopaminergic Neurodegeneration in Rotenone Model of Parkinson's Disease. *Frontiers in Neuroscience,* 10.

JEONG, H. J., KIM, S. J., MOON, P. D., KIM, N. H., KIM, J. S., PARK, R. K., KIM, M. S., PARK, B. R., JEONG, S. & UM, J. Y. 2007. Antiapoptotic mechanism of cannabinoid receptor 2 agonist on cisplatin-induced apoptosis in the HEI-OC1 auditory cell line. *Journal of neuroscience research,* 85**,** 896-905.

JULIEN, B., GRENARD, P., TEIXEIRA-CLERC, F., VAN NHIEU, J. T., LI, L., KARSAK, M., ZIMMER, A., MALLAT, A. & LOTERSZTAJN, S. 2005. Antifibrogenic role of the cannabinoid receptor CB2 in the liver. *Gastroenterology,* 128**,** 742-755.

KALINEC, G., THEIN, P., PARK, C. & KALINEC, F. 2016. HEI-OC1 Cells as a Model for Investigating Drug Cytotoxicity. *Hearing Research*, 335, 105-117.

KALINEC, G. M., WEBSTER, P., LIM, D. J. & KALINEC, F. 2003. A cochlear cell line as an in vitro system for drug ototoxicity screening. *Audiol Neurootol,* 8**,** 177-189.

KARA, M., TÜRKÖN, H., KARACA, T., GÜÇLÜ, O., UYSAL, S., TÜRKYıLMAZ, M., DEMIRTAŞ, S. & DEREKÖY, F. S. 2016. Evaluation of the protective effects of hesperetin against cisplatin-induced ototoxicity in a rat animal model. *International journal of pediatric otorhinolaryngology,* 85**,** 12-18.

KARASAWA, T. & STEYGER, P. S. 2015. An integrated view of cisplatin-induced nephrotoxicity and ototoxicity. *Toxicology letters,* 237**,** 219-227.

KARSAK, M., GAFFAL, E., DATE, R., WANG-ECKHARDT, L., REHNELT, J., PETROSINO, S., STAROWICZ, K., STEUDER, R., SCHLICKER, E. & CRAVATT, B. 2007. Attenuation of allergic contact dermatitis through the endocannabinoid system. *science,* 316**,** 1494-1497.

KAUR, T., MUKHERJEA, D., SHEEHAN, K., JAJOO, S., RYBAK, L. & RAMKUMAR, V. 2011. Short interfering RNA against STAT1 attenuates cisplatin-induced ototoxicity in the rat by suppressing inflammation. *Cell death & disease,* 2**,** e180.

KIM, D.-K., PARK, S.-N., PARK, K.-H., PARK, C. W., YANG, K.-J., KIM, J.-D. & KIM, M.-S. 2015a. Development of a drug delivery system for the inner ear using poly (amino acid)-based nanoparticles. *Drug delivery,* 22**,** 367-374.

KIM, H.-J., OH, G.-S., SHEN, A., LEE, S.-B., KHADKA, D., PANDIT, A., SHIM, H., YANG, S.-H., CHO, E.-Y. & SONG, J. 2015b. Nicotinamide adenine dinucleotide: An essential factor in preserving hearing in cisplatin-induced ototoxicity. *Hearing research,* 326**,** 30-39.

KIM, H. J., SO, H. S., LEE, J. H., PARK, C., LEE, J. B., YOUN, M. J., KIM, S. J., YANG, S. H., LEE, K. M. & KWON, K. B. 2008. Role of proinflammatory cytokines in cisplatin-induced vestibular hair cell damage. *Head & neck,* 30**,** 1445-1456.

KIM, S.-J., HUR, J. H., PARK, C., KIM, H.-J., OH, G.-S., LEE, J. N., YOO, S.-J., CHOE, S.-K., SO, H.-S. & LIM, D. J. 2015c. Bucillamine prevents cisplatin-induced ototoxicity through induction of glutathione and antioxidant genes. *Experimental & molecular medicine,* 47**,** e142.

KIM, S. K., IM, G. J., AN, Y. S., LEE, S. H., JUNG, H. H. & PARK, S. Y. 2016. The effects of the antioxidant α-tocopherol succinate on cisplatin-induced ototoxicity in HEI-OC1 auditory cells. *International journal of pediatric otorhinolaryngology,* 86**,** 9-14.

KNOP, K., HOOGENBOOM, R., FISCHER, D. & SCHUBERT, U. S. 2010. Poly (ethylene glycol) in drug delivery: pros and cons as well as potential alternatives. *Angewandte Chemie International Edition,* 49**,** 6288-6308.

KOTTSCHADE, L. A., SLOAN, J. A., MAZURCZAK, M. A., JOHNSON, D. B., MURPHY, B. P., ROWLAND, K. M., SMITH, D. A., BERG, A. R., STELLA, P. J. & LOPRINZI, C. L. 2011. The use of vitamin E for the prevention of chemotherapy-induced peripheral neuropathy: results of a randomized phase III clinical trial. *Supportive Care in Cancer,* 19**,** 1769-1777.

KRUSPIG, B., ZHIVOTOVSKY, B. & GOGVADZE, V. 2013. Contrasting effects of α-tocopheryl succinate on cisplatin-and etoposide-induced apoptosis. *Mitochondrion,* 13**,** 533-538.

LARDNER, A. 2001. The effects of extracellular pH on immune function. *Journal of leukocyte biology,* 69**,** 522-530.

LEE, E. S., NA, K. & BAE, Y. H. 2005. Super pH-sensitive multifunctional polymeric micelle. *Nano Letters,* 5**,** 325-329.

LEE, J. E., NAKAGAWA, T., KIM, T. S., ENDO, T., SHIGA, A., IGUCHI, F., LEE, S. H. & ITO, J. 2004. Role of reactive radicals in degeneration of the auditory system of mice following cisplatin treatment. *Acta oto-laryngologica,* 124**,** 1131-1135.

LI, G., LIU, W. & FRENZ, D. 2006. Cisplatin ototoxicity to the rat inner ear: a role for HMG1 and iNOS. *Neurotoxicology,* 27**,** 22-30.

LIM, D. J. & ANNIKO, M. 1985. Developmental morphology of the mouse inner ear: a scanning electron microscopic observation. *Acta Oto-Laryngologica,* 99**,** 5-69.

LIM, D. J. R., J. 1992. Structural development of the cochlea. *In:* REMAND, R. (ed.) *Development of Auditory and Vestibular Systems.* Amsterdam: El Sevier.

LIU, J., HUANG, Y., KUMAR, A., TAN, A., JIN, S., MOZHI, A. & LIANG, X.-J. 2014a. pH-sensitive nano-systems for drug delivery in cancer therapy. *Biotechnology advances,* 32**,** 693-710.

LIU, Z., WANG, Y., ZHAO, H., ZHENG, Q., XIAO, L. & ZHAO, M. 2014b. CB2 receptor activation ameliorates the proinflammatory activity in acute lung injury induced by paraquat. *BioMed research international,* 2014.

MA, W., HU, J., CHENG, Y., WANG, J., ZHANG, X. & XU, M. 2015a. Ginkgolide B protects against cisplatin-induced ototoxicity: enhancement of Akt–Nrf2–HO-1 signaling and reduction of NADPH oxidase. *Cancer chemotherapy and pharmacology,* 75**,** 949-959.

MACCARRONE, M. 2008. CB2 receptors in reproduction. *British journal of pharmacology,* 153**,** 189-198.

MALLAT, A., TEIXEIRA-CLERC, F., DEVEAUX, V., MANIN, S. & LOTERSZTAJN, S. 2011. The endocannabinoid system as a key mediator during liver diseases: new insights and therapeutic openings. *British journal of pharmacology,* 163**,** 1432-1440.

MARTÍN-SALDAÑA, S., PALAO-SUAY, R., TRINIDAD, A., AGUILAR, M. R., RAMÍREZ-CAMACHO, R. & SAN ROMÁN, J. 2016. Otoprotective properties of 6α-methylprednisolone-loaded nanoparticles against cisplatin: In vitro and in vivo correlation. *Nanomedicine: Nanotechnology, Biology and Medicine,* 12**,** 965-976.

MARULLO, R., WERNER, E., DEGTYAREVA, N., MOORE, B., ALTAVILLA, G., RAMALINGAM, S. S. & DOETSCH, P. W. 2013. Cisplatin induces a mitochondrial-ROS response that contributes to cytotoxicity depending on mitochondrial redox status and bioenergetic functions. *PLoS ONE,* 8.

MCCALL, A. A., SWAN, E. E. L., BORENSTEIN, J. T., SEWELL, W. F., KUJAWA, S. G. & MCKENNA, M. J. 2010. Drug delivery for treatment of inner ear disease: current state of knowledge. *Ear and hearing,* 31**,** 156.

MCHUGH, D., TANNER, C., MECHOULAM, R., PERTWEE, R. G. & ROSS, R. A. 2008. Inhibition of human neutrophil chemotaxis by endogenous cannabinoids and phytocannabinoids: evidence for a site distinct from CB1 and CB2. *Molecular pharmacology,* 73**,** 441-450.

MIMURA, T., OKA, S., KOSHIMOTO, H., UEDA, Y., WATANABE, Y. & SUGIURA, T. 2012. Involvement of the endogenous cannabinoid 2 ligand 2-arachidonyl glycerol in allergic inflammation. *International archives of allergy and immunology,* 159**,** 149-156.

MOGHIMI, S. M., HUNTER, A. C. & MURRAY, J. C. 2005. Nanomedicine: current status and future prospects. *The FASEB journal,* 19**,** 311-330.

MUKHERJEA, D., JAJOO, S., SHEEHAN, K., KAUR, T., SHETH, S., BUNCH, J., PERRO, C., RYBAK, L. P. & RAMKUMAR, V. 2011. NOX3 NADPH oxidase couples transient receptor potential vanilloid 1 to signal transducer and activator of transcription 1-mediated inflammation and hearing loss. *Antioxidants & redox signaling,* 14**,** 999-1010.

MUKHERJEE, S., ADAMS, M., WHITEAKER, K., DAZA, A., KAGE, K., CASSAR, S., MEYER, M. & YAO, B. B. 2004. Species comparison and pharmacological characterization of rat and human CB 2 cannabinoid receptors. *European journal of pharmacology,* 505**,** 1-9.

MUKHOPADHYAY, P., BAGGELAAR, M., ERDELYI, K., CAO, Z., CINAR, R., FEZZA, F., IGNATOWSKA-JANLOWSKA, B., WILKERSON, J., GILS, N. & HANSEN, T. 2016. The novel, orally available and peripherally restricted selective cannabinoid CB2 receptor agonist LEI-101 prevents cisplatin-induced nephrotoxicity. *British journal of pharmacology,* 173**,** 446-458.

MUKHOPADHYAY, P., PAN, H., RAJESH, M., BÁTKAI, S., PATEL, V., HARVEY-WHITE, J., MUKHOPADHYAY, B., HASKÓ, G., GAO, B. & MACKIE, K. 2010a. CB1 cannabinoid receptors promote oxidative/nitrosative stress, inflammation and cell death in a murine nephropathy model. *British journal of pharmacology,* 160**,** 657-668.

MUKHOPADHYAY, P., RAJESH, M., PAN, H., PATEL, V., MUKHOPADHYAY, B., BÁTKAI, S., GAO, B., HASKÓ, G. & PACHER, P. 2010b. Cannabinoid-2 receptor limits inflammation, oxidative/nitrosative stress, and cell death in nephropathy. *Free Radical Biology and Medicine,* 48**,** 457-467.

MUNRO, S., THOMAS, K. L. & ABU-SHAAR, M. 1993. Molecular characterization of a peripheral receptor for cannabinoids. *Nature,* 365**,** 61-65.

MUSAZZI, U. M., YOUM, I., MUROWCHICK, J. B., EZOULIN, M. J. & YOUAN, B.-B. C. 2014. Resveratrol-loaded nanocarriers: Formulation, optimization, characterization and in vitro toxicity on cochlear cells. *Colloids and Surfaces B: Biointerfaces,* 118**,** 234-242.

N ABI-HACHEM, R., ZINE, A. & R VAN DE WATER, T. 2010. The injured cochlea as a target for inflammatory processes, initiation of cell death pathways and

application of related otoprotective strategies. *Recent patents on CNS drug discovery,* 5**,** 147-163.

NEUZIL, J., WEBER, T., GELLERT, N. & WEBER, C. 2001. Selective cancer cell killing by α-tocopheryl succinate. *British journal of cancer,* 84**,** 87.

NIKI, E. 2014. Role of vitamin E as a lipid-soluble peroxyl radical scavenger: in vitro and in vivo evidence. *Free Radical Biology and Medicine,* 66**,** 3-12.

OFEK, O., KARSAK, M., LECLERC, N., FOGEL, M., FRENKEL, B., WRIGHT, K., TAM, J., ATTAR-NAMDAR, M., KRAM, V. & SHOHAMI, E. 2006. Peripheral cannabinoid receptor, CB2, regulates bone mass. *Proceedings of the National Academy of Sciences of the United States of America,* 103**,** 696-701.

OKA, S., YANAGIMOTO, S., IKEDA, S., GOKOH, M., KISHIMOTO, S., WAKU, K., ISHIMA, Y. & SUGIURA, T. 2005. Evidence for the involvement of the cannabinoid CB2 receptor and its endogenous ligand 2-arachidonoylglycerol in 12-O-tetradecanoylphorbol-13-acetate-induced acute inflammation in mouse ear. *Journal of Biological Chemistry,* 280**,** 18488-18497.

OSEN, K. K., FURNESS, D. N. & HACKNEY, C. M. 2011. The border between the central and the peripheral nervous system in the cat cochlear nerve: A light and scanning electron microscopical study. *Hearing research,* 277**,** 44-53.

ÖZEL, H., ÖZDOĞAN, F., GÜRGEN, S., ESEN, E., GENÇ, S. & SELÇUK, A. 2016. Comparison of the protective effects of intratympanic dexamethasone and methylprednisolone against cisplatin-induced ototoxicity. *The Journal of laryngology and otology,* 130**,** 225-234.

PAKSOY, M., AYDURAN, E., ŞANLı, A., EKEN, M., AYDıN, S. & OKTAY, Z. A. 2011. The protective effects of intratympanic dexamethasone and vitamin E on cisplatin-induced ototoxicity are demonstrated in rats. *Medical Oncology,* 28**,** 615-621.

- - -

- -

, J. S. 2015a. Anticancer and Antiangiogenic Activity of Surfactant-Free Nanoparticles Based on Self-Assembled Polymeric Derivatives of Vitamin E: Structure–Activity Relationship. *Biomacromolecules,* 16**,** 1566-1581.

PALAO-SUAY, R., RODRIGÁÑEZ, L., AGUILAR, M. R., SÁNCHEZ-RODRÍGUEZ, C., PARRA, F., FERNÁNDEZ, M., PARRA, J., RIESTRA-AYORA, J., SANZ-FERNÁNDEZ, R. & ROMÁN, J. S. 2015. Mitochondrially Targeted Nanoparticles Based on α-TOS for the Selective Cancer Treatment. *Macromolecular bioscience,* 16, 395-411.

PAN, H., MUKHOPADHYAY, P., RAJESH, M., PATEL, V., MUKHOPADHYAY, B., GAO, B., HASKÓ, G. & PACHER, P. 2009. Cannabidiol attenuates cisplatin-induced nephrotoxicity by decreasing oxidative/nitrosative stress, inflammation, and cell death. *Journal of Pharmacology and Experimental Therapeutics,* 328**,** 708-714.

PARNES, L. S., SUN, A. H. & FREEMAN, D. J. 1999. Corticosteroid pharmacokinetics in the inner ear fluids: an animal study followed by clinical application. *The Laryngoscope,* 109**,** 1-17.

PATIL, K. V., CANLON, B. & CEDERROTH, C. R. 2015. High quality RNA extraction of the mammalian cochlea for qRT-PCR and transcriptome analyses. *Hearing research,* 325**,** 42-48.

PAULSON, D. P., ABUZEID, W., JIANG, H., OE, T., O'MALLEY, B. W. & LI, D. 2008. A novel controlled local drug delivery system for inner ear disease. *The Laryngoscope,* 118**,** 706-711.

PÉREZ-GÓMEZ, E., ANDRADAS, C., BLASCO-BENITO, S., CAFFAREL, M. M., GARCÍA-TABOADA, E., VILLA-MORALES, M., MORENO, E., HAMANN, S., MARTÍN-VILLAR, E. & FLORES, J. M. 2015. Role of cannabinoid receptor CB2 in HER2 Pro-oncogenic signaling in breast cancer. *Journal of the National Cancer Institute,* 107**,** djv077.

PERTWEE, R., HOWLETT, A., ABOOD, M. E., ALEXANDER, S., DI MARZO, V., ELPHICK, M., GREASLEY, P., HANSEN, H. S., KUNOS, G. & MACKIE, K. 2010. International Union of Basic and Clinical Pharmacology. LXXIX. Cannabinoid receptors and their ligands: beyond CB1 and CB2. *Pharmacological reviews,* 62**,** 588-631.

PERTWEE, R. G. 1997. Pharmacology of cannabinoid CB 1 and CB 2 receptors. *Pharmacology & therapeutics,* 74**,** 129-180.

PINILLA, M., RAMÍREZ-CAMACHO, R., JORGE, E., TRINIDAD, A. & VERGARA, J. 2001. Ventral approach to the rat middle ear for otologic research. *Otolaryngology--Head and Neck Surgery,* 124**,** 515-517.

PRITZ, C. O., BITSCHE, M., SALVENMOSER, W., DUDÁS, J., SCHROTT-FISCHER, A. & GLUECKERT, R. 2013a. Endocytic trafficking of silica nanoparticles in a cell line derived from the organ of Corti. *Nanomedicine,* 8**,** 239-252.

PRITZ, C. O., DUDÁS, J., RASK-ANDERSEN, H., SCHROTT-FISCHER, A. & GLUECKERT, R. 2013b. Nanomedicine strategies for drug delivery to the ear. *Nanomedicine,* 8**,** 1155-1172.

PUNNIA-MOORTHY, A. 1987. Evaluation of pH changes in inflammation of the subcutaneous air pouch lining in the rat, induced by carrageenan, dextran and Staphylococcus aureus. *Journal of Oral Pathology & Medicine,* 16**,** 36-44.

PYYKKÖ, I., ZOU, J., SCHROTT-FISCHER, A., GLUECKERT, R. & KINNUNEN, P. 2015. An Overview of Nanoparticle Based Delivery for Treatment of Inner Ear Disorders. *Methods in molecular biology (Clifton, NJ),* 1427**,** 363-415.

RAJESH, M., MUKHOPADHYAY, P., HASKO, G., HUFFMAN, J., MACKIE, K. & PACHER, P. 2008. CB2 cannabinoid receptor agonists attenuate TNF-α-induced human vascular smooth muscle cell proliferation and migration. *British journal of pharmacology,* 153**,** 347-357.

RAMIREZ-CAMACHO, R., CITORES, M., TRINIDAD, A., VERDAGUER, J., GARCÍA-BERROCAL, J., MARTÍN MARERO, A., PUENTE, A., GONZÁLEZ-GARCÍA, J. & VARGAS, J. 2007. HSP-70 as a nonspecific early marker in cisplatin ototoxicity. *Acta oto-laryngologica,* 127**,** 564-567.

RAO, J. P. & GECKELER, K. E. 2011. Polymer nanoparticles: preparation techniques and size-control parameters. *Progress in Polymer Science,* 36**,** 887-913.

REYES-ORTEGA, F., RODRÍGUEZ, G., AGUILAR, M. R., LORD, M., WHITELOCK, J., STENZEL, M. H. & SAN ROMÁN, J. 2013. Encapsulation of low molecular weight heparin (bemiparin) into polymeric nanoparticles obtained from cationic block copolymers: properties and cell activity. *Journal of Materials Chemistry B,* 1**,** 850-860.

ROCHE, R., HOAREAU, L., BES-HOUTMANN, S., GONTHIER, M.-P., LABORDE, C., BARON, J.-F., HAFFAF, Y., CESARI, M. & FESTY, F. 2006. Presence of

the cannabinoid receptors, CB1 and CB2, in human omental and subcutaneous adipocytes. *Histochemistry and cell biology,* 126**,** 177-187.

RYBAK, L. P., MUKHERJEA, D., JAJOO, S. & RAMKUMAR, V. 2009. Cisplatin ototoxicity and protection: clinical and experimental studies. *Tohoku J Exp Med,* 219**,** 177-86.

RYBAK, L. P. & RAMKUMAR, V. 2007. Ototoxicity. *Kidney Int,* 72**,** 931-5.

RYBAK, L. P., WHITWORTH, C. A., MUKHERJEA, D. & RAMKUMAR, V. 2007. Mechanisms of cisplatin-induced ototoxicity and prevention. *Hearing research,* 226**,** 157-167.

SHIRE, D., CARILLON, C., KAGHAD, M., CALANDRA, B., RINALDI-CARMONA, M., LE FUR, G., CAPUT, D. & FERRARA, P. 1995. An amino-terminal variant of the central cannabinoid receptor resulting from alternative splicing. *Journal of Biological Chemistry,* 270**,** 3726-3731.

SO, H., KIM, H., KIM, Y., KIM, E., PAE, H.-O., CHUNG, H.-T., KIM, H.-J., KWON, K.-B., LEE, K.-M. & LEE, H.-Y. 2008. Evidence that cisplatin-induced auditory damage is attenuated by downregulation of pro-inflammatory cytokines via Nrf2/HO-1. *Journal of the Association for Research in Otolaryngology,* 9**,** 290-306.

SO, H., KIM, H., LEE, J.-H., PARK, C., KIM, Y., KIM, E., KIM, J.-K., YUN, K.-J., LEE, K.-M. & LEE, H.-Y. 2007. Cisplatin cytotoxicity of auditory cells requires secretions of proinflammatory cytokines via activation of ERK and NF-κB. *Journal of the Association for Research in Otolaryngology,* 8**,** 338-355.

SO, H., KIM, H., LEE, J., PARK, S., PARK, C., KIM, Y., KIM, J., LEE, K., KIM, K. & CHUNG, S. 2006. Flunarizine induces Nrf2-mediated transcriptional activation of heme oxygenase-1 in protection of auditory cells from cisplatin. *Cell Death & Differentiation,* 13**,** 1763-1775.

STÄNDER, S., SCHMELZ, M., METZE, D., LUGER, T. & RUKWIED, R. 2005. Distribution of cannabinoid receptor 1 (CB1) and 2 (CB2) on sensory nerve fibers and adnexal structures in human skin. *Journal of dermatological science,* 38**,** 177-188.

STORR, M., GAFFAL, E., SAUR, D., SCHUSDZIARRA, V. & ALLESCHER, H. 2002. Effect of cannabinoids on neural transmission in rat gastric fundus. *Canadian journal of physiology and pharmacology,* 80**,** 67-76.

SUÁREZ, P., ROJO, L., GONZÁLEZ-GÓMEZ, Á. & ROMÁN, J. S. 2013. Self-Assembling Gradient Copolymers of Vinylimidazol and (Acrylic) ibuprofen With Anti-Inflammatory and Zinc Chelating Properties. *Macromolecular bioscience,* 13**,** 1174-1184.

SUN, C., WANG, X., CHEN, D., LIN, X., YU, D. & WU, H. 2016. Dexamethasone loaded nanoparticles exert protective effects against Cisplatin-induced hearing loss by systemic administration. *Neuroscience letters,* 619**,** 142-148.

SUN, C., WANG, X., ZHENG, Z., CHEN, D., WANG, X., SHI, F., YU, D. & WU, H. 2015. A single dose of dexamethasone encapsulated in polyethylene glycol-coated polylactic acid nanoparticles attenuates cisplatin-induced hearing loss following round window membrane administration. *International journal of nanomedicine,* 10**,** 3567.

SUROVTSEVA, E. V., JOHNSTON, A. H., ZHANG, W., ZHANG, Y., KIM, A., MURAKOSHI, M., WADA, H., NEWMAN, T. A., ZOU, J. & PYYKKÖ, I. 2012. Prestin binding peptides as ligands for targeted polymersome mediated drug delivery to outer hair cells in the inner ear. *International journal of pharmaceutics,* 424**,** 121-127.

TENG, X. W., DAVIES, N. M., FUKUDA, C., GOOD, R. L. & FARISS, M. W. 2005. Pharmacokinetics and tissue distribution of d-alpha-tocopheryl succinate formulations following intravenous administration in the rat. *Biopharmaceutics & drug disposition,* 26**,** 195-203.

TERANISHI, M.-A., NAKASHIMA, T. & WAKABAYASHI, T. 2001. Effects of α-tocopherol on cisplatin-induced ototoxicity in guinea pigs. *Hearing research,* 151**,** 61-70.

TOAL, K. L., RADZIWON, K. E., HOLFOTH, D. P., XU-FRIEDMAN, M. A. & DENT, M. L. 2016. Audiograms, gap detection thresholds, and frequency difference limens in cannabinoid receptor 1 knockout mice. *Hearing research,* 332**,** 217-222.

TORCHILIN, V. P. 2006. *Nanoparticulates as drug carriers,* Imperial college press.

TRAITEL, T., GOLDBART, R. & KOST, J. 2008. Smart polymers for responsive drug-delivery systems. *Journal of Biomaterials Science, Polymer Edition,* 19**,** 755-767.

UCHEGBU, I. F. & SIEW, A. 2013. Nanomedicines and nanodiagnostics come of age. *Journal of pharmaceutical sciences,* 102**,** 305-310.

VELASCO, D., RÉTHORÉ, G., NEWLAND, B., PARRA, J., ELVIRA, C., PANDIT, A., ROJO, L. & SAN ROMÁN, J. 2012. Low polydispersity (N-ethyl pyrrolidine methacrylamide-co-1-vinylimidazole) linear oligomers for gene therapy applications. *European Journal of Pharmaceutics and Biopharmaceutics,* 82**,** 465-474.

WAISSBLUTH, S., SALEHI, P., HE, X. & DANIEL, S. J. 2013. Systemic dexamethasone for the prevention of cisplatin-induced ototoxicity. *European Archives of Oto-Rhino-Laryngology,* 270**,** 1597-1605.

WANG, J., LADRECH, S., PUJOL, R., BRABET, P., VAN DE WATER, T. R. & PUEL, J.-L. 2004. Caspase inhibitors, but not c-Jun NH2-terminal kinase inhibitor treatment, prevent cisplatin-induced hearing loss. *Cancer Research,* 64**,** 9217-9224.

WANG, X. & QUINN, P. J. 1999. Vitamin E and its function in membranes. *Progress in lipid research,* 38**,** 309-336.

WATANABE, K., INAI, S., JINNOUCHI, K., BADA, S., HESS, A., MICHEL, O. & YAGI, T. 2001. Nuclear-factor kappa B (NF-kappa B)-inducible nitric oxide synthase (iNOS/NOS II) pathway damages the stria vascularis in cisplatin-treated mice. *Anticancer research,* 22**,** 4081-4085.

WILSON, W. R., BYL, F. M. & LAIRD, N. 1980. The efficacy of steroids in the treatment of idiopathic sudden hearing loss: a double-blind clinical study. *Archives of Otolaryngology,* 106**,** 772-776.

WILLIAMS, H. D., TREVASKIS, N. L., CHARMAN, S. A., SHANKER, R. M., CHARMAN, W. N., POUTON, C. W. & PORTER, C. J. 2013. Strategies to address low drug solubility in discovery and development. *Pharmacological reviews,* 65**,** 315-499.

WORLD HEALTH ORGANIZATION, W. H. 2015. Fact sheet N°300. *Deafness and hearing loss.* World Health Organization.

YANG, L., LI, F.-F., HAN, Y.-C., JIA, B. & DING, Y. 2015. Cannabinoid receptor CB2 is involved in tetrahydrocannabinol-induced anti-inflammation against lipopolysaccharide in MG-63 cells. *Mediators of inflammation,* 2015.

YOO, J., HAMILTON, S. J., ANGEL, D., FUNG, K., FRANKLIN, J., PARNES, L. S., LEWIS, D., VENKATESAN, V. & WINQUIST, E. 2014. Cisplatin otoprotection using transtympanic L-N-acetylcysteine: A pilot randomized study in head and neck cancer patients. *The Laryngoscope,* 124**,** E87-E94.

YOON, J. Y., YANG, K.-J., KIM, D. E., LEE, K.-Y., PARK, S.-N., KIM, D.-K. & KIM, J.-D. 2015. Intratympanic delivery of oligoarginine-conjugated nanoparticles as a gene (or drug) carrier to the inner ear. *Biomaterials,* 73**,** 243-253.

YOUM, I. & YOUAN, B.-B. C. 2013. Uptake mechanism of furosemide-loaded pegylated nanoparticles by cochlear cell lines. *Hearing research,* 304**,** 7-19.

YUMUSAKHUYLU, A. C., YAZICI, M., SARI, M., BINNETOGLU, A., KOSEMIHAL, E., AKDAS, F., SIRVANCI, S., YUKSEL, M., UNERI, C. & TUTKUN, A. 2012. Protective role of resveratrol against cisplatin induced ototoxicity in guinea pigs. *International journal of pediatric otorhinolaryngology,* 76**,** 404-408.

ZHANG, C., BECKERMANN, B., KALLIFATIDIS, G., LIU, Z., RITTGEN, W., EDLER, L., BÜCHLER, P., DEBATIN, K.-M., BÜCHLER, M. W. & FRIESS, H. 2006. Corticosteroids induce chemotherapy resistance in the majority of tumour cells from bone, brain, breast, cervix, melanoma and neuroblastoma. *International journal of oncology,* 29**,** 1295-1301.

ZHANG, W., ZHANG, Y., LOBLER, M., SCHMITZ, K.-P., AHMAD, A., PYYKKO, I. & ZOU, J. 2011a. Nuclear entry of hyperbranched polylysine nanoparticles into cochlear cells. *Int J Nanomedicine,* 6**,** 535-546.

ZHANG, Y., ZHANG, W., LÖBLER, M., SCHMITZ, K.-P., SAULNIER, P., PERRIER, T., PYYKKÖ, I. & ZOU, J. 2011b. Inner ear biocompatibility of lipid nanocapsules after round window membrane application. *International journal of pharmaceutics,* 404**,** 211-219.

ZHENG, Y., REID, P. & SMITH, P. F. 2015. Cannabinoid CB1 Receptor Agonists Do Not Decrease, but may Increase Acoustic Trauma-Induced Tinnitus in Rats. *Frontiers in neurology,* 6.

ZHU, Z., LI, Y., LI, X., LI, R., JIA, Z., LIU, B., GUO, W., WU, W. & JIANG, X. 2010. Paclitaxel-loaded poly(N-vinylpyrrolidone)-b-poly(epsilon-caprolactone) nanoparticles: preparation and antitumor activity in vivo. *J Control Release,* 142**,** 438-446.

ZINE, A. & ROMAND, R. 1996. Development of the auditory receptors of the rat: a SEM study. *Brain research,* 721**,** 49-58.

ZOPPI, S., MADRIGAL, J., CASO, J., GARCÍA-GUTIÉRREZ, M., MANZANARES, J., LEZA, J. & GARCÍA-BUENO, B. 2014. Regulatory role of the cannabinoid CB2 receptor in stress-induced neuroinflammation in mice. *British journal of pharmacology,* 171**,** 2814-2826.

ZORATTI, C., KIPMEN-KORGUN, D., OSIBOW, K., MALLI, R. & GRAIER, W. F. 2003. Anandamide initiates Ca2+ signaling via CB2 receptor linked to phospholipase C in calf pulmonary endothelial cells. *British journal of pharmacology,* 140**,** 1351-1362.

ZOU, J., FENG, H., MANNERSTRÖM, M., HEINONEN, T. & PYYKKÖ, I. 2014. Toxicity of silver nanoparticle in rat ear and BALB/c 3T3 cell line. *Journal of nanobiotechnology,* 12**,** 1.

ZOU, J., HANNULA, M., MISRA, S., FENG, H., LABRADOR, R. H., AULA, A. S., HYTTINEN, J. & PYYKKÖ, I. 2015. Micro CT visualization of silver nanoparticles in the middle and inner ear of rat and transportation pathway after transtympanic injection. *Journal of nanobiotechnology,* 13**,** 1.

ZOU, J., SOOD, R., RANJAN, S., POE, D., RAMADAN, U. A., PYYKKÖ, I. & KINNUNEN, P. K. 2012. Size-dependent passage of liposome nanocarriers with preserved posttransport integrity across the middle-inner ear barriers in rats. *Otology & Neurotology,* 33**,** 666-673.

Anexos

Anexos

Anexos